

**Haemodynamic correlates of interictal and ictal  
epileptic discharges and ictal semiology using  
simultaneous scalp video-EEG-fMRI  
and intracranial EEG-fMRI**

**Umair Javaid Chaudhary, MBBS, MSc**

DEPARTMENT OF CLINICAL AND EXPERIMENTAL EPILEPSY  
INSTITUTE OF NEUROLOGY  
UNIVERSITY COLLEGE LONDON (UCL)  
UNITED KINGDOM

THESIS SUBMITTED TO UNIVERSITY COLLEGE LONDON  
FOR THE DEGREE OF DOCTOR OF PHILOSOPHY, 2013

## **DECLARATION OF OWN WORK**

I, Umair Javaid Chaudhary, confirm that the work presented here is my own.

Where information has been derived from other sources, I confirm that this has been indicated in the thesis.

The scientific studies presented in this thesis reflect the contributions of a team of researchers including other colleagues from the DCEE, ION UCL. However, this thesis presents only studies where I conducted most steps of data collection, data analysis and the complete interpretation of the results following discussions at supervision meetings. I have outlined my own individual contribution to each of the studies published here and the contributions of my main co-workers and collaborators.

All the figures and illustrations are my own.

Information derived from other sources has been indicated and referenced in this thesis.

A handwritten signature in black ink, appearing to read 'Umair Javaid Chaudhary', written over a horizontal line.

Signature

## ABSTRACT

Interictal and ictal epileptic discharges are produced by focal and widespread dysfunctional neuronal networks. Identification and characterization of epileptic discharges underlie the diagnosis and the choice of treatment for epilepsy patients. A better knowledge of the generation, propagation and localisation of epileptic discharges, and their interaction with the physiological and pathological brain networks can be very helpful in planning epilepsy surgery and minimizing the risk of damaging the physiological brain networks.

This work describes a number of methodological developments and novel applications investigating the epileptic networks in humans using EEG-fMRI. First, I implemented synchronized video recording inside the MRI-scanner during simultaneous EEG-fMRI studies, which did not deteriorate the imaging and EEG data quality. Secondly, I used video recordings to identify physiological activities to be modelled as confounds in the functional imaging data analysis for interictal activity, thus increasing the sensitivity of video-EEG-fMRI. Thirdly, I applied this modelling approach to investigate seizure related functional networks in patients with focal epilepsy. Video recordings allowed partitioning seizures into phases separating the ictal onset related functional networks from propagation related networks. Localisation of the ictal onset related networks may be useful in the planning for epilepsy surgery in a selected group of patients, as demonstrated by their comparison with intracranial-EEG recordings. Further, I investigated haemodynamic changes during preictal period which suggested recruitment of an inhibitory followed by an excitatory network prior to the ictal onset on scalp EEG. In the next step, I used simultaneous intracranial-EEG-fMRI in patients undergoing invasive evaluation, demonstrating that local and remote networks associated with very focal interictal discharges recorded on intracranial-EEG may predict the surgical outcome. Finally, I investigated the interaction of epileptic discharges with the working memory, using scalp video-EEG-fMRI, showing that the presence of epileptic activity may alter the working memory related networks. Methodological constraints, clinical applications and future perspectives are discussed.

## TABLE OF CONTENTS

ABSTRACT .....	3
TABLE OF CONTENTS .....	4
LIST OF FIGURES .....	11
LIST OF TABLES .....	13
LIST OF ABBREVIATIONS .....	14
ACKNOWLEDGEMENTS .....	19
FUNDING SOURCES .....	21
FOREWORD.....	22
OUTLINE AND STATEMENT OF PERSONAL CONTRIBUTION .....	24
PUBLICATIONS ASSOCIATED WITH THIS THESIS .....	26
CONFERENCE POSTERS AND TALKS RELATED TO THIS THESIS .....	30
AWARDS.....	31
SECTION 1: LITERATURE REVIEW .....	32
<b>Chapter 1: Epilepsy in historical perspective .....</b>	<b>32</b>
1.1    Pre-Greek and Classical Greek Era (Before 500 BC - 400 AD) .....	32
1.1.1    Theories about Epilepsy .....	32
1.1.2    Clinical Concepts .....	34
1.1.3    Diagnosis and Treatment.....	34
1.2    Middle-Ages around the World: 401-1500 AD .....	35
1.3    Western Renaissance (1501-1700 A.D.).....	36
1.4    Enlightenment (1701-1815) .....	36
1.5    Early Nineteenth Century - Pre-Hughlings Jackson.....	37
1.6    Era of Hughlings Jackson (1835-1911).....	38
1.7    Century of New Advancements .....	41
1.8    Perspectives and conclusion .....	41
<b>Chapter 2: Epileptology: where do we stand? .....</b>	<b>42</b>
2.1    Definition of seizure and epilepsy.....	42
2.2    Burden of epilepsy.....	42
2.3    Aetiology of epilepsy .....	43

2.4	Mechanism of seizure generation.....	44
2.4.1	Absence seizures .....	44
2.4.2	Focal epileptic activity .....	46
2.4.2a	Interictal epileptiform discharges .....	46
2.4.2b	Transition to focal seizures.....	47
2.4.2c	Onset and progression of focal seizures .....	48
2.5	Classification of seizures and epilepsy.....	50
2.5.1	New ILAE classification of seizures and epilepsy.....	52
2.5.2	Pros and cons of the new ILAE classification.....	54
2.6	Investigation techniques .....	56
2.6.1	Electroencephalography .....	56
2.6.2	Structural magnetic resonance imaging in epileptology .....	60
2.6.3	Positron emission tomography .....	61
2.6.4	Magneto-encephalography .....	62
2.6.5	Ictal single photon emission computed tomography.....	63
2.6.6	Functional magnetic resonance imaging .....	64
2.7	Medical and surgical treatments.....	64
2.7.1	Antiepileptic drugs .....	65
2.7.2	Refractory epilepsy and epilepsy surgery .....	65
2.8	Perspectives and conclusion.....	68
<b>Chapter 3: Simultaneous EEG-fMRI in epilepsy.....</b>		<b>69</b>
3.1	Mechanism of the BOLD effect .....	69
3.1.1	Types of neuronal activity recorded on EEG .....	69
3.1.2	Relationship between neuronal activity, energy metabolism and haemodynamic changes.....	70
3.1.3	What is the BOLD effect?.....	71
3.1.4	BOLD effect and neuronal activity .....	72
3.2	Methodological considerations for simultaneous EEG-fMRI.....	74
3.2.1	Patient selection.....	74
3.2.1a	Studies on IED related haemodynamic changes .....	75
3.2.1b	Studies on ictal related haemodynamic changes .....	75
3.2.2	Recording EEG inside MRI scanner .....	81
3.2.3	Identification of interictal and ictal activity in EEG-fMRI studies.....	82
3.2.4	Data quality .....	83

3.2.4a	Removing artefacts in EEG data recorded during fMRI.....	83
3.2.4b	Artefacts in fMRI data: physiological and non-physiological	85
3.2.5	fMRI data analysis.....	88
3.2.5a	Identification of variations in MR signal intensity.....	88
3.2.5b	Correlation analysis: general linear model.....	89
3.2.5c	Independent component analysis.....	93
3.2.5d	What are the respective roles of GLM or ICA based analyses?	94
3.2.6	Validation of fMRI findings.....	95
3.3	Applications of EEG-fMRI in epilepsy.....	102
3.3.1	How many patients will show BOLD changes?.....	103
3.3.2	IED related networks.....	104
3.3.3	Localisation of seizure onset in focal epilepsy.....	105
3.3.4	Preictal BOLD changes, seizure evolution and propagation in focal epilepsy.....	107
3.3.5	Haemodynamic networks in idiopathic generalized epilepsy.....	107
3.3.6	Seizure related networks in other forms of epilepsy.....	110
3.3.7	Haemodynamic mapping of cognitive networks during GSWDs.....	111
3.3.8	Role of EEG-fMRI in management of epilepsy.....	112
3.4	Perspectives on the application of simultaneous EEG-fMRI in epilepsy.....	113
SECTION 2: EXPERIMENTAL STUDIES.....		115
<b>Chapter 4: Common Methods.....</b>		<b>115</b>
4.1	Patient recruitment.....	115
4.2	MRI acquisition.....	115
4.3	Video-EEG acquisition:.....	116
4.3.1	EEG recording and artefact correction.....	116
4.3.2	Video recording.....	117
4.4	fMRI processing and statistical analysis.....	120
<b>Chapter 5: Implementation and Evaluation of Simultaneous video-EEG-fMRI.....</b>		<b>121</b>
5.1	Background.....	121
5.2	Methods.....	122

5.2.1	Subjects .....	122
5.2.2	MRI acquisition .....	122
5.2.2a	Test object .....	122
5.2.2b	Human subjects .....	123
5.2.3	Video- EEG acquisition.....	123
5.2.3a	EEG recording and artefact correction.....	123
5.2.3b	Video recording.....	123
5.2.4	Experimental design for hand motor task.....	123
5.2.5	Data Analysis .....	123
5.2.5a	Image, EEG and video quality .....	123
5.2.5b	fMRI analysis: hand motor task .....	125
5.3	Results .....	125
5.4	Discussion .....	132
5.5	Conclusion.....	134
<b>Chapter 6: Improving the sensitivity of vEEG-fMRI studies of IED by modelling video-EEG detected physiological confounds .....</b>		<b>135</b>
6.1	Background .....	135
6.2	Methods .....	137
6.2.1	Subjects .....	137
6.2.2	MRI acquisition.....	137
6.2.3	Video-EEG recording and artefact correction.....	137
6.2.4	Data processing and analysis.....	137
6.2.4a	EEG and fMRI Processing .....	137
6.2.4b	fMRI Modelling .....	139
6.2.5	Assessment of BOLD changes and level of concordance.....	139
6.3	Results .....	142
6.3.1	IED related BOLD changes.....	142
6.3.2	BOLD changes linked to physiological activities .....	150
6.4	Discussion .....	155
6.5	Conclusion.....	159
<b>Chapter 7: Mapping ictal haemodynamic networks using vEEG-fMRI .....</b>		<b>160</b>
7.1	Background .....	160
7.2	Methods .....	161
7.2.1	Subjects .....	161

7.2.2	MRI acquisition.....	162
7.2.3	Video-EEG recording and artefact correction.....	162
7.2.4	Data processing and analysis.....	162
7.2.4a	EEG and fMRI Processing .....	162
7.2.4b	fMRI Modelling .....	163
7.2.5	Assessment of BOLD changes, significance, visualization and level of concordance.....	164
7.2.6	Quantification of head motion events .....	166
7.3	Results .....	166
7.3.1	Ictal BOLD changes .....	177
7.3.1a	Comparison of ictal BOLD changes with invasively defined SOZ and surgical outcome .....	177
7.3.1b	Comparison of ictal BOLD changes with presumed SOZ ..	191
7.3.2	Ictal propagation related BOLD networks .....	194
7.3.3	Direction of BOLD change .....	197
7.3.4	Head motion and ictal BOLD patterns .....	197
7.4	Discussion .....	200
7.4.1	Methodological considerations.....	201
7.4.2	Neurobiological significance.....	203
7.4.3	Clinical significance .....	205
7.5	Conclusion.....	208
<b>Chapter 8: Mapping preictal haemodynamic networks using vEEG-fMRI 209</b>		
8.1	Background .....	209
8.2	Methods.....	210
8.2.1	Subjects .....	210
8.2.2	MRI acquisition.....	210
8.2.3	Video-EEG recording and artefact correction.....	210
8.2.4	Data processing and analysis.....	210
8.2.4a	EEG and fMRI Processing .....	210
8.2.4b	fMRI Modelling .....	211
8.2.5	Assessment of BOLD change significance, visualization and level of concordance .....	211
8.3	Results .....	213
8.4	Discussion .....	222



8.5	Conclusion.....	225
<b>Chapter 9: Mapping the interictal haemodynamic networks using simultaneous intracranial EEG-fMRI and comparison with postsurgical outcome..... 226</b>		
9.1	Background .....	226
9.2	Methods .....	227
9.2.1	Subjects .....	227
9.2.2	Intracranial EEG-fMRI acquisition.....	227
9.2.3	Data Processing and analysis .....	231
9.2.3a	Intracranial EEG and fMRI processing.....	231
9.2.3b	fMRI modelling.....	232
9.2.4	Assessment of BOLD changes .....	232
9.2.4a	BOLD changes for individual IED types .....	232
9.2.4b	BOLD changes for combined all IEDs in an individual patient 234	
9.3	Results .....	234
9.3.1	Individual IED related BOLD changes .....	239
9.3.2	Combined IED related BOLD changes.....	244
9.4	Discussion .....	249
9.4.1	Methodological considerations.....	250
9.4.2	Neurobiological significance.....	251
9.4.3	Clinical significance .....	252
9.5	Conclusion.....	254
<b>Chapter 10: Imaging the interaction: epileptic discharges, working memory and behaviour ..... 255</b>		
10.1	Background .....	255
10.2	Methods .....	256
10.2.1	Subjects .....	256
10.2.2	MRI acquisition and working memory task .....	256
10.2.3	Video-EEG recording and artefact correction.....	257
10.2.4	Data processing and analysis.....	257
10.2.4a	EEG and fMRI processing .....	257
10.2.4b	fMRI modelling.....	257

10.2.5	Assessment of BOLD changes, significance and visualization	259
10.2.6	Statistical analysis .....	259
10.3	Results .....	260
10.4	Discussion .....	268
10.5	Conclusion.....	273
SECTION 3: DISCUSSION & CONCLUSION.....		274
<b>Chapter 11: General discussion and future perspectives .....</b>		<b>274</b>
11.1	BOLD mapping for interictal discharges .....	275
11.2	BOLD mapping for seizures.....	277
11.3	Assessment of loss of awareness and EEG-fMRI.....	280
<b>Chapter 12: Conclusion .....</b>		<b>282</b>
APPENDICES.....		283
<b>Appendix 1: Examples of epileptiform discharges.....</b>		<b>283</b>
<b>Appendix 2: IED related BOLD changes for data presented in Chapter 7.</b>		<b>285</b>
<b>Appendix 3: IED related BOLD changes on scalp EEG-fMRI for data presented in Chapter 9.....</b>		<b>287</b>
REFERENCES.....		289

## LIST OF FIGURES

Figure 1.1: Epilepsy tablet -----	33
Figure 1.2: Eminent British neuroscientists in the era of Hughlings Jackson ----	40
Figure 2.1: Intracranial electrodes -----	59
Figure 4.1: Arrangement of equipment -----	119
Figure 5.1: Mean time courses of signal from ROI in a test object -----	127
Figure 5.2: Mean SFNR from EPI volumes for a test object-----	128
Figure 5.3: Mean SFNR from EPI volumes in human subjects -----	129
Figure 5.4: Representative sample of Synchronized Video-EEG -----	130
Figure 5.5: BOLD activations for finger tapping task -----	131
Figure 6.1: Design matrices with and without physiological activities-----	141
Figure 6.2: Bar chart of physiological confounds -----	145
Figure 6.3: BOLD changes for IEDs for GLM 1 and GLM2 -----	148
Figure 6.4: BOLD changes for physiological activities -----	153
Figure 6.5: BOLD changes for physiological activities -----	154
Figure 7.1: Bar charts: identification of seizures and ictal phases -----	176
Figure 7.2: Bar chart showing level of concordance -----	179
Figure 7.3: Ictal BOLD changes for patient #1 -----	185
Figure 7.4: Ictal BOLD changes for patient #10-----	186
Figure 7.5: Ictal BOLD changes patients #4 -----	187
Figure 7.6: Comparison of BOLD changes with implantation and resection----	189
Figure 7.7: Ictal BOLD changes for patient #19-----	192
Figure 7.8: BOLD changes in DMN-----	195
Figure 7.9: Scatter plots showing inter scan head motion -----	198
Figure 7.10: Comparison of BOLD change for seizure, motion and pulse -----	199
Figure 8.1: Bar chart showing level of concordance for preictal BOLD changes vs. Ictal onset/Ictal phases -----	217
Figure 8.2: Preictal BOLD changes for patient #1 -----	218
Figure 8.3: Preictal BOLD changes for patient #10-----	219
Figure 8.4: Time courses of preictal BOLD changes -----	220

Figure 9.1: Implantation Scheme -----	229
Figure 9.2: IEDs and BOLD changes for Patient #2 -----	240
Figure 9.3: IEDs and BOLD changes for Patient #3 -----	242
Figure 9.4: BOLD changes for combined all IED types and surgical resection- 246	
Figure 9.5: BOLD changes, laterality index and postsurgical outcome -----	247
Figure 10.1: Design matrix -----	258
Figure 10.2: Dot chart showing number of GSWDs and responses-----	262
Figure 10.3: Representative sample of EEG -----	263
Figure 10.4: BOLD changes for GSWDs and task -----	264
Figure 10.5: Working memory related BOLD changes with/without GSWDs -	265
Figure 10.6: Predicted BOLD responses-----	267
Figure 10.7: BOLD changes for GSWDs during rest and task -----	271
Figure 10.8: BOLD changes for working memory task -----	272
Figure S1: Example of generalized spike wave discharges -----	283
Figure S2: Example of focal interictal epileptiform discharges -----	284

## LIST OF TABLES

Table 3.1: Publications on mapping seizure related BOLD changes using fMRI or EEG-fMRI .....	77
Table 3.2: Sensitivity, criteria for concordance and degree of concordance from previous publications on seizures using fMRI or EEG-fMRI .....	97
Table 6.1: Summary of electroclinical and imaging findings .....	138
Table 6.2: Epileptic discharges and motion observed during vEEG-fMRI .....	144
Table 6.3: Location, size, statistical significance and degree of concordance (focal cases only) of IED related BOLD changes .....	146
Table 6.4: BOLD changes for physiological activities .....	151
Table 7.1: Clinical characteristics and localisation of epilepsy .....	168
Table 7.2: Interictal and ictal activity recorded during long-term video-EEG monitoring .....	170
Table 7.3: Seizures recorded during vEEG-fMRI .....	175
Table 7.4: Ictal BOLD changes and level of concordance with the SOZ .....	180
Table 7.5: BOLD changes in resting state networks during seizure .....	196
Table 8.1: Preictal BOLD changes and level of concordance with the SOZ .....	215
Table 9.1: Clinical characteristics .....	228
Table 9.2: IED statistics and local and network level BOLD changes .....	235
Table 9.3: BOLD changes for combined all IED types, laterality index and postsurgical outcome .....	245
Table S1: IED related BOLD changes for patients who had seizures during scalp EEG-fMRI .....	286
Table S2: IED related BOLD changes during scalp EEG-fMRI for patients who also underwent icEEG-fMRI .....	288

## LIST OF ABBREVIATIONS

- AD = After death  
AED = Antiepileptic drugs  
Ant. = Anterior  
ATLR = Anterior temporal lobe resection  
AVM = Arterio-venous malformation  
BECTS = Benign childhood epilepsy with centro-temporal spikes  
BG = Basal ganglia  
Bilat. = Bilateral  
BOLD = Blood oxygen level dependent  
BC = Before Christ  
BS = Brainstem  
BSW = Bilateral spike and wave  
C+ = Concordant plus  
C1 = Camera 1: scanner bore mounted camera  
C2 = Camera 2: wall-mounted non-detachable camera inside the scanner room  
CAE = Childhood absence epilepsy  
CT = Computed tomography  
D = Discordant  
DMN = Default mode network  
DNET = Dysembroplastic neuroepithelial tumour  
DR = Drug reduction  
EC = Entirely concordant  
EEG = Electroencephalography  
EEG-fMRI = Simultaneous electroencephalography and functional magnetic resonance imaging  
EMA = Eyelid myoclonia with absences  
EMG = Electromyography  
EOI = Effect of interest  
EPI = echo-planar imaging  
EPSPs = Excitatory post-synaptic potentials  
ETS = Eye tracking system

ExTLE = Extra temporal lobe epilepsy  
Fron.L=Frontal lobe  
FCD = Focal cortical dysplasia  
FDG = Fluoro deoxy-glucose  
FDR = False discovery rate  
FE = Focal epilepsy  
FEF=Frontal Eye-Field  
FLE = Frontal lobe epilepsy  
fMRI = Functional magnetic resonance imaging  
FOS = Fixation-off sensitivity  
FOV = Field of view  
FP = Fronto-polar  
FT = Fronto-temporal  
FTJ = Fronto-temporal junction  
FWE = Family wise error  
GA = Gradient artefact  
GABA =  $\gamma$ -amino butyric acid  
GLM = General linear model  
GM = Global statistical maximum  
GSWDs = Generalized spike and wave discharges  
HFO = High frequency oscillations  
Highlighted green = additional BOLD clusters revealed for GLM2  
HRF = Haemodynamic response function  
HS = Hippocampal sclerosis  
Hz = Hertz  
IC = Independent component  
ICA = Independent component analysis  
icEEG = Intracranial EEG  
icEEG-fMRI = Intracranial electroencephalography and functional magnetic resonance imaging  
IE = Ictal established  
IEDs = Interictal epileptiform discharges  
IFG = Inferior frontal gyrus  
IGE = Idiopathic generalized epilepsy

ILAE = International league against epilepsy  
Inf. = Inferior  
Infin. = Infinity  
IO = Ictal onset  
IPL = Inferior parietal lobe  
IPSPs = Inhibitory post synaptic potentials  
ITG = Inferior temporal gyrus  
IZ = Irritative zone  
JAE = Juvenile absence epilepsy  
kHz = Kilo-hertz  
k $\Omega$  = Kilo-ohm  
L = left  
lat. = Lateral  
LFP = Local field potential  
LI = Late ictal  
LOA = Loss of awareness  
M = Music  
MC = Motor cortex  
MCD = Malformations of cortical development  
ME = Musicogenic epilepsy  
md. / Med. = Medial  
Me.FL = Medial frontal lobe  
Me.TL = Medial temporal lobe  
mEFP = mean extracellular field potential  
MEG = Magneto-encephalography  
MFG = Middle frontal gyrus  
MHz = Mega hertz  
MNI = Montreal neurological institute  
MOC = Medial occipital cortex  
MR-compatible = Magnetic resonance compatible  
MRI = Magnetic resonance imaging  
ms = milliseconds  
MTG = Middle temporal gyrus  
MUA = Multi unit activity



mV = Milli volt  
NA = Not applicable / available  
NHNN = National Hospital for Neurology and Neurosurgery  
NL= Non lesional  
NMDA = N-methyl D-aspartic acid  
OFR = optical fire wire repeater  
OL = Occipital lobe  
OP = Occipital pole  
PA = Pulse artefact  
Par. L = Parietal lobe  
PC = Parietal cortex  
PCA = Principal component analysis  
pCO<sub>2</sub> = partial pressure of carbon di oxide  
PDS = Paroxysmal depolarizing shift  
PET = Positron emission tomography  
Ph = Photic stimulation  
PLE = Parietal lobe epilepsy  
PMC = Pre-motor cortex  
Post. = Posterior  
PPR = Photo paroxysmal response  
PRB = Patient response button  
R=right  
RE = Rasmussen's encephalitis  
Re = Reading  
ReE = Reading epilepsy  
RF = Radio frequency  
RP = Realignment parameters  
SAR = specific absorption rate  
SC = Some concordance  
SD = Sleep deprivation  
sec = seconds  
SEF=Supplementary Eye-Field  
Seq. = Sequential  
SFG=Superior frontal gyrus

SFNR = Signal to fluctuation noise ratio  
SGE = Secondary generalized epilepsy  
SGS = Secondary generalized seizure  
SISCOM = sub-traction of ictal and interictal scans  
SMA=Supplementary motor area  
SMC=Sensory motor cortex  
SOZ = Seizure onset zone  
SPECT = Single photon emission computed tomography  
SPM = Statistical parametric mapping  
SR = Sound/Voice recording  
STG = Superior temporal gyrus  
T = Tesla  
Temp.L = Temporal lobe  
TIRDA = Temporal intermittent rhythmic delta  
TLE = Temporal lobe epilepsy  
TPJ = Temporo-parietal junction  
TR = Time repeat  
UCL = University College London  
UCLH = University College London Hospitals  
NHS = National Health Service  
video-EEG-fMRI/vEEG-fMRI = simultaneous video EEG and fMRI  
vent. = Ventricle  
video-EEG = Simultaneous video and scalp electroencephalography  
VR = Video recording  
WM = Working memory  
Y = Yes  
 $\Delta$  = Change  
 $\mu$  = Micro  
 $\mu$ V = micro volts  
 $^{99m}\text{Tc-ECD}$  = technetium ethyl-cysteinate-dimer  
 $^{99m}\text{Tc-HMPAO}$  = technetium hexa-methyl-propylene-amine-oxime

## ACKNOWLEDGEMENTS

I am deeply grateful to Professor Louis Lemieux, my principal supervisor, and Professor John S. Duncan, my secondary supervisor, for their warm welcome in the research groups, inspiring guidance and mentorship, and constant support throughout the course of this thesis. I am also thankful to Dr. David W. Carmichael, Dr. Roman Rodionov, Dr. Rachel Thornton and Dr. Serge Vulliemoz, who were my main companions and guides in the field of EEG-fMRI research and brought crucial scientific and methodological input in the EEG-fMRI studies. I am very grateful to Dave Gasston for designing the filter box for wall camera making simultaneous video-EEG-fMRI possible. Dr. Caroline Micallef very kindly provided her help and guidance for the anatomic localization of functional imaging maps and I am greatly thankful to her. I would like to thank Professor Mathias Koepp for his co-supervision in the cognition and epileptic activity study described in Chapter 10. I would like to thank to all other researchers of the Epilepsy Research Group whom I met during my time at the Epilepsy Society, Chalfont St. Peter: Dr. Maria Centeno, Jason Stretton, Vasily Kokkinos, Dr. Karin Rosenkrantz, Dr. Matteo Pugnaghi, Dr. Anna Vaudano, Suejen Perani, Dr. Silvia Bonelli, Dr. Christian Vollmar, Dr. Gavin Winston, Dr. Meneka Sidhu and Dr. Anja Haag. I had enthusiastic scientific exchanges and friendly chats with all.

The radiographers at the MRI unit, Epilepsy Society: Philippa Bartlett, Jane Burdett and Elaine Williams, offered their experience for high quality data acquisition and friendly collaboration. Peter Gilford very kindly solved all IT issues. The medical secretaries at Pearman house, Epilepsy Society and the medical staff at Gowers Assessment Unit, Epilepsy Society most graciously provided their support for recruiting patients for my research studies.

I am very thankful to Professor Karl Friston, from the Wellcome Trust Centre for Neuroimaging, for his guidance on methodological aspects of EEG-fMRI studies for seizures, and cognition and epileptic activity.

At the National Hospital for Neurology and Neurosurgery, Dr. Beate Diehl, Professor Matthew Walker and Catherine Scott together with the clinical team of the Telemetry ward were very helpful in discussing electroclinical findings of patients included in this work. Together with Mr Andrew McEvoy, the epilepsy neurosurgeon, they greatly facilitated the logistics and data collection for simultaneous intracranial-EEG-fMRI recordings for patients undergoing invasive presurgical evaluations. John Thornton, head MR physicist and the MR radiographers Lisa Strycharczuk, Catherine Green, Alison Duncan, Prashanth Kesara and Bruce Metheringham also played a key role in data collection for simultaneous intracranial-EEG-fMRI studies. Professor Sanjay Sisodiya, Dr. Fergus Rugg-Gunn, Dr. Dominic Heany and Dr. Sofia Eriksson very kindly provided me access to their patients for my research studies.

I would also like to thank both examiners of this thesis work, Prof. Mark Richardson and Prof. Xavier Golay, for their critical reading and helpful suggestions which improved the quality of this thesis.

Last but not the least, my work is indebted to the continuous loving support from my parents Chaudhary Manzoor-ul-Haq Javed and Nahid Javed, who always encouraged me to follow my endeavours in scientific and medical education, and love, support and motivation given to me by my wife Qurat-ul-Ain Alavi helped me to make best choices and complete my work.

## **FUNDING SOURCES**

During this PhD thesis, I was supported by an overseas scholarship for MS/MPhil Leading to PhD in Selected Fields Phase II, Batch II (10% seats) from Higher Education Commission Islamabad, Pakistan for the first three years. I am also thankful to Action Medical Research for the funding (AMR grant AP1163) provided to me for the fourth year. I acknowledge the financial support of the UK Medical Research Council (MRC grant G0301067) which funded the scalp EEG-fMRI research group. This work was undertaken at UCLH/UCL who receives a proportion of funding from the Department of Health's NIHR Biomedical Research Centers funding scheme. I am grateful to the Big Lottery Fund, Wolfson Trust and the Epilepsy Society for supporting the 3T MRI scanner at the Epilepsy Society.

## FOREWORD

This thesis investigates the haemodynamic networks associated with epileptic activity in the brain of persons with epilepsy. The scientific studies performed to understand this association and presented in this work are based on the combination of neurophysiologic (i.e., EEG) and neuroimaging (i.e., fMRI) methods utilizing their specific strengths. Individually each of these methods results from years of research into the methodological development and clinical application, a detailed description of which is beyond the scope of this thesis. References for further reading are provided throughout the work.

This work was made possible with the valuable contribution of several persons, working more or less closely with my specific projects, from the identification of the patients to the optimization of MR acquisition sequences and data storage. This work was performed under the umbrella of internal and external collaborations at UCL Institute of Neurology. The main scientific collaborations are acknowledged below and other collaborators are mentioned in acknowledgement section.

The first study (Chapter 5) describes the advances in EEG-fMRI data collection using simultaneous video recordings which can be used for the identification of epileptic events inside the MRI scanner. The second study (Chapter 6) shows that the sensitivity of EEG-fMRI studies for interictal activity can be increased by incorporating the information regarding physiological activities, obtained from simultaneous video recordings, into the models of fMRI data analysis. The third and fourth studies (Chapters 7 and 8) investigate the localisation of seizure related epileptic networks using simultaneous video-EEG-fMRI in comparison to the localisation provided by other non-invasive and invasive techniques. I describe the methodological developments in modelling seizures in the context of functional imaging data, and the clinical applications of these findings. Intracranial EEG is considered to be the gold standard for the localisation of epileptic focus / network in patients undergoing presurgical evaluation, however it has certain limitations and it would be very beneficial if these limitations are

addressed. The fifth study (Chapter 9) is a step in this direction investigating the localisation of epileptic networks associated with interictal epileptic discharges using simultaneous intracranial-EEG-fMRI as compared to the postsurgical outcome. In addition, loss of awareness during epileptic activity has major social and clinical consequences and the sixth study (Chapter 10) focuses on this issue describing the changes in the working memory related functional networks in the presence of epileptic activity during the performance of working memory task using simultaneous video-EEG-fMRI. In Chapter 11, I discuss the future applications and perspectives of EEG-fMRI.

# **OUTLINE AND STATEMENT OF PERSONAL CONTRIBUTION**

This thesis is structured as follows:

## **SECTION 1: LITERATURE REVIEW**

Chapter 1 presents key historical aspects of Epilepsy, highlighting the importance of seizure semiology as a major tool for the diagnosis of seizures since the earliest times.

Chapter 2 describes the current understanding of the mechanism of seizure generation, classification scheme of seizures and epilepsy, investigation tools applied to diagnose seizures and possible treatment options.

Chapter 3 summarises the fMRI methods that are important to understand the following work which is based on simultaneous EEG and fMRI. I discuss the neurophysiological basis of fMRI signals and the methodological considerations of investigating epileptic discharges using EEG-fMRI with a review of clinical applications in patients with epilepsy.

## **SECTION 2: EXPERIMENTAL STUDIES**

Chapter 4 describes the common methods used in the most experimental studies described in this thesis.

Chapters 5-10 describe experimental studies.

In Chapter 5, I present my work on combining synchronised video recording with simultaneous EEG and fMRI. In this first application of simultaneous video and EEG-fMRI (video-EEG-fMRI), I evaluate the effects of video recording inside the MRI scanner room on fMRI data quality and vice versa. I also show that this additional information on behaviour, obtained from video recordings during EEG-fMRI, can be helpful in fMRI data analysis.

In Chapter 6, I show that how the sensitivity of video-EEG-fMRI studies for interictal epileptic discharges can be improved by modelling the different



physiological activities performed by the patients during resting video-EEG-fMRI. I identify these physiological activities video-EEG and use them as confounds in the fMRI data analysis design matrix.

In Chapter 7, I present my work on modelling seizures recorded during video-EEG-fMRI, by dividing them into different phases. I compare the localisation of ictal networks during different phases with that of intracranial EEG providing evidence that video-EEG-fMRI may be helpful in localising the seizure onset zone.

In Chapter 8, I describe haemodynamic changes taking place prior to the seizure onset on scalp EEG, highlighting the possible mechanism underlying seizure generation. Here, I would like to thank Teresa Murta for her help in using Matlab for making Figures.

In Chapter 9, I show my work on mapping epileptic networks using simultaneous intracranial EEG-fMRI. I compare the localisation of interictal epileptic discharges with the surgical resection and postsurgical outcome, showing that the localisation provided by intracranial EEG-fMRI may have a predictive value for postsurgical outcome.

In Chapter 10, I present my work on the interaction between epileptic discharges and haemodynamic networks active during performance of a highly demanding task. I demonstrate that the presence of epileptic discharges during a working memory task may alter the working memory related haemodynamic network.

### **SECTION 3: DISCUSSION AND CONCLUSION**

In this section, I discuss future research directions and suggestions to improve current methodological constraints in the context of principal experimental findings.

## **PUBLICATIONS ASSOCIATED WITH THIS THESIS**

Parts of the introduction (Chapters 1 and 3) and experimental studies (Chapters 5, 6 and 10) presented in this thesis have been published as first author articles in international peer-reviewed scientific journals:

### **Chapter 1**

- **Chaudhary UJ**, Duncan JS, Lemieux L. A dialogue with historical concepts of epilepsy from the Babylonians to Hughlings Jackson: Persistent beliefs. *Epilepsy Behav.* 2011 Jun; 21(2):109-14.

### **Chapter 3**

- **Chaudhary UJ**, Duncan JS, Lemieux L. Mapping Haemodynamic Correlates of Seizures using fMRI: A Review. *Hum Brain Mapp.* 2011 Nov 14. doi: 10.1002/hbm.21448. [Epub ahead of print].

### **Chapter 5**

- **Chaudhary UJ**, Kokkinos V, Carmichael DW, Rodionov R, Gasston D, Duncan JS, Lemieux L. Implementation and evaluation of simultaneous video-electroencephalography (Video-EEG) and functional magnetic resonance imaging (fMRI). *Magn Reson Imaging.* 2010 Oct; 28(8): 1192-9.

### **Chapter 6**

- **Chaudhary UJ**, Rodionov R, Carmichael DW, Thornton RC, Duncan JS, Lemieux L. Improving the sensitivity of EEG-fMRI studies of epileptic activity by modelling eye blinks, swallowing and other video-EEG detected physiological confounds. *Neuroimage.* 2012 Jul 16; 61(4): 1383-93.

## Chapter 10

- **Chaudhary UJ**, Centeno M, Carmichael DW, Vollmar C, Rodionov R, Bonelli S, Stretton J, Pressler R, Eriksson SH, Sisodiya S, Friston K, Duncan JS, Lemieux L, Koepp M. Imaging the interaction: epileptic discharges, working memory and behaviour. *Hum Brain Mapp.* 2012 Jun 19. doi: 10.1002/hbm.22115. [Epub ahead of print].

In addition to the experimental studies mentioned above in Chapters 5-10, I was involved as co-investigator in the following studies and publications:

- Thornton R, Vulliemoz S, Rodionov R, Carmichael DW, **Chaudhary UJ**, Diehl B, Laufs H, Vollmar C, McEvoy AW, Walker MC, Bartolomei F, Guye M, Chauvel P, Duncan JS, Lemieux L. Epileptic Networks in Focal Cortical Dysplasia revealed using EEG-fMRI. *Ann Neurol.* 2011 Nov; 70(5): 822-37.

Personal contribution: I participated in data acquisition, EEG-fMRI analysis and interpretation of the results for some of the patients, and writing of the article.

- Katschnig P, Schwingenschuh P, **Chaudhary UJ**, Edwards MJ, Lemieux L, Walker MC, Bhatia KP. Paroxysmal limb dyskinesia induced by weight: an unusual case of cortical reflex seizures. *Mov Disord.* 2011 Nov; 26(13): 2438-9.

Personal contribution: I participated in EEG-fMRI data acquisition, analysis and interpretation of the results and writing of the article.

- Centeno M, Feldmann M, Harrison NA, Rugg-Gunn FJ, **Chaudhary U**, Falcon C, Lemieux L, Thom M, Smith SJ, Sisodiya SM. Epilepsy causing pupillary hippus: an unusual semiology. *Epilepsia.* 2011 Aug; 52(8):e93-6.

Personal contribution: I participated in EEG-fMRI data acquisition, analysis and interpretation of the results and writing of the article.

I also contributed in writing part of a book chapter on EEG-fMRI for seizures:

- Walker MC, Chaudhary UJ and Lenz D. EEG-fMRI in adults with focal epilepsy. Mulert, C, Lemieux, L (Eds), EEG-fMRI - Physiological Basis, Technique, and Applications. Berlin Heidelberg: Springer, 2009, 309-26.

The posters I presented in conferences have been published in peer-reviewed journals as conference proceedings:

- **Chaudhary UJ**, Carmichael DW, Rodionov R, Vulliemoz S, Thornton RC, Pugnaghi M, Micallef C, McEvoy AW, Scott CA, Diehl B, Walker MC, Duncan JS, Lemieux L. Mapping the irritative zone using intracranial EEG-fMRI and comparison with postsurgical outcome. *Epilepsia*. 2012 Sep;53(s5):14. *Conference Proceedings*.
- Pugnaghi M, Carmichael DW, Vaudano V, **Chaudhary UJ**, Benuzzi F, Di Bonaventura C, Giallonardo AT, Rodionov R, Walker MC, Duncan JS, Meletti S, Lemieux L. The effect of generalized spike and wave discharge duration and IGE sub-syndrome on brain networks as revealed by EEG-fMRI. *Epilepsia*. 2012 Sep;53(s5):58. *Conference Proceedings*.
- Vaudano AV, Pedreira C, Thornton R, **Chaudhary U**, Vulliemoz S, Laufs H, Rodionov R, Quiñero Quiroga R, Lemieux L. A novel method for the classification of interictal EEG abnormalities in partial epilepsy: an EEG-fMRI validation study. *Epilepsia*. 2012 Sep;53(s5):62. *Conference Proceedings*.
- Carmichael DW, Hu L, **Chaudhary UJ**, Iannetti G, Vulliemoz S, Rodionov R, Thornton R, Lemieux L. Intracranial EEG-fMRI in epilepsy: a preliminary approach to modelling very frequent spike discharges. *Epilepsia*. 2012 Sep;53(s5):200. *Conference Proceedings*.
- **Chaudhary UJ**, Rodionov R, Carmichael DW, Thornton R, Diehl B, Walker M, Duncan JS, Lemieux L. Mapping preictal and ictal haemodynamic changes for refractory focal seizures. *Epilepsy Curr*. 2012 Jan-Feb; 12(s1): 208. doi: 10.5698/1535-7511-12.s1.1. *Conference Proceedings*.
- **Chaudhary U J**, Centeno M, Carmichael DW, Vollmar C, Rodionov R, Bonelli S, Stretton J, Pressler R, Eriksson S, Sisodiya S, Duncan JS, Lemieux L, Koepp M. Imaging the interaction: working memory, epileptic

discharges and behavioural performance. *Epilepsia*. 2011 Aug;52(s6):174. *Conference Proceedings*.

- Pugnaghi M, **Chaudhary UJ**, Rodionov R, Diehl B, Mc Evoy A, Walker M, Duncan JS, Carmichael DW, Lemieux L. Hippocampal activation in simultaneous intracranial EEG-fMRI: A case report. *Epilepsia*. 2011 Aug;52(s6):179. *Conference Proceedings*.
- **Chaudhary UJ**, Kokkinos V, Rodionov R, Carmichael DW, Vulliemoz S, Thornton R, Gasston D, Diehl B, Duncan JS, Lemieux L. Implementation of video-EEG-fMRI to investigate epileptic activity. *Epilepsia*. 2009. 50:72-73. *Conference Proceedings*.

## CONFERENCE POSTERS AND TALKS RELATED TO THIS THESIS

- Mapping the irritative zone using simultaneous icEEG-fMRI and comparison with postsurgical outcome. 10<sup>th</sup> Annual Meeting European Congress on Epileptology (Sep 2012), London, UK.
- Mapping preictal and ictal haemodynamic changes for refractory focal seizures. 65<sup>th</sup> Annual Meeting American Epilepsy Society (Dec 2011), Baltimore, USA.
- Imaging the interaction: working memory, epileptic discharges and behavioural performance. 29<sup>th</sup> International Epilepsy Congress (Sep 2011), Rome, Italy.
- Imaging the interaction: working memory, epileptic discharges and behavioural performance. UCL Neuroscience Symposium 2011, University College London, UK.
- Hippocampal activation in simultaneous intracranial EEG-fMRI: A case report. 29<sup>th</sup> International Epilepsy Congress (Sep 2011), Rome, Italy.
- Effect of modelling physiological regressors in ictal video-EEG-fMRI: a GLM based analysis. Human Brain Mapping 2010, Barcelona, Spain.
- Effect of modelling physiological regressors in ictal video-EEG-fMRI: a GLM based analysis. Queen Square Symposium 2010, UCL Institute of Neurology, Queen Square, UK.
- Implementation of video-EEG-fMRI to investigate epileptic activity, American Epilepsy Society Conference 2009, Boston, USA.
- Investigation of seizures using simultaneous video-EEG-fMRI. International League against Epilepsy-UK Chapter, 2009, Sheffield, UK.
- Evaluation of simultaneous video, electroencephalography (EEG) and functional magnetic resonance imaging (fMRI) for future studies of epileptic events. Queen Square Symposium 2009, UCL Institute of Neurology, Queen Square, UK.

## **AWARDS**

- UCL CNT Early Career Investigator in Neuroimaging Techniques Award for 2012
- Oral presentation in PhD student category. Queen Square Symposium 2010, UCL Institute of Neurology, Queen Square London.
- Overseas Scholarship for Masters Leading to PhD. Higher Education Commission Islamabad, Pakistan. From Sep 2007 to Sep 2011.

## SECTION 1: LITERATURE REVIEW

### Chapter 1: Epilepsy in historical perspective<sup>1</sup>

Epilepsy is one of the few neurological disorders to be recognised in Antiquity. Thoughts on the aetiology of epilepsy have evolved from affliction of evil spirits and bad omens to an organic disease of the brain. In this chapter the course of history is followed from Babylonians to the twentieth century mapping the conceptual development of epilepsy.

#### 1.1 Pre-Greek and Classical Greek Era (Before 500 BC - 400 AD)

The earliest account of epilepsy comes from a Babylonian Tablet (1067-1046 BC) (Figure 1.1) describing symptoms and supernatural aetiology [Wilson and Reynolds 1990; Reynolds and Wilson 2008]. Other early descriptions of disease recognisable as epilepsy come from Ayurvedic collection of treaties “Charaka Samhita” (400 BC) [WHO Media centre. 2001], traditional Chinese Wade system [Lai and Lai 1991] and Persian text on health, “Avesta” (600 BC) [Vanzan and Paladin 1992]. These early descriptions of a condition analogous to epilepsy run independently and in parallel in geographically separate areas.

##### 1.1.1 Theories about Epilepsy

The Greeks used the term epilepsy (meaning: ‘to seize’, ‘to attack’) because they thought that the disease was caused by an attack from a demon or god [Temkin 1971; Todman 2008a]. An anonymous monograph entitled “On the Sacred Disease” (contentiously related to the Hippocratic collection of manuscripts) refuted the divine character of epilepsy and supernatural means for the treatment. Hippocrates viewed epilepsy as a disease of brain without any associated divine nature, which happens due to the excess of phlegm entering into the blood [Hippocrates. 1923; Temkin 1971; Magiorkinis *et al.* 2010].

---

<sup>1</sup> This chapter forms the basis of the article [Chaudhary *et al.* 2011].



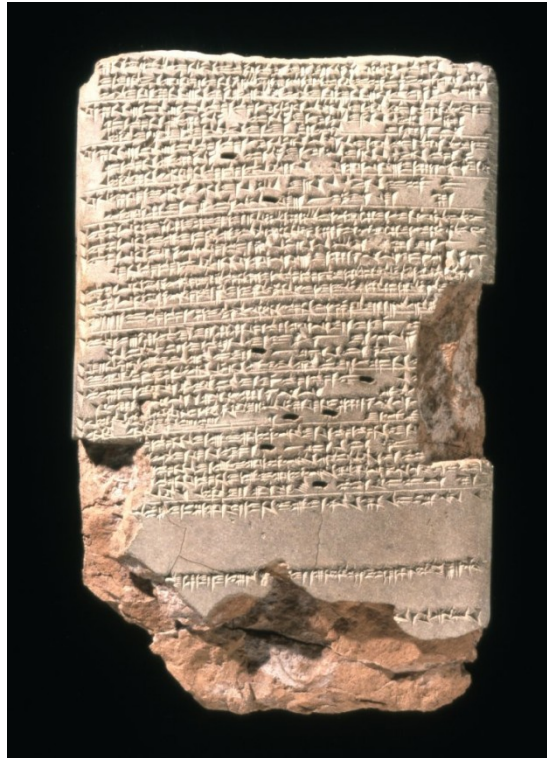


**Figure 1.1: Epilepsy tablet**

Epilepsy tablet (47753) from the Babylonian collection of British Museum, written in Neo-Babylonian script dated middle of the first millennium BC approximately. This Tablet is part of a medical diagnostic series “Sakikku (meaning: all diseases)” which consists of 40 tablets in total. In this tablet epilepsy is called as “Sakikku miqtu” (meaning: falling disease). The aetiology of epilepsy is presumed to be the effect of demons and ghosts, and features of generalized seizures, gelastic seizures, nocturnal epilepsy, chronic epilepsy and post ictal states are described. This is by far the first written account of epilepsy [Wilson and Reynolds 1990; Reynolds and Wilson 2008]. Image © The Trustees of the British Museum

The religious literature mixed possessions and epilepsy under one umbrella. The description of Jesus driving out an unclean spirit from a boy with epilepsy promoted the spiritual nature of epilepsy. However, physicians noted that epileptics lost consciousness during convulsions whereas those who were possessed were partly conscious during convulsions. Galen separated idiopathic epilepsy: resulting from the obstruction of cerebral ventricles by phlegmatic and melancholic humors, from sympathetic epilepsy: originating in other body parts with a subsequent involvement of brain. Meninges, contusions and mechanical factors were other implicated causes of epilepsy [Temkin 1934; DRABKIN 1951; Temkin 1971; Todman 2008b].

### 1.1.2 Clinical Concepts

Epilepsy was considered to be a chronic and hereditary disease with unpredictable and repetitive attacks with impairment of leading functions affecting men more commonly than women [Celsus 1938], (a trend that persists today in certain subtypes of epilepsy [Christensen *et al.* 2005]). External factors: climate, geographical location, food habits, sexual activity and abstinence, alcohol and physical exercise were noted to trigger attacks [Hippocrates. 1923; Temkin 1971]. Galen introduced the concept of aura (Greek, meaning: breeze) for the first time and identified various types; however, loss of consciousness and falling to the ground were the two main clinical features. Apoplectic attacks were distinguished from convulsions; stillness, paleness and unresponsiveness in the former and jerky movements, discharge of urine, excrements and semen, and frothing at the mouth in the latter [Temkin 1971]. A typical epileptic attack was divided into: manifestation (insensibility and convulsions), abatement (discharge of urine, excrements and semen and frothing at mouth) and cessation (physical and psychic discomfort) [Temkin 1971; Temkin 1985; Garcia-Albea 2009].

### 1.1.3 Diagnosis and Treatment

Clinical observation and description of attacks were pivotal for the diagnosis. Attacks were provoked by rotating potter's wheel before the eyes, fumigation with kindled jet (a mineraloid) and bathing new born with undiluted wine.

Magicians used carystian stone (some kind of asbestos), amulets, lichen of horses, camel's hair, gall and rennet of seal, human blood and bones and fixing iron nails in the ground at the site of the first epileptic fit to ward off epilepsy. In contrast,

Hippocrates considered that magical practices were immoral and suggested treating epilepsy before becoming chronic, especially sympathetic epilepsy in mentally fit patients [Hippocrates. 1923;Temkin 1971].

Galen treated idiopathic epilepsy by bleeding lower arm or thigh and using purgatives; and sympathetic epilepsy by binding the body part first affected during attacks and following a diet and exercise plan [Temkin 1934;Green 1951]. Other proposed treatments included venesection, trephining and cauterization of skull [Temkin 1971;Garcia-Albea 2009].

## 1.2 Middle-Ages around the World: 401-1500 AD

During Sui dynasty Chinese scholars classified seizures on the basis of the age of onset, clinical symptoms and presumed aetiology [Lai and Lai 1991]. As for the Greek tradition, the effects of the moon on the sufferer gave epilepsy the name lunacy in Byzantine and Latin literature. Epilepsy continued to be known as infectious till 16<sup>th</sup> century when Fernelius dispelled this notion [Temkin 1971;Diamantis *et al.* 2010].

Three main categories of attacks were proposed: epileptic (originating from brain), analeptic (originating from stomach) and cataleptic (originating from other parts of body). Fever was associated with catalepsy and frothing with epilepsy. However, later in the medieval period these three categories were confused under one umbrella “Falling Evil” [Temkin 1971;Langslow 2000;Engel 2007].

Muslim scholars translated the Latin work into Arabic and incorporated the Islamic principles of medical hygiene from “Quran” and “Tibb-al-Nabi” into Greek theories. Ibn-Abbas explained that compressive skull fractures resulted in epilepsy. Avicenna, in his book “The Canon of Medicine”, discussed the incurable nature of hereditary epilepsy and differentiated between epilepsy from brain and epilepsy from nerves [Temkin 1971;Bakhtiar *et al.* 1999;Browne 2001;Diamantis *et al.* 2010].

The diagnosis and treatment of epilepsy continued to follow the Greek literature. Al-Razi advocated the use of “tariaq” (mixture of laurel seeds, myrrh, aristolochia and Greek gentian) to cure epilepsy. Avicenna wrote extensively on tailoring treatments according to the individual needs, regularising eating habits and avoiding seizure provoking factors such as: shrill noises, bright lights and lack of sleep [Vanzan and Paladin 1992;Bakhtiar *et al.* 1999]. Pre-Columbian American

physicians used plants such as “Carlo-Santo” root and “Mechoacan” root for treating epilepsy [Elferink 1999].

### **1.3 Western Renaissance (1501-1700 A.D.)**

The theories proposed during this period revolved around various chemical particles causing epilepsy. Thomas Willis explained that particles in the blood called “spasmodi copula” explode the animal spirit in the middle part of brain, resulting in a convulsion. Marcello Malpighi viewed the cerebral cortex as a mass of glands and suggested that arsenical particles in the nervous juice irritate cerebral fibres causing epileptic attack.

Contrary to the prevalent beliefs, an effort was made to separate epilepsy from unnatural causes, and features such as failure of rational treatment, speaking in foreign languages, opened eyes and reaction of pupils to the light during attacks were identified as signs of possession. Charles Le Pois refuted the existence of sympathetic epilepsy and proposed that all epilepsies originated from the brain and symptoms in distant parts of the body were actually initial symptoms before spread [Temkin 1971;Eadie 2003;Diamantis *et al.* 2010].

### **1.4 Enlightenment (1701-1815)**

This is the era of systematic questioning of ancient dogma and the emergence of rationalism. Giorgio Baglivi elaborated a mechanical theory that the disturbed elastic equilibrium of fibres in dura mater was a cause of epilepsy. Alternatively, Stahl refuted the role of mechanical particles in epilepsy and proposed that symptomatic convulsions may occur in other diseases where as epileptic convulsions occur independently [Temkin 1971;Schouten 1974;Cappelletti 2000;Lama and vanWijngaarden 2002].

Crucially, physicians fought against superstitions and emphasized the importance of provoking factors. Samuel Tissot disapproved the influence of moon and pregnancy on epilepsy and formally identified absences as a seizure type for the first time. However, some new superstitions were developed such as masturbation as a causative factor for epilepsy, and clitoridectomy and castration were performed until 1881 when Gowers dispelled the role of castration in curing epilepsy [Temkin 1971;Cappelletti 2000;Lama and vanWijngaarden 2002].

William Cullen differentiated grand mal and petit mal seizures and sub-classified epilepsy: epilepsia cerebialis (from brain), epilepsia sympathetic (from manifest

causes) and epilepsia occasionalis (from manifest irritation) [Gowers 1881;Duffy 1963;Temkin 1971;McGirr 1991;Karbowski 2001].

### **1.5 Early Nineteenth Century - Pre-Hughlings Jackson**

In the nineteenth century specialist hospitals for epilepsy were established in England (National Hospital for the Paralysed and Epileptic, Queen Square, London), Germany (Heil-und Pflegeanstalt für Schwachsinnige und Epileptische, Stetten) and America. Additionally, the terminology for different seizure types was described: “le grand mal” (severe attacks with loss of consciousness and convulsions), “le petit mal” (slight attacks), absence seizures (seizures without physical symptoms and inability to respond) and “état de mal” (seizures occurring uninterruptedly and continuously; status epilepticus in today’s epileptology).

Robert Todd ascribed a primary role to cerebral hemispheres and quadrigeminal bodies in seizures and discussed epileptic hemiplegia after seizures [Todd 1855;McIntyre 2008]. The weakness in hemiplegic seizures was later termed as “Todd’s paralysis”. In his thesis Horing discussed the incompletely developed seizures with dreamy state behaviour, which were later named as psychomotor symptoms by Griesinger [Sigerist 1941;Schott. 1968;Temkin 1971;Lishman *et al.* 1998;Eadie 2010].

In England, Marshall Hall proposed a theory describing “centric and eccentric epilepsy”, inculcating a new interest in reflex nature of epilepsy [Temkin 1971;Manuel 1996]. Later, Brown Sequard in agreement with Hall investigated blockade of reflex arc, by applying ligatures or sectioning nerves, as a possible treatment for seizures [Koehler 1994] and Astley Cooper’s experiments on animals established the fact that change in blood flow to the brain can lead to seizures [Nuland 1976].

Here again the description of clinical semiology was the cornerstone for diagnosis. Administration of Bromide and Iodide of potassium was claimed to be very successful at reducing seizures by physicians. It became so popular that 2.5 tons of Bromide was used every year at the National Hospital in London [Temkin 1971;Pearce 2002]. Victor Horsley (Figure 1.2) at the National Hospital in London and other neurosurgeons from across the Europe revived surgery as a cure for epilepsy and published the results of their successful interventions and laid down the foundations of modern epilepsy surgery [Smith 1852;Billings 1861;Temkin 1971].

### 1.6 Era of Hughlings Jackson (1835-1911)

Epileptology in the latter part of nineteenth century and early part of the twentieth century can truly be named after Hughlings Jackson (Figure 1.2). He proposed philosophical explanations, combining pathology (from neuroanatomical dissections) with clinical symptoms. He defined seizures as occasional, sudden, excessive, rapid and local discharges of grey matter lesions analogous to hemiplegia resulting from locally destroying lesions. He explained that seizures spread from one part to other parts of brain through ascending and descending fibres. He gave utmost importance to lesion localisation for understanding the mechanism of convulsions and labelled the first symptom as “the signal symptom.” He also proposed that grey matter in cerebral cortex is the seat for epilepsy, but did not disregard the role of grey matter in corpus striatum. Hughlings Jackson divided the brain theoretically into three levels; lowest at pontobulbar, middle at sensorimotor cortex and the highest at frontal lobes from where epilepsy started when consciousness was lost before generalized convulsions.

Hughlings Jackson explained the mechanism of cortical spread of seizures marching from one part to the other parts of body, which were previously described by Bravais and Bright and later these seizures were called as Jacksonian epilepsy. He described aphasia in epilepsy (epileptic aphemia) ascribing it to fluctuations in blood supply.

Jackson also elaborated on seizures starting with a dream like state without any motor signs and automatic behaviours, and anatomically localised it to gyrus uncinatus. Jackson along with David Ferrier and William Gowers (Figure 1.2) was the founding father of a specialist epilepsy centre in the Buckinghamshire countryside, 30km west of London, in 1894 [Head 1921; Jackson JH 1958; Tyler 1984; Swash 2005; Khalsa *et al.* 2006; Reynolds 2007; Reynolds and Andrew 2007; Silvester 2009; York and Steinberg 2009].

The anatomical description of conductive fibres by David Ferrier verified Jackson’s theory about partial epilepsy that localised convulsions are a result of localised injuries of cerebrum and may spread if the discharge involved wider area. William Gowers further elaborated that a mere absence of any visible brain abnormality does not mean that the patient would not develop epilepsy rather it is the absence of an active brain pathology which determines whether the patient

will develop epilepsy. Gowers described that epileptic convulsions were more coordinated where as hysterical attacks had quasi-purposive movements, though some difficult cases fall in the grey area between hysteria and epilepsy [Gowers 1881;Temkin 1971].

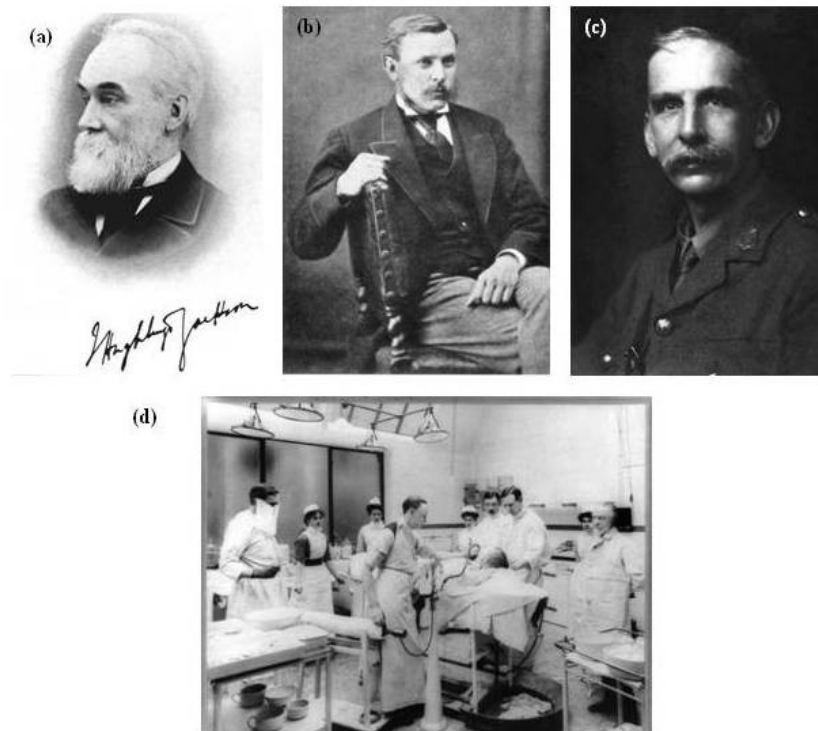


**Figure 1.2: Eminent British neuroscientists in the era of Hughlings Jackson**

(a) John Hughlings Jackson (1835-1911), (b) William Gower (1845-1915) and (c) Victor Horsley (1857-1916). (d) Victor Horsley performing surgery at National Hospital in London, UK.

“Image courtesy of the Queen Square Library, Archive and Museum. Copyright National Hospital for Neurology & Neurosurgery



### **1.7 Century of New Advancements**

The twentieth century can be named the century of new advancements as far as epilepsy is concerned. The term epileptologist was coined by William Spratling in 1904 for the person specializing in epilepsy [Dasheiff 1994]. The International league against epilepsy (ILAE) was founded in 1909 and worked towards unification and standardization of epilepsy nomenclature [Meinardi H 2009].

Progress in the field of neurophysiology led to the recording of brain rhythms from the surface of skull and directly from the brain (depth recordings) [Niedermeyer and Lopes da Silva 2005]. Advancements in physics and radiology set in motion the possibilities to view structures inside the skull cavity without opening it with computed tomography (CT) scan (by Sir Godfrey Hounsfield in early 1970s) [Richmond C 2004], magnetic resonance imaging (MRI) [Edelstein *et al.* 1980;Lauterbur 1989] and many other imaging tools which are discussed in Chapter 2.

### **1.8 Perspectives and conclusion**

It can be said that the history of the concept epilepsy is intrinsically linked to our understanding of the working of the mind. People have sought help from religion, magic and science to cure epilepsy. In the quest to unravel the truth behind epilepsy, scientists and physicians have been successful at times to suggest mechanisms closer to today's understanding of the condition. However, it is important to note that since antiquity to date the diagnosis of epilepsy has heavily depended on thorough investigation of seizure types and their semiological description.

## Chapter 2: Epileptology: where do we stand?

### 2.1 Definition of seizure and epilepsy

The ILAE published a glossary of descriptive terminology for ictal phenomenology [Blume *et al.* 2001] and defined an epileptic seizure as a manifestation of epileptic (excessive and/or hyper-synchronous), usually self-limited activity of neurons in the brain; epileptic disorder as “a chronic neurologic condition characterized by recurrent epileptic seizures”; and epilepsies as “those conditions involving chronic re-current epileptic seizures that can be considered epileptic disorders”.

These definitions were updated [Fisher *et al.* 2005] whereby epileptic seizure was defined as “a transient occurrence of signs and/or symptoms due to abnormal excessive or synchronous neuronal activity in the brain”, and epilepsy was defined as “disorder of the brain characterized by an enduring predisposition to generate epileptic seizures and by the neurobiological, cognitive, psychological, and social consequences of this condition”.

It has been argued that this updated definition will make single provoked seizures such as single febrile seizures without consequent electroclinical abnormalities and acute symptomatic seizure to come under the diagnosis of epilepsy, thus increasing the therapeutic and epidemiological burden unnecessarily [Beghi *et al.* 2005]. On the other hand, authors of the definition [Fisher *et al.* 2005] have explained that the current definition is a mechanistic definition of seizures and will not affect the diagnosis of epilepsy since single febrile seizure without consequent electroclinical abnormalities and acute symptomatic seizure do not meet the proposed definition of epilepsy.

### 2.2 Burden of epilepsy

The incidence of first unprovoked seizure ranges from 50 to 70 per 100,000 in the developed countries [Hauser and Beghi 2008]. The incidence of epilepsy in developed countries is around 50/100000/year, in comparison it is much higher (100-190/100000/year) in the resource poor countries [Sander and Shorvon 1996]. The life time prevalence of seizures is found to be between 2 and 5% [Sander and Shorvon 1996] and the life time prevalence of epilepsy in general ranges from 2.7 to 12.4 per 1000 in western countries [Ngugi *et al.* 2010]. The

prevalence of active epilepsy in western countries ranges from 2.3 to 10.3 per 1000 [Ngugi *et al.* 2010].

Partial seizures occur in 55% of patients and generalized seizures in 45% of patients in the developed countries [Kotsopoulos *et al.* 2002]. In contrast, generalized seizures predominate (Pakistan= 80%, Turkey= 65.4%) in resource poor countries [Aziz *et al.* 1997]. The proportion of patients with partial seizures changed from 34% (diagnosed clinically) to 53% when diagnosed on the basis of electroclinical data [Nicoletti *et al.* 1999].

In the UK, around 30000 people develop epilepsy every year [MacDonald *et al.* 2000;Duncan 2007] with an incidence of 46/100,000/year and a life time prevalence of 4/1000 [MacDonald *et al.* 2000].

### **2.3 Aetiology of epilepsy**

Over the last 20 years the proportion of patients with unknown (cryptogenic and idiopathic 45% to 67% [Oun *et al.* 2003;Olafsson *et al.* 2005]) causes of epilepsy have remained similar in different studies [Sander *et al.* 1990;Benn *et al.* 2008]. The Community based studies [Sander *et al.* 1990;Hauser *et al.* 1993;Forsgren *et al.* 1996] have shown that the major causes of epilepsy are: cerebrovascular diseases (11-21%), head trauma (2-6%), brain infections (0-3%), neoplasms (4-7%) and idiopathic/cryptogenic (45-65%). Other causes also include neurodegenerative diseases and learning disabilities [Sander *et al.* 1990;Benn *et al.* 2008]. Considering the importance of understanding the causes of epilepsy in the management of epilepsy, it has been proposed that aetiology should be one axis of ILAE classification. An aetiological classification of epilepsy enlisting the subclasses on the basis of varying aetiologies has also been suggested [Shorvon 2011a;Shorvon 2011b].

Large neuropathological studies performed on patients undergoing epilepsy surgery have helped to understand the underlying aetiologies of refractory epilepsy. These include: hippocampal sclerosis (HS: 35%), tumours (gangliogliomas, dysembryoplastic neuroepithelial tumours (DNET: 27%), malformations of cortical development (MCD: 13%, including focal cortical dysplasia (FCD) and polymicrogyria), vascular malformations (6%, including arterio-venous malformations (AVM) and cavernomas), ischemic or traumatic brain injuries (5%) and encephalitic lesions (2%) [Blumcke 2009]. Around 4% of

patients had dual pathologies and no structural lesions were seen in 7% of patients [Blumcke 2009].

Recent developments in the field of genetics in epilepsy have also helped to identify genetic aetiologies for some previously idiopathic and cryptogenic epilepsy. When seizures are the main symptom of the disease, epilepsy can be due to a single gene disorder (e.g., progressive myoclonic epilepsies, benign familial neonatal convulsions, autosomal dominant nocturnal frontal lobe epilepsy and familial temporal lobe epilepsy); or complex inheritance pattern (e.g., juvenile myoclonic epilepsy, childhood absence epilepsy and idiopathic partial epilepsies). On the other hand, seizures can be part of a symptom complex defining a syndrome with an underlying single gene disorder (e.g., tuberous sclerosis, neurofibromatosis type I, malformation of cortical development) or a chromosomal abnormality (e.g., Down syndrome, Fragile X syndrome, ring chromosome 20) [Shorvon 2011b].

## **2.4 Mechanism of seizure generation**

The mechanisms underlying epilepsy have been investigated in-vitro and in-vivo experimental studies over the last 60 years. The proposed mechanisms can be widely divided into two main categories on the basis of epileptic activity type: 1) absence seizures, and 2) focal epileptic activity.

### **2.4.1 Absence seizures**

In 1941, Jasper and Kershman proposed that absence seizures have a subcortical origin because no evidence was found for a cortical focus on electroencephalography (EEG). The stimulation of intralaminar thalamus at 3Hz produced a 3Hz spike and wave discharge (see Appendix 1) on EEG with a behavioural correlate similar to absence seizures [Meeren *et al.* 2005] and Penfield in 1952 introduced the concept of a centrencephalic mechanism for absence seizures [Penfield and Jasper 1954]. At the same time, Gibbs and Gibbs and Bennett and Gloor performed experiments in patients with absence seizures suggesting a leading role of cortex in the generation of absence seizures [Meeren *et al.* 2005]. The availability of depth intracranial recordings in patients with absence seizures (no longer performed) and the advanced signal processing techniques further consolidated the concept of the driving role of the cortex by

revealing latency in the recruitment of thalamus during absence seizures [Bancaud 1969].

Gloor and colleagues went on to perform experiments on feline penicillin generalized epilepsy model, showing that an hyperexcitable cortex is prerequisite to respond to afferent thalamocortical volleys producing spike and wave discharges of absence seizures, thus proposing corticoreticular theory [Gloor 1968;Gloor 1969]. In 1991 Buzsaki investigated the thalamocortical mechanism of spontaneous spike and wave discharges and intrathalamic network using unit recordings in rats. He showed that reticular thalamic nucleus has pacemaker characteristic and local high voltage spindle field potentials start a few cycles earlier than cortex proposing a thalamic clock model for absence seizures [Buzsaki 1991] confirmed by others in rat models [Avanzini *et al.* 1992].

Meeren [Meeren *et al.* 2002] argued that the cortical recordings in earlier studies were performed at sites distant from the actual cortical focus. It was proposed that both functionally intact thalamus and cortex are prerequisite for producing spike and wave discharges in absence seizures. Further, the cortico-cortical, intra-thalamic and cortico-thalamic relationships were quantified, using advanced signal analysis methods, and a consistent cortical focus was found in perioral region of somatosensory cortex to lead in the first 500ms as compared to thalamus.

Further evidence to the theory that a cortical focus is responsible for the initiation of absence seizures is provided recently in the studies using high density EEG [Tucker *et al.* 2007;Tucker *et al.* 2009] and functional imaging techniques [Vaudano *et al.* 2009].

At the cellular level, spike and wave discharges represent inhibitory post synaptic potentials (IPSPs) in the cortex and thalamus mediated by the  $\gamma$ -amino butyric acid (GABA) receptors. Physiological spindle waves are produced by thalamus during sleep and blockade of GABA<sub>A</sub> receptors transforms the spindle waves into strong and synchronous spike and wave discharges at 2-3Hz through disinhibition from other thalamic reticular neurons and activation of GABA<sub>B</sub> mediated IPSPs [Huguenard and Prince 1994;Bal *et al.* 1995a;Bal *et al.* 1995b;Kim *et al.* 1997;Sanchez-Vives *et al.* 1997;Sanchez-Vives and McCormick 1997;Steriade *et al.* 1998]. Similarly, the topical application of GABA<sub>A</sub> receptor antagonist on the cortex also resulted in the transformation of spindle waves into spike and

wave discharges as long as the corticothalamic network is intact [Gloor 1968;Gloor 1969;Gloor *et al.* 1990]. Other cellular mechanisms which participate in the generation of spike and wave discharges also include the loss of  $K^+$  currents which regulate the burst length in thalamus or the increase in low threshold  $Ca^{2+}$  currents [Tsakiridou *et al.* 1995].

These spike and wave discharges also require both anatomic connections and physiologically intact networks for fast synchronisation across thalamus and cortex and appear generalized from the onset [Gloor *et al.* 1990;Contreras *et al.* 1996;Contreras and Steriade 1997]. From the above discussion, it appears that both cortex and thalamus have been identified to have driving role in the generation of spike and wave discharges of absence seizures at different times. Nonetheless, functionally intact cortex and thalamus are required to produce and sustain spike and wave discharges.

#### **2.4.2 Focal epileptic activity**

In order to comprehend the mechanism of focal seizure generation, it is important to understand the underlying mechanism of interictal epileptiform discharges (IEDs), therefore I will discuss IEDs first and what do they represent.

##### **2.4.2a Interictal epileptiform discharges**

IED commonly referred to as ‘epileptic spikes’ (see Appendix 1) are the expression of epilepsy observed most frequently in the clinical context in humans. These are synchronous high amplitude ( $> 50$  uV) fast transients (50-200 ms) recorded on scalp EEG with specific temporal and spatial characteristics. These temporal characteristics include single discharges, periodic discharges or discharges in clusters, and spatial characteristics include localised or generalized/widespread across brain regions [Gotman 1980;Niedermeyer and Lopes da Silva 2005].

At the cellular level, IEDs are produced by a paroxysmal depolarizing shift (PDS), also known as intracellular burst discharge, resulting in excitatory post synaptic potentials (EPSPs: mediated by glutamate receptors) or IPSPs (mediated by GABA receptors), as shown in different models including: impaired GABAa mediated inhibition model [Schwartzkroin and Wyler 1980;deCurtis *et al.* 1999], low magnesium model [Mody and Heinemann 1987;Mody *et al.* 1987], high

potassium model [Rutecki *et al.* 1985], low calcium model [Haas and Jefferys 1984; Haas *et al.* 1984] and kindling model [McIntyre and Wong 1986].

The bursting neurons which produce PDS are found in hippocampus (CA1-CA3 regions) [Johnston *et al.* 1980], superficial layers of piriform cortex [Forti *et al.* 1997], deep layers of entorhinal cortex [Fountain *et al.* 1998] and layer IV-V of neocortex [Connors *et al.* 1982]. These neurons synchronize across a population of neurons through excitatory and inhibitory synaptic interactions [Chamberlin *et al.* 1990; Cobb *et al.* 1995] as well as non synaptic mechanisms such as gap-junctions [Jefferys 1995a; Jefferys 1995b]. As a result local field potentials (LFP) are recorded on scalp EEG which is visible as IEDs. An estimate shows that 10000 to 50000 pyramidal cells must be firing simultaneously to produce an IED on EEG [Murakami and Okada 2006]. The propagation of IEDs takes place in vertical and tangential directions depending upon the preferred circuitry and physiological and anatomical connectivity [deCurtis and Avanzini 1994; Albowitz and Kuhnt 1995].

The energy metabolism during the occurrence of IEDs and the role of functional imaging studies in understanding the underlying mechanism is described in sections 2.6.3 and 3.1.

#### **2.4.2b Transition to focal seizures**

It is noteworthy that IEDs and seizures cannot be equated as two reflections of the same underlying phenomenon. There is evidence from experimental and human studies that IEDs are produced in regions (clinically termed as irritative zone: IZ) which can be remote from the regions producing seizures (clinically termed as seizure onset zone: SOZ) [Luders and Comair 2000; Luders *et al.* 2006]. The epileptogenic zone (EZ) which is clinically required to be removed to render someone seizure free may include both IZ and SOZ with dynamic boundaries reflecting underlying neuronal synchronization [Alarcon *et al.* 1994; Luders and Comair 2000; Luders *et al.* 2006]. There can be other IZs in the same brain tissue which continue to produce IEDs (green spikes) and do not need to be resected with EZ [Luders *et al.* 2006].

It has been shown that the occurrence of IEDs may decrease the probability to produce an ictal event [Barbarosie and Avoli 1997] and some spike quantification studies have shown that IEDs cease before the ictal onset [Marciani *et al.* 1985; Gotman 1985], while others have found that the frequency of IEDs does not

change before seizure onset [LeVan Quyen *et al.* 2001a;LeVan Quyen *et al.* 2001b;Avoli *et al.* 2006]. In vitro and in vivo studies have shown that preictal discharges are qualitatively different from IEDs and may precede the ictal onset by seconds to minutes [Bragin *et al.* 2007;Gnatkovsky *et al.* 2008;Huberfeld *et al.* 2011]. It has been shown, both in vitro and in vivo that some high frequency oscillations (HFOs: 50-500Hz) are probably another type of interictal pattern produced by highly interconnected principal neurons and that the power amplitude of HFOs has been found to increase minutes to seconds before the seizure onset, but there is no clear evidence for their role in seizure generation [Jacobs *et al.* 2008a;Engel, Jr. *et al.* 2009;Khosravani *et al.* 2009].

#### **2.4.2c Onset and progression of focal seizures**

The commonly observed ictal patterns (~ 87%) identified on scalp EEG at the ictal onset include: rhythmic activity (alpha, theta or delta frequencies), paroxysmal fast activity (>13Hz) and repetitive epileptiform activity [Foldvary *et al.* 2001]. However, epileptic activity revealed on scalp EEG may be delayed as compared to intracranial EEG (icEEG) [Ray *et al.* 2007]. Intracranial EEG (icEEG) recordings in temporal and neocortical human seizures have shown low amplitude fast activity commonly at the ictal onset [Allen *et al.* 1992;Alarcon *et al.* 1995;Wendling *et al.* 2002;Wendling *et al.* 2003;Wendling *et al.* 2005]. Two different mechanisms have been proposed for this fast activity: synchronization (strong intrinsic temporal correlation between regions at seizure onset) [Babb *et al.* 1987;Monto *et al.* 2007] and desynchronization (spatial decorrelation of regions at seizure onset) [Bartolomei *et al.* 2001;Wendling *et al.* 2003]. More recently unit recordings of human neurons have also favoured the desynchronization in different regions at seizure onset [Truccolo *et al.* 2011]. This is in line with the concept that there is complex recruitment of a pathologic network rather than single focus at seizure onset [Bragin *et al.* 2000;Bartolomei *et al.* 2004], and the thalamus is recruited late in the seizure [Arthuis *et al.* 2009]. It has also been shown that the paroxysmal fast activity (15 to 40 Hz) at the ictal onset evolves into a slow activity (3 to 10 Hz) during the ictal activity over time [Wendling *et al.* 2005].

Several cellular mechanisms maintaining normal physiological balance may fail to produce seizures. These include changes in the extra and intracellular volumes, ion concentrations, buffering mechanisms and cerebral blood flow compensatory



mechanisms. As a result an imbalance between excitatory and inhibitory pathways (through N-methyl D-aspartic acid (NMDA) and GABAergic receptors) is produced which leads to seizure generation. The commonly understood mechanisms of seizure generation postulates that there is gradual loss of burst after-hyperpolarisation and progressive increases in the number of bursts with prolonged after-depolarization, followed by a tonic depolarization of the membrane potential. The tonic activity is followed by irregular periodic bursts termed clonic phase which ends up in hyperpolarized membrane potential corresponding to postictal depression [McCormick and Contreras 2001].

The experimental data suggests that seizures with low voltage fast oscillations at the onset have a transient reduction in GABAergic inhibition causing paradoxical reinforcement of inhibitory networks and principal neurons become silent. This is followed by synchronous and rhythmic firing of principle neurons which is associated with an increase in extracellular potassium levels (due to excessive firing of inhibitory interneurons or nonsynaptic transmission of potassium wave) leading to inactivation of GABA mediated IPSPs and recurrent excitation and progression of seizure activity [Gnatkovsky *et al.* 2008]. A possible explanation proposed for reduction in GABA mediated inhibition may be the exhaustion of GABA nerve terminals. Others have suggested the role of depolarization secondary to the increased firing of GABAergic interneurons [Ziburkus *et al.* 2006] or increased synaptic excitability with maintained inhibition [Derchansky *et al.* 2008] in seizure generation. Functional imaging studies have further elaborated on the energy metabolism at the ictal onset and are described in sections 2.6.5 and 3.1.

In comparison to the cortical onset of focal seizures, it has been shown in animal models of reflex epilepsy that brainstem reticular formation plays a vital role in the initiation of generalized seizures. Increased brain reticular formation neuronal responses are induced in response to sensory stimuli after administration of subconvulsant dose of pro-convulsant drugs, and is considered a major mechanism for sensory initiation of seizures [Faingold 2012].

The majority of our knowledge regarding the underlying mechanisms of focal seizure generation comes from animal models of temporal lobe epilepsy, posttraumatic epilepsy and stimulated seizures, and a limited number of studies on spontaneous seizures in humans. In comparison, the majority of focal seizures in

humans are spontaneous with diverse aetiologies and multiple sub-types. The above described mechanisms, therefore, may hold true for some types of focal interictal and ictal activity; it is unknown if these mechanisms may be postulated to all types of spontaneous seizures in humans.

## **2.5 Classification of seizures and epilepsy**

Classification systems divide heterogeneous disease patterns into homogeneous groups to understand the biology of the disease. They can highlight the causes, pathophysiology and management of the disease, and can be applied as a tool for communication between physicians and scientific community [Engel, Jr. 1998;Beghi 2009;Beghi 2011].

In 1969, one of the earliest classifications of seizures was proposed by Gastaut which incorporated the modern technology of the time i.e., EEG. Seizures were divided into four categories: partial, generalized, unilateral and unclassified, on the basis of clinical characteristics, interictal and ictal features on EEG, anatomical substrates, aetiology and age of onset [Gastaut 1970]. After the availability of simultaneous recording and display of video and EEG, a revised classification scheme for epileptic seizures was proposed [ILAE 1981]. The categories for anatomical substrates, aetiology and age of onset were discarded and partial seizures were divided into two categories on the basis of retaining/loss of consciousness: simple and complex partial seizures [ILAE 1981]. Consciousness was defined as “that integrating activity by which man grasps the totality of his phenomenal field” [Evans 1972].

An international classification of epilepsies and epileptic syndromes [ILAE 1985] was proposed which maintained the two dichotomies separating epilepsies with generalized and focal seizures and epilepsies with known and unknown causes. The terms “idiopathic”, “symptomatic” and “localisation related epilepsies” replaced the terms “primary”, “secondary” and partial epilepsies respectively, and a group “special syndromes” was introduced which consisted of epilepsies difficult to be placed in other groups [ILAE 1985]. This classification was revised and updated in 1989 maintaining the same basic structures, however some syndromes/ epilepsies which were better defined now were moved to different categories [ILAE 1989] such as: primary reading epilepsy was defined as idiopathic localisation related epilepsy; chronic progressive epilepsia partialis continua of childhood and epilepsies with specific modes of seizure precipitation

were moved to symptomatic localisation related epilepsies from special syndromes [ILAE 1985;ILAE 1989].

The practical value of these classification systems was assessed in clinics and research studies. A consensus was developing that ILAE classifications were satisfactory in the majority of cases in tertiary centres, but the applicability was uneven in identifying homogeneous subpopulations [ILAE 1996]. Therefore, it was suggested that a reappraisal is required and ILAE started working on four documents: descriptive terminology for ictal phenomenon, classification of epileptic seizures, classification of epilepsy syndromes and classification of functional disability [Engel, Jr. 1998]. Hans Luders proposed a scheme for describing ictal semiology [Luders *et al.* 1998], which was succinct and focussed on clinical features and also introduced new terms such as: dialeptic seizures and automotor seizures. It was proposed that each type of ictal semiology is one component and different types can be linked together to describe propagation of seizures [Luders *et al.* 1998]. Others argued that it was good to describe seizures for epilepsy surgery [Engel, Jr. 1998] or as a diagnostic guide at bedside [Wolf 2003] but missed some critical information including: frequency, precipitating factors and postictal behaviours [Engel, Jr. 1998].

As new investigation techniques provided detailed information on the anatomic substrates of ictal semiology, different types of seizures, syndromes, causes and prognosis of different classes of epilepsy, especially in the context of epilepsy surgery, a diagnostic scheme with five axes was put forward [Engel, Jr. 2001]. In the same year Wieser *et al.*, proposed a new ILAE classification for postsurgical outcome [Wieser *et al.* 2001], which was a step forward from Engel's outcome classification [Engel 1993]. According to the new ILAE classification [Wieser *et al.* 2001] postsurgical outcome is divided in six categories: Class I (completely seizure free; no auras); Class II (only auras; no other seizures); Class III (one to three seizure days per year; auras); Class IV (four seizure days per year to 50% reduction of baseline seizure days; auras); Class V (less than 50% reduction of baseline seizure days to 100% increase of baseline seizure days; auras); Class VI (more than 100% increase of baseline seizure days; auras).

In 2006 a core group of ILAE [Engel, Jr. 2006] presented a report on possible further changes in classification of epilepsy. They proposed to classify seizures on the basis of pathophysiologic mechanism, anatomic substrates, response to anti-

epileptic drugs (AEDs), ictal onset and propagation patterns on EEG and associated epileptic syndromes. Epilepsy syndromes were classified according to seizure types, age of onset, progressive nature, interictal EEG and associated clinical features, pathophysiologic mechanism and genetic basis [Engel, Jr. 2006]. The syndromic classification of different epilepsy types is important since epilepsy is a symptom complex and the heterogeneity of the disease can only be justified by combining variable aetiology and differing clinical, electrophysiologic, imaging, and pathologic patterns in syndromes which can be used for diagnostic, prognostic, and therapeutic purposes [Beghi 2009]. In comparison, a newer concept of system epilepsies (involving one (or more) functionally defined brain system(s)) was introduced in Monreale workshop, and epilepsies were classified as type I-IV on the basis of aetiology rather using terms idiopathic or symptomatic [Capovilla *et al.* 2009]. However, some did not agree with the idea of system classification [Luders *et al.* 2009] and the current classification of seizures and epilepsies was proposed by ILAE in 2010 [Berg *et al.* 2010].

### 2.5.1 New ILAE classification of seizures and epilepsy

In the current classification of epileptic seizures and epilepsy [Berg *et al.* 2010], the basic structure was maintained as for 1981 classification of seizures [ILAE 1981] and 1989 classification of epilepsies [ILAE 1989]. The concepts which do not follow our current understanding of epilepsies have been revised and confusing terminologies which have been a source of debate in the last two decades have been replaced with new terminology [Berg *et al.* 2010]. The changes in the new classification of seizures [Berg *et al.* 2010] as compared to 1981 classification of seizures [ILAE 1981] include:

- Generalized seizures are conceptualized to originate at some point within, and rapidly engaging, bilaterally distributed networks but do not include the entire cortex necessarily.
- The sub-classification of absence seizures has been modified and myoclonic absence seizures and eyelid myoclonia are now recognized.
- Myoclonic astatic seizures have been renamed as myoclonic atonic seizures.

- Focal seizures are conceptualized as originating within networks which may be discretely localised or more widely distributed.
- The previously known simple and complex partial seizures have been combined together under the term focal seizures.
- A new term ‘dyscognitive’ has been coined to describe impairment of consciousness.
- The secondarily generalized seizures have now been renamed as bilateral convulsive seizures.
- Neonatal seizures are no longer regarded as a separate entity.
- Spasms were not acknowledged in the 1981 classification of seizures, and are termed as epileptic spasms in the new classification.
- It has been suggested that the focal seizures can be described according to clinical features as described in the semiological seizure classification [Luders *et al.* 1998] or the glossary of ictal semiology [Blume *et al.* 2001].

The changes in the new classification of epilepsies [Berg *et al.* 2010] compared to the 1989 classification of epilepsies [ILAE 1989] include:

- The terms idiopathic, symptomatic, and cryptogenic have been replaced with genetic, structural/metabolic and unknown, respectively.
- The term benign has been replaced by self-limiting.
- Cause is no longer equated with prognosis, in the current classification [Berg *et al.* 2010] and the notion of idiopathic epilepsies being benign is intentionally discarded.
- Dravet syndrome is now considered as genetic epilepsy.
- Electroclinical syndromes are better defined on the basis of: typical age of onset, specific EEG characteristics, seizure types, and other features permitting a specific diagnosis. These electroclinical syndromes are differentiated from less well defined epilepsies.
- Constellations is a category containing syndromes or nonsyndromic epilepsies which cannot be classified as electroclinical syndromes but should be recognized based on their clinical or other features.
- Epilepsies associated with structural or metabolic conditions are labelled differently from 1989 classification so that their localisation

and aetiology can be identified e.g., epilepsy with focal seizures secondary to cortical dysplasia in the temporal lobe.

- The concept of epileptic encephalopathy has been recognized: the epileptic activity itself may contribute to severe cognitive and behavioural impairments above and beyond what might be expected from the underlying pathology alone, which can worsen over time.

### 2.5.2 Pros and cons of the new ILAE classification

Many arguments have been put forward for and against the new classification of seizures and epilepsy. Speaking in favour, the new classification provides a framework reflecting the scientific understanding and improvements in the clinical care by incorporating the new information on genetics [Berg and Scheffer 2011].

- The further development of this classification is a dynamic process reflecting the transition in concepts on the basis of our current knowledge.
- The old system has been updated rather than discarded and it will take time before the non-specialist adopt the new system [Shinnar 2010].
- Flexibility [Berg and Scheffer 2011;Wong 2011;Duncan 2011a] to describe syndromes, incorporating information on multiple axes, e.g., “syndrome x” secondary to “y gene mutation” [Wong 2011] is another main feature of this system.
- Controversial terms including: idiopathic, symptomatic, cryptogenic, simple partial and complex partial have been removed [Wong 2011;Jackson 2011;Berg and Scheffer 2011].
- Using the descriptive terminology [Luders *et al.* 1998;Blume *et al.* 2001] lateralizing and localising features of seizures can be highlighted [Duncan 2011a] and aetiology can be listed using the database proposed by Shorvon [Shorvon 2011b] which will be particularly helpful in the context of epilepsy surgery.
- The application of new classification scheme may give information on outcome measures and prognostic value [Moshe 2011] specifically in epilepsy surgery on the basis of aetiology [Menzler *et al.* 2011].

Much has been discussed regarding the shortcomings of this new classification system some of which are highlighted here:

- The ILAE Classification Core Group report incorporate advanced current knowledge of pathophysiologic, clinical, interictal, and ictal manifestations derived from EEG and other modes of modern investigative procedures which has been largely discarded in the new classification [Panayiotopoulos 2011].
- The dichotomy, suggested by epidemiologists, between unprovoked seizures (a clear manifestation of epilepsy) and acute symptomatic seizures (a risk factors but not really a symptom of epilepsy) has been discarded [Panayiotopoulos 2011].
- New terms used may not be better understood or/and may be as easily misconstrued [Ferrie 2010;Panayiotopoulos 2011].
- The new classification has stressed on replacing idiopathic with genetic epilepsies. However, substituting idiopathic with genetic does not clarify the concept as the true genetic basis of most idiopathic epilepsies is not known and very few epilepsies are exclusively genetic in nature [Engel, Jr. 2001;Shinnar 2010;Shorvon 2011a;Duncan 2011a]. Moreover, the long established term idiopathic truly meaning “sui generis” (of own kind), reflects the nature of epilepsies in this group, but are not necessarily of genetic origin [Ferrie 2010;Shorvon 2011a]. Therefore, it has been suggested to classify epilepsies into groups: genetic epilepsies (with true genetic nature identified), idiopathic epilepsies (with the meaning as currently used), structural epilepsies (as defined in the new proposals), metabolic epilepsies (also as defined in the new proposals), and cryptogenic/probably symptomatic (with the meaning as currently used) [Ferrie 2010].
- No specific classification is recommended for focal seizures which defy the essence of any classification, as the use of descriptions of the various types of focal seizure [Luders *et al.* 1998;Blume *et al.* 2001] can be employed for differential diagnosis but should not be used as a classification system.
- Focal myoclonic seizures and status epilepticus have been completely ignored [Panayiotopoulos 2011] despite advances in the understanding of the later [Colloquium on Status Epilepticus 2007;Colloquium on Status Epilepticus 2009].

- The new classification recognises that focal and generalized seizures originate in focal and widespread neuronal networks; it does not take into account the emerging evidence from functional imaging studies [Wolf 2011] on the involvement of distributed networks in idiopathic localisation related epilepsies [Salek-Haddadi *et al.* 2009], and the involvement of localised networks in generalized seizures [Moeller *et al.* 2010c].

In conclusion, the new ILAE classification is part of a transition phase until we develop a rational, scientifically justifiable and clinically implementable classification of seizures and epilepsies reflecting the advanced state of knowledge regarding epilepsy. The most important aspect of this new classification is its flexibility and will absorb the developing information. Further updates to this new classification will be required in near future specially inclusion of the information being obtained from structural and functional imaging techniques. To take the new classification further, classifications of malformations of cortical development and focal cortical dysplasia have been proposed [Blumcke *et al.* 2009; Blumcke *et al.* 2011].

## **2.6 Investigation techniques**

The clinical investigation of seizures heavily depends upon the identification of seizure types and associated clinical semiology, electrophysiological rhythms on EEG and structural abnormalities on MRI. The precise localisation of the seizure onset becomes all the more important for patients being considered for surgery to stop their focal seizures. Here, I briefly discuss the clinical utility and application of different investigation techniques.

### **2.6.1 Electroencephalography**

Caton described the spontaneous electrical activity from the brain surface for the first time in 1875. In 1929 Hans Berger recorded the brain rhythms in humans from the surface of skull which was later named as electroencephalogram (EEG) [Swartz and Goldensohn 1998]. The application of EEG recordings in clinical science led to the identification of abnormalities on EEG which can be used for diagnosis of different types of epilepsy. In 1935, Gibbs, Davis and Lennox described 3Hz pattern of absence seizures and a year later IEDs were reported to be the focal signatures of epilepsy by Gibbs and Jasper [Swartz and Goldensohn 1998]. Efforts were made to record behaviour on cameras and electrical signals on



EEG simultaneously by Schwaub in 1938; it was in 1966 that first closed-circuit television EEG recordings were made by Goldensohn [Swartz and Goldensohn 1998]. Penfield and Jasper performed intracranial stimulation and its effect on behaviour in epilepsy patients in 1954 [Swartz and Goldensohn 1998]. Simultaneous recording of video and EEG by Stalberg (1976), Kamp (1979) and Binnie (1981) [Binnie *et al.* 1981;Niedermeyer and Lopes da Silva 2005] and digitization of the recorded EEG signal by Duffy [Duffy *et al.* 1979] provided the opportunity to record the seizure semiology and underlying brain rhythms at the same time over long periods of time. The digital recording of EEG opened a new window for analysing the electrical signal using mathematical algorithms to reveal the underlying source of epileptiform activity [Swartz 1998].

Interictal and ictal patterns [Lee *et al.* 2000;Foldvary *et al.* 2001] and clinical semiology [Loddenkemper and Kotagal 2005;Foldvary-Schaefer and Unnwongse 2011] are important for the diagnosis and localisation of epilepsy (up to lobar level), as recorded on simultaneous video and scalp EEG (video-EEG) with good temporal resolution. Currently, video-EEG plays a major role in diagnostic clarification, classification of seizure types and epilepsy syndromes, localisation of epileptic activity, detecting the frequency of minor seizures, sub-clinical status epilepticus and transient cognitive impairment. It is prudent to note that interictal EEG cannot approve or disprove the diagnosis of epilepsy, rather it supports the diagnosis. Similarly, EEG cannot be used to monitor a therapeutic response of AEDs by disappearance of interictal activity or for the prognosis of epilepsy [Binnie and Prior 1994;Smith 2005]. The sensitivity of scalp EEG ranges from 25 to 56%, with a specificity of 78-98% [Smith 2005] and the patterns seen on scalp EEG may localise paradoxically or have incongruity with the EZ [Catarino *et al.* 2011;Remi *et al.* 2011].

The simultaneous recording of scalp EEG and icEEG has shown that at least 6-10cm<sup>2</sup> area of brain needs to be recruited before electrical activity could be seen on scalp EEG and the patterns on scalp EEG are delayed up to 8 sec reflecting propagated electrical activity [Tao *et al.* 2005;Ray *et al.* 2007]. It is noteworthy that icEEG recordings are performed only in a small sub population of patients undergoing presurgical evaluation. Intracranial electrodes as shown in Figure 2.1 are placed on the basis of a clinical hypothesis generated by consensus to localise the SOZ, EZ and eloquent cortex when epileptogenic lesions are nearer to seizure

focus. The duration of implantation is decided on clinical grounds [Luders and Comair 2000; Duncan 2007] but usually is in the order of days to weeks and not months considering the increasing risk of complications e.g., infection and bleeding with longer durations of implantation. The intracranial recordings are stopped once a sufficient number of ictal events have been captured. Both micro and macro electrodes (subdural grids and stereo-tactically placed depth electrodes) can be used, although the latter is much more common. The spectrum of activity recorded on icEEG extends much beyond that of scalp EEG. The spatial resolution of icEEG largely depends on the type of electrodes. Micro electrodes record single and multi unit activity (MUA), and macro electrodes used in majority of clinical studies record LFPs from smaller population of neurons as compared to LFPs recorded on scalp EEG, with a range of the order of 1cm for depth electrodes [Lachaux *et al.* 2003]. Intracranial EEG provides localisation of interictal/ictal patterns and high frequency signals up to sub-gyral level and is considered the holy grail of clinical neurophysiology [Ray *et al.* 2007; Jacobs *et al.* 2008a]. One of the limitations of icEEG is its limited spatial sampling. At least 10000 recording sites would be required to cover the whole brain properly [Halgren *et al.* 1998] whereas the number of implanted electrodes rarely exceeds 100 in clinical practice. It has been suggested that interpretation of icEEG findings in combination with MEG and fMRI can address this issue for localisation and cognitive studies [Lachaux *et al.* 2003].

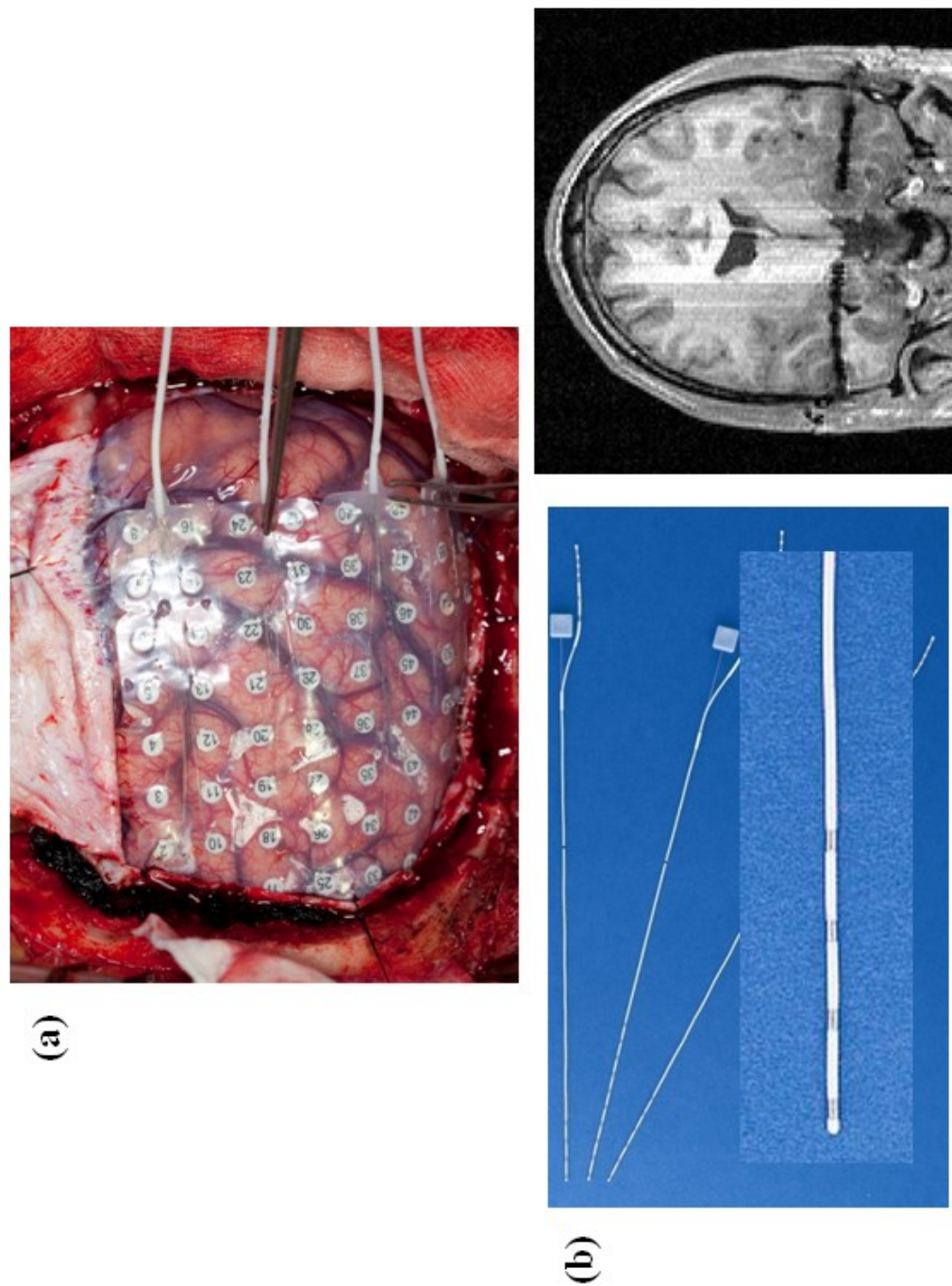


**Figure 2.1: Intracranial electrodes**

(a) Grid electrodes placed directly on the surface of brain (left frontal lobe). (b) Depth electrodes; Coronal section MRI scan reveals depth electrodes in both temporal lobes.

### 2.6.2 Structural magnetic resonance imaging in epileptology

Since the advent of MRI, the progress in the field of neuroimaging has established MRI's superiority over CT-scans in terms of sensitivity and specificity and revolutionised the investigative and therapeutic procedures [McLachlan *et al.* 1985;Dowd *et al.* 1991;Kuzniecky *et al.* 1993;Duncan *et al.* 1997b;Bartlett *et al.* 2002]. In the acute situations though CT-scan is obtained as the first investigation, MRI is preferably the first choice investigation in all patients with epilepsy except those patients who have a definite diagnosis of idiopathic generalized epilepsy (IGE) or other types of epilepsy known to have no structural abnormality [Duncan 1997].

The indications [Duncan 2010] for MRI in patients with epilepsy include:

- Onset of partial seizures at any age.
- Onset of generalized or unclassified seizures in the first year of life or adulthood.
- Evidence of a fixed deficit on neurological or neuropsychological examination.
- Difficulty in obtaining seizure control with first line antiepileptic drugs.
- Loss of seizure control or a change in the pattern of seizures.

The neuroimaging commission of the ILAE has recommended imaging protocol for epilepsy patients ensuring that the structural abnormalities are detected uniformly where these protocols are used, which includes high resolution thin cut MRI with T1-weighted, T2-weighted, FLAIR and proton density sequences [ILAE 1998].

The commonest abnormalities detected on MRI in patients with epilepsy include: HS, MCD, vascular malformations, tumours (DNET and glioma), cavernomas, granulomas especially cysticercosis, traumatic injuries, haemorrhages and ischemic damage [Duncan 2010]. It has been shown that the structural MRI scanning at higher resolution e.g., at 3 Tesla (T) can identify the previously undetected (e.g., at 1.5 T) lesion in 20% of cases [Strandberg *et al.* 2008]. Manual [Cook *et al.* 1992] and automated [Bonilha *et al.* 2009] hippocampal volumetry has revealed hippocampal damage unilaterally or bilaterally. Voxel-based analysis of MRI scans has shown subtle abnormalities which were not visible previously in 10-30% of patients overall [Salmenpera *et al.* 2007], and in 14% of patients with refractory focal epilepsy, half of which were

concordant with scalp EEG data [Focke *et al.* 2008;Focke *et al.* 2009]. Diffusion tensor imaging allows the mapping of the diffusion process of molecules. Diffusion tensor imaging for brain tissue mainly utilises diffusion of water molecules in white matter fibres in the brain. This diffusion can be in the direction or perpendicular to the direction of white matter fibres and a value (fractional anisotropy) between zero and 1 is calculated to demonstrate the anisotropy of the diffusion process. Diffusion tensor imaging has shown diffusion abnormalities in 50% of patients with refractory focal epilepsy which were concordant with epileptiform abnormalities on EEG [Thivard *et al.* 2006;Guye *et al.* 2007], and also reorganization in the language networks postoperatively [Yogarajah *et al.* 2010].

### 2.6.3 Positron emission tomography

Positron emission tomography (PET) utilizes positron emitting radionucleotide such as  $^{18}\text{F}$ -fluro deoxy-glucose (FDG) in combination with X-ray CT-scan to visualize and quantify the areas on the basis of the principle that the brain metabolism is decreased below normal in areas of cerebral dysfunction during interictal periods in patients with focal seizures [Theodore *et al.* 1986;Debets *et al.* 1990;Theodore *et al.* 1997]. It has been shown that PET can identify focal areas of hypometabolism in 55-80% of patients with focal abnormalities such as IEDs on EEG [Theodore *et al.* 1986;Theodore *et al.* 1997].

The area of hypometabolism revealed by PET is usually more extensive than the structural abnormality revealed by MRI [Duncan *et al.* 1997a;Duncan 2010]. More specifically, using FDG PET imaging, focal areas of hypometabolism were seen in 75-90% of patients with focal cortical dysplasia [Lerner *et al.* 2009] and seizure focus was identified in 70% of patients with temporal lobe epilepsy [Knowlton *et al.* 1997;Markand *et al.* 1997]. Another study showed that the findings of FDG PET imaging influenced the clinical decision, made on the basis of long-term video-EEG monitoring and MRI, to change in 71% of patients undergoing presurgical assessment [Uijl *et al.* 2007]. Ipsilateral hypometabolism on FDG PET scans has been shown to be a predictor of good postoperative outcome [Van Bogaert *et al.* 2000;Willmann *et al.* 2007].

The major limitations of PET include false localisation [Nagarajan *et al.* 1996], and the localisation of interictal activity rather than seizures. The reasons for false localisation are likely to be medication effects, structural abnormalities or

propagation of interictal activity. There have been only a few PET studies of seizures due to short half life of the tracer, difficulties in interpretation of ictal hypermetabolism and unpredictable nature of seizures [Alavi and Hirsch 1991;Chugani *et al.* 1994].

In the current settings the clinical role of PET has been limited to that 20-25% of patients with refractory focal epilepsy where structural imaging cannot reveal a lesion. In such cases, re-review of structural imaging in the light of PET findings may reveal a previously hidden lesion in the area of hypometabolism. The area of hypometabolism can also serve as a guide for the placement of intracranial electrodes to identify seizure focus during presurgical evaluation [Duncan 1997;Duncan 2010].

#### **2.6.4 Magneto-encephalography**

Magneto-encephalography (MEG) can record the magnetic fields generated by the normal and abnormal electrical activity produced by different brain areas [Knake *et al.* 2006]. MEG requires only 4cm<sup>2</sup> area to be recruited to produce a visually recognisable MEG spike above the background noise [Oishi *et al.* 2002] and can record IEDs which are not visible on scalp EEG from the neocortex, inter hemispheric and orbito-frontal cortices [Agirre-Arrizubieta *et al.* 2009]. On the other hand, IEDs from medial temporal lobes can be better detected on EEG than on MEG [Agirre-Arrizubieta *et al.* 2009]. The dipole source imaging of IEDs has shown that the orientation of the sources relative to the skull is very important because MEG is better suited for tangential than radial sources. In comparison, scalp EEG can record both radial and tangential sources but is better suited for radial sources. Therefore, both techniques are complementary to reveal the full picture [Ebersole and Ebersole 2010].

The clinical role of MEG has been found to be helpful in distinguishing the area of onset of IEDs from the area of propagation, placement of intracranial electrodes, the decision of resection, and predicting seizure freedom to some extent [Knowlton *et al.* 1997;Knowlton *et al.* 2008a;Knowlton *et al.* 2008b;Knowlton *et al.* 2009]. In addition, MEG has also been used in mapping the eloquent cortex (language area); however it cannot replace the cortical stimulation for mapping language area in patients undergoing a resection near language cortex and needs further evaluation in larger sample [McDonald *et al.* 2009;Doss *et al.* 2009;Frye *et al.* 2009].

### 2.6.5 Ictal single photon emission computed tomography

Ictal single photon emission computed tomography (Ictal SPECT) measures regional cerebral blood flow [O'Brien *et al.* 1998] on the basis that the increased ictal neuronal activity during seizures is associated with increased metabolism and blood flow to focal areas involved by using radio-labelled tracers. The <sup>123</sup>Iodine labelled tracers require 20 minutes to reach peak brain activity [Nishizawa *et al.* 1989]. Therefore, technetium hexa-methyl-propylene-amine-oxime (<sup>99m</sup>Tc-HMPAO) and technetium ethyl cysteinate dimer (<sup>99m</sup>Tc-ECD) are preferred currently which reach the peak within 2 minutes of injection [la Fougere *et al.* 2009]. Both interictal and ictal SPECT have been shown to help in localisation and lateralization; however ictal SPECT has higher sensitivity (73-97%) than interictal-SPECT (50%) for patients with temporal lobe epilepsy [Spanaki *et al.* 1999;Zaknun *et al.* 2008]. The sensitivity of ictal SPECT for extra temporal epilepsy (66%) is lower than for temporal lobe epilepsy [Weil *et al.* 2001]. Using digital analysis techniques by sub-traction of ictal and interictal scans (SISCOM), SPECT has been found to be helpful in predicting the postsurgical outcome [Ahnlide *et al.* 2007;Wichert-Ana *et al.* 2008a;Wichert-Ana *et al.* 2008b]. One of the study showed that 75% of patients whose SISCOM findings were within the margins of the resected area were rendered seizure free. In comparison, when SISCOM findings were outside the resection margins seizures continued in all the patients [Wichert-Ana *et al.* 2008b].

Currently, ictal SPECT is used during presurgical evaluation of refractory focal epilepsy when no structural abnormality is visible on MRI scan and a re-review of MRI scans of the area of hyperperfusion on ictal SPECT may also reveal previously hidden lesion. If the area of hyperperfusion on ictal SPECT is concordant with electroclinical information and not close to the eloquent cortex, resection can be recommended without confirmation with icEEG recordings. In other patients, the findings of ictal SPECT can be used as a guide for the placement of intracranial electrodes during presurgical assessment [Van Paesschen *et al.* 2003;Van Paesschen *et al.* 2007;Duncan 2010].

One of the limitations of ictal SPECT is that the areas of hyperperfusion shown may include both the ictal onset and propagated patterns because of low temporal resolution and delay in injecting the tracer [Van Paesschen *et al.* 2007]. A study showed that in 78% of patients hyperperfusion extended to areas involved in

propagation and was limited to epileptic focus only in 27% of patients when the injection was given within 5 seconds of seizure onset [Fukuda *et al.* 2006]. This limitation has been encountered more commonly in patients with frontal lobe epilepsy [Lee *et al.* 2006]. Moreover, additional areas of hyperperfusion which are homotopic and contralateral to the seizure onset zone are also commonly seen forming mirror imaging effect [Huberfeld *et al.* 2006].

### **2.6.6 Functional magnetic resonance imaging**

The development of Functional Magnetic Resonance Imaging (fMRI) by Ogawa and Kwong in 1990s [Ogawa *et al.* 1990a;Ogawa *et al.* 1990b;Kwong *et al.* 1992;Ogawa *et al.* 1992] made it possible to identify changes in blood oxygen level dependent (BOLD) associated with physiological and pathological activities in brain. The literature and application of fMRI has increased exponentially over the last two decades. Task modulated fMRI studies are the subject of the vast majority of fMRI studies. It is being used to localise language areas and networks non-invasively in patients undergoing presurgical evaluation [Bonelli *et al.* 2011] and has replaced Wada test in many centres [Wagner *et al.* 2012]. The investigation of memory using fMRI has revealed the underlying networks suggesting that the findings may have predictive value for patients undergoing epilepsy surgery [Richardson *et al.* 2004;Richardson *et al.* 2006a;Bonelli *et al.* 2010;Stretton *et al.* 2012].

Simultaneous and synchronized recording of good quality EEG and fMRI (EEG-fMRI) data in 2001 [Lemieux *et al.* 2001] further broadened the range of neural events, effects and states that could be studied using fMRI, particularly in the resting state. The methodological details and applications of EEG-fMRI are discussed in Chapter 3.

## **2.7 Medical and surgical treatments**

The two most important questions regarding the treatment of epilepsy are:

- When to start?
- What to start?

AEDs are usually not started after the first provoked/unprovoked seizure. However, seizures associated with acute brain injury from trauma or infections require treatment for acute episodes but it does not prevent from the development of epilepsy in future [Schierhout and Roberts 2000]. AEDs do not appear to



change the prognosis of the disease and the likelihood of remission of seizures remains same if the treatment is started early or late [Schierhout and Roberts 2000;Marson *et al.* 2005;Marson *et al.* 2007]. The risk of recurrence of seizures is higher when there is an underlying structural abnormality, learning disability or epileptiform abnormalities on EEG [Hart *et al.* 1990;Kim *et al.* 2006]. In addition, the risk such as of sudden unexpected death in epilepsy increases with chronic epilepsy. Therefore, the decision to start antiepileptic drugs is largely an individual decision and requires a balance between risks associated with seizures and antiepileptic drugs.

### 2.7.1 Antiepileptic drugs

AEDs can be classified according to their mechanism of action as follows;

- Action on Sodium ion channels: Phenytoin, Carbamazepine, Lamotrigene, Topiramate, Valproic acid, Zonisamide, Lacosamide, Rufinamide
- Action on Calcium ion channels: Ethosuximide, Valproic acid, Levetiracetam, Zonisamide, Gabapentin, Pregabalin
- Action on Potassium ion channels: Retigabine
- Enhancement of GABA transmission: Benzodiazepines (Diazepam, Clonazepam), Gabapentin, Phenobarbital, Valproic acid, Topiramate, Vigabatrin, Felbamate, Zonisamide
- Inhibition of excitatory amino acid transmission: Felbamate and Topiramate, Zonisamide, Perampanel
- Carbonic anhydrase inhibitors: Acetazolamide, Zonisamide

The choice of AEDs for different types of seizures is different. Generally it can be divided into “first and second line” and “drugs to be avoided” for focal, generalized, myoclonic and absence seizures. The choice of right antiepileptic drug is of prime importance as some antiepileptic drugs can worsen seizures in idiopathic generalized epilepsy [Hitiris and Brodie 2005;Bergey 2005].

### 2.7.2 Refractory epilepsy and epilepsy surgery

Around 64-70% of patients with epilepsy achieve remission during the early years of epilepsy either spontaneously or with antiepileptic drugs [MacDonald *et al.* 2000;Kwan and Brodie 2000;Beleza 2009]. Seizures can be controlled with the first AED in 47% of patients, with the second AED in another 13% and with the third AED in an additional 4% [Kwan and Brodie 2000].

Seizures continue despite treatment with antiepileptic drugs in 30-40% of patients [Beleza 2009] and the proportion of continuing seizures is higher in patients with symptomatic and cryptogenic epilepsy (40%) than idiopathic epilepsy (26%) [Kwan and Brodie 2000]. These patients are regarded as having refractory epilepsy. The definition of refractory epilepsy depends upon three main factors:

- Number of AEDs previously taken
- Frequency of seizures
- Duration of uncontrolled epilepsy

Therefore, refractory epilepsy has been defined when there is absence of response to 2 AEDs at reasonable doses keeping in mind the frequency of continuing seizures and the duration of uncontrolled epilepsy [Beleza 2009].

Before considering epilepsy surgery it is important to ensure that:

- The diagnosis of epilepsy and its subtype is correct
- Adherence to antiepileptic drugs is maintained
- Correct type of antiepileptic medication was used for the type of epilepsy.

One out of two patients with refractory epilepsy can be offered further treatment with epilepsy surgery, provided that they have a focal seizure onset, which is estimated to be around 3% of people who develop epilepsy [Duncan 2011b]. Before surgery these patients undergo thorough presurgical evaluation [Duncan 2011c]. In developed countries, for every 50 million people, around 1000 people need such assessment and 50% of these will undergo epilepsy surgery [Lhatoo *et al.* 2003]. The purpose of presurgical evaluation is to localise the focal epileptogenic area, by consensus of converging data from different investigation techniques, which can be removed with surgery without additional risks; to decide the type of possible surgery; and to assess the risk and benefits of surgery postsurgically [Duncan 2007]. The presurgical evaluation includes: detailed clinical history taking and examination, long-term scalp video-EEG, MRI, neuropsychological and neuropsychiatric assessments. MRI may fail to reveal an abnormality in 25% of cases and other investigations: PET, ictal-SPECT, MEG or EEG-fMRI recordings are performed to further localise the epileptic focus [Duncan 2010]. A small proportion of these patients also undergo icEEG recordings to confirm a predefined hypothesis regarding seizure onset and epileptogenic areas prior to surgery [Duncan 2007; Miller and Cole 2011].

The surgical procedures performed in epilepsy surgery include: anterior temporal lobe resection (ATLR), lesionectomy, neocortical resection, hemispherectomy, corpus callosotomy and multiple subpial transaction [Duncan 2007]. Relative proportion of different epilepsy surgery procedures has changed over time and also varies in different centres and countries. At the National Hospital for Neurology and Neurosurgery ATLR (77-81%) is the predominant surgical procedure performed in patients undergoing epilepsy surgery followed by extra-temporal lesionectomy (7-14%), temporal lesionectomy (7%), extra-temporal resections (3%) and hemispherectomy (2-3%) [Lhatoo *et al.* 2003; deTisi *et al.* 2011]. It has been shown that in children with temporal lobe epilepsy undergoing surgery between 1989 and 1993 in Germany, ATLR was performed in 80%, lesionectomies plus hippocampectomies in 11.4% and lateral neocortical resections in 8.6% [Clusmann *et al.* 2004]. In comparison, between 1994 and 2000 in Germany in the same centre, ATLR was performed in 13%, amygdalohippocampectomies in 50%, lesionectomies plus hippocampectomies in 16.7% and lateral neocortical resections in 20.3%, in children with temporal lobe epilepsy undergoing surgery [Clusmann *et al.* 2004]. In addition to the above mentioned procedures, gamma knife surgery is also performed for hippocampal sclerosis, cavernous angiomas and hypothalamic hamartomas in other centres [Regis *et al.* 2000]

Overall, 60% of patients who undergo temporal lobe surgery achieve long-term seizure freedom, and 30–40% of patients who undergo extratemporal surgery remain seizure free [Tellez-Zenteno *et al.* 2005]. The best remission rates at 2 years and 5 years postsurgically are achieved in patients who undergo anterior temporal lobe resections for neuroepithelial tumours and vascular malformations [Berkovic *et al.* 1995; deTisi *et al.* 2011]. The postsurgical seizure freedom rate is reported to be 52-62% at 5 years in patients with HS. Patients with FCD and MCD have early recurrence of seizures [deTisi *et al.* 2011]. Overall remission rates at 5 and 10 year postsurgically for all types of epilepsy surgery are 52% and 47% respectively [deTisi *et al.* 2011]. In 30-50% of patients with refractory epilepsy who are not suitable for surgery, vagus nerve stimulation can be used resulting in a 50% reduction in seizures in 30% of patients [Theodore and Fisher 2004].

## **2.8 Perspectives and conclusion**

The invention of new tools during the last century has revolutionised the process of diagnosis of epilepsy. These tools investigating the structure (using MRI), electrical and magnetic activity (using scalp and intracranial EEG, and MEG) and functional networks (using fMRI) of brain can provide scientific evidence regarding the seat of epilepsy. In its true sense this phase of new advancements is continuing even today. Although much work has been done there is still abundant room for improvement as far as the non-invasive localisation of epilepsy is concerned because the patients with refractory epilepsy continue to suffer.

## Chapter 3: Simultaneous EEG-fMRI in epilepsy<sup>2</sup>

Since its inception [Ogawa *et al.* 1990a;Kwong *et al.* 1992], fMRI has been used as a tool to map physiological and pathological BOLD networks in research and clinical settings. These applications include mapping: language [Bonelli *et al.* 2011] and memory networks [Richardson *et al.* 2006a;Bonelli *et al.* 2010;Stretton *et al.* 2012]; haemodynamic changes associated with epileptic activity; and brain state related haemodynamic changes in the resting state [Gusnard *et al.* 2001;Laufs *et al.* 2006;Fox *et al.* 2009] and during sleep [Czisch *et al.* 2004;Laufs *et al.* 2007a]. Functional MRI has good spatial resolution but low temporal resolution for investigating epileptic activity. On the other hand, EEG has good temporal resolution but low spatial resolution. Therefore, EEG was incorporated in the fMRI set up for the first time in 1993 by Ives [Ives *et al.* 1993], with the later development of EEG-triggered fMRI [Warach *et al.* 1996], and simultaneous (continuous) EEG-fMRI [Lemieux *et al.* 2001]. In this chapter, I discuss the mechanism of BOLD contrast, its relationship with neuronal activity and main methodological constraints and applications of simultaneous EEG-fMRI in epilepsy.

### 3.1 Mechanism of the BOLD effect

Research in animals and humans have shed some light on the underlying mechanism of BOLD contrast [Menon *et al.* 1997;Krakow *et al.* 1999;Krakow *et al.* 2000b;Logothetis *et al.* 2001]. EEG displays the electromagnetic field patterns generated by the neuronal signals; therefore, it is important to describe different activities briefly which can be recorded by EEG before embarking on establishing their relationship with haemodynamic changes and BOLD contrast.

#### 3.1.1 Types of neuronal activity recorded on EEG

Electrical signals recorded by EEG include: single unit activity, MUA and LFP. An electrode placed near a neural site measures the mean extracellular field potential (mEFP) which represents the weighted sum of activity along multiple cells. When a microelectrode with a small tip is placed close to the soma or

---

<sup>2</sup> This chapter forms the basis of the article [Chaudhary *et al.* 2013].

axon of a neuron or inside the cell body, the measured mEFP represents the spiking activity (action potentials), its latency, amplitude and shape [Halgren *et al.* 1998; Harris *et al.* 2000] reflecting instantaneous firing of a neuron (single unit activity). MUA reflects the weighted sum of the output signal of a neuronal population within a radius of 50-350 microns and the activity from each point within the sphere is weighted by its distance from the recording electrode site [Grover and Buchwald 1970; Legatt *et al.* 1980; Gray *et al.* 1995]. LFPs are weighted sum of synchronized post-synaptic potentials of excitatory and inhibitory neurons, after potentials, dendrosomatic spikes and voltage gated membrane oscillations, reflecting the input signal of a neuronal population within 0.5 to 3 mm of a recording electrode [GRANIT *et al.* 1963; Harada and Takahashi 1983; Walton and Fulton 1986; Mitzdorf 1987; Higashi *et al.* 1993; Chandler *et al.* 1994; Kobayashi *et al.* 1997; Juergens *et al.* 1999]. LFPs represent the low frequency mEFP signal, as shown by the combined EEG and intracortical recordings [Fromm and Bond 1964; Buchwald *et al.* 1965; Fromm and Bond 1967], which is not correlated with cell size. IEDs recorded on human scalp EEG represent LFPs from 6-10 cm<sup>2</sup> area of brain [Tao *et al.* 2005; Ray *et al.* 2007].

### **3.1.2 Relationship between neuronal activity, energy metabolism and haemodynamic changes**

Brain requires energy for its functioning (neuronal activity) which is provided through oxygen and glucose supply which in turn is mediated by cerebral blood flow. The evidence for the coupling between blood flow and neuronal activity is known for long [Roy and Sherrington 1890; Logothetis and Pfeuffer 2004]. Later studies using the <sup>14</sup>C deoxy-glucose confirmed the relationship between neuronal activity and glucose metabolism [Sokoloff *et al.* 1977; Sokoloff 1977]. Another interesting observation has been that the haemodynamic changes may result from the neurotransmitter signalling rather the local energy requirements. The role of neurotransmitter (GABA and glutamate) related signalling has also been proposed in deriving the haemodynamic responses in different brain structures including: neocortex, cerebellum and hippocampus [Attwell and Iadecola 2002; Logothetis and Pfeuffer 2004; Logothetis and Wandell 2004]. The inhibitors of non-NMDA glutamate receptors and adenosine receptors have been shown to block increase in blood flow [Li and Iadecola 1994], whereas application of glutamate have

vascular effects to increase blood flow [Faraci and Breese 1993;Yang and Iadecola 1996;Fergus and Lee 1997]. Therefore, the brain energy requirement is dependent on both neuronal and neurotransmitter signalling, and in turn blood flow is also mediated by these mechanisms.

### 3.1.3 What is the BOLD effect?

Increased neuronal activity requires increased energy demands. This increased energy requirement is fulfilled by regional changes in cerebral blood flow, cerebral blood volume and blood oxygenation. As a result the ratio of diamagnetic oxy-haemoglobin and paramagnetic deoxy-haemoglobin changes; and, in the presence of a strong magnetic field, the inhomogeneities induced by deoxy-haemoglobin in the intracellular space of red blood cells and the surrounding tissue generate a magnetic field gradient which can be detected as the blood oxygen level dependent: BOLD contrast [Ogawa *et al.* 1990a;Kwong *et al.* 1992;Mulert and Lemieux 2010]. This intrinsic contrast mechanism provides a means of mapping function related haemodynamic changes non-invasively over the entire brain with good spatial resolution.

The time course of the transient BOLD signal for a brief neuronal stimulus is also called the haemodynamic response function (HRF). It starts with an initial dip [Hu *et al.* 1997;Logothetis *et al.* 1999] followed by an increase which is delayed by 2-3s and reaches a plateau or peak value with a rapid rise in 6-12s. The signal returns through baseline with a post-stimulus undershoot resolving approximately 20 to 30 seconds post stimulus. It has been shown that the initial dip in the signal is attributed to the rapid increase in deoxy-haemoglobin [Malonek and Grinvald 1996] and local tissue hypoxia [Geneslaw *et al.* 2011]. The increase in BOLD signal reflects increased oxygen consumption as a result of increased neuronal activity. Increased blood flow to the areas of increased oxygen consumption supply additional oxygen requirements and overcompensates for the decreased oxygen. The under shoot of BOLD signal reflects changes in blood volume. It is suggested that the decrease in BOLD signal from peak may also reflect neuronal inhibition [Fox *et al.* 1988;Frahm *et al.* 1996;Logothetis *et al.* 1999;Logothetis *et al.* 2001;Logothetis and Wandell 2004;Logothetis and Pfeuffer 2004;Mulert and Lemieux 2010].

### 3.1.4 BOLD effect and neuronal activity

Over the last decade, efforts have been made to understand the exact relationship between the haemodynamic changes and the neuronal activity. Logothetis and colleagues [Logothetis *et al.* 2001] dissected the relationship between single unit activity, MUA, LFPs and BOLD responses which were recorded simultaneously from visual cortex. The sustained BOLD responses for single/multi unit activity show strong adaptation 2.5s after neuronal firing. In comparison, the BOLD responses for LFPs were sustained for the duration of the neuronal firing and highly correlated with it. It was suggested thus: strong association of BOLD responses with LFPs actually reflects that BOLD signal represents the summated input signals to neuronal population and the local processing of these signals. Moreover, MUA lacks synchronization and the signal decreases on summation which may be another cause of its lesser contribution towards BOLD responses [Logothetis *et al.* 2001].

The contribution of LFP activity to the BOLD signal has also been suggested by the studies addressing the issue of energy consumption underlying neuronal signals. The neuronal signals from post-synaptic effects of glutamate neurons account for the largest proportion of energy consumption (74% in humans and 34% in rodents) [Attwell and Laughlin 2001;Lennie 2003]. There is also a relationship between energy expenditure and neurotransmitters [Shulman and Rothman 1998;Rothman *et al.* 1999;Magistretti *et al.* 1999], energy expenditure and synaptic activity [Takahashi *et al.* 1995] (specifically that of glutamatergic neurons as they account for 80-90% of glucose usage for energy requirements [Pan *et al.* 2000]), and energy expenditure and astrocytes [Magistretti *et al.* 1994;Pellerin and Magistretti 1994]. In turn, this energy expensive synaptic activity which underlies the LFPs generated by neuronal population is associated with haemodynamic signal changes.

It has been shown that selective blocking of MUA has minimal effect on BOLD contrast and spikes/single unit activity are not dependent on cerebral blood flow refuting a quantitative relationship between spiking rate of neurons and haemodynamic signals [Mathiesen *et al.* 1998;Logothetis *et al.* 1999;Rees *et al.* 2000;Logothetis and Pfeuffer 2004;Logothetis and Wandell 2004]. Therefore, it can be said that BOLD contrast is closely related to LFPs and reflects the input activity to a cortical or subcortical neuronal population and its local processing.



An important question to address here is the nature of the relationship between the BOLD effect and neuronal activity. The BOLD response increases as a compressive, nonlinear, saturating function of stimulus energy [Wandell 1999; Logothetis and Wandell 2004]. This nonlinearity can result from a nonlinear association between the neuronal signal and stimulus energy or the neuronal signal and BOLD effect. Some studies have suggested a linear relationship between the neuronal signals and associated BOLD response; which if true should enable to infer neuronal signal from BOLD response [Mathiesen *et al.* 1998; Logothetis *et al.* 1999; Brinker *et al.* 1999; Rees *et al.* 2000; Ogawa *et al.* 2000; Logothetis *et al.* 2001; Smith *et al.* 2002; Logothetis and Pfeuffer 2004]. Logothetis and colleagues [Logothetis *et al.* 2001] showed that the neuronal signal and BOLD response increase proportionally for stimuli of varying strength, however it is not a time variant and did not extend to zero, suggesting that the whole relationship is nonlinear.

The sustained BOLD increases [Logothetis and Wandell 2004] and decreases [Shmuel *et al.* 2002] for a particular stimulus or a task can be conceptualized to reflect a balance between local neuronal excitation and inhibition. The regional energy demands change when there is net excitation, inhibition, or simple adjustments resulting in the regulation of cerebral blood flow. A simplistic explanation is that stimulus specific increase in excitatory neuronal activity results in increase in BOLD signal. This might be true in some cases but increases in BOLD signal can also occur when there is increase in both excitatory and inhibitory neuronal activity without a net gain. It can be argued that an increase in inhibitory activity with simultaneous decrease in excitation would result in decreased BOLD signal [Logothetis 2008]. Though, the energy expenditure may increase with increased inhibition or with sustained suppression of spiking activity of neurons due to longstanding stimulation [Ackermann *et al.* 1984; Nudo and Masterton 1986; Jueptner and Weiller 1995; Stefanovic *et al.* 2004]. This increased metabolism may be attributed to the pre-synaptic input activity despite decreased neuronal spiking [Logothetis 2008]. Human fMRI studies have suggested an association between neuronal inhibition/decreased neuronal spiking and down-regulation of haemodynamic signals and metabolism for BOLD signal decreases [Shmuel *et al.* 2002; Shmuel *et al.* 2006; Devor *et al.* 2007; Carmichael *et al.* 2008a]. Therefore, it is difficult to say that decreases in BOLD signal

reflect decreased metabolism and neuronal inhibition, unless the association between inhibitory neuronal activity and energy metabolism are clearly understood.

From the above discussion it is evident that the generation of BOLD response is highly dependent on local blood flow. White matter energy consumption is one fourth that of gray matter and is rarely reported to have BOLD signal changes [Mosier and Bereznaya 2001;Tettamanti *et al.* 2002]. Moreover, the BOLD signal may differ between regions, even when the regions are nearby. Our current understanding of BOLD mechanism does not allow determining a quantitative relationship between BOLD signal and its underlying neural activity, whether for number of spikes per unit time per BOLD increase or for perisynaptic activity, even if BOLD is calibrated for local perfusion of the tissue [Kida *et al.* 2000;Hyder *et al.* 2000].

### **3.2 Methodological considerations for simultaneous EEG-fMRI**

The aims of performing EEG-fMRI for patients of epilepsy include the localisation of interictal and ictal epileptic networks and understanding the relationship between neuronal activity and the associated haemodynamic changes. Studies using fMRI and/or EEG-fMRI as an investigation tool in epilepsy face a number of methodological issues pertaining to patient recruitment, identification of epileptic activity on EEG and data analysis which makes simultaneous EEG-fMRI data acquisition complex. Here, I discuss these issues within the specific context of their demonstrated application in epilepsy.

#### **3.2.1 Patient selection**

EEG-fMRI studies investigating the epileptic functional networks depend upon EEG to identify epileptic activity and therefore suffer from the limitations of EEG as described in Chapter 2, Section 2.6.1. Moreover, the aim of exploring functional networks varies from understanding the mechanism generating epileptic discharges (e.g., EEG-fMRI studies in generalized epilepsy) to localise the epileptic focus (e.g., EEG-fMRI studies in focal epilepsy). Therefore, patient selection has an important role to play in EEG-fMRI studies. In this section, I summarize the concerns relating to patient selection and their possible solutions adopted for EEG-fMRI studies of epileptic activity.

### 3.2.1a Studies on IED related haemodynamic changes

Initial studies investigating haemodynamic changes related to IEDs have been single case reports providing proof of the concept [Lemieux *et al.* 1997; Krakow *et al.* 1999; Lemieux *et al.* 2001; Archer *et al.* 2003b]. Majority of later studies are case series and have included patients with IGE [Aghakhani *et al.* 2004; Gotman *et al.* 2005; Hamandi *et al.* 2006; Hamandi *et al.* 2008; Carmichael *et al.* 2008a; Moeller *et al.* 2008a; Moeller *et al.* 2008b; Moeller *et al.* 2010a] and focal epilepsy with frequent IEDs on standard clinical EEG recordings and attending epilepsy clinics at tertiary care level [Krakow *et al.* 1999; Benar *et al.* 2002; Al-Asmi *et al.* 2003; Benar *et al.* 2003; Archer *et al.* 2003a; Bagshaw *et al.* 2004; Bagshaw *et al.* 2005; Salek-Haddadi *et al.* 2006; Kobayashi *et al.* 2006d; Jacobs *et al.* 2007; Zijlmans *et al.* 2007; Tyvaert *et al.* 2008; Jacobs *et al.* 2009; Vulliemoz *et al.* 2009; LeVan *et al.* 2010a; Thornton *et al.* 2010a; Grouiller *et al.* 2011; Thornton *et al.* 2011; Vulliemoz *et al.* 2011].

A number of studies have focussed on specific sub-types of epilepsy: refractory focal epilepsy [Salek-Haddadi *et al.* 2006; Jacobs *et al.* 2007; Zijlmans *et al.* 2007; Tyvaert *et al.* 2008; Jacobs *et al.* 2009; Vulliemoz *et al.* 2009; Thornton *et al.* 2010a; LeVan *et al.* 2010b; Grouiller *et al.* 2011; Thornton *et al.* 2011; Vulliemoz *et al.* 2011], secondary generalized epilepsy (SGE) [Hamandi *et al.* 2006; Hamandi *et al.* 2008], benign childhood epilepsy with centro-temporal spikes (BECTS) [Archer *et al.* 2003b; Masterton *et al.* 2010], childhood absence epilepsy (CAE) and reading epilepsy [Archer *et al.* 2003a]; and on specific structural abnormalities: MCDs [Tyvaert *et al.* 2008], cavernous angiomas [Kobayashi *et al.* 2007], tuberous sclerosis [Jacobs *et al.* 2008a] and FCDs [Tyvaert *et al.* 2008; Thornton *et al.* 2011]. A few studies have recruited patients undergoing presurgical evaluation and have compared the localisation of BOLD changes with postsurgical outcome retrospectively [Lazeyras *et al.* 2000a; Zijlmans *et al.* 2007; Thornton *et al.* 2010a; Thornton *et al.* 2011].

### 3.2.1b Studies on ictal related haemodynamic changes

Patient recruitment for ictal studies using fMRI has been either fortuitous, in cases when seizures have occurred during studies of the interictal state, or targeted. The majority of series published to date have resulted from the former. The targeted selection of patients based on the specific aim of capturing seizures has generally

been when seizures were provoked by certain triggers such as fixation off sensitivity (FOS) [Krakow *et al.* 2000c;Iannetti *et al.* 2002;Di Bonaventura *et al.* 2005], music [Morocz *et al.* 2003], reading [Salek-Haddadi *et al.* 2009] and photo paroxysmal response (PPR) [Moeller *et al.* 2009b]. Most studies have been single case reports or small series of patients with specific subgroups of epilepsy (Table 3.1). The unpredictable nature of seizures (except when seizures can be triggered) explains this situation.

Vigorous head or body movements inside an MRI scanner may be hazardous from the patient safety perspective [Lemieux *et al.* 1997] and can adversely affect data quality [Lemieux *et al.* 2007]. Patient recruitment has, therefore, been limited to specific seizure types which can be scanned without patient safety and data quality concerns.

**Table 3.1: Publications on mapping seizure related BOLD changes using fMRI or EEG-fMRI**

Study	Syndrome	Subjects	EEG/Channels	Motion Cut-off (mm)	Seizure Activation	Seizure Detection	Data Analysis Approach
<b>Adults: fMRI Only Studies</b>							
[Detre <i>et al.</i> 1995]	FE	1	N	-	N	Visually Observed	$\Delta$ Signal Intensity
[Detre <i>et al.</i> 1996]	FE	1	N	-	N	NM	$\Delta$ Signal Intensity
[Krakow <i>et al.</i> 2000c]	FOS	1	N	-	Fixation	Eye tracking system	GLM
[Kubota <i>et al.</i> 2000]	FE	1	N	-	N	Visually Observed	$\Delta$ Signal Intensity
[Krings <i>et al.</i> 2000]	FE	1	N	-	N	Visually Observed, Video recording	$\Delta$ Signal Intensity
[Morocz <i>et al.</i> 2003]	ME	1	N	-	Music	Patient response button	GLM, ICA
[Archer <i>et al.</i> 2006]	FE	1	N	-	N	Video recording	GLM
[Auer <i>et al.</i> 2008]	FE	1	N	0.2	N	Visually Observed	$\Delta$ Signal Intensity
[Donaire <i>et al.</i> 2009b]	FE	1	N	0.5	N	Visually Observed	Seq.GLM, ICA
[Iannetti <i>et al.</i> 2002]	FOS	3	Y/32	-	Fixation	EEG	GLM
[Salek-Haddadi <i>et al.</i> 2002]	FE	1	Y/11	-	N	EEG	GLM
[Salek-Haddadi <i>et al.</i> 2003b]	JAE	1	Y /NM	-	N	EEG	GLM

**Table 3.1: contd.**

Study	Syndrome	Subjects	EEG/Channels	Motion Cut-off (mm)	Seizure Activation	Seizure Detection	Data Analysis Approach
<b>Adults: EEG-fMRI Studies</b>							
[Aghakhani <i>et al.</i> 2004]	IGE	25	Y/21	-	N	EEG	GLM
[Gotman <i>et al.</i> 2005]	IGE	25	Y/21	1	N	EEG	GLM
[Federico <i>et al.</i> 2005b]	FE	3	*	-	SD	Video recording	GLM
[Di Bonaventura <i>et al.</i> 2005]	FOS	3	Y /NM	-	Fixation	EEG	GLM
[Di Bonaventura <i>et al.</i> 2006a]	RE	1	Y /NM	-	N	EEG	GLM
[Di Bonaventura <i>et al.</i> 2006b]	FE/ IGE	32/ 11	Y/18	-	N	EEG, Video recording, Patient response button	GLM
[Kobayashi <i>et al.</i> 2006a]	FE	1	Y/27	1	N	EEG	GLM
[Hamandi <i>et al.</i> 2006]	IGE/ SGE	30/ 16	Y/12	-	N	EEG	GLM
[Laufs <i>et al.</i> 2006]	JAE	1	Y/29	-	N	EEG	GLM
[Hamandi <i>et al.</i> 2008]	IGE/ SGE	2/2	Y/32	-	N	EEG	GLM
[Carmichael <i>et al.</i> 2008a]	IGE/ SGE	2/2	Y/32	-	N	EEG	GLM

**Table 3.1: contd.**

Study	Syndrome	Subjects	EEG/Channels	Motion Cut-off (mm)	Seizure Activation	Seizure Detection	Data Analysis Approach
<b>Adults: EEG-fMRI Studies</b>							
[Salek-Haddadi <i>et al.</i> 2009]	ReE	9	Y/11	-	Reading	EEG, Sound recording, EMG, Patient response button	GLM
[Tyvaert <i>et al.</i> 2008]	FE	8	Y/25	-	N	EEG	GLM
[Donaire <i>et al.</i> 2009a]	FE	10	Y/27	-	N	Visually Observed	Seq.GLM
[Tyvaert <i>et al.</i> 2009]	FE	17	Y/25	1	N	EEG, Video recording	Seq.GLM
[LeVan and Gotman 2009]	FE	15	Y/25	-	N	EEG	ICA
[Chassagnon <i>et al.</i> 2009]	FE	1	Y/27	-	N	EEG	GLM
[Marrosu <i>et al.</i> 2009]	ME	1	Y	-	N	EEG	GLM
[Thornton <i>et al.</i> 2010b]	FE	83	Y/32 -64	-	N	EEG	GLM, ICA
<b>Children</b>							
[Jackson <i>et al.</i> 1994]	FE	1	N	-	N	-	$\Delta$ Signal Intensity
[Labate <i>et al.</i> 2005]	IGE	1	Y/18	-	N	EEG	GLM
[Liu <i>et al.</i> 2008]	EMA	4	Y/21	-	N	EEG	GLM
[Moeller <i>et al.</i> 2008a]	CAE	10	Y/30	-	N	EEG	GLM
[Moeller <i>et al.</i> 2008b]	IGE	10	Y/30	-	N	EEG	GLM
[Moeller <i>et al.</i> 2009b]	IGE/ PPR	16/ 14	Y/30	-	Photic	EEG	GLM

**Table 3.1: contd.**

Study	Syndrome	Subjects	EEG/Channels	Motion Cut-off (mm)	Seizure Activation	Seizure Detection	Data Analysis Approach
<b>Children</b>							
[Li <i>et al.</i> 2009]	CAE	15	Y/34	-	N	EEG	GLM
[Moeller <i>et al.</i> 2009a]	IGE	1	Y/30	-	Photic	EEG	GLM
[Bai <i>et al.</i> 2010]	CAE	42	Y/21	>3	DR, SD	EEG	GLM
[Moeller <i>et al.</i> 2010a]	IGE	12	Y/25	-	N	EEG	GLM, ICA
[Berman <i>et al.</i> 2010]	CAE	37	Y/21 -32	-	DR	EEG	GLM
[Moeller <i>et al.</i> 2010b]	IGE	1	Y/32	-	-	EEG	GLM
[Moeller <i>et al.</i> 2010c]	CAE / JAE	14	Y/25 -30	1	-	EEG	Seq.GLM
[Carney <i>et al.</i> 2010]	CAE	11	Y/18	-	DR	EEG	GLM

Abbreviations: FE = Focal Epilepsy, FOS = Fixation off Sensitivity, ME = Musicogenic Epilepsy, JAE = Juvenile Absence Epilepsy, IGE = Idiopathic Generalized Epilepsy, RE = Rasmussan's Encephalitis, SGE = Secondary Generalized Epilepsy, ReE = Reading Epilepsy, EMA = Eyelid Myoclonia with Absences, CAE = Childhood Absence Epilepsy, PPR = Photo paroxysmal Response, N = None, Y = Yes, SD = Sleep Deprivation, Photic = Photic Stimulation, DR = Drug Reduction, EMG = Electromyography,  $\Delta$  = Change, GLM = General Linear Model, ICA = Independent Component Analysis, Seq.= Sequential, EEG = Electroencephalography

\*One patient had simultaneously recorded EEG



### 3.2.2 Recording EEG inside MRI scanner

The recording of scalp EEG and MRI independently are believed to be safe for all practical purposes. Combining these two techniques together raises challenges for EEG data quality, image data quality and patient safety. Acquiring a good quality EEG during fMRI scanning which can be interpreted at the same level as the EEG recorded outside the scanner is the foremost requirement for a successful EEG-fMRI study.

Scalp EEG recording inside the scanner requires the electrodes and leads to be placed within the imaging field of view (FOV) which can result in possible interactions between strong magnetic field of the scanner and metal electrodes. The main sources of artefact on EEG recorded inside the scanner include: strong static magnetic field, switching magnetic gradient fields, electrical and magnetic components of radio frequency (RF) pulses ( $\sim 10 \mu\text{T}$  and 100 MHz), cardiac pulse and head and body movements. Any change in magnetic flux (essentially the component of the magnetic field that is perpendicular to a surface) over time through a conducting medium (loop, surface, volume) can produce an electromotive force in the material resulting in an induced current. This change in magnetic flux and the induced current can be caused by movement (change of position, orientation or shape) of the conducting medium in a magnetic field or change in the magnetic field to which the conducting medium is exposed, which can cause additional health hazards and EEG quality degradation in the form of pulse related and image acquisition (gradient switching and RF) related artefacts [Lemieux *et al.* 1997; Goldman *et al.* 2000; Krakow *et al.* 2000a; Krakow *et al.* 2000b; Lemieux *et al.* 2001; Benar *et al.* 2003; Mirsattari *et al.* 2004; Laufs *et al.* 2008].

It has been recommended to insert one 10 k $\Omega$  current-limiting resistor serially at each electrode lead and twisting (for immobilisation purposes) of the electrode leads in a bundle to reduce the possibility of formation of large loops between subject's head, electrode, electrode lead and EEG amplifier. In turn this avoids health hazards from induced currents flowing through loops and heating of EEG components in contact with the subject. Other important considerations are: using RF transmit/receive coil; avoiding RF antenna effect by ensuring that the length of wires (exposed to the electrical component of the field) is as short as possible and the wires are not resonating and duly secured in place by sand bags [Lemieux

*et al.* 1997;Goldman *et al.* 2000;Konings *et al.* 2000;Krakow *et al.* 2000a;Krakow *et al.* 2000b;Lemieux *et al.* 2001;Benar *et al.* 2003;Mirsattari *et al.* 2004;Laufs *et al.* 2008].

Early EEG-fMRI studies have used magnetic resonance compatible (MR-compatible) electrodes placed individually on the scalp [Krakow *et al.* 2000a;Krakow *et al.* 2000b;Lemieux *et al.* 2001;Salek-Haddadi *et al.* 2006]. Recent studies have used commercially available MR-compatible EEG system and electrode caps (32-64 channels) [Tyvaert *et al.* 2008;Vulliemoz *et al.* 2009;Thornton *et al.* 2010a;Thornton *et al.* 2011] which have incorporated current-limiting resistors in their product design. It is also important that the scalp electrodes used should not touch the skin, have good artefact characteristics and ease of use. The amount of conductive agent between electrodes and scalp should be minimised to avoid forming bridges between electrodes [Laufs *et al.* 2008].

Safety, feasibility as well as human studies for recording EEG signals from implanted intracranial electrodes during MRI scanning have also been conducted [Carmichael *et al.* 2008a;Carmichael *et al.* 2010;Vulliemoz *et al.* 2011], proposing that simultaneous intracranial EEG-fMRI is safe provided head transmit coil is used, electrode leads are separated, and specific absorption rates are limited.

The signal recorded by EEG electrodes is relayed to the EEG recording amplifier through wires. Previously, the wires (metallic) carrying electrical signals from scalp used to be passed to the outside of the electromagnetically shielded room, amplified and digitized using conventional EEG recording hardware. Currently, with the availability of MR-compatible equipment, the EEG signals are amplified and digitized within the scanner room using MR-compatible amplifiers and passed to the recording equipment, outside of the electro-magnetically shielded room, through optical fibres. Moreover, EEG clock is synchronized with the MRI clock which also improves scanner artefact removal from EEG [Allen *et al.* 2000;Laufs *et al.* 2008].

### **3.2.3 Identification of interictal and ictal activity in EEG-fMRI studies**

IEDs are identified on scalp EEG recorded inside the scanner [Aghakhani *et al.* 2004;Bagshaw *et al.* 2004;Bagshaw *et al.* 2005;Salek-Haddadi *et al.* 2006;Tyvaert *et al.* 2008;Vulliemoz *et al.* 2009;Thornton *et al.* 2010a;Thornton *et al.* 2011]. The low sensitivity of routine 20 minute scalp EEG (25 to 56%)

[Smith 2005] may result in spike less EEG-fMRI studies i.e., EEG-fMRI studies without IEDs to be modelled for haemodynamic changes. More recently, a solution has been proposed to correlate the voltage maps of averaged IEDs recorded during the long-term video-EEG monitoring with the voltage maps of scalp EEG recorded inside scanner. This correlation produces a regressor which in turn is applied to evaluate IED related haemodynamic changes [Grouiller *et al.* 2011]. I will call this method as topographical voltage map correlation based analysis [Grouiller *et al.* 2011] in the rest of the thesis.

For identification of seizures, various means of identification have been applied in fMRI studies. These methods include online and retrospective review of EEG, Electromyography (EMG), video recording, observation of ictal semiology (for example: by person inside the scanner room), eye tracking technology, patient response button and sound/voice recording (Table 3.1). Using simultaneous video-EEG recording is a well established method and video recording can provide additional valuable information to identify seizures when EEG is not helpful [Binnie *et al.* 1981;Smith 2005]. In this respect, synchronisation of EEG and video is pivotal, as there may be a time delay for the electrical activity to propagate from the SOZ to the symptomatogenic zone to produce clinical symptoms [Luders *et al.* 2006]. Thus depending solely on video or sound recording may be inaccurate or sub-optimal. Similarly, if consciousness is affected immediately at the beginning of a seizure, the use of patient signal (e.g. via a button press) may not be a reliable way of identifying seizure onset because the patient may not be able to press the button at all due to impairment of consciousness. EMG recordings may also prove helpful during EEG-fMRI studies for atonic/tonic seizures and myoclonic jerks [Richardson *et al.* 2006b].

### **3.2.4 Data quality**

Combined multimodal measurements are generally prone to data quality degradation due to interactions between the recording instruments e.g., EEG and fMRI. Here, I discuss these issues in some detail.

#### **3.2.4a Removing artefacts in EEG data recorded during fMRI**

For most applications, in particular those relying on the quantitative EEG analysis, it is necessary to minimize artefacts on EEG during fMRI acquisition and remove subsequently before any further processing. The EEG quality is

affected by the presence of the scanner's magnetic fields: static, gradient and RF through induction and recording good quality EEG inside the MRI scanner is a challenging task [Parkes *et al.* 2006;Laufs and Duncan 2007;Laufs *et al.* 2008]. Generally speaking EEG recordings inside an MRI scanner are obscured by two main types of artefacts; gradient artefact (GA) and pulse artefact (PA). The GA is produced by the rapidly changing magnetic field used for fMRI acquisition and superimposes the EEG signal making it uninterpretable [Warach *et al.* 1996;Allen *et al.* 2000]. Initial EEG-fMRI studies circumvented this problem by leaving gaps in the fMRI acquisition i.e., acquiring spike triggered fMRI. Thus, EEG features of interest were identified between these gaps of sufficient duration [Warach *et al.* 1996;Kraus *et al.* 1999;Symms *et al.* 1999;Lazeyras *et al.* 2000b;Al-Asmi *et al.* 2003;Archer *et al.* 2003a;Archer *et al.* 2003b]. This technique limits experimental efficiency, therefore, attempts were made to record EEG of sufficient quality throughout fMRI acquisition i.e., continuous EEG-fMRI. The spectral signature of the GA ranges from  $1/TR$  (TR: slice acquisition repetition time) to around 1 kHz (corresponding to the readout gradient) and can appear artificially benign when recorded using standard EEG equipment [Ives *et al.* 1993]. It has been shown that equipment with sufficient bandwidth, sampling rate (1-20KHz) and dynamic range (~20 mV) can capture the artefact with adequate accuracy [Allen *et al.* 2000].

It is assumed that the time gap between acquired volumes and slices remains stable and the pattern of the GA is repeated exactly across slices [Allen *et al.* 2000]. However, the GA is subject to variations in time due to changes in the electrode/lead configuration caused by subject motion. Therefore, immobilisation of head using vacuum cushions and avoiding loop formation by twisting and immobilising the wires using sand bags is advised for recording good quality EEG [Benar *et al.* 2002]. Further reduction in the GA can be done by low-pass filtering, modification of the MR sequence and synchronization of EEG and MRI clocks [Allen *et al.* 2000;Laufs *et al.* 2008]. Commercially available MR compatible equipment has implemented these principles and significantly improved the quality of EEG recorded inside the scanner [Laufs *et al.* 2008;Mulert and Lemieux 2010].

A number of methods have been devised over the years with varying degrees of efficacy to remove GA including frequency domain method [Hoffmann *et al.*

2000], average image artefact subtraction, average image artefact subtraction and adaptive noise cancellation [Allen *et al.* 2000] and principal component analysis (PCA) [Negishi *et al.* 2004; Niazy *et al.* 2005]. To date the most commonly used method is average image artefact subtraction and adaptive noise cancellation [Allen *et al.* 2000], which is used both for online and off-line EEG artefact removal. This works on the basis of the principle that physiological signals and the GA are not correlated and the gap between acquired volumes and slices and the pattern of the GA remains stable. As a result, the GA is estimated and removed by averaging the EEG over a number of epochs corresponding to individual scan repetitions for example [Allen *et al.* 2000].

The PA is also often called the ballistocardiographic (BCG) artefact. This effect results at least in part from the pulsatile movement of the head and scalp in relation to the cardiac cycle which results in induced voltages (artefacts) in the EEG recording circuit. Although a contribution from the Hall effect [Yan *et al.* 2010] which is not ballistic cannot be excluded and hence the terminology pulse related artefact is preferred. This effect may make the identification of epileptic events difficult in most patients. Here again methods based on the average artefact subtraction principle [Allen *et al.* 1998] are the most commonly applied technique for removing the PA. Other methods include applying adaptive filtering [Bonmassar *et al.* 2002], weighted average subtraction [Goldman *et al.* 2000], median filter template [Ellingson *et al.* 2004] or statistical algorithms in independent component analysis (ICA) [Srivastava *et al.* 2005]. All these methods have been validated in a number of studies and provide adequate solutions facilitating the identification of epileptic discharges.

Methods to improve the quality of EEG inside the scanner are under continuous development. Despite these improvements, it is a common view that a certain degree of loss of EEG data quality cannot be avoided [Debener *et al.* 2007; Debener and Herrmann 2008; Debener *et al.* 2008] making the interpretation of events on EEG inside the MRI scanner difficult to some extent [Benar *et al.* 2003].

### **3.2.4b Artefacts in fMRI data: physiological and non-physiological**

The imaging sequence used most for simultaneous EEG-fMRI is gradient echo-planar imaging (EPI) which is prone to distortion and local signal dropout [Schmitt *et al.* 1998; Krakow *et al.* 2000b]. The quality of the fMRI data acquired

during EEG recording in general and seizures in particular can be severely degraded by a number of factors, namely: electromagnetic interference caused by the EEG recording system (passive: distortion from metallic electrodes and leads; active: contamination of MR signal by RF waves generated by the EEG electronics), head motion and pulse and respiration related artefacts. Artefacts produced in the imaging data due to electromagnetic interference can be minimized by proper selection, design and placement of EEG recording equipment as explained in Section 3.2. Here, I describe the methods used to minimize artefacts in the fMRI from head motion, pulse and respiration.

### **Head motion related artefact in fMRI**

Head and body movements as small as a fraction of a millimetre can affect fMRI data quality adversely and may make them unusable or impossible to interpret [Hajnal *et al.* 1994], unless special post-processing steps are utilized [Friston *et al.* 1995a]. Motion is integral to most seizure types. Therefore physical means to limit motion such as vacuum cushions can play an important role at the acquisition stage [Benar *et al.* 2003].

The most common and widely applied motion correction method in fMRI is post acquisition realignment of the fMRI time series using six rigid body realignment parameters (RP). The RPs are the 3 rotation angles and 3 translation shifts that describe the rigid-body relationship between an individual volume in the fMRI time series and the first/mean volume in the series, estimated using a least squares approach and expressed as 6 time series [Friston *et al.* 1995a]. Some investigators [Gotman *et al.* 2005] have used a cut off limit of 1 mm and 1 degree inter-scan motion above which the whole data set is discarded from the analysis. Each seizure related fMRI dataset is potentially unique, in contrast to most cognitive studies in healthy subjects; therefore, another approach is to systematically attempt to extract as much information as possible from every dataset through adapted signal modelling strategies. For example, residual motion related signal may be treated as confound within the general linear modelling framework. These effects can be modelled based on the motion RPs derived from the scan realignment procedure [Friston *et al.* 1995a] and by calculating additional linear and nonlinear motion related effects (using Volterra-expansion of motion RPs) [Salek-Haddadi *et al.* 2003a; Hamandi *et al.* 2006].

For large motion effects, the inclusion of ‘scan nulling’ regressors has also been proposed [Lemieux *et al.* 2007], instead of discarding the scans, on the basis of the principle that inclusion of nuisance effects into models of the fMRI signal, in addition to the effects of interest, can increase sensitivity [Friston *et al.* 1995b]. These regressors attempt to explain the signal variation due to severe head motion events (i.e. above a pre-fixed cut-off value of the inter-scan motion derived from the RP), by representing the effect as a series of four regressors each consisting of a one TR duration Heaviside function corresponding to the scan affected by head motion and the 3 subsequent scans [Lemieux *et al.* 2007].

### **Cardiac pulse and respiration related effects in fMRI: physiological noise**

The cyclical variability of the pulse causes changes in oxygenated blood volume in the brain, and small displacements of the brain tissue from compression and decompression during the cardiac cycle. Similarly, respiration related physiological noise also affects fMRI data quality through changes in magnetic field secondary to chest movements and due to changes in  $p\text{CO}_2$  (partial pressure of  $\text{CO}_2$  in blood) levels causing fluctuations in BOLD. Though these signal variations are present in all fMRI studies, their effect becomes more significant for EEG-fMRI studies of epilepsy in view of the greater imperative of extracting as much information as possible from individual unique datasets and due to the possible clinical implications of the result for the patient’s management in some cases. This is in contrast with most fMRI studies in which a dataset of sub-optimal quality can be replaced with a better one, possibly from a different subject.

Image data correction and regression methods based on the phase of the cardiac cycle relative to the scan acquisition [Glover *et al.* 2000;Liston *et al.* 2006] and ICA based identification of physiological noise related components and removal [Perlberg *et al.* 2007] have been used. For respiration related signals, modelling of respiratory volume per minute and changes in depth and height of respiration as confounds [Birn *et al.* 2006;van Houdt *et al.* 2010] have been employed. It has been shown in EEG-fMRI studies of IEDs [Glover *et al.* 2000;Liston *et al.* 2006] and alpha rhythms [van Houdt *et al.* 2010] that inclusion of these additional regressors as confounds improves sensitivity. In addition cardiac effects have also been modelled in fMRI analysis of seizures [Thornton *et al.* 2010b].

The inclusion of as complete and thorough a model of the effects of motion and physiological confounds such as pulse on the fMRI signal is the best possible

means of avoiding false positive findings and therefore guaranteeing maximum specificity of the observed BOLD signal changes in relation to neural activity. A novel approach to this problem will be presented in detail in Chapter 6.

### **3.2.5 fMRI data analysis**

The overall aim of the analysis is to identify haemodynamic patterns reflecting the epileptic activity. Three types of data analysis approaches have been proposed for this purpose: the identification of regions showing particular patterns of signal fluctuations; the general linear model (GLM); and data-driven such as ICA. Within the GLM framework, the choice and specification of the model embody the investigator's hypotheses. These differ in their underlying assumptions and in particular the degree to which they rely on the use of other data such as synchronously recorded EEG to reveal these patterns.

#### **3.2.5a Identification of variations in MR signal intensity**

Early studies investigating haemodynamic changes during seizures used fMRI without simultaneous EEG or video. In these, fluctuations in signal intensity relative to the mean signal [Jackson *et al.* 1994; Detre *et al.* 1995] or the baseline signal [Krings *et al.* 2000; Kubota *et al.* 2000] were identified to produce maps of ictal fMRI change. Detre and colleagues performed a cross-correlation analysis between regions of the earliest signal change including the well characterised focus and the rest of the brain [Detre *et al.* 1996]. More recently, Auer and colleagues correlated the signal at every voxel in the brain to an internal reference curve defined by visually examining the signal alterations of the voxels in the area responsible for seizures to map changes in other regions [Auer *et al.* 2008].

Detection of variation in signal intensity, as applied in these studies [Jackson *et al.* 1994; Detre *et al.* 1995; Krings *et al.* 2000; Kubota *et al.* 2000], lacks the concurrent information from EEG on seizure onset and evolution. In addition, mapping of putative ictal haemodynamic changes based on visual identification of regions of raw signal intensity changes may be particularly unreliable due to the effects of motion and MR signal drift.

Spike triggered fMRI studies [Ives *et al.* 1993; Warach *et al.* 1996; Krakow *et al.* 1999; Symms *et al.* 1999; Al-Asmi *et al.* 2003] also measured MR signal variations above a certain threshold between active (spike triggered) and resting (without spikes) fMRI data.



### 3.2.5b Correlation analysis: general linear model

The analysis of most fMRI time series data relies on the application of the GLM which is a correlation based technique in a mass univariate (voxel by voxel) approach where the signal is expressed as a weighted sum of effects, fitted to the data at each voxel and subsequent mapping of the fitted weight statistics [Friston 1996]. In practice, it is most commonly implemented in the form of a design matrix encompassing all known effects on the signal either as effects of interest (EOI) or confounds. This is also the case in most EEG-fMRI applications, where the effects associated with epileptic discharges identified on EEG are incorporated into the GLM as a regressor of interest, to map the degree of correlation of this regressor with the measured signal across all voxels. Each EOI to be included as a regressor in a GLM design requires the choice of a mathematical representation, and is convolved with an HRF.

A number of questions need to be considered and explored further in detail to find an appropriate and more realistic way of modelling IEDs and seizures in fMRI data analysis. For example, can it be presumed that the haemodynamic changes that take place during a seizure that lasts 10 seconds correspond to a neuronal event with fixed intensity over that duration? More specifically, can a seizure be realistically represented as an event block analogous to those used in block design cognitive fMRI studies? There is also the issue of the seizure onset and the preictal state; do they correspond to distinct states that fundamentally differ from the baseline or is there a gradual haemodynamic transition from interictal to ictal state? Similarly, can multiple seizures be considered as the same phenomenon and therefore be grouped as a single effect for the purpose of modelling?

#### **Event representation**

The EOI are usually represented as box-car functions for example in the fMRI studies following a paradigm such as cognitive studies, or idealised zero-duration stick functions for example in the fMRI studies of random brief events such as IEDs [Salek-Haddadi *et al.* 2006; Tyvaert *et al.* 2008; Vulliemoz *et al.* 2009; Thornton *et al.* 2010a; Thornton *et al.* 2011].

However, seizures are dynamic in nature and potentially involve a complex sequence of various combinations of brain regions over time. This complexity makes their mathematical representation for GLM model building much more

difficult, which is reflected by the variety of approaches used to analyse ictal fMRI data.

In the case of provoked seizures this is somewhat simplified by the possibility of identifying a clear seizure onset using the timing of provoking factor such as: eye closure in FOS [Krakow *et al.* 2000c;Iannetti *et al.* 2002;Di Bonaventura *et al.* 2006b], music in musicogenic seizures [Morocz *et al.* 2003;Marrosu *et al.* 2009] and reading in reading epilepsy [Salek-Haddadi *et al.* 2009]. In some case it may be possible to provoke repeated seizures, separated by periods of rest which may therefore be considered repetitions of the same type of event (similar to the block design of conventional cognitive fMRI studies) and represented mathematically as box-car [Krakow *et al.* 2000c;Iannetti *et al.* 2002;Morocz *et al.* 2003;Marrosu *et al.* 2009] or as series of stick functions [Salek-Haddadi *et al.* 2009]. An important issue which has not been taken into account for provoked seizures is the possible time lag between stimulus presentation and seizure onset, which could allow further exploration of the mechanisms of seizure generation.

In contrast, spontaneous seizures such as focal or absence seizures which occur at random may have uncertainty in the identification of the event onset given the available means. Ictal events must be identified employing different methods (Section 3.2.3 and Table 3.1), and categorised using the same data. Onset and offset timings of single or multiple seizures or preictal states have been used to define the EOI to be modelled and represented as variable duration blocks (depending upon the seizure duration) to be included in the design matrix as regressors [Salek-Haddadi *et al.* 2002;Hamandi *et al.* 2006;Tyvaert *et al.* 2008;Salek-Haddadi *et al.* 2009].

When seizures are modelled as a single block, though they reveal BOLD changes, the ability to differentiate seizure onset from propagated activity is diminished. Based on this hypothesis, peri-ictal haemodynamic changes have been mapped sequentially; from prior to the seizure onset (preictal: 120s prior to clinical seizure onset [Donaire *et al.* 2009a], 9s prior to the ictal discharge onset on EEG [Tyvaert *et al.* 2009]) up to pre-specified time following the seizure offset (postictal: 60s after clinical seizure end [Donaire *et al.* 2009a], 10s after the EEG discharge offset [Tyvaert *et al.* 2009]). Donaire and co-workers divided the preictal, ictal and postictal blocks into sequential fixed width 10s blocks each representing a different effect (i.e. independent regressors in the GLM) and

compared with a baseline period (20s temporally unrelated to the seizure). Secondly, the signals in each 10s block were also compared with that in the contiguous 10s block within the GLM framework [Donaire *et al.* 2009a;Donaire *et al.* 2009b]. This approach provides the ability to map and differentiate seizure onset and seizure propagation; however it makes minimum use of the simultaneously recorded EEG. More recently, Thornton and co-workers have modelled seizures by dividing each seizure into three distinct and consecutive phases (representing each as a block of variable durations): early ictal, clinical ictal and late ictal, based on the onset, duration and electrical evolution over time. The authors argued that this modelling approach makes better use of the available physiological information and allows for the better understanding of propagation of haemodynamic effects between phases [Thornton *et al.* 2010b].

Based on the principle that all quantifiable effects should be included in the GLM design matrix to reduce the amount of unmodelled residual signal variance, IEDs and confounds: RP and pulse regressors have also been represented in the same design matrix as separate regressors and confounds respectively (Section 2.4.1 and 2.4.2) [Salek-Haddadi *et al.* 2002;Gotman *et al.* 2005;Hamandi *et al.* 2006;Laufs *et al.* 2006;Tyvaert *et al.* 2008;Chassagnon *et al.* 2009;Salek-Haddadi *et al.* 2009;Thornton *et al.* 2010b]. As yet, however, there is no consensus on the degree to which such confounds must be modelled.

An important question here is; how should one represent multiple seizures in the design matrix? This is of utmost importance because; unless all seizures recorded are electroclinically stereotyped, they may be manifestations of a variety of underlying epileptogenic networks, in which case they must be represented as different effects (different regressors) in the GLM. Three different approaches have been applied:

- Similar repeated seizures as variable duration blocks in a single regressor [Tyvaert *et al.* 2008].
- Each epileptic event of variable duration represented as a separate regressor and the event with the longest duration and clear electrical and spatial propagation represented as seizure [Tyvaert *et al.* 2009].
- Ictal phase specific effects represented as variable duration blocks across seizures [Thornton *et al.* 2010b].

**Epilepsy related HRF**

Once the events are identified and represented mathematically they must convolve with an informed basis set representing the shape of the HRF<sup>3</sup> for the purpose of inclusion in the GLM. The creation of regressors to represent the ictal events themselves and the choice of HRF for ictal events are particularly problematic given that ictal events can last many minutes, and may involve multiple brain regions at different times as demonstrated by seizure semiology and electrophysiology. In addition, the nature of BOLD changes associated with ictal events is not completely known. They may remain stationary in a particular brain region once started, or may evolve and diminish before propagating to other brain areas. Thus, longer duration and dynamic nature of seizures increase the difficulty to select a basis set or shape of HRF for seizures.

On the other hand, an important consequence of the univariate aspect of the GLM approach and the choice of basis set is the possibility of accounting for spatial variability in the shape of HRF as it has been shown in interictal and ictal studies that the shape and timing of the peak HRF may deviate from the canonical shape in relation to generalised activity [Benar *et al.* 2002; Bagshaw *et al.* 2004; Hawco *et al.* 2007; Moeller *et al.* 2008b; Jacobs *et al.* 2009; Siniatchkin *et al.* 2010; Masterton *et al.* 2010; Moeller *et al.* 2010c; Grouiller *et al.* 2011]. It has also been shown that the shape of HRF may be epilepsy syndrome specific and the use of syndrome specific HRF may improve the localisation of BOLD signal changes [Masterton *et al.* 2010]. The lesser the flexibility of the basis set the fewer the questions that can be addressed related to the time course of the ictal related changes. For single-term basis sets, such as the canonical HRF, the only question that can be addressed is the sign of the putative BOLD changes. Therefore, inter-dependence between the temporal and spatial aspects of the analysis is embodied in the necessary choice of HRF for GLM model building,

---

<sup>3</sup> In this work, the use of the conventional ‘response function’ terminology (as in HRF, which is derived from cognitive experiments with clear causality) does not imply a causal relationship between epileptic events and putative BOLD signal change. In the context of resting-state EEG-fMRI experiments, the use of features identified on scalp EEG does not guarantee that any fMRI signal change associated with these events will occur *after* the event. This is due to the possibility of a degree of decoupling due to the limited sensitivity of scalp EEG: for example, one could imagine physiological changes (associated with haemodynamic changes) taking place in the brain *before* they appear on the scalp and in a time-locked fashion. In the same spirit, I use the ‘epileptic event related BOLD *signal change*’ terminology in preference to ‘BOLD *response*’.

which reflects the investigator's specific hypotheses about the inter-relationship between the ictal phenomenology and the fMRI signals [Salek-Haddadi *et al.* 2002;Archer *et al.* 2006;Hamandi *et al.* 2006;Laufs *et al.* 2006;Hamandi *et al.* 2008;Salek-Haddadi *et al.* 2009;Donaire *et al.* 2009a;Donaire *et al.* 2009b;Thornton *et al.* 2010b].

For more extensive basis sets such as the Fourier set consisting of a linear combination of  $n$  sine and  $n$  cosine functions, the time course can be evaluated over the specified time window [Salek-Haddadi *et al.* 2002;Thornton *et al.* 2010b]. Multiple GLMs each with different gamma functions (time to peak: 3, 5, 7, and 9s) have also been used to account for some variability in the timing of the HRF [Aghakhani *et al.* 2004;Kobayashi *et al.* 2006b;Tyvaert *et al.* 2008;Chassagnon *et al.* 2009;Jacobs *et al.* 2009].

### **Common features: mapping group effects**

The GLM framework has been used to explore group effects by combining the single subject analyses using spatial normalisation [Penny and Holmes 2004] for the purpose of making population level inferences [Friston *et al.* 1999a;Worsley *et al.* 2002]. This is particularly useful to identify shared features and is probably most relevant in stereotypical syndromes such as IGE [Gotman *et al.* 2005], CAE [Moeller *et al.* 2008a] and some types of SGE [Hamandi *et al.* 2006].

### **3.2.5c Independent component analysis**

ICA is a well established and powerful data-driven approach based on basic assumptions regarding the properties of the sources responsible for the observed signals, particularly their statistical independence. It can be used to decompose multi-channel time series data into spatially or temporally independent components by maximising their statistical independence. If the signal satisfies the necessary conditions, each independent component represents the activity of one of the sources of the signal [Calhoun *et al.* 2001;McKeown *et al.* 2003]. A common assumption in ICA algorithms is that the sources are spatially stationary [McKeown *et al.* 1998;McKeown *et al.* 1999] which is helpful in separating the signal related sources from noise sources which are presumed to be non-stationary [DeMartino *et al.* 2007]. However seizures involve complex spatial and temporal propagation; therefore, the applicability of ICA to such a dynamic process must be questioned in principle. Nonetheless, ICA has been used to study ictal

haemodynamic patterns with some interesting results as discussed below, making this assumption of stationarity less relevant.

The components identified by ICA cannot be ranked by degree of importance, in contrast to PCA. Furthermore for spatial ICA of fMRI time series data, the number of components can be up to the number of scans. Therefore, some form of data dimensionality reduction step is commonly employed either by pre-specifying or calculating (using PCA [McKeown *et al.* 1998]) or using a model of the noise [Beckmann and Smith 2004] and the number of sources are identified. Furthermore, spatiotemporal characterisation of BOLD signals on one hand and fMRI artefacts on the other combined with a pattern recognition technique has also been used to automatically classify components [DeMartino *et al.* 2007; Rodionov *et al.* 2007].

#### **Applications of ICA in epilepsy**

Morocz and colleagues [Morocz *et al.* 2003] and Donaire and colleagues [Donaire *et al.* 2009b] applied ICA on ictal fMRI time series data, and visually compared the activity maps with the GLM based statistical maps of BOLD changes. LeVan and co-workers [LeVan *et al.* 2010b] have used an iterative fixed-point method [Hyvarinen and Oja 2000] to compute independent components (IC), and repeated the decomposition 20 times to identify stable and reproducible sources. They separated ictal components from physiological components, artefacts, residual motion, and cerebral BOLD activity by applying GLM based modelling assumptions whereby: HRF convolved with seizures was fitted to IC time courses in an auto-regressive model and activation maps for ictal components were generated. For multiple seizures in the same patient, single HRF shape was calculated presuming it remains the same for each seizure [LeVan *et al.* 2010b]. It is also argued that although ICA can reveal BOLD changes and noise separately [McKeown and Sejnowski 1998; McKeown *et al.* 1998] it cannot specifically separate the different types of structured noise [LeVan *et al.* 2010b]. Rodionov *et al.*, [Rodionov *et al.* 2007] and Thornton *et al.* [Thornton *et al.* 2010b] applied cortex based spatial ICA with automated component classification to identify IED and seizure related ICs spatially concordant with the epileptogenic areas in patients with focal epilepsy.

#### **3.2.5d What are the respective roles of GLM or ICA based analyses?**

The GLM embodies an approach to fMRI data analysis based on fitting a postulated model of the fMRI time series to the data. It therefore relies entirely on the ability of the investigator to devise a suitable model to allow the identification of the brain regions for which the degree of fit is sufficiently high (in relation to the level of unexplained variance and given the number of voxels at which the degree of fitness is tested). In other words, this approach can only be used to answer questions of the type: in which parts of the brain does the fMRI signal match a pre-specified pattern? Assuming the availability of suitable models for each effect, this approach can be used to account for multiple effects simultaneously such as the BOLD changes related to seizure and interictal activity on one hand [Tyvaert *et al.* 2008;Chassagnon *et al.* 2009;Salek-Haddadi *et al.* 2009;Thornton *et al.* 2010b] and various sources of physiological noise through the inclusion of pulse [Liston *et al.* 2006], respiration [van Houdt *et al.* 2010] and motion effects [Salek-Haddadi *et al.* 2009]. Therefore, this requires the proper identification of events of interest, the mathematical representation of these events in the GLM framework and a choice of haemodynamic kernel as discussed above. Given that the aim of such studies is to reveal BOLD changes specifically related to seizures in any part of the brain and that this depends on the separation between the ictal and interictal states, it is crucial to realise that the GLM approach effectively attempts to explain all fMRI signal variations across the entire brain based on EEG (and possibly video).

In comparison, ICA of fMRI by not relying on a postulated specific model of the signal time course, can be seen as a way of freeing the analysis from the bias of scalp EEG. However, this lack of prior model shifts the problem to the interpretation of the often very numerous components. Nonetheless, ICA of fMRI can reveal BOLD patterns that can be associated with seizures through post-hoc comparison with EEG [Thornton *et al.* 2010b]. Simultaneous intracranial EEG-fMRI [Vulliemoz *et al.* 2011] will provide important validation data.

### 3.2.6 Validation of fMRI findings

Given that the aim of fMRI studies of interictal and ictal activity is localisation, validation requires two elements: a gold standard (icEEG is used as gold standard in most epilepsy surgery programmes) and a method to compare the fMRI maps with the gold standard. Notwithstanding the precise nature of the gold standard, the latter usually requires the application of co-registration of the fMRI maps and

gold standard onto a structural MR image of the subject's brain. Because of the complex nature of the fMRI maps, summarising the level of spatial agreement can be challenging and various criteria (Table 3.2) have been applied which can be grouped into the following broad categories:

1. Localisation of the most statistically significant BOLD change cluster, and also taking into account the localisation of other BOLD change clusters [Salek-Haddadi *et al.* 2006;Vulliemoz *et al.* 2009;Thornton *et al.* 2010a;Thornton *et al.* 2010b;Thornton *et al.* 2011]
2. Localisation of the cluster corresponding to the earliest BOLD increase, with a cut-off threshold for statistical significance and spatial extent [Donaire *et al.* 2009a].
3. Localisation of the most statistically significant BOLD change cluster with a cut-off threshold for spatial extent (greatest number of voxels) [Di Bonaventura *et al.* 2006b].
4. Localisation of the most statistically significant BOLD change cluster [Tyvaert *et al.* 2008].
5. Localisation of all clusters of BOLD change above predefined statistical and spatial threshold [Gotman *et al.* 2005].
6. Localisation of the most statistically significant BOLD cluster, and also the most statistically significant cluster in the individual lobes [Hamandi *et al.* 2006].

In some instances concordance relative to the gold standard is defined (Table 3.2) in terms of Cartesian [Iannetti *et al.* 2002;Salek-Haddadi *et al.* 2003a;Hamandi *et al.* 2006;Carney *et al.* 2010] or cortically informed [Thornton *et al.* 2010b] distance, while in others it is defined at the lobar level [Salek-Haddadi *et al.* 2006;Salek-Haddadi *et al.* 2009;Tyvaert *et al.* 2009].

In the experimental studies described in the following chapters, I use a concordance scheme based on the approach described in the above mentioned category 1 and compare the localisation of BOLD with the localisation defined independently from other non-invasive and invasive techniques. Where available, I compare the localisation from EEG-fMRI with that of gold standard i.e., icEEG and also postsurgical outcome. The pros and cons of this approach are discussed in the relevant chapters.



**Table 3.2: Sensitivity, criteria for concordance and degree of concordance from previous publications on seizures using fMRI or EEG-fMRI**

Study	Subjects	Selection Criteria	Subjects with Seizures	Subjects with fMRI Results	Criteria for concordance and localisation of BOLD changes	Degree of Concordance
Iannetti <i>et al.</i> 2002	3	Refractory epilepsy triggered by fixation off sensitivity	3	3	Localisation of all BOLD clusters according to co-ordinates system in MNI space at sub-lobar level	NA
Aghakhani <i>et al.</i> 2004	25	IGE patients with 2-4 Hz GSWDs	15	15	Co-registration and localisation of all BOLD clusters with individual anatomical scans	NA
Gotman <i>et al.</i> 2005	25	IGE patients with 2-4 Hz GSWDs	15	15	Localisation of all BOLD clusters according to co-ordinates system in MNI space at lobar level	NA
Federico <i>et al.</i> 2005	3	FE patients undergoing pre-surgical evaluation	3	3	Visual comparison of the statistically most significant BOLD cluster with; icEEG based (Cases:1/3) or electroclinical, MRI and Ictal SPECT based (Cases:2/3) SOZ	1/3
Di Bonaventura <i>et al.</i> 2006	43	FE/ IGE patients with well-defined epileptic syndrome, easily recognizable EEG activity and without extensive motion during seizures	13	9	Visual comparison of the location of all BOLD clusters (threshold for amplitude ( $p < 0.05$ ) and extent ( $350 \text{ mm}^3$ )) with electroclinical and MRI based SOZ. All clusters were labelled using Talairach atlas according to co-ordinates system in MNI space at lobar	8/9

**Table 3.2: Contd.**

<b>Study</b>	<b>Subjects</b>	<b>Selection Criteria</b>	<b>Subjects with Seizures</b>	<b>Subjects with fMRI Results</b>	<b>Criteria for concordance and localisation of BOLD changes</b>	<b>Degree of Concordance</b>
Hamandi <i>et al.</i> 2006	46	IGE /SGE patients with frequent GSWDs	33	22	Localisation of all BOLD clusters according to co-ordinates system in MNI space at lobar level	NA
Salek-Haddadi <i>et al.</i> 2008	9	Reading epilepsy patients	6	6	Visual identification and localisation of the statistically most significant and other BOLD clusters for individual patients	
Tyvaert <i>et al.</i> 2008	8	From the EEG-fMRI data-base, patients with MCD and interictal and ictal Events	8	8	Visual comparison of the location of the most statistically significant BOLD clusters with; icEEG (Cases:2/8), or electroclinical and lesions on MRI based (Cases:6/8) SOZ	8/8
Donaire <i>et al.</i> 2009	10	From the EEG-fMRI data-base, patients with at least 1 clinical seizure during fMRI, with Ictal SPECT and with icEEG Evaluation	10	5	Co-registration and comparison of the earliest BOLD cluster (threshold for extent (minimum 5 contiguous voxels) and statistical significance ( $t > 3$ )) with; icEEG (Cases:2/5) or electroclinical, MRI and Ictal SPECT based (Cases:3/5) SOZ	4/5
Tyvaert <i>et al.</i> 2009	17	From the EEG-fMRI database, patients with spontaneous seizure during fMRI	17	10	Visual comparison of the location of the earliest BOLD cluster (threshold for extent and statistical significance) with; icEEG (Cases: 3/10) or electroclinical, lesion on MRI based (Cases: 7/10) SOZ.	9/10

**Table 3.2: Contd.**

Study	Subjects	Selection Criteria	Subjects with Seizures	Subjects with fMRI Results	Criteria for concordance and localisation of BOLD changes	Degree of Concordance
LeVan <i>et al.</i> 2009	15	From the EEG-fMRI database, patients with seizure during EEG-fMRI	15	14	Visual comparison of the location of the statistically most significant BOLD cluster (threshold for extent (minimum 5 contiguous voxels) and statistical significance ( $t > 3$ )) or ICA based clusters correlated with GLM, with; icEEG (Cases:4/15) or electroclinical and MRI based (Cases:11/15) SOZ	13/ 15
Thornton <i>et al.</i> 2010	83	Refractory focal epilepsy patients undergoing pre-surgical evaluation	9	7	Co-registration and comparison of all the statistically significant BOLD clusters with icEEG (Cases:8/9) based SOZ, and defined as: Concordant: when all significant BOLD clusters were within the SOZ and the area of maximal signal change was in the same gyrus and within 2 cm of the icEEG electrode concordant plus: when the statistically most significant BOLD cluster was concordant but additional discordant clusters were also present	4/9
Liu <i>et al.</i> 2008	4	Eye lid myoclonia associated with absences patients	4	4	Visual identification and localisation of all BOLD clusters threshold for extent (minimum 5 contiguous voxels) and statistical significance ( $t > 3$ ) for individual patients at lobar and sub-lobar level	NA

**Table 3.2: Contd.**

<b>Study</b>	<b>Subjects</b>	<b>Selection Criteria</b>	<b>Subjects with Seizures</b>	<b>Subjects with fMRI Results</b>	<b>Criteria for concordance and localisation of BOLD changes</b>	<b>Degree of Concordance</b>
Moeller <i>et al.</i> 2008	10	Newly diagnosed CAE patients	6	6	Visual identification and localisation of all BOLD clusters, co-registered with individual MRI (MNI space), threshold for extent (minimum 5 contiguous voxels) and statistical significance ( $t > 4.7$ )	NA
Li <i>et al.</i> 2009	15	CAE patients with frequent GSWDs	6	6	Visual identification and localisation of all BOLD clusters threshold for extent (minimum 5 contiguous voxels) and statistical significance ( $t > 3$ ) for individual patients at lobar and sub-lobar level	NA
Moeller <i>et al.</i> 2009	16/ 14	IGE patients/healthy subjects with PPR	6	6	Visual identification and localisation of all BOLD clusters, co-registered with individual MRI (MNI space), threshold for extent (minimum 5 contiguous voxels) and statistical significance ( $t > 4.7$ )	NA
Bai <i>et al.</i> 2010	42	CAE patients with 3-4 Hz GSWDs	9	9	Visual identification and localisation of all BOLD clusters, co-registered with individual MRI (MNI space), threshold for statistical significance ( $p < 0.05$ , FDR)	NA
Berman <i>et al.</i> 2010	37	CAE patients with 3-4 Hz GSWDs, without additional seizure types or structural brain abnormality or neurologic disorders	9	9	Visual identification and localisation of all BOLD clusters, co-registered with individual MRI (MNI space), threshold for extent (minimum 3 contiguous voxels) and statistical significance ( $p < 0.05$ , FDR)	NA

**Table 3.2: Contd.**

Study	Subjects	Selection Criteria	Subjects with Seizures	Subjects with fMRI Results	Criteria for concordance and localisation of BOLD changes	Degree of Concordance
Moeller <i>et al.</i> 2010	14	CAE patients with 3 Hz GSWDs (3-30s, inducible by hyperventilation), transient impairment of consciousness	9	9	Visual identification and localisation of all BOLD clusters, co-registered with individual MRI (MNI space), threshold for extent and statistical significance ( $F > 5.7$ )	NA
Carney <i>et al.</i> 2010	11	Children with absences as exclusive seizure type, not on medications, with 3-3.5 Hz GSWDs inducible with hyperventilation, with normal early development and normal structural imaging	11	11	Visual identification and localisation of all BOLD clusters, co-registered with individual MRI (MNI space), threshold for statistical significance ( $p < 0.001$ )	NA

Abbreviations: SOZ = Seizure Onset Zone, BOLD = Blood Oxygen Level Dependent, NA = Not Applicable, IGE = Idiopathic Generalized Epilepsy, GSWDs = Generalized Spike Wave Discharges, FE = Focal Epilepsy, MNI = Montreal Neurological Institute, SGE = Secondary Generalized Epilepsy, MCD = Malformations of Cortical Development, icEEG = Intracranial EEG, CAE = Childhood Absence Epilepsy, PPR = Photo paroxysmal Response, FDR = False Discovery Rate

### 3.3 Applications of EEG-fMRI in epilepsy

Simultaneous EEG-fMRI can provide new and unique insight on the localisation of brain networks involved in interictal and ictal discharges. Following investigations into the feasibility, sensitivity and specificity of EEG-fMRI findings in epilepsy [Lemieux *et al.* 1997; Krakow *et al.* 2000b; Lemieux *et al.* 2001; Al-Asmi *et al.* 2003; Salek-Haddadi *et al.* 2006], the literature on EEG-fMRI has expanded rapidly especially on: the study of IED related haemodynamic changes in focal [Archer *et al.* 2003b; Bagshaw *et al.* 2005; Salek-Haddadi *et al.* 2006; Kobayashi *et al.* 2006d; Jacobs *et al.* 2009; LeVan *et al.* 2010a] and generalized epilepsy [Hamandi *et al.* 2006], the effects of epilepsy on neurovascular coupling [Carmichael *et al.* 2008a], localisation of epileptogenic zone in focal epilepsy [Federico *et al.* 2005b; Salek-Haddadi *et al.* 2006; Zijlmans *et al.* 2007; Jacobs *et al.* 2008b; Thornton *et al.* 2010a] and the involvement of epileptic networks for 3Hz generalized spike wave discharges (GSWDs) [Gotman *et al.* 2005; Hamandi *et al.* 2006; Hamandi *et al.* 2008].

However, the delineation of the brain areas producing IEDs may not suffice to localise the SOZ, which is clinically more important than IZ localised by IEDs [Luders *et al.* 2006]. Thus there has been an increasing interest in investigating specific seizure related haemodynamic changes using fMRI [Jackson *et al.* 1994; Detre *et al.* 1995; Federico *et al.* 2005b; Archer *et al.* 2006; Hamandi *et al.* 2006; Tyvaert *et al.* 2008; LeVan and Gotman 2009; Tyvaert *et al.* 2009; Donaire *et al.* 2009a; Donaire *et al.* 2009b; Archer *et al.* 2010; Bai *et al.* 2010; Berman *et al.* 2010; Carney *et al.* 2010; LeVan *et al.* 2010b; Thornton *et al.* 2010b], however the data on seizure related haemodynamic changes is not as extensive as for the interictal state due to methodological and practical issues as discussed in Section 3.2.

EEG-fMRI has advantages over other methods (scalp EEG, MEG, PET and SPECT) available for investigating epilepsy including: non-invasive nature; no exposure to radioactive material; and high spatiotemporal resolution [Laufs *et al.* 2008; Logothetis 2008]. Evidence relevant to assessing the potential clinical value of EEG-fMRI applied to ictal activity, either in relation to localisation of the SOZ or syndrome classification, is very limited. To the best of my knowledge, no systematic comparison of the findings of EEG-fMRI with ictal SPECT or PET has been performed to date. Validation in individual cases by comparison with icEEG

and or ictal SPECT or PET, is generally encouraging while keeping in mind the limitations of these techniques and of our general understanding of seizure initiation and propagation. No formal assessment of sensitivity and specificity has been done to date, possibly reflecting both the technique's novelty and an early realization of the difficulties in modelling the relationship between EEG and semiology on one hand and fMRI on the other and interpreting the resulting maps. Therefore, we are limited to relatively anecdotal observations.

### 3.3.1 How many patients will show BOLD changes?

The sensitivity of EEG-fMRI to map IED related BOLD changes had been limited in part by the lack of epileptiform activity during fMRI, with roughly 40% of cases showing no clear IED, but also because of sub-optimal modelling of the fMRI signal, with 30% of cases with IED not showing significant BOLD changes [Salek-Haddadi *et al.* 2006]. Due to recent advances in modelling interictal BOLD changes, the technique's sensitivity has been shown to increase to 78% in one study using topographical voltage map correlation based analysis [Grouiller *et al.* 2011]. However, prospective studies will be required to establish the clinical utility of this method.

On the other hand, the sensitivity in terms of patients who will have a seizure during EEG-fMRI acquisition varies from 4% to 100% in the published literature, and the sensitivity in terms of patients revealing BOLD changes out of patients with seizures during EEG-fMRI acquisition varies from 66% to 100% [Jackson *et al.* 1994; Detre *et al.* 1995; Federico *et al.* 2005b; Archer *et al.* 2006; Hamandi *et al.* 2006; Tyvaert *et al.* 2008; LeVan and Gotman 2009; Salek-Haddadi *et al.* 2009; Tyvaert *et al.* 2009; Donaire *et al.* 2009a; Donaire *et al.* 2009b; Archer *et al.* 2010; Bai *et al.* 2010; Berman *et al.* 2010; Carney *et al.* 2010; LeVan *et al.* 2010b; Thornton *et al.* 2010b]. This wide range of sensitivity largely depends on the variable patient selection criteria used in different studies (Table 3.2). Similarly, the ability of EEG-fMRI studies to localise the SOZ in focal epilepsy is also quite variable depending upon the various modelling approaches and concordance criteria applied (Tables 3.1 and 3.2).

### 3.3.2 IED related networks

EEG-fMRI has been employed to investigate IED related haemodynamic networks in patients undergoing presurgical evaluation, and also in different epilepsy syndromes and pathologies.

In patients undergoing presurgical evaluation of epilepsy, localisation of IED related BOLD changes provide additional information at lobar level having good concordance with the epileptic focus [Krakow *et al.* 1999; Lazeyras *et al.* 2000b; Al-Asmi *et al.* 2003; Salek-Haddadi *et al.* 2006; Vulliemoz *et al.* 2009; Thornton *et al.* 2010a; Grouiller *et al.* 2011; Thornton *et al.* 2011] which can be used as target areas for placing intracranial electrodes. Localisation of IED related BOLD changes has also been compared with the electrical source localisation, suggesting good concordance between the two techniques [Seeck *et al.* 1998; Lemieux *et al.* 2001; Bagshaw *et al.* 2006; Benar *et al.* 2006; Vulliemoz *et al.* 2009]. There are only a few studies comparing the localisation of BOLD changes with icEEG [Seeck *et al.* 1998; Lazeyras *et al.* 2000b; Al-Asmi *et al.* 2003; Benar *et al.* 2006; Thornton *et al.* 2011] which is still widely considered as the gold standard in presurgical evaluation of epilepsy, albeit with severe constraints in terms of the limited spatial sampling of the brain.

In a recent study [Zijlmans *et al.* 2007], it has been shown that EEG-fMRI proved very useful in presurgical evaluation of epilepsy to confirm or to refute multifocality in patients who had been rejected from epilepsy surgery on conventional presurgical assessment, and opened new aspects to be confirmed with icEEG. Further studies on IED related BOLD networks in refractory focal epilepsy and their comparison with postsurgical outcome have suggested that EEG-fMRI may have a predictive role in future [Thornton *et al.* 2010a; Thornton *et al.* 2011]. There has been only one simultaneous icEEG-fMRI study [Vulliemoz *et al.* 2011], in two patients undergoing presurgical evaluation with implanted electrodes, revealing that IEDs recorded on icEEG from very focal areas can also show BOLD changes in focal areas and distributed networks.

EEG-fMRI has been applied to study the following sub-types of epilepsy: temporal lobe epilepsy (TLE), extra-temporal lobe epilepsy (ExTLE) [Salek-Haddadi *et al.* 2006; Kobayashi *et al.* 2006d; Laufs *et al.* 2007b; Kobayashi *et al.* 2009], BECTS [Archer *et al.* 2003b; Masterton *et al.* 2010] and lesional and focal epilepsy in children [Jacobs *et al.* 2007; Jacobs *et al.* 2008a; Jacobs *et al.* 2009],



revealing IED related BOLD networks in an attempt to possibly classify epilepsies on the basis of BOLD networks. Investigation of IED related BOLD changes in TLE has been particularly important in the context that scalp EEG may not detect deep sources of IEDs. The yield of EEG-fMRI studies in TLE has been variable from high [Kobayashi *et al.* 2006d;Kobayashi *et al.* 2009] to moderate/low [Salek-Haddadi *et al.* 2006] in different studies. Moreover, IED related BOLD decreases have been seen in the so-called ‘default mode network’ (DMN) [Raichle *et al.* 2001] more commonly in TLE [Laufs *et al.* 2007b] as compared to ExTLE [Salek-Haddadi *et al.* 2006]. It is argued that these BOLD decreases in DMN may reflect changes in consciousness [Laufs *et al.* 2007b].

IED related BOLD decreases have also been observed in epileptic focus [Salek-Haddadi *et al.* 2006;Kobayashi *et al.* 2006d] and in and around areas of dysplastic cortex in MCDs [Federico *et al.* 2005a;Kobayashi *et al.* 2006c;Tyvaert *et al.* 2008]. The possible reasons suggested for IED related BOLD decreases in these studies include: vascular steal, abnormal coupling or neuronal inhibition; however, it is difficult to prefer one reason over the other. Other studies have also investigated IED related BOLD changes in cavernous angiomas [Kobayashi *et al.* 2007], tuberous sclerosis [Jacobs *et al.* 2008b] and FCD [Tyvaert *et al.* 2008;Thornton *et al.* 2011] and have revealed focal changes in the areas of pathology as well as widespread changes in distributed networks.

Widespread IED related BOLD changes in cortical and subcortical structures, in addition to focal BOLD changes in epileptic focus, have been observed. These findings suggest that IEDs may recruit an epileptic network involving thalamus specifically when they are bilateral and synchronous [Federico *et al.* 2005a;Aghakhani *et al.* 2006;Hamandi *et al.* 2006]. Moreover, BOLD changes prior to IED onset on scalp EEG have also been shown, which are found to be more focal than BOLD changes at IED onset [Jacobs *et al.* 2009] suggesting increased neuronal activity which is not yet visible on scalp EEG because of its low sensitivity [Ray *et al.* 2007].

### **3.3.3 Localisation of seizure onset in focal epilepsy**

Early case reports with fMRI alone showed MR signal build up and recovery to baseline in the presumed seizure onset zone for clinical/subclinical seizures [Jackson *et al.* 1994;Detre *et al.* 1995;Kubota *et al.* 2000]. In another case-report, Krings and colleagues observed, temporally and spatially distinct, early

MR signal change in perilesional cortex prior to the clinical seizure and an increase in MR signal intensity in eloquent cortex during clinical seizure (symptomatogenic zone)[Krings *et al.* 2000].

In two case reports [Salek-Haddadi *et al.* 2002;Kobayashi *et al.* 2006a] and a case series [Donaire *et al.* 2009a], using EEG-fMRI and GLM based data analysis approach, time locked BOLD increase within the presumed SOZ was revealed during seizures. The amplitude of BOLD signal increase was found to be generally higher in the presumed SOZ in comparison to other areas. In a series of patients with MCDs [Tyvaert *et al.* 2008], using GLM based data analysis approach, the spatial localisation of seizure related haemodynamic response was shown to be different in various pathological lesions. In nodular heterotopias (4/4 cases) the maximum BOLD increase was observed in the overlying cortex of heterotopias whereas in FCD (2/2 cases) and band heterotopias (2/2 cases) maximum BOLD increase was found within the structural lesion, however, other smaller and less significant clusters of BOLD signal change were also observed remotely [Tyvaert *et al.* 2008]. Thornton and colleagues [Thornton *et al.* 2010b] investigated seizures by dividing into three phases (see Section 2.5.2a for details). Using GLM based data analysis approach they showed significant BOLD changes in 7/9 cases, and the concordance of BOLD localisation with the SOZ (defined using icEEG) was found to be greatest for the early ictal phase and the combined phases. Moreover, they argued that as the ictal activity spreads on EEG, the BOLD changes should also evolve temporally. Therefore, BOLD changes during clinical ictal and late ictal phases discordant with SOZ may represent propagated activity. Using ICA on the data from the same group of patients, it was demonstrated that ICs were spatially concordant with SOZ in all cases (confirmed in 8/9 cases with icEEG), making an argument that ICA is helpful to reveal ictal BOLD changes when GLM based approach fails [Thornton *et al.* 2010b].

It has also been shown that the spatial extent of BOLD signal change was larger for the combined effect of multiple seizures than single seizures [Kobayashi *et al.* 2006a], and the BOLD changes for seizures were widespread in comparison to the BOLD changes for IEDs [Kobayashi *et al.* 2006a;Tyvaert *et al.* 2008]. The significance of BOLD signal decrease is not clearly known, however, additional areas of BOLD signal decrease during seizures were observed; within perilesional cortex and opposite hemisphere of brain [Kobayashi *et al.* 2006a]; within the

presumed SOZ [Donaire *et al.* 2009a]; within surrounding areas of BOLD signal increase and remotely from the presumed SOZ/SOZ [Tyvaert *et al.* 2008;Thornton *et al.* 2010b]. These remote areas were often part of the DMN [Raichle *et al.* 2001], in common with many studies of IEDs [Salek-Haddadi *et al.* 2006;Laufs *et al.* 2006].

### **3.3.4 Preictal BOLD changes, seizure evolution and propagation in focal epilepsy**

Federico and colleagues focussed specifically on preictal BOLD changes in three cases and revealed BOLD increase (2/3 cases) and decrease (1/3 cases) starting prior to the clinical seizure, however preictal BOLD increase (~4min) was concordant with SOZ in only one case [Federico *et al.* 2005b]. Using series of sequential fixed-width block model for seizure representation in the GLM framework, Donaire and colleagues [Donaire *et al.* 2009a] described widespread BOLD decrease in default mode network 10–26s prior to the first BOLD increase which in itself preceded the first clinical (6–52s) or electrographic change (8–12s) in 5/10 cases. In contrast, using a similar model to Donaire’s, Tyvaert and colleagues [Tyvaert *et al.* 2009] found that on average BOLD changes started  $5.2 \pm 2.6$ s after EEG-onset of seizure and returned to baseline  $28.8 \pm 12.9$ s after EEG onset in 10/17 cases, roughly in line with what would be expected in response to a physiological block stimulus. The initial area of BOLD increase was found to be concordant with the SOZ/presumed SOZ (Table 3.2) [Tyvaert *et al.* 2009;Donaire *et al.* 2009a]. Moreover, by relaxing the statistical threshold additional BOLD change clusters concordant with the SOZ/presumed SOZ were noticed in 2/17 cases prior to ictal onset on EEG. [Tyvaert *et al.* 2009]. They argued that other areas of BOLD signal increase demonstrated propagation of seizures as it spreads in time. Though these observations were made in small studies, this may point towards EEG-fMRI’s ability to identify preictal haemodynamic changes even when epileptic discharges are not yet visible on scalp EEG.

### **3.3.5 Haemodynamic networks in idiopathic generalized epilepsy**

Salek-Haddadi and colleagues [Salek-Haddadi *et al.* 2003b], using GLM based data analysis approach, described haemodynamic involvement of deeper structures of the brain during absence seizures, identifying two patterns of simultaneous BOLD change: BOLD increase (+3 % from baseline) in thalamic

nuclei and symmetrical, widespread decreases in cerebrum, maximum in the frontal lobes (-8 % from baseline) in relation to four long (mean duration: 30 sec) absence seizures. Subsequent group studies of IGE patients [Aghakhani *et al.* 2004;Gotman *et al.* 2005;Hamandi *et al.* 2006;Laufs *et al.* 2006] also revealed common patterns of BOLD decrease in the frontal and parietal cortices, posterior cingulate, caudate and precuneus, and predominant BOLD increase in the thalamus, medial frontal region and insula.

The areas involved in GSWDs related cortical BOLD decrease resemble the DMN [Raichle *et al.* 2001]. The BOLD signal decrease in these areas, in relation to GSWDs, can be argued to represent the suspension of physiologic conscious rest or an fMRI signature of the negative clinical phenomenology of absences during which cognitive processes may be impaired [Laufs *et al.* 2006]. The studies of absence seizures in animal models [Danober *et al.* 1998] and in humans using transcranial Doppler, H<sub>2</sub><sup>(15)</sup>O and PET [Prevett *et al.* 1995;Diehl *et al.* 1998] and invasive recordings have also pointed towards the involvement of cortico-thalamic network in the generation of absence seizures [Avoli and Gloor 1981;Avoli and Gloor 1982;Avoli and Kostopoulos 1982;Avoli *et al.* 2001]. However, fMRI non-invasively provides the evidence for the association of the cortico-subcortical/striato-cortico-thalamic network with GSWDs recorded on EEG.

The effect of duration of GSWDs on the spatial distribution of BOLD changes is complex. Aghakhani and colleagues showed that the BOLD changes for shorter (< 3 sec) and longer (> 3 sec) bursts of GSWDs were similar in 3/4 cases and one case did not reveal any BOLD change for shorter discharges [Aghakhani *et al.* 2004]. On the contrary, it has also been discussed that BOLD changes were of greater magnitude [Carney *et al.* 2010] or tended to be more frequent in the thalamus [Hamandi *et al.* 2006;Li *et al.* 2009] when GSWDs were of longer duration and higher in number. This may be due to improved signal to noise ratio or may reflect the role of thalamus in maintaining the GSWDs [Avoli *et al.* 2001] for longer duration discharges.

Studies using simultaneous EEG-fMRI and perfusion mapping techniques (arterial spin labelling) have shown a positive correlation between BOLD changes and cerebral blood flow irrespective of the sign of BOLD change. This association is stronger during GSWDs than during background activity suggesting preserved

(i.e. within normal limits) neurovascular coupling [Hamandi *et al.* 2008; Carmichael *et al.* 2008a].

Timing of the BOLD changes relative to the EEG onset of GSWDs is also under-debate. Using conventional GLM based data analysis approach: GSWDs modelled as box-car and convolved with a standard HRF [Glover *et al.* 2000], it was shown that BOLD increase in the thalamus, occipital cortex, cerebellum, temporal lobes, insula, caudate and pons; and decrease in the parietal cortex, precuneus, cingulate gyrus, basal ganglia and pons started after EEG onset, and BOLD increases peaked earlier than BOLD decreases [Aghakhani *et al.* 2004; Hamandi *et al.* 2006; Moeller *et al.* 2008a; Bai *et al.* 2010; Carney *et al.* 2010; Berman *et al.* 2010]. It can be argued that this analysis approach may not be perfect physiologically; assuming electrophysiological and haemodynamic changes during seizures start and end abruptly. Therefore, by modelling the HRF before the EEG onset of GSWDs in the GLM framework [Moeller *et al.* 2008b], and by investigating the mean time course of GSWDs related haemodynamic change in specific areas (selected on the basis of location of significant BOLD cluster) [Bai *et al.* 2010; Carney *et al.* 2010], it was shown that temporal pattern of BOLD changes was different from the conventionally reported pattern. The BOLD increase in the thalamus, [Moeller *et al.* 2008b], parietal cortex and precuneus [Carney *et al.* 2010] preceded the GSWDs onset on EEG. Bai and colleagues also suggested that the BOLD increase in orbital frontal cortex, frontal polar, cingulate, parietal cortex, precuneus and occipital cortex preceded the GSWDs onset on EEG followed by BOLD decrease in the same areas lasting 20s after GSWDs [Bai *et al.* 2010]. Animal models of absence seizures investigated with optical imaging also showed changes in concentration of oxy/deoxy-haemoglobin prior to the onset of GSWDs [Roche-Labarbe *et al.* 2010], illustrating all the more need to correlate the findings of animal models with human studies. The inconsistency of temporal evolution of GSWDs related BOLD changes in IGE may result from variable modelling strategies applied [Moeller *et al.* 2008b; Bai *et al.* 2010], different types of epileptic discharges (polyspikes and waves and GSWDs) and age related biological differences between adults [Hamandi *et al.* 2006] and children [Moeller *et al.* 2008b]. The pre-GSWDs BOLD changes may reflect early electrophysiological changes which are not evident on scalp EEG, however, this needs to be investigated further.

Moeller and colleagues investigated the patient specific BOLD changes for absence seizure, using series of sequential fixed width blocks to represent seizures in the GLM framework, and found that BOLD changes were consistent for several absences within one patient but varied across patients [Moeller *et al.* 2010c]. Moreover, the BOLD changes in various anatomical areas; thalamus, cortex and caudate, were dynamic (evolving at different time points) throughout the duration of absence seizure rather than being static [Moeller *et al.* 2010c]. They also showed that the BOLD increase in cortex (6/9 cases) and decrease in caudate (5/9 cases) preceded the BOLD increase in the thalamus (9/9 cases) [Moeller *et al.* 2010c]. These absence seizures related focal BOLD increases in cortex [Bai *et al.* 2010;Carney *et al.* 2010;Moeller *et al.* 2010c] are consistent with the cortical focus theory of initiation of absences [Meeren *et al.* 2002;Polack *et al.* 2007;Vaudano *et al.* 2009;Westmijse *et al.* 2009].

### 3.3.6 Seizure related networks in other forms of epilepsy

Seizure related networks explored in FOS using EEG-fMRI have revealed BOLD increase in parieto-occipital regions correlated with 2.5-3Hz activity triggered by eye closure [Krakow *et al.* 2000c;Iannetti *et al.* 2002;Di Bonaventura *et al.* 2005]. In two case reports on musicogenic epilepsy, it was shown that BOLD networks involved the presumed SOZ: right gyrus rectus and left anterior temporal lobe [Morocz *et al.* 2003], and right dorsal frontal cortex and right temporal lobe [Marrosu *et al.* 2009] during presentation of epileptogenic music. Morocz and colleagues argued that the BOLD changes in the left anterior temporal lobe represented the seizure focus (confirmed by ictal EEG and ictal-SPECT) and that the BOLD changes in the ventral frontal lobe and right gyrus rectus were related to presentation and listening of epileptogenic music, in line with previous PET studies [Morocz *et al.* 2003].

For pseudo-absences (three cases) in FLE, focal BOLD increase was revealed in the medial frontal cortex correlated with GSWDs which was not seen in typical absences (six cases) in the same study [Di Bonaventura *et al.* 2006b]. However, more recent studies on absences in children have also shown focal BOLD increases in the cortex (Section 3.3.5), therefore, it needs to be further investigated as to whether these different haemodynamic changes between typical and pseudo-absences can be applied as a differentiating point. Similarly, comparison of the GSWDs related BOLD patterns in patients with IGE and SGE

revealed many similarities in the distribution but greater inter-individual variability in cases of SGE, and did not lead to reliable classification of individual cases [Hamandi *et al.* 2006].

In patients with reading epilepsy, BOLD networks involving the motor and premotor cortex, striatum, medial temporal lobe and thalamus were revealed in correlation with orofacial reflex myoclonus and EEG discharges triggered by reading. These changes were also differentiated from the BOLD activations observed during language and facial motor tasks [Salek-Haddadi *et al.* 2009]. EEG-fMRI has also helped to demonstrate the coexistence of separate epileptic networks for GSWDs and for focal facial twitching in a single patient, and the BOLD changes for the latter helped to ascertain that the FCD previously seen on MRI was epileptogenic [Chassagnon *et al.* 2009].

In children with PPR (6 cases; 4=IGE/CAE, 2=PPR only) [Moeller *et al.* 2009b], focal BOLD increases were observed in premotor and parietal cortex (adjacent to intra-parietal sulcus) 3 sec prior to PPR (corresponding to gamma activity on EEG), followed by BOLD decrease in the same areas during PPR. It is possible that the early BOLD changes in parietal cortex indicate its possible role in the generation of PPR, or may reflect it being part of the fronto-parietal visual networks responsible for saccades and visual attention, which needs to be elucidated further [Moeller *et al.* 2009b]. Additionally, most of the subjects (5 cases) did not show any BOLD changes in the thalamus [Moeller *et al.* 2009b], and it can be argued that the thalamus may play a less important role in the generation of PPR in comparison to typical GSWDs in IGE for which an intact thalamo-cortical network is deemed necessary [Avoli *et al.* 2001].

Liu and colleagues, investigating children with eyelid myoclonia associated with absences (EMA) showed BOLD increase in thalamus, temporal lobes, midline structures and BOLD decrease in parietal and frontal cortex. This epileptic network in EMA is similar to the epileptic network identified in IGE, which can be explained by the presence of GSWDs both in EMA and IGE [Liu *et al.* 2008].

### **3.3.7 Haemodynamic mapping of cognitive networks during GSWDs**

The haemodynamic changes for GSWDs associated with cognitive impairment have been investigated only recently using various attention tasks during EEG-fMRI [Berman *et al.* 2010; Bai *et al.* 2010; Moeller *et al.* 2010b].

BOLD increases in thalamus, frontal cortex, primary visual, auditory, somatosensory, and motor cortex, and BOLD decreases in the lateral and medial parietal cortex, cingulate gyrus, and basal ganglia have been revealed for GSWDs during which behavioural performance was poor (4/9 cases, 100% error rate). In comparison, for GSWDs during which behavioural performance was good (2/9 cases, 0% error rate), no significant BOLD changes were observed [Berman *et al.* 2010]. These findings provide supplementary evidence that structures playing an active role during attention tasks [Riccio *et al.* 2002] become involved during GSWDs as revealed by haemodynamic changes in cortico-thalamic network, thus impairing consciousness and performance.

On the contrary, in a case report it was shown that performance was not impaired during GSWDs, and the associated BOLD changes were observed in the same cortico-thalamic network [Moeller *et al.* 2010b]. The authors have argued that the BOLD changes in cortico-thalamic network for these GSWDs involved the same structures which are associated with clinical absences. However, GSWDs related BOLD changes can be very patient specific (Section 3.3.5) and findings of a single case cannot be generalized. The impairment of consciousness during GSWDs and the associated BOLD changes is a complex question which needs to be explored systematically.

### 3.3.8 Role of EEG-fMRI in management of epilepsy

In single case reports, EEG-fMRI has also demonstrated the ability to help in diagnosis and management of epilepsy. Spatial location of BOLD changes associated with myoclonic jerks of right foot helped to localise an FCD from left frontal lobe which was confirmed with intraoperative cortical mapping as SOZ and resected resulting in complete abolition of seizures [Archer *et al.* 2006]. In another patient with refractory epilepsy, who had undergone epilepsy surgery twice without any appreciable success, fMRI showed widespread BOLD changes involving the cortex, caudate nucleus, thalamus and other areas during the seizure (a pattern known to be present in generalized epilepsy). Consequently, the antiepileptic drugs were changed to control generalized epilepsy and seizure frequency reduced from 10/day to 1/month [Auer *et al.* 2008].

Overall, EEG-fMRI has been helpful in localising the haemodynamic networks associated with GSWDs and focal interictal and ictal discharges, and has also generated new hypotheses to be explored in further detail.



### 3.4 Perspectives on the application of simultaneous EEG-fMRI in epilepsy

I have discussed the methodological constraints and clinical applications of simultaneous EEG-fMRI in epilepsy in Sections 3.2 and 3.3 respectively. Here, I present my perspectives briefly on EEG-fMRI in relation to the experimental studies presented in the following chapters.

The sensitivity of EEG-fMRI is highly dependent on capturing and identifying events of interest on EEG recorded inside the scanner, in most instances. It will be most useful if two or more of the different methods used to identify events of interest (as described in Section 3.2.3) can be combined together without affecting the data quality. The sensitivity of fMRI studies can also be increased by explaining the variance in the data and reducing the amount of residual noise as thoroughly as possible. Synchronised video recordings during resting EEG-fMRI can help to identify and model physiological activities (e.g., eye blinks and hand movements, which are performed by patients voluntarily), thus decreasing unmodelled residual variance in the data.

EEG-fMRI studies in focal epilepsy have demonstrated the technique's ability to localise the epileptic focus as described in Sections 3.3.2 and 3.3.3. Given that epileptic activity most commonly happens spontaneously whether be IEDs or seizures and IEDs occur more frequently than seizures, the majority of EEG-fMRI studies have investigated IED related haemodynamic networks. However, IEDs localise IZ only and it is necessary to localise SOZ to perform surgery in patients with refractory focal epilepsy. This raises interest in capturing and investigating seizures using EEG-fMRI. Since seizures occur randomly and are likely to be associated with head or body motion, it seems that the application of ictal EEG-fMRI will be limited to a subset of cases with very carefully defined selection criteria e.g., patients with daily seizures and with seizure types without large head movements. Methodologically robust and consistent strategy which can separate seizure related BOLD changes from artefactual changes need to be applied to analyse seizure related fMRI data. However, I believe that such studies can also provide crucial new insights into the spontaneous transition from the interictal to ictal state in humans. Moreover, synchronized video-EEG inside the MRI scanner can help to identify and classify seizures into different phases on the basis of their evolution which may in turn help to separate haemodynamic networks at seizure onset from those during seizure propagation, complementing icEEG studies.

For all clinical purposes, icEEG is considered the gold standard for the localisation of epileptic activity. However, it has limited spatial coverage leaving the possibility that the epileptic activity recorded on icEEG may also have reflections in the other parts of brain which are not covered with icEEG raising doubts about the nature of the gold standard. Investigating fMRI haemodynamic networks associated with epileptic activity identified on simultaneously recorded icEEG can present a solution to this question.

EEG-fMRI studies on GSWDs have progressed more rapidly, possibly due to the presumed more uniform underlying phenomenology, and have improved our knowledge of the underlying epileptic networks such as cortico-thalamic network in IGE. However, the effects of GSWDs on the networks involved in cognition and maintaining awareness remains to be explored properly. Experimental studies in the following Chapters 5-10 present my work addressing the above mentioned issues systematically.

## SECTION 2: EXPERIMENTAL STUDIES

### Chapter 4: Common Methods

In this chapter, I describe the experimental methods used in common for the research studies using simultaneous video-EEG and fMRI (video-EEG-fMRI) in Chapters 5 to 8 and 10. These methods are common practice in the epilepsy imaging group at the MRI Unit, Epilepsy Society, Chalfont St Peter. The detailed methods for each experimental study and specifically for the study in Chapter 9 for intracranial EEG-fMRI (icEEG-fMRI) are described in relevant chapters.

#### 4.1 Patient recruitment

All patients participating in research studies were attending the National Hospital for Neurology and Neurosurgery, Queen Square, London. All patients had had a detailed clinical history taken and a full neurological examination, MRI scanning following our epilepsy protocol [Duncan 2010], long-term video-EEG monitoring and neuropsychology assessment. All subjects gave informed, written consent and the study was approved by the joint research ethics committee of the National Hospital for Neurology and Neurosurgery (UCLH NHS Foundation Trust) and UCL Institute of Neurology, Queen Square, London, UK.

#### 4.2 MRI acquisition

The MRI scanning was performed at the Epilepsy Society's MRI Unit (Chalfont St. Peter, Buckinghamshire, UK). Patients were fitted with an EEG cap (see section 4.3 Video-EEG acquisition below), ear plugs, their head was immobilised using a vacuum cushion and they were asked to remain still during scanning. Images were acquired using a 3T GE Signa® Excite HDX Echospeed MRI scanner (GE, Milwaukee, USA) with a standard transmit/receive head coil. Each patient underwent one to three 20-minute imaging sessions and each fMRI dataset consisted of 404 volumes of T2\* weighted gradient echo EPI. The EPI scan parameters were as follows: TE = 30 ms, TR = 3000 ms, flip angle = 90°, slices = 44, slice thickness = 2.4 mm with 0.6 mm gap, FOV = 24x24 cm<sup>2</sup>, matrix =

64x64, voxel size = 3.75 x 3.75 x 3. A slice trigger was generated by the scanner for the acquisition of each EPI slice which was recorded by the EEG recording software to be used subsequently for scanner artefact removal. For the purpose of anatomical localisation I also acquired one volumetric 3D T1-weighted image at the same time (Image parameters: TE = 3.1 ms, TR = 8.3 ms, TI = 450 ms, flip angle = 20°, slices = 170, slice thickness = 1.1 mm with zero gap, FOV = 24x18, matrix = 256x256 cm<sup>2</sup>, excitations = 1, voxel size = 1.09 x 1.09 x 1.5).

### **4.3 Video-EEG acquisition:**

#### **4.3.1 EEG recording and artefact correction**

Scalp EEG was recorded during the MRI scanning using a 64 channel MR-compatible electrode cap (62 EEG electrodes, 1 ECG electrode and 1 reference electrode; BrainCap MR, Germany), 2x32 MR-compatible amplifiers (Brain Products, Munich, Germany) and Brain Vision Recorder software version 1 (Brain Products, Munich, Germany). The electrodes were arranged according to the modified combinatorial nomenclature referenced to FCz electrode. EEG was recorded continuously during fMRI with a sampling rate of 5000 Hz and was synchronized to the scanner's 20 KHz gradient clock. Other recording parameters for EEG were: resolution = 0.5  $\mu$ V; high pass filter = 0.016 Hz and low pass filter = 250 Hz (applied after amplification but prior to data recording); digitization = 16-bit. ECG was recorded with a single electrode which was placed just below left clavicle and connected to the same amplifier as for EEG electrodes.

Prior to MRI acquisition, a resting EEG (with eyes closed) for 15 minutes was recorded outside the scanner. Patients were put into the scanner with the EEG wires straightened, immobilized (using sand bags) and connected to MR-compatible amplifiers at the back of the scanner. EEG data was transmitted from the amplifiers to the recording computer located in the control room via fibre-optic cable.

The artefacts (GA and PA) from EEG recorded inside the scanner were removed offline using average artefact subtraction methods [Allen *et al.* 1998; Allen *et al.* 2000] in Brain Vision Analyzer software version 2 (Brain Products, Munich, Germany). The artefact corrected EEG was resampled to 250 Hz and infinite impulse filters (implemented as phase shift-free Butterworth filters; Low-pass

filter = 70 Hz; High-pass filter = 0.3 Hz; Slope = 12 db/octave) were applied to identify IEDs and seizures. These events recorded on video-EEG inside the scanner were visually compared with IEDs and seizures recorded on long-term video-EEG monitoring and coded by consensus.

### 4.3.2 Video recording

Two cameras were used to monitor and record the subject's behaviour during MR scanning (schematic representation in Figure 4.1). An MR-compatible camera (C1: MR-Cam 12M, MRC Systems GmbH, Heidelberg, Germany) was positioned inside the bore of the scanner focusing on the subject's face, recording facial expressions and head movements. The video signals from C1 were transmitted to the recording computer placed outside the scanner room through shielded cable and low-pass filter (1MHz: MRC Systems GmbH, Heidelberg, Germany) to provide RF shielding. The low-pass filter box was also grounded to the scanner room shield.

A second video camera (C2: Handicam DCR-HC51E, Sony Corporation, San Diego, CA, USA) was positioned on the wall facing the scanner bore allowing a view of the subject's entire body. The video signals from C2 to the recording computer were transmitted using a custom-built filter system (designed by Dave Gasston) consisting of electric power supply sockets for camera and optical fire wire (IEEE 1394B) repeater (OFR), a low-pass filter (BLP-1.9, 50Ω DC to 1.9 MHz) and OFR transmitter box enclosed in an aluminium box. Both C2 and filter box were permanently attached at a safe distance of 3m and a height of 2.5m in front of the scanner.

A video multiplexer (HA-402TX Quad Processor, Ultima Precision Co Ltd, Taiwan) was used to get a picture-in-picture video display from both cameras. The video output signals from C1 (analogue signal) and C2 (digital signal) were different where as the video multiplexer could receive only analogue signals. Therefore, I used a bi-directional analogue/digital video converter (ADVC110 – high-quality, Thomson Worldwide, Cergy Pontoise Cedex, France) to convert digital video signals from C2 to analogue. Thus, analogue signals from both cameras were fed into the video multiplexer. Another bi-directional analogue/digital video converter (ADVC110 – high-quality, Thomson Worldwide, Cergy Pontoise Cedex, France) converted the analogue signals from the video multiplexer back to digital video signals for display and input to the recording

computer. The second conversion of signals from analogue to digital was done because the software (Brain Vision Recorder version 1; Brain Products, Munich, Germany) recording video and EEG could receive only digital signals. The above described video input system has a maximum transmission delay of  $\approx 150\text{ms}$  as specified by the manufacturers.

Video and EEG were recorded synchronously using Brain Vision Recorder version 1 software (Brain Products, Munich, Germany) with an online display of video-EEG without scanner artefacts using RecView software (Brain Products, Munich, Germany).

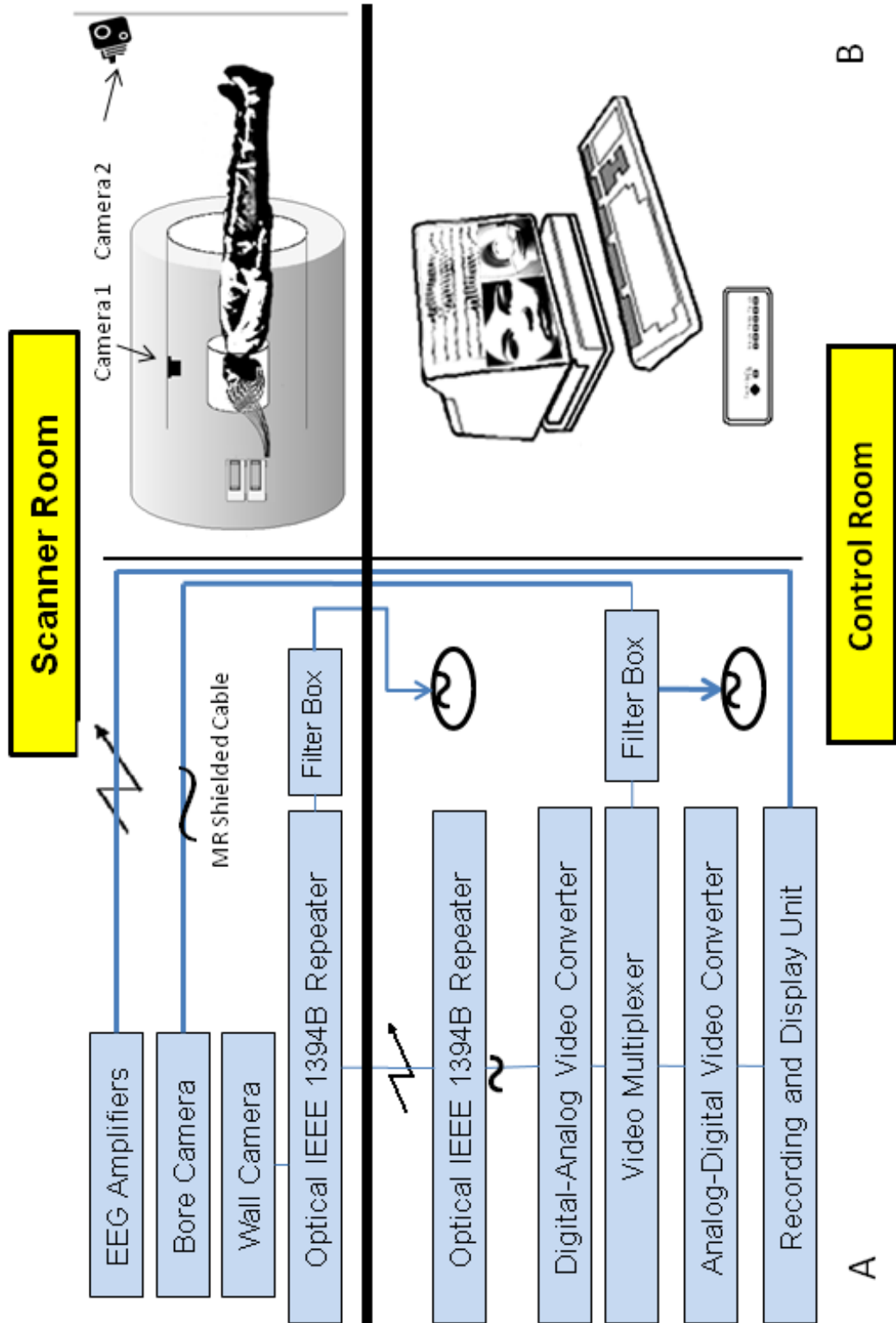


**Figure 4.1: Arrangement of equipment**

(A) Circuit Diagram (B) System Set up

#### 4.4 fMRI processing and statistical analysis

All fMRI data were analysed using software package Statistical Parametric Mapping (SPM: version 5 for Chapters 5, 6, 7 and 8; version 8 for Chapter 9 and 10) (<http://www.fil.ion.ucl.ac.uk/spm>) running under Matlab (Mathworks Inc., U.S.A.). After discarding the first four image volumes to avoid T1-saturation effect, the EPI time series images were realigned to the mean and spatially smoothed using an isotropic Gaussian kernel of 8mm FWHM [Friston *et al.* 1995a].

The fMRI data was analysed within the GLM framework to map interictal and ictal related haemodynamic changes. The EOIs: IED or ictal discharges, were represented as zero-duration stick function or blocks of variable duration depending upon the length of the discharge. EOIs were convolved with canonical HRF and temporal and dispersion derivatives which resulted in three regressors for each event [Friston *et al.* 1998]. When a patient had more than one type of IED or ictal discharges, they were modelled as separate regressors [Salek-Haddadi *et al.* 2002; Salek-Haddadi *et al.* 2009; Thornton *et al.* 2010b]. Twenty four inter-scan realignment parameters (6 realignment parameters from image pre-processing and a Volterra-expansion of these [Friston *et al.* 1996]) were included in the GLMs as confounds to account for motion related effects. Forty four additional regressors (one for each slice) were also included in the GLM as confounds to explain pulse-related artefact [Liston *et al.* 2006]. A high-pass filter of 128s was included to remove slow scanner drift related effects [Ashburner *et al.* 2008].

SPM-[F] contrasts across three regressors for each event type were used to generate F-maps to reveal event related BOLD changes. The presence of significant BOLD changes was assessed by applying a threshold of  $p < 0.05$ , corrected for family wise error (FWE), and additionally a less conservative statistical threshold  $p < 0.001$ , uncorrected for FWE. The resulting SPM-[F] maps were co-registered with T1-weighted MRI scans to evaluate the anatomical localisation [Ashburner and Friston 1997]. BOLD time courses were plotted for each BOLD cluster to classify the BOLD change as increases or decreases according to the sign of the peak change relative to baseline [Ashburner *et al.* 2008].



## Chapter 5: Implementation and Evaluation of Simultaneous video-EEG-fMRI<sup>4</sup>

### 5.1 Background

The majority of EEG-fMRI studies have focussed on IED related BOLD changes reflecting the IZ [Luders *et al.* 2006], which may be different from the SOZ [Rosenow and Luders 2001]. This indicates the need to study the haemodynamic correlates of seizures, which has been investigated in a relatively small number of cases as discussed in Chapter 3, Section 3.3. A variety of strategies have been applied for identification of seizures during EEG-fMRI data acquisition. These strategies include online and retrospective review of EEG [Tyvaert *et al.* 2008; Salek-Haddadi *et al.* 2009; Tyvaert *et al.* 2009; Moeller *et al.* 2009b; Thornton *et al.* 2010b; Moeller *et al.* 2010c], Electromyography (EMG) [Salek-Haddadi *et al.* 2009], non-synchronized video recording [Federico *et al.* 2005b; Di Bonaventura *et al.* 2006b; Tyvaert *et al.* 2009], , observation of ictal semiology (for example: by person inside the scanner room) [Di Bonaventura *et al.* 2006b], eye tracking technology, patient response button [Di Bonaventura *et al.* 2006b; Salek-Haddadi *et al.* 2009] and sound/voice recording as discussed in Chapter 3, Section 3.2. However, these methods may not be entirely reliable as markers of the ictal events particularly in the absence of reliable data synchronization mechanism [Salek-Haddadi *et al.* 2009]. In addition simple partial seizures may not have a definite signature on EEG [Smith 2005]. In this respect video-EEG recording has proven to be pivotal in identifying and localising the seizure onset and seizure propagation with a good diagnostic yield [Binnie *et al.* 1981; Kaplan PW and Lesser RP 1996; Cascino 2002].

In this chapter, I present my work on implementing the use of two video cameras, one capturing facial semiology (C1) and a second one monitoring limb and body movements (C2) for synchronized video recording during EEG-fMRI (video-EEG-fMRI). The aim was to combine the capability of video-EEG to characterise the type of events of interest (as for clinical video-EEG monitoring) with the

---

<sup>4</sup>This chapter forms the basis of the article [Chaudhary *et al.* 2010].

localising power of fMRI, allowing greater precision and specificity in building models for the analysis of the fMRI time series. I investigated the compatibility of dual video recording synchronised with EEG-fMRI equipment inside a 3T MRI scanner based on the evaluation of possible noise production in EEG, video and fMRI data quality secondary to the introduction of the video recording equipment in the EEG-fMRI data acquisition set up. I also evaluated video-EEG-fMRI (vEEG-fMRI) in a hand motor paradigm to utilize supplementary information from video in fMRI data analysis.

## **5.2 Methods**

The common methods are described in Chapter 4, and the specific methods for this study are described here.

### **5.2.1 Subjects**

The effect of video cameras on EEG-fMRI data quality was assessed in a test object (17 cm diameter spherical plastic vessel filled with a doped agar gel, Dielectric, Inc., Madison, WI, USA) and 24 human subjects, with and without video cameras from August 2008 to April 2009. Five subjects undergoing vEEG-fMRI were also asked to perform repetitive finger thumb opposition task.

### **5.2.2 MRI acquisition**

#### **5.2.2a Test object**

The test object was scanned with and without video recording at variable camera positions:

- 1) With video recording: C1 at positions P1 (edge of scanner bore) and P2 (inside the scanner bore); C2 switched on (S1).
- 2) Without video recording: C1 at P0 (removed from the scanner room); and C2 switched off (S0).

Five minute sessions of gradient echo T2\*-weighted EPI were performed with RF amplifier switched on and off for test object. The EPI parameters are described in Chapter 4.

### **5.2.2b Human subjects**

Twenty minute resting state EPI sessions were performed for human subjects with RF amplifier switched on, and video cameras in place (C1 at P2 and C2 at S1) in 12 subjects, and without video cameras in 12 subjects (C1 at P0 and C2 at S0). In addition, five minute task related EPI sessions were also performed in 5 subjects. The MRI acquisition parameters are described in Chapter 4.

### **5.2.3 Video- EEG acquisition**

#### **5.2.3a EEG recording and artefact correction**

In human subjects, scalp EEG was recorded during MR scanning using a 64 channel MR-compatible electrode cap (BrainCap MR, Easy cap, Herrsching-Breitbrunn, Germany), according to the extended international 10-20 system. Two additional electrodes were used to record electro-oculogram (EOG) and electrocardiogram (ECG). The rest of the details for EEG recording and removal of scanner artefact are described in Chapter 4, Section 4.3a.

#### **5.2.3b Video recording**

The details of video recording are described in Chapter 4 section 4.3b.

### **5.2.4 Experimental design for hand motor task**

Repetitive finger thumb opposition task started with left hand, followed by right hand and then rest, each lasting 30 seconds over a period of 5 minutes. The subjects were instructed to focus on the head coil mirror through which they could see the radiographers in control room and follow the cue for changing hands and rest.

### **5.2.5 Data Analysis**

#### **5.2.5a Image, EEG and video quality**

The signal to fluctuation noise ratio (SFNR) was calculated in to evaluate MR data quality in relation to the presence of video recording. The SFNR was defined

as mean signal intensity divided by its temporal standard deviation. I calculated SFNR voxel-wise as follows:

$$\text{Mean signal in an image voxel } (\hat{S}) = \frac{\sum_{i=1}^N S_i}{N}$$

When,  $S$  is the signal in an image voxel and  $N$  is the image volume number

$$\text{Temporal standard deviation } (F) = \frac{\sqrt{\sum_{i=1}^N (\hat{S} - S_i)^2}}{N}$$

$$\text{SFNR} = \frac{\hat{S}}{F}$$

A region of interest was selected automatically as the central 11x11x11 voxels (Figure 5.1) of the volume (presuming accurate positioning of the phantom / subject head in the centre of the field of view). The average SFNR within this region was then calculated which will be used for further analysis.

Secondly, SFNR values were also calculated by dividing squareroot of two times the mean signal intensity by the temporal standard deviation of the difference between two sequentially acquired volumes. These calculations were made on the EPI images using an in house script written by an experienced physicist (Dr. David W Carnichael) in Matlab version 6.5 R13 (MathWorks, Natick, MA, U.S.A.) and SPM 5 software (available from: <http://www.fil.ion.ucl.ac.uk/spm>) running on a Dell Inspiron 1525 under Red Hat Linux 9. The script displayed standard deviation summary maps and created movies of EPI images with RF amplifier switched off for review to detect transient noise effects. I used Mann-Whitney test (SPSS version 13) to compare SFNR from EPI acquired at variable camera positions in the test object, as well as from EPI acquired with and without video recording in human subjects. The synchronized video-EEG was reviewed visually with two expert observers (Dr. Roman Rodionov, Dr. David W Carnichael) having experience of EEG recording inside MRI scanner using Brain Vision Analyzer software version 2 (Brain Products, Munich, Germany).

### 5.2.5b fMRI analysis: hand motor task

The fMRI time series data was analysed using SPM 5 (available from: <http://www.fil.ion.ucl.ac.uk/spm>) after pre-processing as described in Chapter 4, Section 4.4. Two GLMs were built to determine the presence of experimental condition related BOLD effects. A first GLM was built based on the specified block design with a canonical basis set. A second GLM was built based on review of the video to identify left and right hand finger tapping blocks, convolved with canonical basis set. Six scan realignment parameters from image pre-processing were included as confounds in both the GLMs and SPM[T] maps were generated (corrected for FWE: threshold at  $p < 0.05$ , uncorrected for FWE: threshold at  $p < 0.001$ ).

## 5.3 Results

Visual inspection of the movie of raw EPI image time series with RF amplifier switched off did not reveal any artefact (e.g., related to spike noise or electrostatic interference) and comparison of standard deviation maps of the time series with and without RF amplification in test object did not reveal any RF interference for any of the camera configurations (Figure 5.1). The difference between SFNR estimates for cameras at variable positions (P1, P2, S1, P0 and S0) was not statistically significant (Figures 5.1 and 5.2).

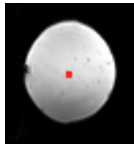
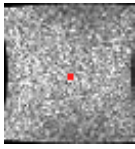
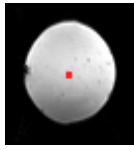
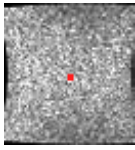
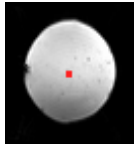
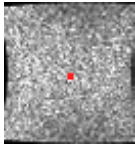
The SFNR for 12 subjects without the camera ranged from 26.7 to 73.9 with a mean of 50.9 (95% CI; 42.5 – 59.3), and SFNR for 12 subjects with camera ranged from 33.7 to 75.7 with a mean of 49.5 (95% CI; 42.9- 56.2). The comparison of SFNR from EPI of human subjects with / without camera showed no significant difference ( $p > 0.05$ ) (Figure 5.3).

Visual inspection and comparison of the video and EEG inside and outside the MR scanner did not reveal any additional interference as assessed with expert observers with experience in EEG-fMRI (Figure 5.4).

BOLD activations were observed in expected hand motor areas which were concordant for both analysis strategies in 4/5 subjects. Review of video revealed that subject 4 performed the task randomly alternating between right and left

hand. The paradigm based block design analysis did not reveal any significant BOLD response. Incorporation of video-derived information in the second GLM showed significant BOLD activations in the motor cortex [Left: Cluster Size = 18, Voxel  $t = 5.7$  ( $Z$  equivalent = 5.2); Right: Cluster Size = 18, Voxel  $t = 5.8$  ( $Z$  equivalent = 5.2)] and supplementary motor cortex (SMA) [Cluster Size = 98, Voxel  $t = 6$  ( $Z$  equivalent = 5.5)]. By lowering the threshold, SPM[T] maps (uncorrected for FWE) for paradigm based block design revealed BOLD activations around motor cortex [Right: Cluster Size = 509, Voxel  $t = 4.87$  ( $Z$  equivalent = 4.57); Left: Cluster Size = 178, Voxel  $t = 4.15$  ( $Z$  equivalent = 3.95)] and SMA [Cluster Size = 136, Voxel  $t = 4.36$  ( $Z$  equivalent = 4.14)]. In comparison, SPM[T] maps for the second video based GLM showed BOLD response in hand motor cortex [Right: Cluster Size = 689, Voxel  $t = 4.52$  ( $Z$  equivalent = 4.26); Left: Cluster Size = 764, Voxel  $t = 5.7$  ( $Z$  equivalent = 5.2)], SMA [Cluster Size = 4587, Voxel  $t = 6$  ( $Z$  equivalent = 5.52)] and pre-motor cortex [Right: Cluster Size = 4587, Voxel  $t = 5.78$  ( $Z$  equivalent = 5.29); Left: Cluster Size = 523, Voxel  $t = 5.13$  ( $Z$  equivalent = 4.77)] (Figure 5.5).

(a)

Camera Position	RF ON	RF OFF
C1 at P0 C2 at S0		
C1 at P1 C2 at S1		
C1 at P2 C2 at S1		

(b)

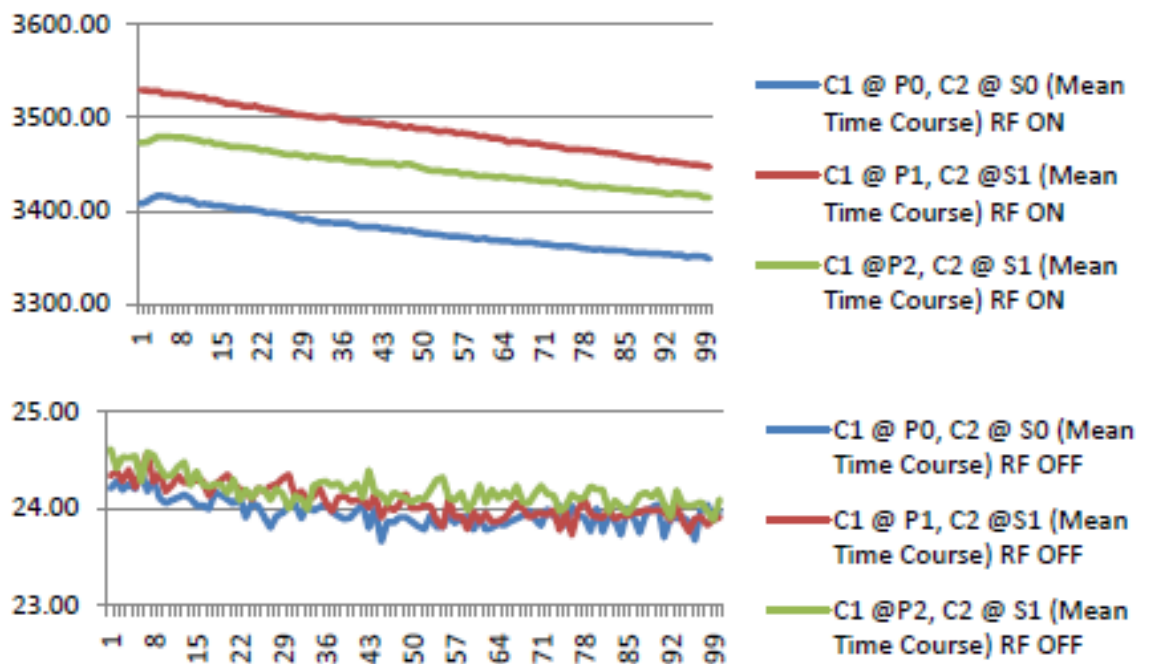


**Figure 5.1: Mean time courses of signal from ROI in a test object**

(a) Display of single slices of EPI in the test object at variable camera positions showing region of interest (ROI) in the centre (marked red). (b) Mean time courses for different acquisitions with radiofrequency (RF) amplifier on and off are also shown.

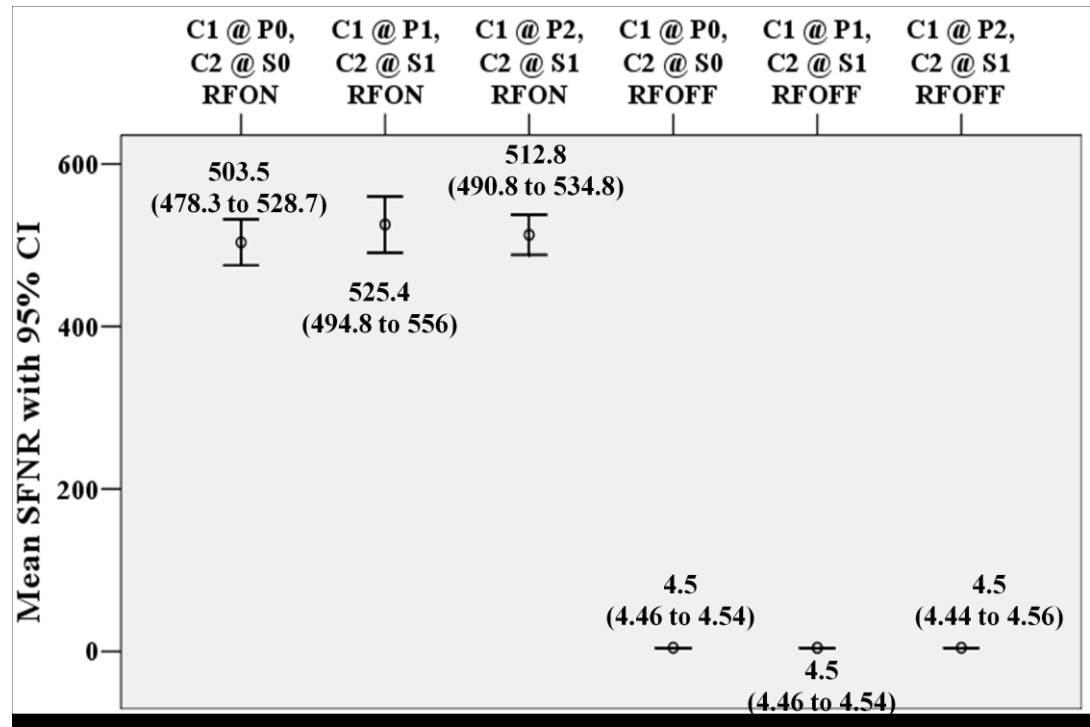


**Figure 5.2: Mean SFNR from EPI volumes for a test object**

Mean SFNR (95% Confidence Interval) (CI) calculated from different volumes of EPI from a test object with RF amplifier on and off, at variable camera positions. The difference between SFNR at variable camera position was not statistically significant: RF On

C1 @ P0 and C2 @ S0 versus C1 @ P1 and C2 @ S1:  $p = 0.2$

C1 @ P0 and C2 @ S0 versus C1 @ P2 and C2 @ S1:  $p = 0.7$

RF Off

C1 @ P0 and C2 @ S0 versus C1 @ P1 and C2 @ S1:  $p = 0.1$

C1 @ P0 and C2 @ S0 versus C1 @ P2 and C2 @ S1:  $p = 0.8$

Abbreviations: C1 = Scanner bore mounted detachable camera, C2 = Wall-mounted camera inside the scanner room, P0 = C1 removed from the scanner room, P1 = C1 at the edge of scanner bore, P2 = C1 inside the scanner bore, S0 = C2 switched off, S1 = C2 switched on.



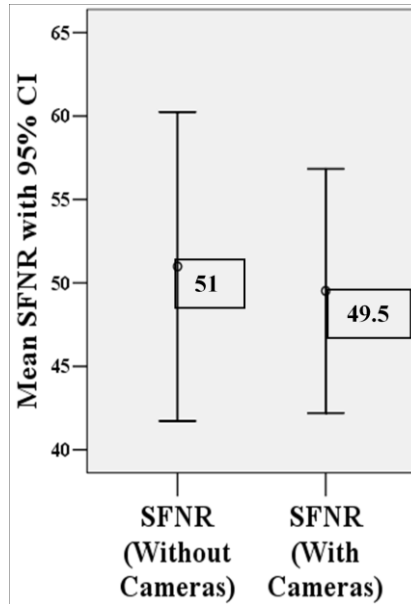


**Figure 5.3: Mean SFNR from EPI volumes in human subjects**

Mean SFNR with 95% CI from EPI volumes in human subjects (12 Subjects with and 12 subjects without camera). The difference between SFNR in two groups was not statistically significant ( $p = 0.6$ ).

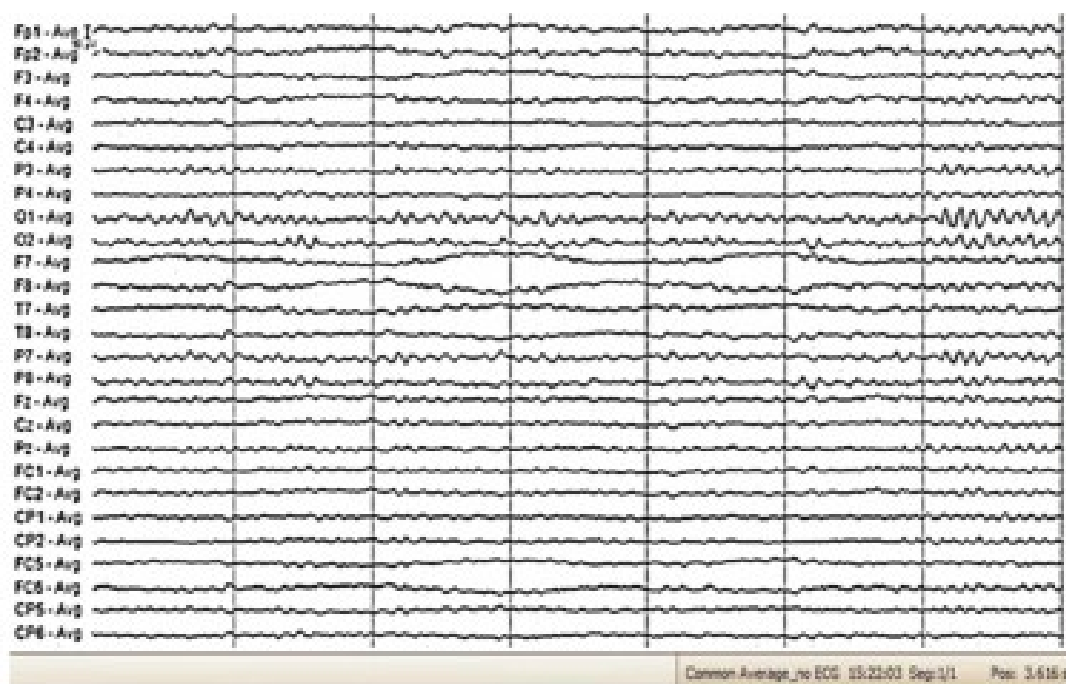


**Figure 5.4: Representative sample of Synchronized Video-EEG**

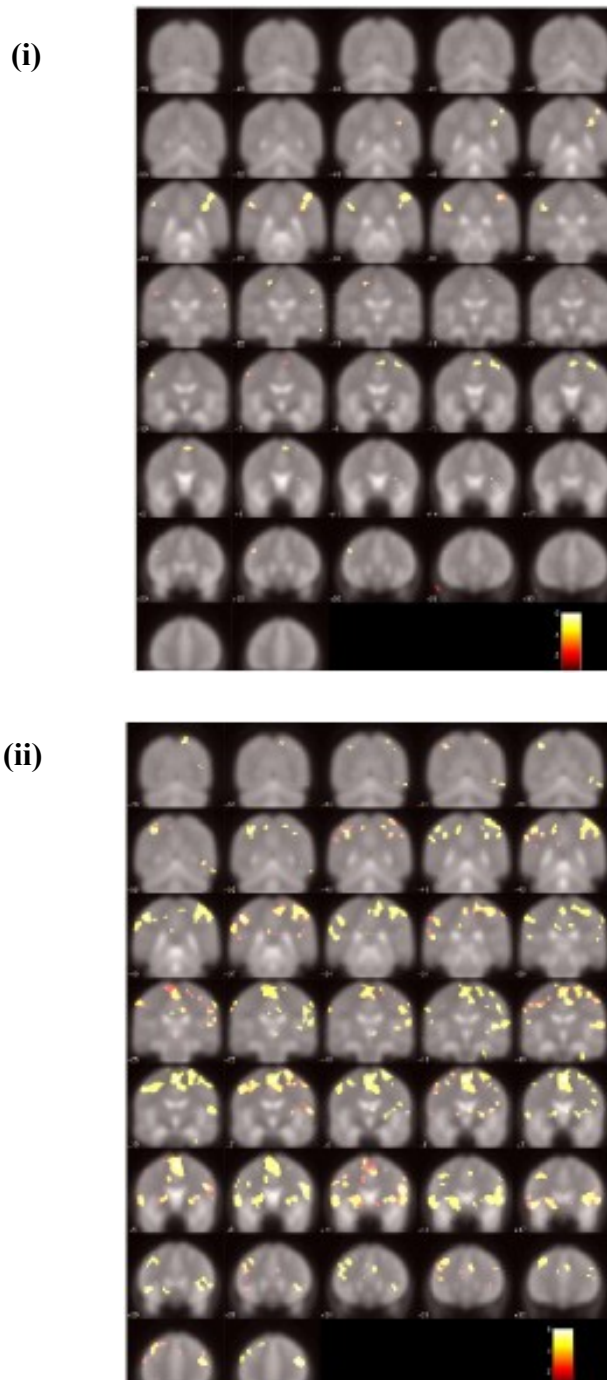


**Figure 5.5: BOLD activations for finger tapping task**

Subject 4: BOLD activations for left and right hand finger tapping overlaid on normalized EPI (i) paradigm specific block design analysis revealed BOLD responses around primary motor cortex in subject 4 (being non-compliant to the paradigm design). (ii) Incorporation of video information about timing of finger tapping into video based block design GLM, revealed additional BOLD responses in primary motor cortex, supplementary motor cortex and pre-motor cortex.

#### 5.4 Discussion

The effect of using two powered video cameras on simultaneously acquired EEG and fMRI data quality was evaluated. The results demonstrate that there was no significant deterioration of the data quality and therefore simultaneous vEEG-fMRI was implemented successfully.

Generally, in-built and standard camera systems provided by MR manufacturers have limitations including low video quality/resolution and limited view of the patient's body [Neuner *et al.* 2007]. Though video recording has been employed previously to record patient's behaviours during EEG-fMRI data acquisition [Krings *et al.* 2000;Federico *et al.* 2005b;Archer *et al.* 2006;Tyvaert *et al.* 2009], but to the best of my knowledge there has been no report on the effect of this on the image quality. Moreover, the video recordings were not synchronized with the EEG thus raising the issue of possible delay between video and EEG signals. Hence, the information obtained from video to be included in the design matrix for fMRI data analysis may become unreliable especially on the temporal scale. The video component of the vEEG-fMRI system proposed in this chapter is compatible with the EEG recording system, thus providing synchronised video-EEG which is in turn synchronized with the MR scanner clock and scan acquisition. In this manner, EEG sampling remains constant relative to the scanner gradient switching and facilitates [Mandelkowitz *et al.* 2006] the removal of imaging and pulse artefact [Allen *et al.* 1998;Allen *et al.* 2000]. Furthermore, the video recording system enables to record two different views of the patient. One camera records the subject's facial expressions and head movement and the second camera records body and limb movements. The necessary equipment includes commercially available and custom made equipment and the set up can be assembled and disassembled in any MRI suite. In comparison to other camera systems established in an MRI scanner environment [Wild *et al.* 2000;Neuner *et al.* 2007] the current system does not need any additional mirrors to reflect images of the patient or extra illumination of the subject. Therefore, there is no vibration related video quality reduction in the currently proposed system as compared to other systems using additional mirrors. The image of the subject is

recorded directly and the ambient scanner room and bore lighting provide sufficient luminescence to record video (Figure 5.4).

The wall camera which is a commercially available camera provided a wider view of the patient's body. It was mounted at a sufficient distance (3 metres) from the scanner so that it does not interfere with the scanner's magnetic field which could result in artefacts and degraded image quality, as I noted it contains magnetic material and must be secured permanently  $> 2\text{m}$  from the scanner bore entrance to maintain safety. An in-house built power and data line filter was used to reduce any electromagnetic interference from the power supply and data inputs of the wall camera. The conversion of digital electrical signals to optical signals was performed to ensure that electrical signals do not contribute to the noise production and eliminate the possibility of transmission of unwanted RF signals through the Faraday cage.

MR image quality assessment is routinely performed by calculating SNR [Glover and Law 2001] and specifically SFNR for functional time series [Glover and Lai 1998;Friedman and Glover 2006]. The bore camera was tested by the manufacturer (MR-Cam 12M, MRC Systems GmbH, Heidelberg, Germany), in a Siemens 1.5T Symphony scanner using fast gradients sequences on a water phantom. The manufacturer calculated mean and standard deviation of noise in the MR images to evaluate the interference caused by the camera and found that this remained stable (personal communication). In this study, I tested two cameras in a 3T MRI scanner with an EPI sequence on a test object and human subjects for vEEG-fMRI. I did not observe any significant artefact production due to the video recording. The SFNR was not significantly altered by the video recording. Similarly video recording inside MR scanner was also free of any major artefact. Thus, video recording can be implemented without any significant decline in the data quality.

The information provided by the video recording may be used efficiently for modelling and data analysis in subjects not complying with the experiment design. This was evident from the analysis of finger tapping motor paradigm as shown in the results, where by incorporation of information provided by video recording into the design matrix revealed additional clusters of BOLD activations

in SMA and pre-motor cortex. These findings are concordant with the previously published findings for the brain areas responsible for finger tapping [Boecker *et al.* 1994;Moritz *et al.* 2000a;Moritz *et al.* 2000b]. I propose that the additional information provided by video will also be very useful in the identification of epileptic events and differentiation of physiological activities from epileptic events specifically seizures. I will evaluate the utility of vEEG-fMRI in the experimental studies on epileptic activity in Chapters 6 to 8.

### **5.5 Conclusion**

In conclusion, the compatibility of video cameras with EEG-fMRI equipment was evaluated in this chapter, and no significant deterioration in image quality was detected in the fMRI images or in the EEG quality. The incorporation of video is useful for monitoring task compliance and can also be used for the identification of epileptic events.

## Chapter 6: Improving the sensitivity of vEEG-fMRI studies of IED by modelling video-EEG detected physiological confounds<sup>5</sup>

### 6.1 Background

The sensitivity of EEG-fMRI is limited in part, due to its dependence on EEG to identify epileptic activity during fMRI and because of difficulties in choosing appropriate modelling strategy of the fMRI signal (for details see Chapter 3, Section 3.2). Topographical voltage map correlation based analysis [Grouiller *et al.* 2011] has shown to increase the technique's sensitivity, however, it does not address the nuisance factors: confounds present in fMRI time series data.

Moreover, EEG-fMRI studies demonstrated often complex BOLD patterns [Vulliemoz *et al.* 2009;Vulliemoz *et al.* 2010;Thornton *et al.* 2010a;Thornton *et al.* 2011]}, raising the issue of specificity of the findings and the unknown clinical relevance of individual BOLD clusters. Therefore, IED and seizure related BOLD changes are localised and interpreted in combination with the information available from other non-invasive and invasive tests [Tyvaert *et al.* 2008;Thornton *et al.* 2010a;Thornton *et al.* 2011].

The maximum clinically relevant information may be derived from individual datasets by careful consideration of the following factors: 1) the sensitivity of EEG-fMRI to numerous confounding effects such as motion and heartbeat; 2) the weakness of the epileptic activity in some cases, because of its variable and unpredictable nature (corresponding to low experimental efficiency [Dale 1999;Friston *et al.* 1999b]) reducing sensitivity to the effects of interest. This is in contrast to conventional cognitive fMRI studies aimed at identifying population level effects, in which entire datasets that do not satisfy some quality criterion (e.g. motion above a certain threshold) can often be discarded with little or no consequence. A similar approach has also been employed in epilepsy [Tyvaert *et al.* 2009;Bai *et al.* 2010] resulting in patients being unable to benefit from the test.

---

<sup>5</sup>This chapter forms the basis of the article [Chaudhary *et al.* 2012a].

At the data acquisition stage and during the fMRI data pre-processing various measures have been applied to reduce interferences from the effects of no interest which is discussed in Chapter 3, Section 3.2. However, there are also other physiological activities or events which can potentially account for a significant degree of fMRI signal variance. For example, voluntary and spontaneous eye blinks [Volkman 1986;Bodis-Wollner *et al.* 1999;Bristow *et al.* 2005a;Bristow *et al.* 2005b], swallowing [Mosier and Bereznaya 2001;Suzuki *et al.* 2003;Peck *et al.* 2010], chewing and related tongue movements [Shinagawa *et al.* 2004;Byrd *et al.* 2009;Bracco *et al.* 2010] and hand and foot movements [Lotze *et al.* 2000;Chainay *et al.* 2004] activate specific networks. Voluntary eye blinks have been associated with significant BOLD activations in pre-central and posterior middle frontal gyrus (MFG) (frontal eye fields (FEF)), medial superior frontal gyrus (SFG) (supplementary eye-fields (SEF)), parietal and occipital cortex [Bodis-Wollner *et al.* 1999;Bristow *et al.* 2005a;Bristow *et al.* 2005b]. Swallowing saliva has been shown to involve a network of BOLD changes in the sensorimotor cortex (SMC), inferior frontal gyrus (IFG), SFG, MFG, superior temporal gyrus (STG), inferior parietal lobe (IPL), insula, cingulate gyrus, thalamus and cerebellum [Mosier and Bereznaya 2001;Suzuki *et al.* 2003;Peck *et al.* 2010]. Chewing and related tongue movements activate a network involving SMC, supplementary motor area (SMA), insula and basal ganglia (BG) [Shinagawa *et al.* 2004;Byrd *et al.* 2009;Bracco *et al.* 2010]. Similarly, hand and foot movements show activations in motor cortex (MC), SMA, premotor cortex (PMC) and cerebellum [Lotze *et al.* 2000;Chainay *et al.* 2004]. When these physiological activities are somehow correlated with the effect of interest but not modelled, this will increase the chances of false positive BOLD changes, decreasing the reliability of EEG-fMRI findings.

In this chapter, I propose that the availability of synchronous video-EEG [Chaudhary *et al.* 2010] will allow to identify and model the fMRI changes associated with non-epileptic physiological activities, leading to decreased residual variance and potential increase in the sensitivity to the effects of interest. I evaluated two design matrices: with and without additional regressors for these physiological activities, and compared the resulting BOLD maps for statistical significance and extent of BOLD clusters. The following effects were considered: spontaneous eye movements and blinks, head jerks, voluntary chewing and



speech, facial twitches, swallowing, coughing, yawning and brief hand or foot movements. For the focal epilepsy cases, I also compared the degree of concordance of the maps in relation to the IZ as defined on the basis of electroclinical and radiological information.

## **6.2 Methods**

The common methods are described in Chapter 4, and the specific methods for this study are described here.

### **6.2.1 Subjects**

Six patients with refractory focal epilepsy and four patients with IGE who had IEDs and no seizure during the vEEG-fMRI acquisition were selected for this study. A summary of the clinical details on these patients can be found in Table 6.1.

### **6.2.2 MRI acquisition**

Two 20 minute EPI sessions were performed for each subject. The details of MRI acquisition are described in Chapter 4 Section 4.2.

### **6.2.3 Video-EEG recording and artefact correction**

Synchronous video-EEG was recorded during the MRI scanning. The details of video-EEG recording and removal of pulse and scanner artefact are described in Chapter 4, Section 4.3.

### **6.2.4 Data processing and analysis**

#### **6.2.4a EEG and fMRI Processing**

I reviewed video-EEGs to identify and label IEDs and the following physiological activities: spontaneous eye movements and blinks, head jerks, voluntary chewing and speech, facial twitches, swallowing, coughing, yawning and brief hand or foot movements. These physiological activities were differentiated from ictal semiology by comparing them with the patient's habitual seizure semiologies recorded during the long-term video-EEG monitoring. The details of fMRI data pre-processing are described in Chapter 4, Section 4.4.

**Table 6.1: Summary of electroclinical and imaging findings**

Cases	Epilepsy	Scalp EEG Interictal/Ictal onset	MRI results	Other investigations (MEG/FDG-PET/Ictal- SPECT)	Localisation
1	FE	Vertex sharp waves/L medial hemispheric	Ischemic lesion L fronto- temporo-parietal	L fronto-parietal and L fronto-central / hypo- metabolism L frontal, parietal and temporal lobes / -	L medial hemisphere
2	FE	L + R temporal spikes/ R Temp.L ictal rhythm	Non lesional	- / hypo-metabolism R posterior temporal lobe and L temporal lobe / L temporal lobe	Bilateral temporal lobes
3	FE	Bilateral polyspikes and wave complexes/Medial hemispheric	Non lesional	-/-/-	Medial hemisphere
4	FE	L Temp.L spikes/Rapid involvement of both hemispheres	Cortical damage L temporal lobe	-/-/-	L temporal lobe
5	FE	L Temp.L spikes/ L Temp.L spikes before ictal onset with fairly generalized ictal rhythm often R>L	Polymicrogyria L perisylvian area	-/-/-	L perisylvian area
6	FE	TIRDA, L FT spikes/L FT ictal rhythm	L hippocampal sclerosis	-/-/-	L temporal lobe
7	IGE	3 Hz GSWDs	Non lesional	-/-/-	NA
8	IGE	3 Hz GSWDs	Non lesional	-/-/-	NA
9	IGE	3 Hz GSWDs	Non lesional	-/-/-	NA
10	IGE	3 Hz GSWDs	Non lesional	-/-/-	NA

Abbreviations: FE=Focal Epilepsy, IGE=Idiopathic generalized epilepsy, GSWDs=generalized spike and wave discharges, L=left, R=right, Temp.L=Temporal lobe, TIRDA=Temporal intermittent rhythmic delta, FT=Fronto-temporal, NA=Not applicable

### 6.2.4b fMRI Modelling

In order to map BOLD changes related to the IEDs and physiological activities, I analysed fMRI data within GLM framework. Only those EPI sessions of time series data during which IEDs were recorded on EEG were included in the analysis. For each session, two GLMs were built as follows:

- GLM 1: The effects of interest: IEDs (identified on video-EEG), represented as stick functions (single events) or blocks (for runs or series of events) were modelled and convolved with the canonical HRF with temporal and dispersion derivatives [Salek-Haddadi *et al.* 2006]. Motion and pulse related regressors were included in the design matrix as confounds, as described in Chapter 4, Section 4.4, to explain motion and pulse related effects.
- GLM 2: Consisting of GLM 1 plus additional regressors representing the physiological activities as blocks of variable length depending upon the duration identified on video-EEG were convolved with canonical HRF with temporal and dispersion derivatives.

The difference between GLM1 and GLM2 in terms of the number and type of regressors modelled is represented in Figure 6.1.

### 6.2.5 Assessment of BOLD changes and level of concordance

SPM [F] maps (threshold:  $p < 0.05$ , corrected for FWE) were generated for each EOI: IEDs and physiological activities, to reveal significant BOLD changes. For the cases which did not show any significant BOLD changes at FWE correction, additional SPM [F] maps were generated at a less conservative statistical threshold:  $p < 0.001$ , uncorrected for FWE. The cluster containing the most statistically significant change (global statistical maximum: GM) and other clusters except the BOLD clusters in ventricular system, vascular tree and at the edges of brain resulting from the two GLMs were compared for their statistical significance and spatial extent.

For the cases with focal epilepsy the localisation of BOLD maps (excluding the BOLD clusters in ventricular system, vascular tree, edges of brain and base of brain) was visually compared with the IZ defined on the basis of available clinical

electrophysiological (interictal epileptiform discharges recorded on clinical long-term video-EEG monitoring) and radiological information (structural abnormalities on MRI scan) [Thornton *et al.* 2010b]. Each BOLD map was classified as either:

- *Entirely concordant*: all BOLD clusters within 2 cm around the IZ in the same gyrus/lobe as the IZ.
- *Concordant plus*: GM BOLD cluster within 2 cm around the IZ in the same gyrus/lobe as the IZ, and other clusters remote from the IZ.
- *Some concordance*: GM BOLD cluster remote from the IZ, and another cluster within 2 cm around the IZ in the same gyrus/lobe as the IZ.
- *Discordant*: all clusters remote from the IZ.
- *Null*: no significant clusters.

The number of scans affected by head motion  $> 0.2\text{mm}$  and the maximum amount of inter-scan motion for each dataset was also calculated using an in house script [Salek-Haddadi *et al.* 2006].

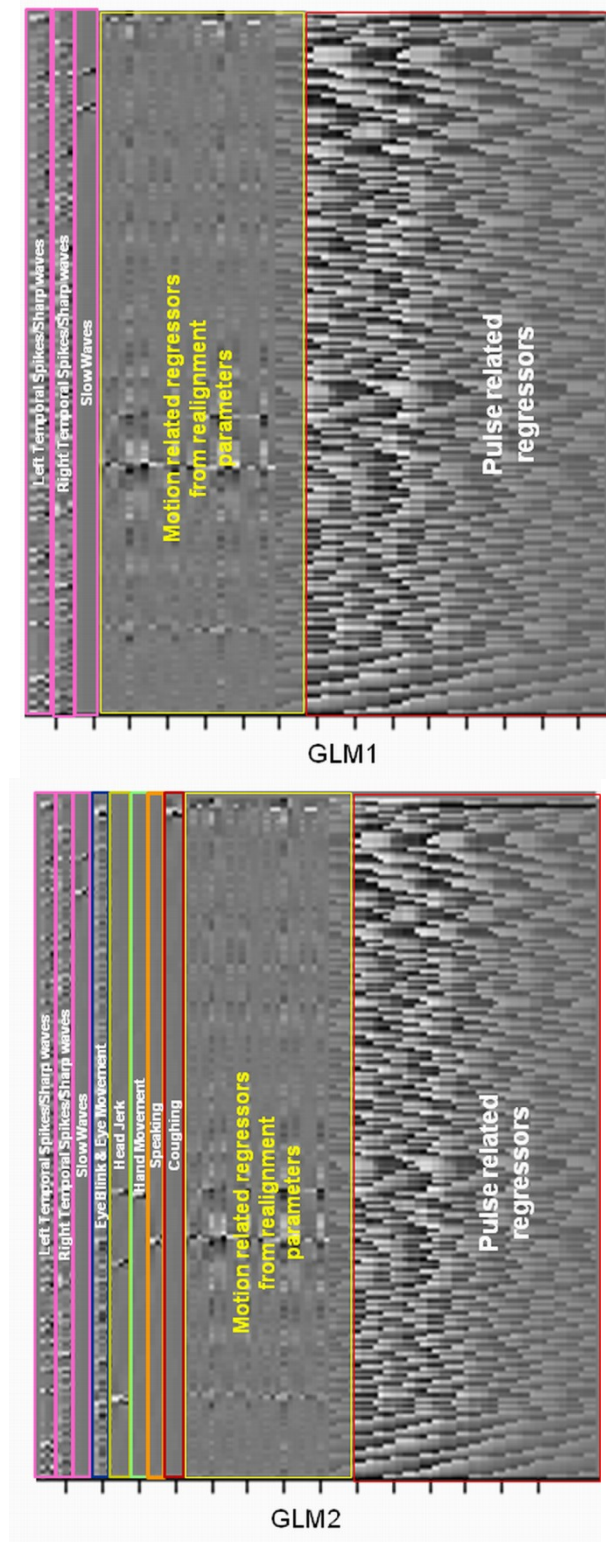


**Figure 6.1: Design matrices with and without physiological activities**

Design matrices for GLM 1 and GLM2 showing the different types of regressors modelled.

### 6.3 Results

The number and type of IED during each session is shown in Table 6.2. 3/10 subjects had more than one type of IED (patients # 2, 4 and 5). The number of IEDs per session ranged from 12 to 575 (Median: 147) in patients with focal epilepsy, and from 1 to 45 (Median: 8) in patients with IGE. Physiological activities were observed in all cases during all sessions and the different types and numbers are shown in Figure 6.2. The number of scans affected by head motion (inter-scan motion > 0.2 mm) ranged from 0 to 46 with a maximum inter-scan motion of 2.3mm (range: 0-2.3; see Table 6.2).

#### 6.3.1 IED related BOLD changes

8/10 subjects revealed IED related BOLD changes for GLM1 and GLM2 at a statistical threshold of  $p < 0.05$  corrected for FWE, and 2/10 subjects showed IED related BOLD changes only  $p < 0.001$  uncorrected for FWE. The location, size and statistical significance and degree of concordance (for the focal epilepsy cases) of BOLD maps for GLM1 with GLM2 are shown in Table 6.3.

In patients with focal epilepsy the size and Z-score of the IED related GM or one of the other BOLD clusters for GLM2 increased in all cases compared to GLM1. For patients #1 and 2 the cluster size and Z-score of the IED related GM and other BOLD clusters increased for all types of IEDs for GLM2 compared to the GLM1 result (highlighted yellow in Table 6.3). The Z-score and cluster size both increased in patients #4 and 5 for GM and other BOLD clusters for type-I IEDs (spikes/sharp waves) (highlighted yellow in Table 6.3), whereas the size and Z-score of the IED related GM and other BOLD clusters for the type-II IED (slow waves) decreased in the same patients. In focal epilepsy patients the Z-score and cluster size for the GM cluster decreased in 2/6 subjects (patients # 3, 6) for GLM2.

Additional IED related BOLD clusters were revealed for 3/6 patients with focal epilepsy subjects (patients #1, 2 and 5) for GLM2 compared to GLM1 (as shown in Figure 6.3 and highlighted in green in Table 6.3), and no cluster was lost. No additional BOLD cluster was seen nor lost, for patients #3, 4 and 6 for GLM2. As shown in Table 6.3, the concordance of the IED related maps was classified as *Concordant plus* for 4/6 subjects (patients #1, 2, 4 and 5) for GLM1 and GLM2. For patient #3, the maps were classified to have *Some concordance* for GLM1 and

GLM2. For patient 6, the IED related maps had *Some concordance* for GLM1 and were classified as *Concordant plus* for GLM2.

In patients with IGE, IED related BOLD changes were revealed in the typical cortico-subcortical network involving the thalamus, basal ganglia, precuneus, cingulate gyrus and parietal and frontal lobes for 3Hz GSWDs for 3 subjects (patients #7, 8 and 9) for both the GLMs. No BOLD changes were seen in the cortico-subcortical network for one IGE patient (#10), rather relatively smaller clusters were seen in and around ventricles. The size and/or Z-score for the GM and other BOLD clusters increased in 2/4 cases (patients #7 and 8; highlighted yellow in Table 6.3) for GLM2 in comparison to GLM1. The Z-score was unchanged and the cluster size decreased in one subject (patient #9), and both the Z-score and cluster size decreased in the other (patient #10) for IED related GM BOLD cluster.

In addition to an increase in Z-score and cluster size of IED related BOLD clusters, Z-score and cluster size of those IED related BOLD clusters also increased which overlapped with BOLD clusters for physiological activities in 7/10 cases (patient #1, 2, 5, 6, 7, 8 and 9) (marked by † in Table 6.3) with GLM 2 than GLM1.

**Table 6.2: Epileptic discharges and motion observed during vEEG-fMRI**

<b>Cases</b>	<b>EPI Session</b>	<b>IEDs during vEEG-fMRI acquisition Description/Number</b>	<b>Head motion (inter-scan &gt; 0.2mm) Number/ <math> \mathbf{d} </math> (mm)</b>
1	1	Vertex sharp waves/184	2/0.2
	2	Vertex sharp waves/575	15/0.6
2	1	Type I-L Temp.L spikes:403, Type II-R Temp.L spikes:37, Type III-Temp.L slow:18	28/1.8
	2	Type I-L Temp.L spikes:331, Type II-R Temp.L spikes:26, Type III-Temp.L slow:3	13/1.7
3	1	BSW:24	32/0.4
	2	BSW:12	46/0.5
4	1	Type I- L Temp.L sharp:2, Type II- L Temp.L slow:108	0/0.1
	2	Type I- L Temp.L sharp:29, Type II- L Temp.L slow:37	1/0.2
5	1	Type I-L Temp.L sharp: 500, Type II- BSW: 46	6/1.1
	2	Type I-L Temp.L sharp: 460, Type II- BSW:86	18/2.3
6	1	L Temp.L spike:25	1/0.3
	2	L Temp.L spike:21	3/0.5
7	1	3 Hz GSWDs:9	10/0.2
	2	3 Hz GSWDs:27	0/0.1
8	1	3 Hz GSWDs:6	5/0.5
	2	3 Hz GSWDs:4	7/0.4
9	1	3 Hz GSWDs:8	8/0.6
	2	3 Hz GSWDs:45	8/0.7
10	1	3 Hz GSWDs:1	0/0.1

Abbreviations: R=Right, L=Left, Temp.L=Temporal lobe, BSW=Bilateral spike and wave, GSWDs=Generalized spike and wave discharges,  $|\mathbf{d}|$  = maximum inter-scan displacement



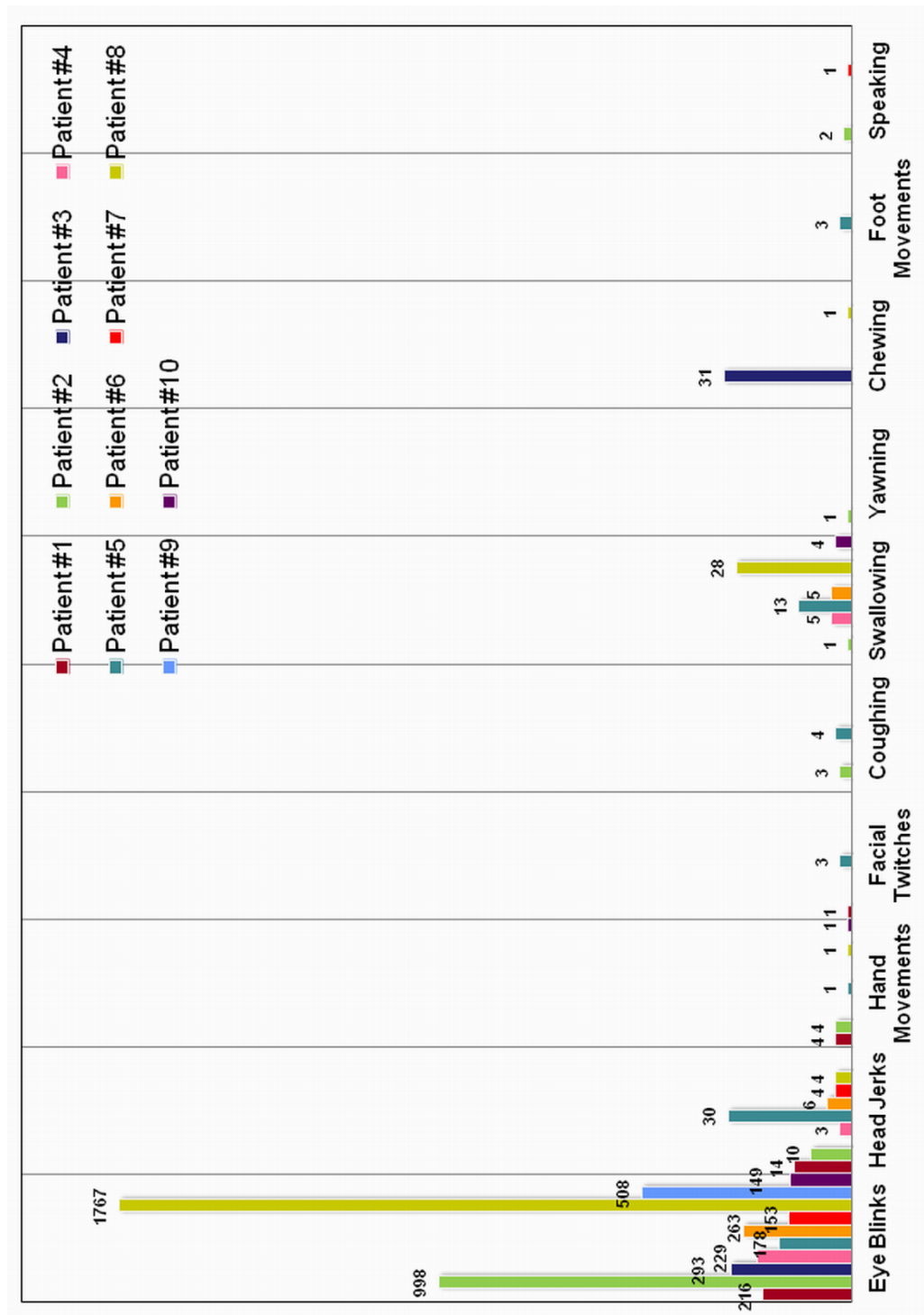


**Figure 6.2: Bar chart of physiological confounds**

Number and type of physiological activities observed during vEEG-fMRI acquisition.

**Table 6.3: Location, size, statistical significance and degree of concordance (focal cases only) of IED related BOLD changes**

ID	IED related BOLD clusters (Location / No. of Voxels / Z-score)		Degree of Concordance	
	GLM1	GLM2	GLM 1	GLM 2
1	1. SMA / 69 / 4.11 2. R IFG / 5 / 3.94 3. L MFG / 9 / 3.78	†1. SMA / 80 / 4.31 2. R IFG / 12 / 4.27 3. L Fronto-temporal / 9 / 3.51 4. L MFG / 5 / 3.34	C+	C+
2	Type I IED 1. L STG (middle) / 25 / 7.33 2. L STG (ant.) / 49 / 7.01 3. L STG (post.) / 23 / 6.71 4. L precuneus / 16 / 3.19 Type II IED- None Type III IED- None	Type I IED 1. L STG (middle) / 30 / 7.83 2. L STG (ant.) / 75 / 7.77 3. L STG (post.) / 27 / 7.18 †4. L precuneus / 17 / 3.74 5. R MTG / 11 / 3.73 Type II IED - None Type III IED- R Par.L / 8 / 3.94	C+	C+
3	1. Precuneus and cingulate / 1840 / Infin. 2. Me.FL / 57 / Infin. 3. L Fron.L / 206 / Infin. 4. L Temp.L / 34 / Infin. 5. Ant. Fron.L / 96 / Infin.	1. Precuneus and cingulate / 1834 / Infin. 2. L Fron.L / 195 / Infin. 3. Me.FL / 56 / Infin. 4. Ant. Fron.L / 98 / Infin. 5. L Temp.L / 33 / Infin.	SC	SC
4	Type I IED 1. L MFG / 105 / 5.63 2. L TPJ / 24 / 4.63 3. L STG / 4 / 3.42 Type II IED 1. L STG / 7 / 3.99 2. L thalamus / 6 / 3.84 3. Cingulate / 11 / 3.65	Type I IED 1. L MFG / 116 / 5.60 2. L TPJ / 58 / 4.68 3. L STG / 9 / 3.58 Type II IED 1. L STG / 7 / 3.89 2. L thalamus / 5 / 3.81 3. Cingulate / 6 / 3.48	C+	C+
5	Type I IED 1. L TPJ / 58 / Infin. 2. R TPJ / 11 / 6.45 3. L Cuneus / 38 / 5.48 4. STG / 2 / 4.90 Type II IED 1. L TPJ / 16 / 5.17	Type I IED 1. L TPJ / 75 / Infin. †2. Bilat. Cuneus / 418 / 6.76 3. R TPJ / 12 / 6.75 †4. STG / 16 / 5.93 †5. L Fron.L (ant.) / 38 / 4.24 †6. L SFG / 28 / 3.91 Type II IED 1. L TPJ / 12 / 5.11	C+	C+
6	1. Cerebellum / 1 / 4.94 2. L Me.TL / 1 / 4.82 3. R ITG / 2 / 4.66 4. R Me.FL / 27 / 4.47 5. R SFG / 12 / 4.39 6. L Inf. Par.L / 44 / 4.35	1. L Me.TL / 1 / 4.79 2. Cerebellum / 1 / 4.78 †3. R ITG / 2 / 4.72 4. R MeFL / 31 / 4.61 †5. L Inf. Par.L / 47 / 4.37 6. R SFG / 12 / 4.30	SC	C+

**Table 6.3: contd.**

ID	IED related BOLD clusters (Location / No. of Voxels / Z-score)		Degree of Concordance	
	GLM1	GLM2	GLM1	GLM2
7	1. Thalamus / 592 / 6.61 2. L caudate / 178 / 6.35 3. L Par.L / 88 / 6.12 4. R caudate / 98 / 5.99 5. BG + precuneus + cingulum / 7638 / 6.61 6. Bilateral Par. L / 2182 / 6.12 7. R cerebellum / 154 / 5.89 8. L FP / 170 / 5.62 9. R SFG / 406 / 4.93 10. L cerebellum / 140 / 4.82	1. Thalamus / 1077 / 7.38 2. L caudate / 169 / 6.51 3. R caudate / 122 / 6.31 4. L Par.L / 138 / 6.31 5. BG + †precuneus + cingulum / 9247 / 7.14 6. Bilateral Par.L / 2547 / 6.31 7. L FP / 140 / 5.60 8. R cerebellum / 139 / 5.57 9. R SFG / 290 / 4.83 10. L cerebellum / 220 / 4.82	NA	NA
8	1. L Par.L / 60 / 6.75 2. Post. cingulum / 146 / 6.36 3. Precuneus / 101 / 6.36 4. R Fron.L / 33 / 6.26 5. Me.FL / 67 / 5.90	1. L Par.L / 89 / 7.13 2. Me.FL / 114 / 6.90 †3. Precuneus / 84 / 6.38 4. R Fron.L / 35 / 6.22 †5. Post. cingulum / 136 / 6.04	NA	NA
9	1. R Par.L / 446 / Infin. 2. Precuneus / 331 / 7.43 3. L Temp.L / 45 / 6.52 4. Post. cingulum / 228 / 5.98 5. L Par.L / 131 / 5.93	1. R Par.L / 428 / Infin. †2. Precuneus / 327 / 7.35 3. L Temp.L / 58 / 6.02 4. Post. cingulum / 223 / 5.79 5. L Par. L / 15 / 5.17	NA	NA
10	1. R Temp.L / 107 / 4.32 2. L lat. vent. / 72 / 4.29 3. L cerebellum / 12 / 4.25 4. White matter R Fron.L / 21 / 3.86 5. White matter L Fron.L / 10 / 3.86	1. L cerebellum / 12 / 4.37 2. Deep WM RT / 27 / 4.04 3. R Temp.L / 17 / 4.02 4. White matter R Fron.L / 13 / 3.93 5. White matter L Fron.L / 7 / 3.83	NA	NA

Abbreviations: R=Right, L=Left, SMA=Supplementary motor area, IFG=Inferior frontal gyrus, MFG=Middle frontal gyrus, Temp.L=Temporal lobe, STG=Superior temporal gyrus, MTG=Middle temporal gyrus, BSW=Bilateral spike and wave, Me.FL=Medial frontal lobe, Fron.L=Frontal lobe, Ant.=Anterior, Infin.=Infinity, OL=Occipital lobe, Post.=Posterior, TPJ=Temporo-parietal junction, Bilat.=Bilateral, Me.TL=Medial temporal lobe, ITG=Inferior temporal gyrus, SFG=Superior frontal gyrus, Inf.=Inferior, Par. L=Parietal lobe, BG=Basal ganglia, FP=Fronto-polar, lat.=Lateral, vent.=Ventricle, † Overlapping BOLD clusters for physiological activities and IEDs, Highlighted green= additional BOLD clusters revealed for GLM2, Highlighted yellow= BOLD clusters for which cluster size and statistical significance increased for GLM2, C+= Concordant plus, SC= Some concordance.

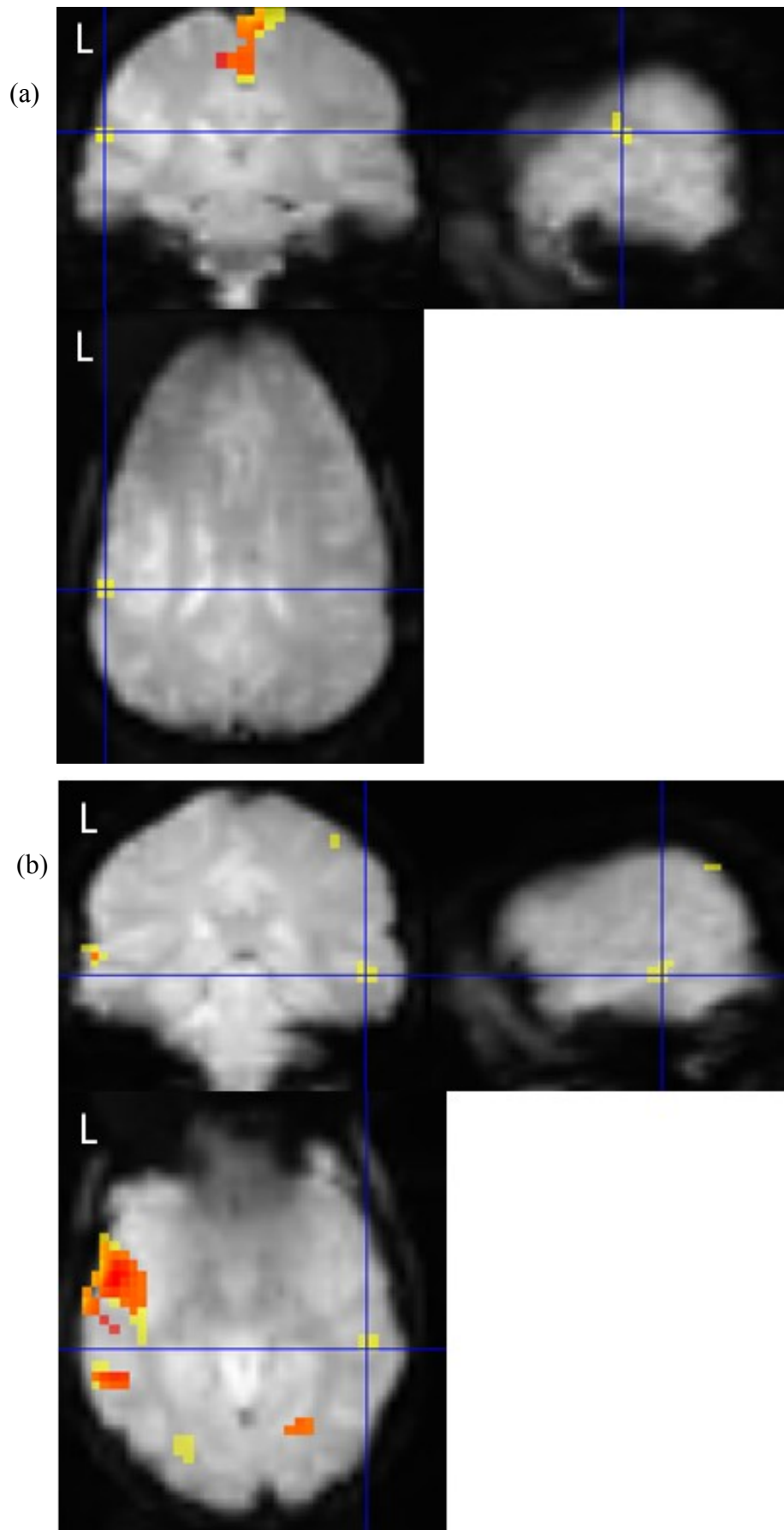
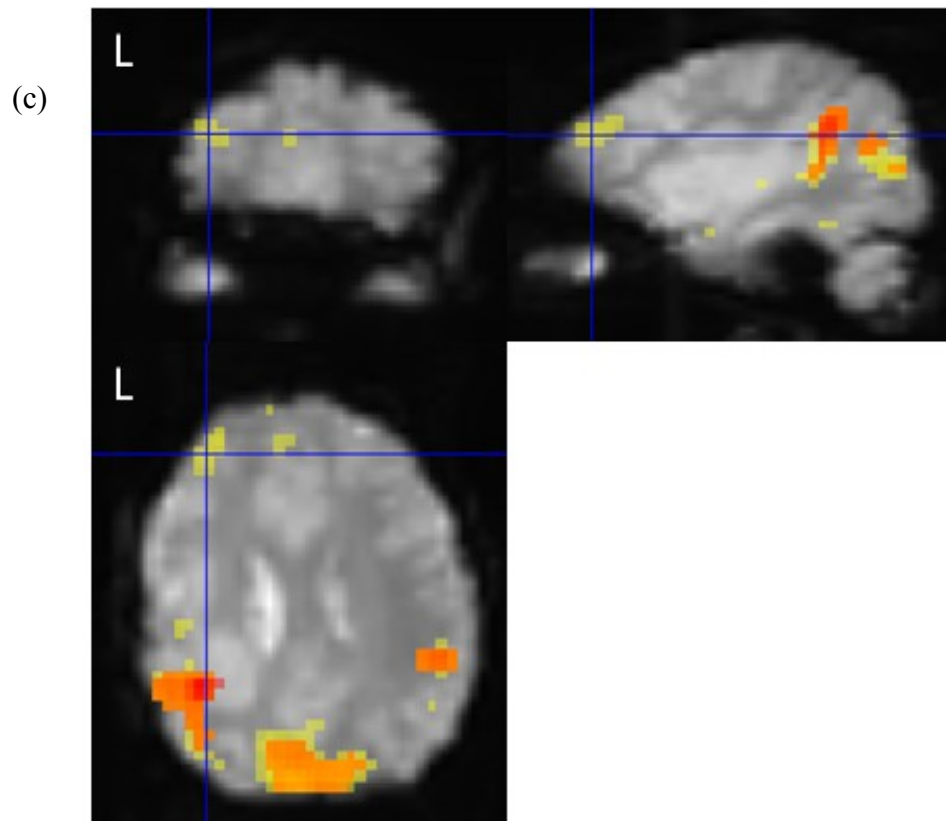


Figure 6.3: BOLD changes for IEDs for GLM 1 and GLM2



**Figure 6.3 (continued)**

SPM[F] maps overlaid on high resolution EPI (at  $p < 0.001$ , uncorrected for FWE) for epileptiform discharges. Red clusters are from GLM1, yellow clusters are from GLM2 and orange clusters represent the overlapping clusters from GLM1 and GLM2; as GLM2 showed all the clusters as shown by GLM1 the overlap of red and yellow resulted in more orange clusters as evident from figure. (a) Case 1: BOLD changes for epileptiform discharges for GLM1 and GLM2. The additional cluster revealed by GLM2 is in yellow colour at the left fronto-temporal junction. (b) Case 2: BOLD changes for type I epileptiform discharges for GLM1 and GLM2. The additional cluster as revealed by GLM2 is in yellow colour in the right middle temporal gyrus. (c) Case 5: BOLD changes for type I epileptiform discharges for GLM1 and GLM2. The additional cluster revealed by including physiological activities as additional regressors in the design matrix is in yellow colour in the left frontal lobe.

### 6.3.2 BOLD changes linked to physiological activities

All patients had eye blinks during vEEG-fMRI acquisition and eye blink related BOLD changes were revealed in areas (see Table 6.4 for details) responsible for vision: predominantly involving medial occipital cortex (MOC), FEF, SEF and cerebellum (Figure 6.4a).

4/10 patients moved their hands (Figure 6.4b) or feet and significant BOLD changes were seen in MC, SMA, and pre-motor cortex.

Overt speech was observed in two patients (#2, 7), when they tried to communicate to the radiographers during acquisition. In one patient (#2, Figure 6.4c) corresponding BOLD changes were revealed in IFG, insula and pre-motor cortex. In the other patient (#7) small speech related BOLD clusters were shown at the edges and base of the brain and inside the ventricles.

6/10 patients were seen to swallow and corresponding BOLD changes were revealed in SFG, cingulate gyrus, IFG, STG, MC, inferior temporal gyrus, cerebellum and inferior parietal lobe as shown in Figure 6.4d.

For head jerks identified on video (Table 6.4, Figure 6.5a,b), BOLD clusters were seen in SMC, premotor cortex, SMA, precuneus, frontopolar and prefrontal cortex, at the edges and base of the brain, inside the ventricles and in the white matter.

For chewing related movements (observed in patients #3 and 8), small BOLD clusters were seen in MC around face area and SMA. A single BOLD cluster was revealed in relation to facial twitches (observed in patients #1 and 5), located in the white matter in patient #5.

For coughing related movements (patient #2 and 5) small BOLD clusters were seen in the MC, SMA, prefrontal cortex, precuneus, medial frontal, cerebellum, base of brain, edges of brain and inside ventricles (Table 6.4, Figure 6.5c).

One patient (#2) was observed to yawn and this was associated with small BOLD clusters predominantly in MC, SMA, precuneus, prefrontal cortex, cerebellum, base of brain and edges of brain (Table 6.4, Figure 6.5d).

**Table 6.4: BOLD changes for physiological activities**

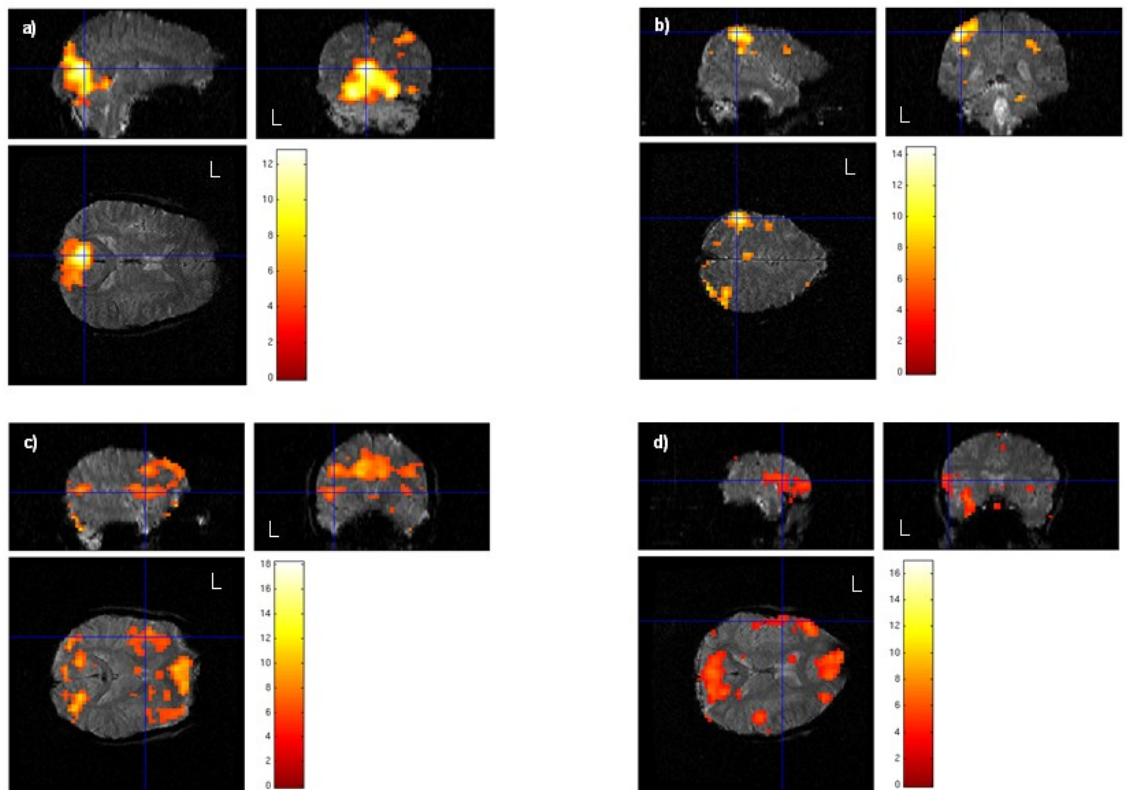
Cases	Eye blinks	Head jerks	Facial Twitches	Hand & foot movements	Speech	Coughing	Swallowing	Yawning	Chewing
1	MOC, OP, PC, FEF, Cerebellum	SMC, SMA, Precuneus, PMC, FP	None	MC, SMA, PMC	-	-	-	-	-
2	PC, FEF, SEF, Precuneus	PMC, SMA, Precuneus, White matter	-	MC, SMA, PMC	IFG, Insula, PMC	MC, SMA, Prefrontal, Ventricles, Edges & base of brain	SFG, Cingulate gyrus	MC, SMA, Precuneus, Prefrontal, Cerebellum, Edges & base of brain	-
3	MOC, OP, PC, FEF, SEF	SMC, SMA, Precuneus, PMC	-	-	-	-	-	-	MC, SMA
4	MOC, OP, SEF, Cerebellum	SMC, SMA, Precuneus, White Matter	-	-	-	-	SFG, Cingulate gyrus	-	-
5	MOC, OP, PC, FEF, SEF, Precuneus	SMC, White matter, Precuneus, Ventricles, Edges & base of brain	White matter	Edges of brain, Falx Cerebri	-	MC, SMA, Prefrontal, Precuneus, Medial Frontal, Cerebellum, Base of brain, Ventricles	Cerebellum, IFG, SFG, STG, SMA, MC	-	-

Table 6.4: contd.

Cases	Eye blinks	Head jerks	Facial Twitches	Hand & foot movements	Speech	Coughing	Swallowing	Yawning	Chewing
6	MOC, SEF, OP, PC	Base of brain	-	-	-	-	Base of brain, MFG, STG, BS, ITG	-	-
7	MOC, FEF, Precuneus, Cerebellum	Prefrontal cortex, Cuneus, White matter, Edges of brain, Base of brain	-	-	Ventricles, Edges & base of brain	-	-	-	-
8	MOC	Prefrontal cortex, SMA, Precuneus, Base of brain	-	None	-	-	IFG, STG, MC, IPL, Cingulate gyrus	-	SMA
9	MOC, FEF, SEF, PC, Precuneus, Cerebellum	White matter, Edges of brain	-	-	-	-	-	-	-
10	MOC, SEF, Cerebellum	-	-	-	-	-	Cingulate gyrus	-	-

Abbreviations: MOC=Medial occipital cortex, PC= Parietal cortex, OP=Occipital pole, FEF=Frontal Eye-Field, SEF=Supplementary Eye-Field, MC=Motor cortex, PMC=Pre-motor cortex, SMA=Supplementary motor area, IFG=Inferior frontal gyrus, SFG=Medial superior frontal gyrus, STG=Superior temporal gyrus, IPL=Inferior parietal lobe, BS=Brain stem, SMC=sensory motor cortex, None=No BOLD changes, “-“=No activity recorded on video-EEG.





**Figure 6.4: BOLD changes for physiological activities**

SPM[F] maps overlaid on high resolution EPI (at  $p < 0.001$ , uncorrected for FWE) for physiological activities. (a) Eye blinks (Case 1): BOLD changes were seen in medial occipital cortex, occipital pole, parietal cortex, frontal eye field and cerebellum, crosshair at maximum BOLD change in medial occipital cortex. (b) Hand movements (Case 1): BOLD changes were seen in motor cortex, supplementary motor area and pre-motor cortex, crosshair at maximum BOLD change in motor cortex. (c) Speech (Case 2): BOLD changes were seen in inferior frontal gyrus, insula and pre-motor cortex, crosshair at BOLD change overlapping inferior frontal gyrus and insula. (d) Swallowing (Case 5): BOLD changes were seen in the cerebellum, inferior frontal gyrus, superior temporal gyrus, supplementary motor area, and motor cortex, crosshair at BOLD change overlapping inferior frontal and superior temporal gyri.

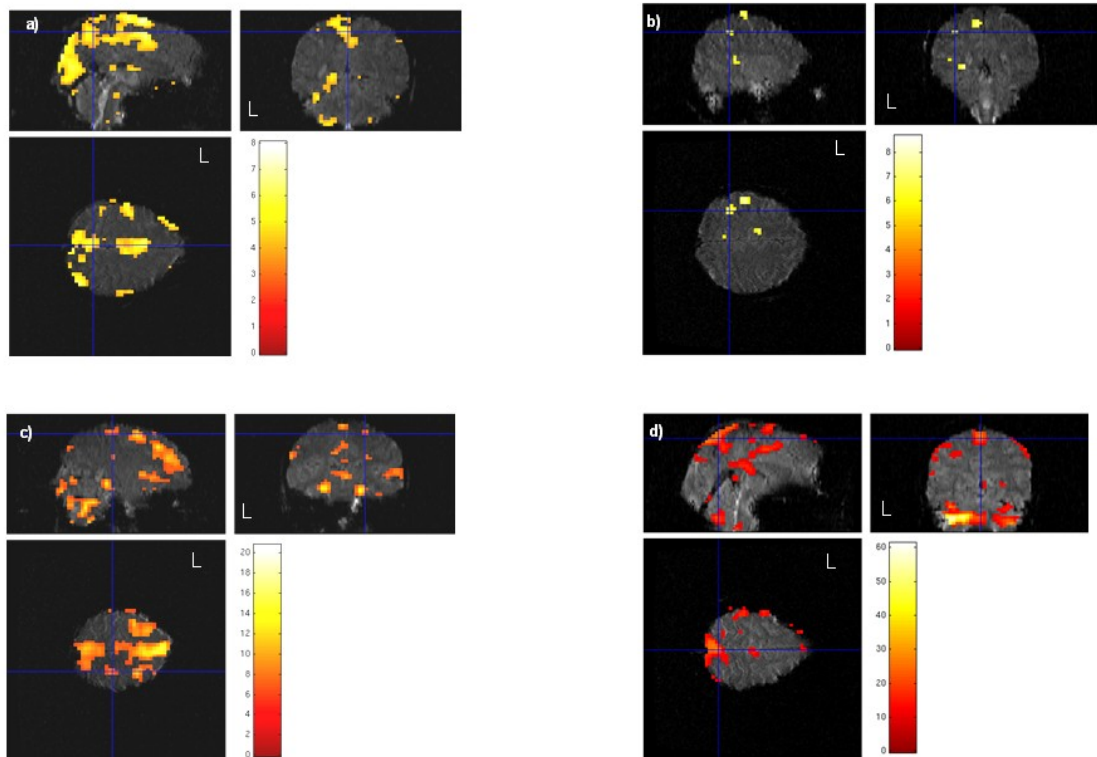


**Figure 6.5: BOLD changes for physiological activities**

SPM[F] maps overlaid on high resolution EPI. (a) Case 1: BOLD changes (at  $p < 0.001$ , uncorrected for FWE) for head jerks were seen in motor cortex, premotor cortex, frontopolar cortex, medial frontal cortex and precuneus. Very small clusters of BOLD changes were also seen around edges of brain and ventricular system. (b) Case 4: BOLD changes (at  $p < 0.001$ , uncorrected for FWE) for head jerks were seen in motor cortex, premotor cortex medial frontal cortex and precuneus. (c) Case 5: BOLD changes (at  $p < 0.05$ , corrected for FWE) for coughing were seen in motor cortex, supplementary motor area, prefrontal cortex, medial frontal cortex, precuneus and cerebellum. Other small clusters of BOLD changes were also seen around edges of brain and inside ventricular system. (d) Case 2: BOLD changes (at  $p < 0.05$ , corrected for FWE) for yawning were seen in motor cortex, premotor cortex, frontopolar cortex, medial frontal cortex and precuneus. Very small clusters of BOLD changes were also seen around edges of brain and ventricular system.

#### 6.4 Discussion

Motivated by the need to maximise the amount of potentially clinically relevant information from each and every vEEG-fMRI dataset in patients with epilepsy, I investigated the effect of including additional regressors for physiological activities: eye blinks, chewing, swallowing, hand or foot movements, coughing, yawning and head jerks. These physiological activities arose spontaneously, identified retrospectively on video-EEG, and were included in the design matrix for fMRI analysis of epileptic activity in patients with focal and generalized epilepsy. In principle this approach should result in more specific and reliable findings if the confounding effects are modelled appropriately through reduction of the amount of residual variance [Friston *et al.* 1995b; Friston *et al.* 1996; Lund *et al.* 2005; Lund *et al.* 2006].

Two models: one without and the second with these additional regressors, were used. I observed increases in the Z-score and cluster size for IED related GM BOLD clusters in 6/10 patients (patients #1, 2, 4, 5, 7 and 8) and decreases in 4/10 patients (patients #3, 6, 9 and 10) as an effect of the inclusion of the physiological activities in the fMRI model. These results also showed additional IED related BOLD clusters in 3/6 focal epilepsy patients as revealed in Figure 6.3. For patients #1 and 5, the additional BOLD cluster revealed by GLM2 (highlighted green in Table 6.3) was in the hemisphere ipsilateral to the lesion on structural MRI and IZ. For patient 2, the additional BOLD cluster by GLM2 (highlighted green in Table 6.3) was located in the hemisphere contralateral to the IZ in line with the PET findings. It has been shown previously that the BOLD changes for IEDs may be more extensive than the electroclinically defined epileptogenic areas [Salek-Haddadi *et al.* 2006; Zijlmans *et al.* 2007] in line with other techniques such as PET where larger areas of metabolic dysfunction are revealed for patients with focal epilepsy [Mauguiere and Ryvlin 2004]. In this study, the additional BOLD clusters revealed by GLM2 (patient #1, 2 and 5) as well as other BOLD clusters (from both GLMs) which are remote from IZ for all patients with focal epilepsy could represent the spread of epileptic activity revealing the epileptic network recruited during IEDs. This may provide new hypotheses to explore in individual cases undergoing presurgical evaluation regarding the epileptic focus and networks especially during seizures [Bartolomei *et al.* 2001].

I showed that the additional IED related BOLD clusters further reinforced the degree of concordance of the IED related BOLD maps with independently derived IZ. The degree of concordance of IED related maps were similar for both GLMs in 5/6 patients (Table 6.3) with focal epilepsy. However, the degree of concordance improved from *Some concordance* to *Concordant plus* for patient 6 (Table 6.3) as a result of a change in statistical significance of BOLD clusters for GLM2.

Similarly, in IGE patients, BOLD changes in the cortico-thalamic network were seen for 3Hz GSWDs which is in agreement with the previous studies [Hamandi *et al.* 2006]. For one IGE case (patient #10), BOLD changes were not seen in cortico-thalamic network as there was only one epoch of 3Hz GSWDs lasting 2 sec. I presume that the correlated BOLD changes in cortico-thalamic network were of low intensity and sub-threshold in patient #10.

EEG-fMRI experiments investigating epileptic activity generally last longer than fMRI studies for cognitive paradigms due to the need to capture as many epileptic events as possible. The physiological activities noticed in patients during vEEG-fMRI acquisition are neither part of experimental design nor related to epilepsy but performed by patients at their own will. I identified these physiological activities on simultaneous video recordings from two cameras synchronised with EEG. Significant BOLD changes were seen for eye blinks, swallowing, chewing and hand movements (Table 6.4) in relevant brain areas as previously reported [Volkman 1986; Bodis-Wollner *et al.* 1999; Lotze *et al.* 2000; Mosier and Bereznaya 2001; Suzuki *et al.* 2003; Shinagawa *et al.* 2004; Chainay *et al.* 2004; Bristow *et al.* 2005a; Bristow *et al.* 2005b; Byrd *et al.* 2009; Peck *et al.* 2010; Bracco *et al.* 2010]. The majority of these BOLD changes were seen at a lower statistical threshold ( $p < 0.001$ , uncorrected for FWE), nevertheless they were seen in areas known to be responsible for the relevant processes. The number and duration of these activities were variable. The most significant and consistent BOLD changes were seen for eye blinks. This may be because there were frequent eye blinks (Figure 6.2). It has been shown that more significant BOLD changes were seen when the number of events such as 3Hz GSWDs was higher [Hamandi *et al.* 2006].

For the physiological activities possible to have associated head motion such as head jerks, coughing and yawning, BOLD changes were seen in the brain areas

known to be involved in producing these activities such as MC and SMA etc. as shown in Figure 6.5 and Table 6.4. This is in agreement with the recent finding [Jansen *et al.* 2012] that motion related artefacts, identified on EEG, when convolved with canonical HRF show neuronally plausible patterns of BOLD changes. Moreover, the signal changes for head motion generally do not overlap significantly with task related BOLD changes [Birn *et al.* 2004] and the latter can be studied even in the presence of task correlated motion if appropriate measures are taken [Birn *et al.* 2009]. Therefore, the BOLD clusters for physiological activities found in relevant anatomical areas in this study are probably genuinely reflecting neuronal activity associated with head movement. Nevertheless this may not be the case in patients with lesions, due to the possible presence of high-contrast edges within the brain, but I did not observe this effect. However, I also observed some signal changes at the edges of the brain for these physiological activities (Figure 6.5) which are in line with the previous findings [Birn *et al.* 2004]. In contrast to Jansen *et al.* (2012) I convolved the EOI with the canonical HRF and its temporal and dispersion derivatives. The additional flexibility thus afforded [Thornton *et al.* 2010b] may capture residual motion related spin history effects [Friston *et al.* 1996]. Moreover, motion related signal changes are well known to be a potential severe confound, although this is less problematic in event-related design when motion is brief and effects of interest are of variable duration [Birn *et al.* 1998;Birn *et al.* 1999] as is the case in this data.

The brain regions active during physiological activities such as those considered here may overlap the epileptogenic network. In fMRI modelling for any EOI the correlated BOLD signal is evaluated in each voxel across the brain. If signal fluctuations in a particular voxel reflect two different types of activity, e.g. epileptic and physiological activities, not modelling this additional signal will increase the residual variance thus decreasing sensitivity to the effect of interest unless the two types of activity are orthogonal [Friston *et al.* 1995b;Friston *et al.* 1996]. In principle the effect should be stronger in regions of overlap between epileptic activity and normal physiological activity. My results support this principle: when more variance was explained in GLM2 the Z-score and cluster size of those IED related BOLD clusters also increased which overlapped with BOLD clusters for physiological activities (BOLD clusters marked by † in Table 6.3). Conventionally, it is important to retain a sufficient number of degrees of

freedom (number of scans minus number of estimated parameters) specially for single subject fMRI modelling; for SPM the recommendation is that there should be at least 30 effective degrees of freedom [Friston *et al.* 1995b], which was the case in this study.

The concordance of SPM maps with independent electroclinical data was evaluated by comparing the location of GM and other BOLD clusters with the IZ. The IZ was defined on the basis of electrophysiological and radiological information. At least 6-10 cm<sup>2</sup> area of the underlying cortex (corresponding to more than one gyrus) needs to be active synchronously to produce an IED on scalp EEG [Ray *et al.* 2007; Tao *et al.* 2007a; Tao *et al.* 2007b]; nonetheless this does not preclude a corresponding smaller region of BOLD change. The extent of BOLD clusters also largely depends on the extent and strength of the underlying haemodynamic changes and the choice of statistical threshold [Bandettini *et al.* 1993; Friston *et al.* 1994]. I used a conventional statistical threshold levels ( $p < 0.05$ , FWE corrected, and  $p < 0.001$ ) in line with other validation studies in epilepsy (Zijlmans *et al.*, 2007). The concordance classification approach, used in this study and applied in many previous publications from my group [Thornton *et al.* 2010b] and others [Grouiller *et al.* 2011], is motivated by the need to summarise sometimes complex maps on one hand, and allow the possibility that the cluster containing the most highly correlated voxel, which has the appealing characteristic of being unique in a given map, has a special biological or clinical significance. It is possible that once fMRI modelling has been sufficiently refined, the GM cluster for IEDs is found to be specifically related to the IZ or the epileptogenic zone.

I discounted the BOLD clusters in the ventricular system, vascular tree, edges of brain and base of brain during the evaluation of GM BOLD cluster as they may represent motion related signal changes. No dataset was discarded because of motion. I used additional regressors (Volterra-expansion of six realignment parameters [Salek-Haddadi *et al.* 2006] and cardiac pulse related regressors [Liston *et al.* 2006]) to reduce motion related fMRI signal variance. The number of scans affected by head motion ( $> 0.2$  mm) and the range for maximum inter-scan motion was in line with previous findings in different subjects [Salek-Haddadi *et al.* 2006; Thornton *et al.* 2010b]; in particular that despite head

motion events greater than one voxel size, BOLD changes can be seen that seem to reflect epileptic activity.

These findings support my hypothesis. I demonstrated that by using this new modelling approach of including physiological activities in the design matrix, the un-modelled residual variance was decreased in principal and new IED related BOLD clusters were revealed. These new IED related BOLD clusters were consistent with the epileptic network as demonstrated by other noninvasive electroclinical (i.e., long-term video-EEG) and radiological (i.e., structural MRI and PET) investigations. The cluster size and statistical significance of BOLD clusters also increased without increasing the amount of data acquired from each subject [Birn *et al.* 2009]. Therefore, I propose that the new modelling approach is worthwhile mainly in studies of individual subjects, where reliability of the results is particularly important.

In the study of seizures the combined effects of seizure related motion and propagating neuronal activity can pose a much greater modelling challenge and widespread BOLD changes are shown [Thornton *et al.* 2010b]. Therefore, I chose to test the new approach on interictal data to facilitate validation in the first instance. In Chapters 7 and 8, I will present my work on including these additional regressors for physiological activities in the design matrices for investigating seizure related haemodynamic changes using vEEG-fMRI.

## 6.5 Conclusion

Modelling epileptic activity to reveal BOLD changes is complex and it is important to separate these BOLD changes from non-epileptic activity related BOLD changes. I showed that inclusion of video-EEG derived additional regressors, for physiological activities, in the design matrix can explain a significant amount of variance. Additional IED related BOLD clusters were revealed in regions concordant with available electroclinical and radiological information in some focal cases, with no apparent degradation of the results in any of the cases, suggesting that this approach constitutes an efficacious addition to fMRI data modelling.

## Chapter 7: Mapping ictal haemodynamic networks using vEEG-fMRI<sup>6</sup>

### 7.1 Background

Focal epilepsy is refractory to medication in 30% of patients [Kwan and Sander 2004]. Epilepsy surgery is potentially curative requiring rigorous presurgical evaluation which focuses on the identification of the brain region: seizure onset zone (SOZ) [Luders and Comair 2000], or network responsible for seizure generation [Spencer 2002]. Synchronized video-EEG is the standard approach to localise SOZ non-invasively [Rosenow and Luders 2001] with good temporal resolution but has low sensitivity (25-56%) and spatial resolution compared to icEEG [Smith 2005; Ray *et al.* 2007]. Therefore, video-EEG may not provide the required information for localising SOZ [Lee *et al.* 2000; Catarino *et al.* 2011; Remi *et al.* 2011] warranting icEEG recordings [Luders *et al.* 2006].

As discussed in Chapter 2, recent advances in neuroimaging such as: high resolution MRI scans, MEG, PET, ictal-SPECT and EEG-fMRI have significantly improved our ability to identify and localise brain areas involved in seizure generation. In Chapter 3, I discussed how EEG-fMRI is able to map ictal related BOLD changes despite its limitations: unpredictable nature of seizures; difficulties with seizure identification inside the scanner; seizure related motion effects; and potentially complex and unknown time course of the ictal haemodynamic patterns represent a challenge for mapping seizures. In Chapters 5 and 6, I demonstrated that a new development of this technique, vEEG-fMRI, can record video synchronously without compromising image and EEG quality which in turn can be used to improve fMRI modelling strategy by identifying physiological confounds, thus explaining more nuisance variance in the fMRI data; since it is crucial to identify and define seizures using all available electroclinical information [Barba *et al.* 2007].

In this chapter, I present my work on the investigation of haemodynamic changes related to seizure onset and during seizure in a series of patients with typical seizures recorded during vEEG-fMRI. I hypothesized that:

---

<sup>6</sup> This chapter forms the basis of the article [Chaudhary *et al.* 2012b]



1) By partitioning seizures into phases, vEEG-fMRI can localise BOLD changes at the seizure onset better than later parts of seizure, providing additional information at the sub-lobar level which is superior to scalp EEG.

2) BOLD networks recruited during later parts of seizure are associated with seizure propagation.

The aim was to localise ictal onset and ictal propagation related BOLD changes non-invasively for comparison with the electroclinically and radiologically defined presumed SOZ and invasively defined SOZ where available, to assess the clinical potential of ictal vEEG-fMRI.

## 7.2 Methods

The common methods are described in Chapter 4, and the methodological aspects specific to this study are described here.

### 7.2.1 Subjects

55 patients with refractory focal epilepsy were invited to undergo vEEG-fMRI scanning if:

- 1) They had  $\geq 2$  seizures /day at the time of scanning.
- 2) Seizures were previously recorded on long-term video-EEG monitoring.
- 3) The seizures did not involve large head motion and deemed suitable for MRI scanning.
- 4) There were no contraindications to undergo MRI scanning.

Drug reduction or sleep deprivation was not used before vEEG-fMRI studies. These patients had had a detailed clinical history and examination, MRI scanning, long-term video-EEG monitoring and neuropsychology assessment. A few patients had a known seizure trigger (Patients: #2: thinking about/lifting a weight in patient's right hand; 9: rubbing right chest wall; 12: lifting/moving limbs; 18: music) which was used to attempt to provoke seizures during vEEG-fMRI. For three of these patients (#2, 9 and 12), the seizure provoking behaviour was used randomly in time and repeated two to three times during the acquisition. For patient #18 a patient specific paradigm was designed where seizure triggering music was presented in blocks of incrementing duration (i.e., 10, 20sec) up to 1-minute alternating with equal duration blocks of non seizure triggering music and without music.

Six patients underwent intracranial electrode implantation based on hypotheses derived from spatial localisation of ictal and IED recorded during long-term vEEG monitoring, structural abnormalities on MRI-scans and other non-invasive investigations such as: PET, MEG or ictal-SPECT where available, as part of their presurgical evaluation. The icEEG was recorded using Nicolet EEG Neurodiagnostic System with the following parameters: sampling rate = 512Hz except one patient (#15) where it was 1024Hz, ADC resolution voltage = 0.153 $\mu$ V, effective digitizer resolution = 22 bit (16 stored).

### **7.2.2 MRI acquisition**

Two 20-minute EPI sessions were acquired. In two cases (patients #: 2 and 7), a third 20-minute EPI session was acquired. The scanning was stopped prematurely in three cases (patients: #6, 9 and 18) to limit the risk of adverse incident. In four cases (patients: #1, 6, 9 and 16) vEEG-fMRI acquisition was repeated on a different day to capture a seizure after the first unsuccessful attempt; also, I had flexible MRI scanning slots and scanned patients at the times they reported that seizures were most likely to occur. The details of MRI acquisition are described in Chapter 4 section 2.

### **7.2.3 Video-EEG recording and artefact correction**

Synchronous scalp video-EEG was recorded during the MRI scanning. The details of video-EEG recording and removal of pulse and scanner artefact are described in Chapter 4, Section 4.3.

### **7.2.4 Data processing and analysis**

#### **7.2.4a EEG and fMRI Processing**

I reviewed video-EEGs jointly with experienced neurophysiologists (Dr. Beate Diehl, Dr. Serge Vulliemoz, Prof. Matthew C Walker) to identify IEDs and ictal rhythms [Luders *et al.* 2000; Foldvary *et al.* 2001] and ictal semiology [Luders *et al.* 1998]. The seizures recorded during vEEG-fMRI were compared with the seizures recorded during long-term video-EEG monitoring, and partitioned into phases based on spatiotemporal evolution [Niedermeyer and Lopes da Silva 2005] of electrophysiologic changes on EEG and ictal semiology on video, in an attempt to separate the seizure onset related BOLD changes from propagation. The ictal phases [Thornton *et al.* 2010b] were defined as follows:

- *Ictal onset*: build up of ictal-EEG-pattern [Foldvary *et al.* 2001] preceding clinical features.
- *Ictal established*: onset of the clinical manifestations along with regional/generalized EEG changes or emergence of myogenic artefact on EEG.
- *Late ictal*: subsequent EEG slowing following the *Ictal established* phase.

Seizures that did not have an electrographic signature (e.g., simple partial seizures) or for which the ictal phases could not be separated clearly due to myogenic artefact on EEG, were labelled as single *Ictal* phase.

Physiological activities: spontaneous eye blinks and eye movements, swallowing, jaw clenching, small head jerk, facial twitches, brief hand/foot movements, as described in Chapter 6, were also identified on video-EEG and distinguished from ictal semiology by comparison with ictal events captured on long-term video-EEG monitoring. The details of fMRI data pre-processing are described in Chapter 4, Section 4.4.

#### 7.2.4b fMRI Modelling

The fMRI-data was analysed within the GLM framework. EPI sessions during which seizures were recorded on video-EEG were analyzed. Eleven patients had more than one seizure during vEEG-fMRI, out of which seven had seizures in more than one EPI-session which were included in a single GLM as separate sessions.

A GLM was built to investigate the BOLD changes associated with the ictal phases in all patients. Each ictal phase was represented mathematically as variable duration block depending upon the duration of the respective phase in a separate regressor. I wanted to identify putative BOLD patterns consistent across seizures. Therefore, in patients with multiple seizures of similar electroclinical characteristics, I modelled a particular ictal phase from multiple seizures within single regressor. IEDs were represented as either stick functions or blocks (for series of events) and treated as confounds. In patients with more than one type of IEDs, each type was modelled as a separate effect. Datasets were analysed irrespective of the amount of head motion. Inter-scan realignment parameters and their Volterra-expansion [Friston *et al.* 1996] were included as confounds to account for motion related effects. Forty four additional regressors (one for each

slice) were also included as confounds to account for pulse related effects [Liston *et al.* 2006]. Physiological activities (described above) were represented as separate blocks and each type was modelled as a single regressor as shown in Chapter 6. The haemodynamic effects of interest: ictal phases, IEDs and physiological activities were convolved with the canonical HRF and its temporal and dispersion derivatives. An exception was patient #9 for whom the effects of interest were convolved with the canonical HRF and its temporal derivative but without the HRF dispersion derivative; because inclusion of the latter resulted in the GLM not being estimable (due to correlation between regressors). The fMRI data was high pass filtered with a cut-off 128sec.

### **7.2.5 Assessment of BOLD changes, significance, visualization and level of concordance**

SPM[F]-maps were obtained for each ictal phase separately, and across combined *all ictal* phases at conventional conservative threshold:  $p < 0.05$ , corrected for FWE. When BOLD changes were not seen at  $p < 0.05$ , I used a less conservative statistical threshold:  $p < 0.001$ , uncorrected for FWE. The resulting maps were co-registered with the patient's anatomical MRI scan. The fitted BOLD time course for each cluster was plotted and classified as increases, decreases or biphasic (including both increases and decreases) according to the sign of the peak change relative to baseline.

To test hypothesis #1, I defined presumed SOZ non-invasively at the lobar level on the basis of IEDs, ictal rhythm, ictal semiology, and structural abnormality where available. The ictal BOLD maps were compared visually with the presumed SOZ along with an experienced neuro-radiologist (Dr. Caroline Micallef) and classified on the basis of the most statistically significant (global maximum: GM) and other clusters as either:

- *Entirely concordant*: All BOLD clusters were within the presumed SOZ (within the same lobe/gyrus).
- *Concordant plus*: The most statistically significant cluster (global maximum: GM) was within the presumed SOZ (within the same lobe/gyrus) and other clusters were remote from the presumed SOZ.

- *Some concordance*: The GM cluster was remote from the presumed SOZ and one of the other clusters was within the presumed SOZ (within the same lobe/gyrus).
- *Discordant*: all clusters were remote (another lobe or opposite hemisphere) from the presumed SOZ.

The BOLD clusters located in the ventricular system, vascular tree, edges and base of brain and cerebellum were not considered [Chaudhary *et al.* 2012a]. Firstly, for patients who underwent icEEG recording during presurgical assessment I compared the sub-lobar localisation provided by vEEG-fMRI with the invasively defined SOZ. The invasively defined SOZ was delineated by two experienced neurophysiologists (Dr. Beate Diehl, Prof. Matthew C Walker) as the location of depth/grid contacts on icEEG where the first and maximal ictal changes were seen. I measured the Euclidean distance between the statistical maximum voxel of GM/other BOLD cluster, within the presumed SOZ for the *Ictal onset/Ictal* phase, and the invasively defined SOZ using the following formula:

$$|d| = \sqrt{((X_1 - X_2)^2 + (Y_1 - Y_2)^2 + (Z_1 - Z_2)^2)}$$

Here,  $X_1$ ,  $Y_1$  and  $Z_1$  represent the position of the icEEG electrode contact in x,y and z plane and  $X_2$ ,  $Y_2$  and  $Z_2$  represent the position of the BOLD change in x,y and z plane. Secondly, for patients who did not have icEEG recording, I compared the sub-lobar localisation of GM BOLD cluster provided by vEEG-fMRI with the level of localisation provided by ictal rhythm on scalp EEG. Thirdly, I compared the level of concordance of BOLD maps with the presumed SOZ between different ictal phases using Spearman's rank Correlation ( $r_s$ ) (IBM SPSS Statistics).

To test hypothesis #2, firstly I assessed the *Ictal established/Ictal* phase related BOLD maps in relation to the symptomatogenic areas (defined on the basis of specific ictal semiology for each patient), and compared the presence/absence of changes in symptomatogenic and non-symptomatogenic areas using Fisher's Exact test in software package IBM SPSS Statistics. Secondly, I assessed *all ictal* BOLD maps in relation to the Resting State Networks (RSNs) [Damoiseaux *et al.*

2006;Mantini *et al.* 2007;van den Heuvel *et al.* 2009]. I also tested for the relationship between presence/absence of loss of consciousness, as reported during long-term video-EEG monitoring for typical seizures, and BOLD changes in the default mode network (DMN) using mean contingency coefficient ( $\Phi$ ); and the association between loss of consciousness in the subgroup with BOLD decreases in the DMN using non-parametric chi-squared test in software package IBM SPSS Statistics.

### 7.2.6 Quantification of head motion events

To assess the potential effects of head motion on the fMRI results, I calculated the number of ‘head jerks’ defined as events of inter-scan displacement  $> 0.2\text{mm}$ , and the mean and maximum inter-scan displacement for each dataset [Salek-Haddadi *et al.* 2006;Lemieux *et al.* 2007]. The level of concordance for *Ictal onset* and *Ictal* phases was also compared as a function of these parameters using chi-squared test for trend (Statistical Package Stata/IC 11.1;StataCorp-LP).

## 7.3 Results

Twenty four of the 55 patients reported or were observed to have ictal events during vEEG-fMRI. When compared to the seizures recorded during long-term video-EEG monitoring, 20/24 patients had typical seizures during vEEG-fMRI. None of the twenty patients with typical seizures during vEEG-fMRI reported an atypical event, and the four patients with atypical events will not be considered further in this work. Of the 20 cases with typical seizures, 6 had frontal lobe, 4 had focal reflex, 4 had multifocal, 2 had temporal lobe, 2 had parietal lobe and 2 had hypothalamic seizures. The median age was 28 years (range: 18-60), median seizure onset was at 9 years (range: 1-32) and there were 12 males. A summary of the clinical details on these patients can be found in Table 7.1. The types of IEDs and ictal rhythms for each patient with typical seizures during long-term video-EEG monitoring are shown in Table 7.2.

The vEEG-fMRI scanning time (median=40 minutes; range=20-80) and seizure statistics for each patient are described in Table 7.3. The seizures were identified on video-EEG in 15/20 patients (75%), on EEG only in 2/20 patients (10%, technical video failure) and on video only in 3/20 patients (15%, no ictal EEG change or EEG obscured by myogenic artefact; Table 7.3, Figure 7.1). In 13/20

(65%) patients distinct ictal phases could be identified and the remainder had single *Ictal* phase.

**Table 7.1: Clinical characteristics and localisation of epilepsy**

ID #	Gender	Age	Seizure onset (age)	Type of Epilepsy	Seizure Onset on Scalp EEG	MRI	Presumed SOZ
<b>Patient who underwent invasive evaluation</b>							
1	F	28	9	PLE	Regional right parieto-occipital	Multiple tubers	Right parieto-occipital
3	M	19	2	Multi focal	Lateralized left hemisphere	FCD: Left Parieto-occipito-temporal	Left parieto-occipito-temporal
10	F	32	2	Multi focal	Lateralized right max. temporal	Ischaemic damage: Right Occipito-parietal	Right temporo-occipital
16	M	28	12	FLE	Regional left fronto-central	FCD: Left posterior SFG + MFG	Left frontal lobe
4	M	28	10	TLE	Regional left temporal	NL	Left temporal lobe
15	M	42	14	TLE	Lateralized left max. fronto-temporal	NL	Left temporal frontal
<b>Patients who did not undergo invasive evaluation</b>							
5	F	23	10	Multi focal	Non-lateralized	MCD: Left Frontal+Parieto-temporal	Left Frontal and Parietal
8	F	31	6	Multi focal	Multi-regional	Right Polymicrogyria and schizencephaly	Right hemisphere
11	F	20	11	FLE	Generalized max. right frontal	Ischaemic damage: Right hemisphere	Right frontal lobe
12	F	24	9	Reflex	Regional fronto-central with left emphasis	FCD: Left paracentral lobule	Left frontal lobe
14	M	60	1	Hypothalamus	None	Hypothalamic Hamartoma	Hypothalamus
17	F	36	17	FLE	Regional right centro-parietal	FCD: Right MFG + pre-central gyrus	Right frontal lobe



**Table 7.1: contd.**

<b>ID #</b>	<b>Gender</b>	<b>Age</b>	<b>Seizure onset (age)</b>	<b>Type of Epilepsy</b>	<b>Seizure Onset on Scalp EEG</b>	<b>MRI</b>	<b>Presumed SOZ</b>
<b>Patients who did not undergo invasive evaluation</b>							
19	M	26	7	PLE	Regional right parieto-central	FCD: Right Angular gyrus	Right parietal lobe
20	M	26	1	Hypothalamus	None	Hypothalamic Hamartoma	Hypothalamus
2	M	36	19	Reflex	Regional left centro-parietal	NL	Left centro-parietal
6	F	37	11	FLE	Non-lateralized	NL	Medial Frontal
7	F	44	1	FLE	Generalized max. fronto-central	NL	Midline fronto-central
9	M	19	5	Reflex	Non-lateralized	NL	Medial hemisphere
13	M	18	7	FLE	Generalized right max. fronto-central	NL	Right frontal lobe
18	M	51	32	Reflex	Generalized max. left fronto-temporal	NL	Left fronto-temporal

Abbreviations: TLE = temporal lobe epilepsy, FLE = frontal lobe epilepsy, PLE = parietal lobe epilepsy, NL = non lesional, FCD = focal cortical dysplasia, MCD = malformation of cortical development, M = male, F = female. SFG=superior frontal gyrus. MFG =middle frontal gyrus.

**Table 7.2: Interictal and ictal activity recorded during long-term video-EEG monitoring**

<b>ID #</b>	<b>Scalp EEG IED Type</b>	<b>IcEEG</b>	<b>Ictal pattern on EEG at seizure onset / Ictal semiology</b>
1	Sharp waves: Right Parieto-occipital	<p><b>Implantation</b>            GRID 8X8: R occipito-temporal and parietal            STRIP 1X6: R superior parietal A            STRIP 1X6: R superior parietal B            DEPTH 1X4: R parieto-occipital superior to tuber            DEPTH 1X4: R parieto-occipital inferior to tuber</p> <p><b>IED Type</b>            Spikes and polyspikes            1)R parieto-occipital tuber depth contact            2)R occipito-temporal grid contact            3)R inferior parietal grid contact</p>	<p><b>Ictal pattern</b> (scalp) = Fast activity: Right Parieto-occipital  <b>Ictal pattern</b> (icEEG) = fast spikes superimposed on irregular 2-5 Hz slow (depth contact superior part of lesion) → 22Hz low voltage fast in all depth contacts → spread to grid contacts covering right parieto-occipital  <b>Ictal semiology</b> = Aura (sensation of being uplifted &gt; visual blurring) &gt; autonomic seizure (blank stare &gt; pupillary hippus &gt; postictal flushing) with LOA</p>
2	None	NA	<p><b>Ictal pattern</b> = Semi-rhythmic theta: Left centro-parietal  <b>Ictal semiology</b> = Right motor seizure: dystonic posturing and myoclonic jerks (median duration: 100ms (range: 50-300ms)) of right index finger &gt; right hand</p>
3	Spikes: 1) Left posterior temporal and occipital 2) Right fronto-temporal	<p><b>Implantation</b>            GRID 8X8: L posterior Temporo-occipit-parietal and frontal            STRIP 1X6: Supplementary motor area            STRIP 1X6: posterior to supplementary motor area            DEPTH 1X4: L parieto-occipital in the lesion</p> <p><b>IED Type</b>            Spikes, polyspikes and fast            1)L posterior temporo-occipital grid contacts            2) synchronously at grid (L posterior temporo-occipital) depth (lesion) and strip (posterior to SMA) contacts</p>	<p><b>Ictal pattern</b> (scalp) = EEG attenuation: Left hemisphere  <b>Ictal pattern</b> (icEEG) = 1. Repetitive spikes/bursts of fast (grid contacts covering left parieto-temporal) → grid contacts covering superior temporal gyrus → midline strip contacts covering posterior to SMA and anterior SMA            2. multifocal spikes with wide field at middle of grid contacts covering left parietal, temporal, inferior frontal and occipital → fast in the same contacts followed by high frequency  <b>Ictal semiology</b> = Aura (left head pain) &gt; tonic seizure with LOA (right arm tonic / bilateral asymmetric posturing) &gt; SGS</p>

**Table 7.2: contd.**

<b>ID</b>	<b>Scalp EEG IED Type</b>	<b>IcEEG</b>	<b>Ictal pattern on EEG at seizure onset / Ictal semiology</b>
4	Sharp waves: left temporal Sharp waves: right temporal	<b>Implantation</b> GRID 4X8: L lateral temporal STRIP 1X6: L superior temporal gyrus STRIP 1X6: L basal temporal anterior STRIP 1X6: L basal temporal posterior DEPTH 1X6: L hippocampus DEPTH 1X6: L amygdale  <b>IED Type</b> Spikes, polyspikes and fast: 1)L medial (posterior) basal temporal strip contacts 2)L anterior inferior temporal grid contacts 3)L anterior temporal polar grid contacts 4)L superior temporal gyrus grid contacts	<b>Ictal pattern</b> (scalp) = Theta rhythm: Left temporal <b>Ictal pattern</b> (icEEG) = burst of polyspikes (left medial (posterior) basal temporal strip) → fast (41 Hz) activity at same contacts → fast activity in left hippocampus and amygdale depth contacts <b>Ictal semiology</b> = Aura (buzzing sensation) > automotor seizure with LOA (orofacial movements > bimanual automatisms > nose wiping left hand)
5	Spikes: 1) Left fronto-temporal/anterior hemisphere 2) Bilateral generalized spike and wave Slow waves: Left fronto-temporal	<b>NA</b>	<b>Ictal pattern</b> = Rhythmical 9 Hz activity: Fronto-central <b>Ictal semiology</b> = Tonic extension of right arm > head turning to right > smile
6	None	<b>NA</b>	<b>Ictal pattern</b> = High amplitude sharp and slow wave complex or fast: fronto-central <b>Ictal semiology</b> = Head lifting > bilateral shoulder posturing > apnoeic > grabbing bed-sides > eye deviation > facial grimacing
7	Spike and wave: Bilateral frontal	<b>NA</b>	<b>Ictal pattern</b> = 1.5-2 Hz slow spike and wave: Bilateral fronto-central <b>Ictal semiology</b> = Dialectic seizures

**Table 7.2: contd.**

<b>ID</b>	<b>Scalp EEG IED Type</b>	<b>IcEEG</b>	<b>Ictal pattern on EEG at seizure onset / Ictal semiology</b>
8	Spike and wave: 1) Right posterior temporal- occipital 2) Left mid- temporal 3) Right mid- temporal 4) 1-1.5 HZ widespread 5) Right frontal spikes	<b>NA</b>	<b>Ictal pattern</b> = Irregular multiple spike and sharp wave discharge: Fronto- temporo-central electrodes <b>Ictal semiology</b> = Small head jerks to the left/upper body stiffening/eye deviation/nystagmus to left
9	Spikes: 1) Fronto-central 2) Left posterior temporal 3) Left parietal	<b>NA</b>	<b>Ictal pattern</b> = Fast and spikes: Fronto- central <b>Ictal semiology</b> = Sensory aura > posturing and stiffening of right arm and leg > jerking of right arm and leg > figure of 4 (right hand bent)/late right eye deviation/apnoea > SGS
10	Sharp: 1) Right mid temporal 2) Right fronto- temporal	<b>Implantation</b> DEPTH 1X6: R hippocampus GRID 4X5: R lateral temporal GRID 8X8: R Temporo- parieto-occipital  <b>IED Type</b> Spikes and poly spikes: 1)R hippocampus depth contacts 2)R occipital grid contacts 3)R parieto-occipital grid contacts	<b>Ictal pattern</b> (scalp) = Sharp wave and theta activity: right hemisphere maximum temporal <b>Ictal pattern</b> (icEEG) = Burst of spike, attenuation and fast (12 Hz)(right hippocampus depth) → fast (18-20 Hz) right lateral temporal superior grid contacts → rhythmic discharge in right occipital grid contacts <b>Ictal semiology</b> = Psychic aura (Déjà vu, jamais vu/ altered visual perception) > automotor seizure with loss of awareness (lip smacking, non forced head turning to right, ictal speech, post ictal nose wipe)
11	Spike and wave: Bilateral Right > Left Sharp: Right frontal/fronto- temporal	<b>NA</b>	<b>Ictal pattern</b> = 2-2.5 Hz slow waves: Right hemisphere maximum frontal <b>Ictal semiology</b> = Dialectic seizures
12	Repetitive runs of spikes: 1) Left fronto- central, post- central 2) Left temporal	<b>NA</b>	<b>Ictal pattern</b> = Rhythmic fast activity: Fronto-central with left emphasis <b>Ictal semiology</b> = Atonic seizures

**Table 7.2: contd.**

<b>ID</b>	<b>Scalp EEG IED Type</b>	<b>IcEEG</b>	<b>Ictal pattern on EEG at seizure onset / Ictal semiology</b>
13	Spike and wave: 1) 1.5-2 Hz Fronto-central Sharp 2) Right fronto-temporal 3) Left fronto-temporal	NA	<b>Ictal pattern</b> = (1) 1.5-2 Hz spike and slow wave complexes: generalized fronto-central, right more than left. (2) EEG attenuation followed by spike and wave: generalized <b>Ictal semiology</b> = (1) Dialeptic seizures, (2) Axial tonic seizures/bilateral asymmetric tonic seizure
14	Sharp: Right temporal & Left temporal	NA	<b>Ictal pattern</b> = None. <b>Ictal semiology</b> = Gelastic seizure
15	Spikes: Left fronto-temporal Polyspikes: Maximum left temporal	<b>Implantation</b> DEPTH 1X8: L orbitofrontal area DEPTH 1X6: L temporal pole DEPTH 1X6: L amygdala DEPTH 1X6: L inferior temporal gyrus DEPTH 1X6: L posterior hippocampus DEPTH 1X6: L superior temporal gyrus  <b>IED Type</b> Spikes: Left fronto-temporal Polyspikes: Maximum left temporal	<b>Ictal pattern</b> (scalp) = Fast activity: left temporal and fronto-central <b>Ictal pattern</b> (icEEG) = Burst of slow and spikes → attenuation → Fast at all contacts but maximum at inferior temporal gyrus, followed by mixed 3-4 HZ delta, theta sharp waves <b>Ictal semiology</b> = Automotor seizure with loss of awareness (mouth automatisms, head deviation to left, right hand dystonic posturing and shaking)
16	Spikes: Left frontal and fronto-central	<b>Implantation</b> GRID 8X8: L dorsolateral frontoparietal GRID 2X8: L parietotemporal (postcentral) DEPTH 1X4: L superior frontal sulcus anterior DEPTH 1X4: L superior frontal sulcus posterior  <b>IED Type</b> Spikes and fast 1)L Superior frontal gyrus/sulcus grid contact 2)L Superior frontal gyrus/sulcus depth contact	<b>Ictal pattern</b> (scalp) = Fast activity: regional left fronto-central. <b>Ictal pattern</b> (icEEG) = Spikes/sharpened theta (left superior frontal gyrus/sulcus grid contacts) → fast (75-80 Hz) at same grid contacts and depth contacts in superior frontal sulcus <b>Ictal semiology</b> = Versive seizure (right head version)

**Table 7.2: contd.**

<b>ID</b>	<b>Scalp EEG IED Type</b>	<b>IcEEG</b>	<b>Ictal pattern on EEG at seizure onset / Ictal semiology</b>
17	Sharp wave: Right Centro-parietal Slow wave: Left temporal	<b>NA</b>	<b>Ictal pattern</b> = Fast spikes: Right central <b>Ictal semiology</b> = Left motor seizure (head turning to left, left arm and/or leg dystonic posturing)
18	None	<b>NA</b>	<b>Ictal pattern</b> = 4 Hz slow waves: maximum left temporal. <b>Ictal semiology</b> = Automotor seizure (oral and right hand automatism)
19	Irregular slow activity: Right centro-parietal	<b>NA</b>	<b>Ictal pattern</b> = Rhythmic fast activity/ Rhythmic theta evolving to rhythmic spikes: Right centro-parietal <b>Ictal semiology</b> = Left arm tonic posturing (adduction/flexion), left leg extension > head leaning forward/arching of back > twitching of orbicularis oculi muscle. No LOA, maintained ictal speech
20	Sharp wave: Right fronto-central	<b>NA</b>	<b>Ictal pattern</b> = None; Late fast right fronto-central in one seizure. <b>Ictal semiology</b> = epigastric aura > autonomic seizure (hyperventilation)

Abbreviations: LOA = loss of awareness, EEG = electroencephalography, Hz = hertz, SGS = secondary generalized seizure, IED = interictal epileptiform discharges, NA = Not available, SMA = Supplementary motor area

**Table 7.3: Seizures recorded during vEEG-fMRI**

ID #	Seizure Trigger	-Duration of Scanning (minutes)	vEEG-fMRI			
			Seizure Identification	Seizure (#)	Ictal Phases	Duration Median (Range)
1	None	*80	Video + EEG	1	IO IE	9 s 15 s
2	Thinking or lifting weight in right hand	60	Video	24	Ictal	10 s (2s-3min)
3	None	40	Video + EEG	2	IO IE LI	27 s (24-30) 11.5 s (11-12) 27.5 s (27-28)
4	None	40	Video + EEG	7	IO IE LI	5.3 s (2-9.2) 4.9 s (1.9-13.3) 7.8 s (7-9.4)
5	None	40	Video + EEG	4	IO IE LI	2.8 s (2.8-10.4) 6 s (5.2-20) 4.2 s (4.2-16)
6	None	*70	Video + EEG	1	IO IE	9.8 s 22.4 s
7	None	60	Video + EEG	30	IO IE LI	3.6 s (1.4-8.6) 14.1 s (5.2-44.2) 4.1 s (1-13.2)
8	None	20	Video + EEG	6	Ictal	13.8 s (8.9-20.4)
9	Rubbing right chest wall	*75	Video + EEG	2	IO IE LI	5.6 s (2.9-8.4) 9.7 s (7.8-11.7) 2 s
10	None	40	Video	1	Ictal	17 s
11	None	40	Video + EEG	17	IO IE LI	5 s (2.4-8.8) 7.8 s (3-50.9) 5.8 s (3.1-18.5)
12	Movement of limbs	40	Video + EEG	15	Ictal	23.2 s (13.7-34.6)
13	None	40	Video + EEG	4	Ictal	11.3 s (8-17.3)
14	None	40	Video	1	Ictal	12 s
15	None	40	EEG	1	IO IE LI	5.7s 5 s 17.4 s
16	None	*80	EEG	1	Ictal	39.5 s
17	None	40	Video + EEG	10	IO IE LI	9.7 s (5-13.2) 4.2 s (2.6-8) 8.1 s (3.8-9.1)
18	Music	45	Video + EEG	1	IO IE	43.6 s 10.4 s
19	None	40	Video + EEG	1	IO IE LI	6.2 s 22.8 s 11.2 s
20	None	40	Video + EEG	1	IO IE	7.6 s 22.2 s

-Total duration of the vEEG-fMRI scanning session. One vEEG-fMRI session had one to three EPI-sessions, each lasting 20 minutes.

\*Patients had two vEEG-fMRI sessions on two different days to capture a seizure. Abbreviations: IO = Ictal onset, IE = Ictal established, LI = Late ictal

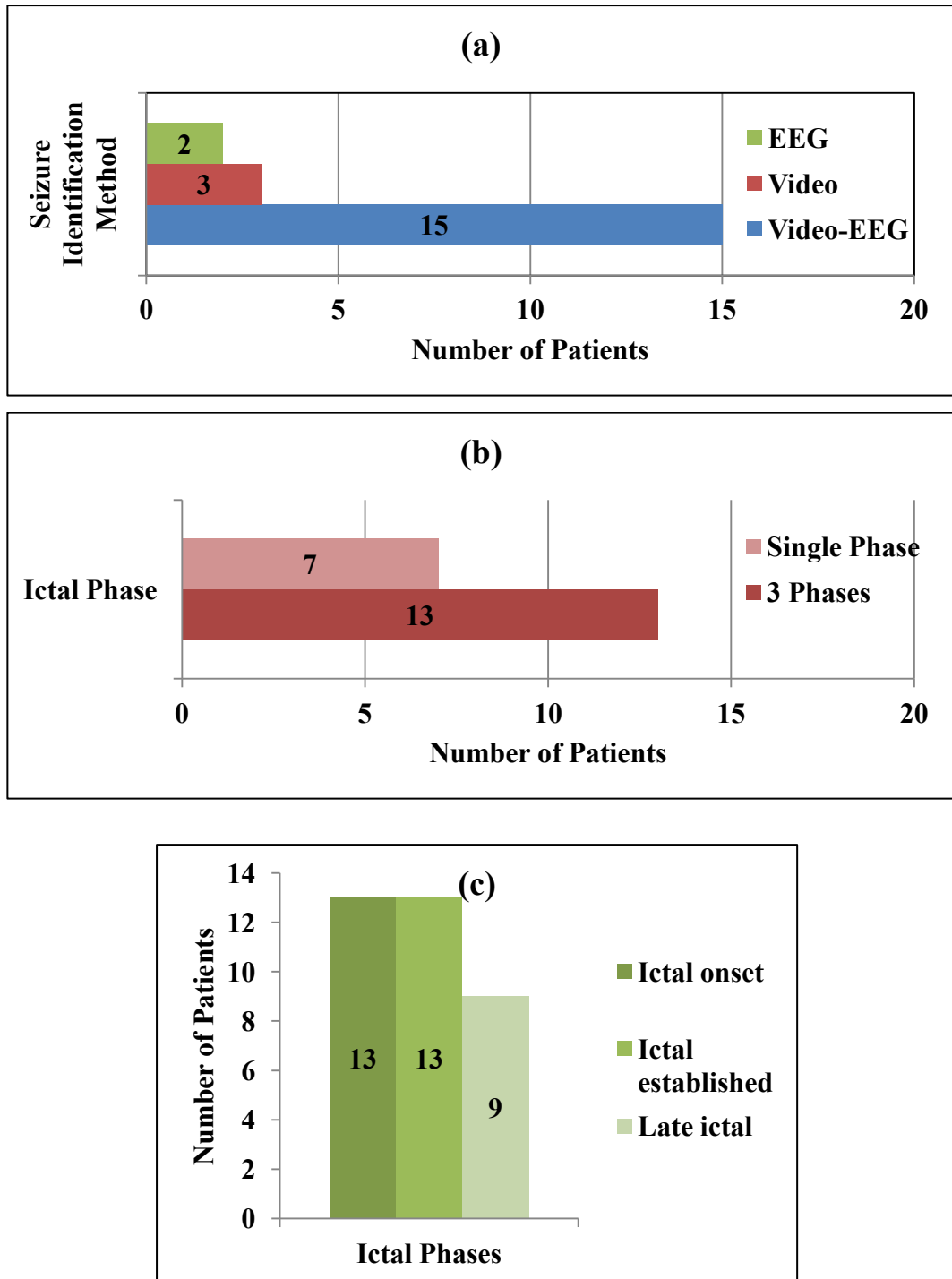


**Figure 7.1: Bar charts: identification of seizures and ictal phases**

(a) Bar chart shows different methods used to identify seizures during vEEG-fMRI. (b) Bar chart shows the number of patients with multiple ictal phases and single ictal phase. (c) Bar chart shows the number of patients with different ictal phases for patients with multiple ictal phases.



### 7.3.1 Ictal BOLD changes

Statistically significant BOLD changes were revealed for all ictal phases except for patient #3 for *Late ictal* phase. BOLD changes were seen at  $p < 0.05$  (corrected for FWE) in 15/20 patients (75%) for all ictal phases, and at  $p < 0.001$  (uncorrected for FWE) for one of the ictal phases in the remaining five patients.

Overall, the level of concordance of the BOLD maps (Figure 7.2) was better for the *Ictal onset/Ictal* phase (*Entirely concordant / Concordant plus* (13/20; 65%) + *Some concordance* (4/20; 20%) = 17/20; 85%) than *Ictal established* (*Entirely concordant / Concordant plus* (5/13; 38%) + *Some concordance* (4/13; 31%) = 9/13; 69%) and *Late ictal* phases (*Concordant plus* (1/9; 11%) + *Some concordance* (4/9; 44%) = 5/9; 55%); and was significantly correlated with the *Ictal onset / Ictal* phase ( $r_s = 0.3, p < 0.05$ ).

The BOLD changes for each ictal phase in each patient are described in Table 7.4.

#### 7.3.1a Comparison of ictal BOLD changes with invasively defined SOZ and surgical outcome

In the 6 patients (#1, 3, 4, 10, 15 and 16) who underwent icEEG recordings, four had epileptogenic structural abnormalities: focal cortical dysplasia (FCD: patients #3 and 16), tuberous sclerosis (patient #1) and ischaemic damage (patient #10; Table 7.1). For these four patients BOLD changes were seen within the presumed SOZ overlapping the structural abnormalities (Figures 7.3 and 7.4). *Ictal onset / Ictal* phase related maps were classified as (Table 7.4) *Entirely concordant or Concordant plus* in three, and to have *Some concordance* in one patient. Two of these four patients had *Ictal established* phase and the maps were classified as *Entirely concordant / Concordant plus* and to have *Some concordance* for one patient each.

For two patients who underwent icEEG recordings and did not have structural abnormalities also showed BOLD changes within the presumed SOZ at lobar level. The *Ictal onset / Ictal* phase related maps were classified as *Entirely concordant / Concordant plus* (Figure 7.5) in two patients; *Ictal established* phase related maps were classified to have *Some concordance* in one patient and were *Discordant* in one patient; and *Late ictal* phase related maps were classified as *Concordant plus* and to have *Some concordance* for one patient each.

The distance between the *Ictal onset / Ictal* phases related GM cluster found to be within the presumed SOZ in 5/6 patients and the invasively defined SOZ was 1.1 to 3.5cm (Table 7.4, Figure 7.6), demonstrating that vEEG-fMRI can localise the SOZ at sub-lobar level non-invasively for the *Ictal onset / Ictal phase*. Three patients proceeded to surgery and the BOLD cluster within the presumed SOZ was resected in two patients (#1 and 16: ILAE Class I postsurgical outcome; Figure 7.6), and was not resected in one patient (#4: ILAE Class III postsurgical outcome; Figure 7.6).

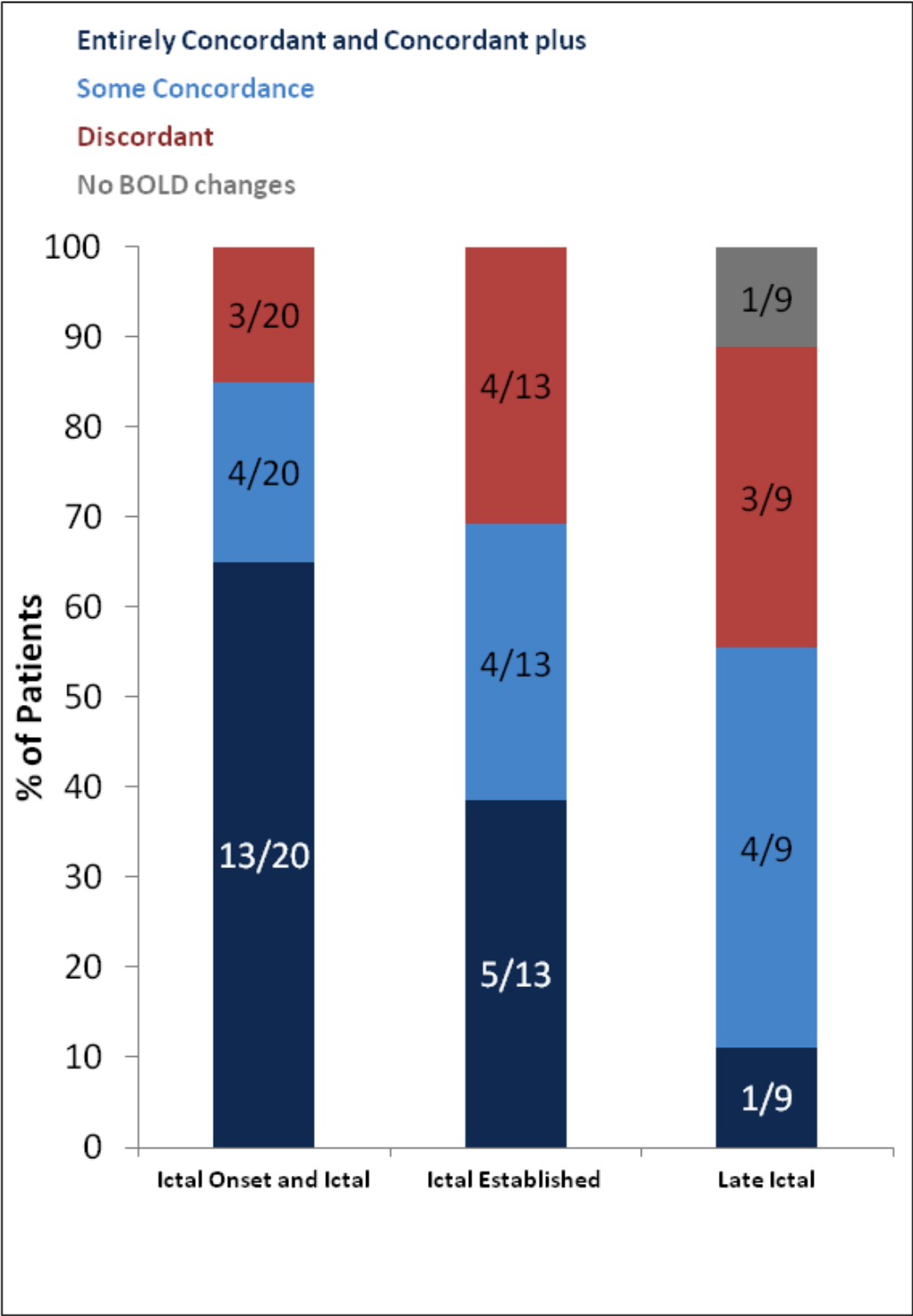


**Figure 7.2: Bar chart showing level of concordance**

Level of concordance of BOLD changes with the SOZ during ictal phases.

**Table 7.4: Ictal BOLD changes and level of concordance with the SOZ**

ID #	Localisation of BOLD changes for each ictal phase (Increases = ↑, Decreases = ↓)							Concordance	icEEG defined SOZ	-  d  (cm)		
	Phase	R Fron.	R Temp.	R Par.	L Fron.	L Temp.	L Par.				Others	
<b>Invasively defined SOZ</b>												
1	IO	↑MFG	-	↑*Inferior	-	-	-	-	-	SC	R parieto-occipital tuber	7/1.9
	IE	↑MFG	-	↑Inferior	-	-	-	-	-	SC		
3	IO	-	-	-	↓*MFG/IFG	-	↓*Superior	-	-	C+	SOZ 1: L TPO SOZ 2: L post. temp. SOZ 3: L IFG	SOZ 1: 4.6/1.7 SOZ 2: 4 SOZ 3: 2.3
	IE	-	-	↑Superior	↑MFG	-	↑Superior	-	↑Superior	C+		
10	Ictal	-	-	↑Superior	-	-	↑Superior	-	↑Superior ↑*R TPO ↑Med. Occ. ↑Precuneus	C+	SOZ 1: R hippocampus SOZ 2: Medial TPO	SOZ 1: 5.6 SOZ 2: 1.8
16	Ictal	-	-	↑Superior	↓*^SFG/MFG	↓STG	↑Superior, ↓SMG	↓Precuneus	↓Precuneus	C+	Left sup. Fron. sulcus and post. SFG	1.5
4	IO	-	-	-	-	↑*STG	-	-	-	EC	L anterior ITG	3.5
	IE	↑MFG	-	-	↑MFG	-	-	-	-	D		
	LI	-	-	-	-	↓Posterior	-	-	-	C+		
15	IO	-	-	-	↑MFG, MC	↑*STG	-	-	-	C+	SOZ 1: L temp. pole SOZ 2: L ITG	SOZ 1: 1.1 SOZ 2: 3
	IE	-	-	-	↓MFG	↑^STG	-	-	-	SC		
	LI	-	-	-	↑MFG	↑Post. Temp. STG	-	-	-	SC		

Table 7.4: contd.

ID #	Localisation of BOLD changes for each ictal phase (Increases = ↑, Decreases = ↓)								Concordance	icEEG defined SOZ	-  d  (cm)	
	Phase	R Fron.	R Temp.	R Par.	L Fron.	L Temp.	L Par.	Others				
<b>Presumed SOZ</b>												
5	IO	-	-	-	-	-	-	↑*Inferior	↑Precuneus	C+	C+	NA
	IE	-	-	-	↓ L Fronto-temporo-parietal	-	-	-	-	C+	C+	NA
	LI	↑FP, ↑Med.SFG	-	-	↑FC, ↑FP, ↑Med.SFG	-	-	-	-	D	D	NA
8	Ictal	↑^MFG, ↓Med.SFG	↑*MTG	-	-	-	-	-	-	C+	C+	NA
11	IO	↑* MFG	-	↑Superior	↑L MFG	-	-	↑Superior	-	C+	C+	NA
	IE	-	-	-	-	-	-	-	↓ Precuneus	D	D	NA
	LI	↑IFG	↑Lat. Parieto-temporal	-	-	-	-	-	-	SC	SC	NA
12	Ictal	↓MFG	-	-	↓*MFG /SFG	↓ Temporoccipital	-	-	-	C+	C+	NA
14	Ictal	↓MFG	-	-	↓MFG	↓STG	-	-	↓Paracentral lobule	D	D	NA

Table 7.4: contd.

ID #	Localisation of BOLD changes for each ictal phase (Increases = ↑, Decreases = ↓)								Concordance	icEEG defined SOZ	- d  (cm)
	Phase	R Fron.	R Temp.	R Par.	L Fron.	L Temp.	L Par.	Others			
17	IO	↑*MC, SMA, SFG	-	↓Superior	-	-	↓Superior	↓Paracentral Lobule, Precuneus	C+	NA	NA
	IE	↑^MC, Med.SFG	-	↑Superior	↑^MC, Med.SFG	-	↑Superior	↑Paracentral lobule Precuneus	SC		
	LI	-	↓MTG	-	-	-	↓Superior	-	D		
19	IO	↑MFG ↓Med.SFG	-	↓*SMG	↓Med.SFG	-	-	-	SC		
	IE	↓MFG ↓Med.SFG	↓SMG	↓Superior	↓MFG, ↓Med.SFG	-	↓Superior	↓Precuneus	C+		
	LI	↓MFG ↓Med.SFG	↓SMG	↓Superior	↓MFG ↓Med.SFG	-	↓Precuneus	↓Precuneus	SC		
20	IO	-	↑Med. Temp	-	↑MC	↑Med. Temp	↑Superior	-	D		
	IE	↓Med.SFG	-	-	↓MFG, MC	-	↓Med. Temp	↓Hypothalamus	SC		

Table 7.4: contd.

ID #	Localisation of BOLD changes for each ictal phase (Increases = ↑, Decreases = ↓)							Concordance	icEEG defined SOZ	- d  (cm)		
	Phase	R Fron.	R Temp.	R Par.	L Fron.	L Temp.	L Par.				Others	
<b>Presumed SOZ</b>												
2	Ictal	-	-	-	↑* <sup>^</sup> MC (hand area)	-	-	-	-	EC	NA	NA
6	IO	-	-	-	↓*SFG, MC	-	-	-	-	EC		
	IE	-	-	-	↓ <sup>^</sup> SFG,MC	-	-	-	-	EC		
7	IO	↓*Med.SFG	-	↓Superior	↓*Med.SFG	-	-	-	-	C+		
	IE	↓Lat. Fron., ↓*Med.SFG	-	↓Superior	↓Lat. Fron., ↓*Med.SFG	-	↓Superior	↓Precuneus, ↓ <sup>^</sup> Cingulum, ↑Thalamus		D		
	LI	↓Lat. Fron., ↓*Med.SFG	-	↓Superior	↓Lat. Fron., ↓*Med.SFG	-	↓Superior	↓Precuneus		D		
9	IO	-	↓MTG	-	↓*Med.SFG	-	-	-	-	SC		
	IE	↑ <sup>^</sup> MFG/IFG	↑MTG	-	↑ <sup>^</sup> Med.SFG	↑MTG	-	-	-	C+		
	LI	-	↓MTG	-	↓Med.SFG	-	-	-	-	SC		
13	Ictal	-	-	↑Superior	-	-	-	-	-	D		
18	IO	↓MFG Med.SFG	-	↓Superior	↓Med. SFG	↓*STG	-	-	-	SC		
	IE	↓MFG	-	↓Superior	-	-	-	↓Precuneus		D		

BOLD changes for different ictal phases are described at  $p < 0.05$  (FWE-corrected) in 15 patients. In five patients one of the ictal phase revealed BOLD changes at less conservative statistical threshold  $p < 0.001$  uncorrected for FWE only (Italicized). For each ictal phase the most statistically significant cluster (GM) is boldened.

\* *Ictal onset/Ictal* phase-related BOLD cluster highlighted non-invasively to be within the presumed SOZ

^ *Ictal established/Ictal* phase related BOLD cluster within the symptomatogenic area as defined on the basis of ictal semiology

¬ |d| = Distance (cm) between the intracranial electrode with first EEG change at seizure onset and GM/nearest BOLD cluster for the *Ictal onset / Ictal* phase highlighted non-invasively to be within the presumed SOZ

Abbreviations: Sup.=Superior, Fron.=Frontal, Temp.=Temporal, Par.=Parietal, Occ.=Occipital, IO=Ictal onset, IE= Ictal established, LI= Late ictal, Med.SFG = medial superior frontal gyrus, MC= motor cortex, SFG = superior frontal gyrus, MTG = middle temporal gyrus, MFG = middle frontal gyrus, SMA = supplementary motor area, IFG = inferior frontal gyrus, STG = superior temporal gyrus, B/L = bilateral, SMG = supra-marginal gyrus, ITG = inferior temporal gyrus, R = right, L = left, SOZ = seizure onset zone, TPO = Temporo-parieto-occipital junction, EC = Entirely concordant, C+ = Concordant plus, SC = Some concordance, D = Discordant



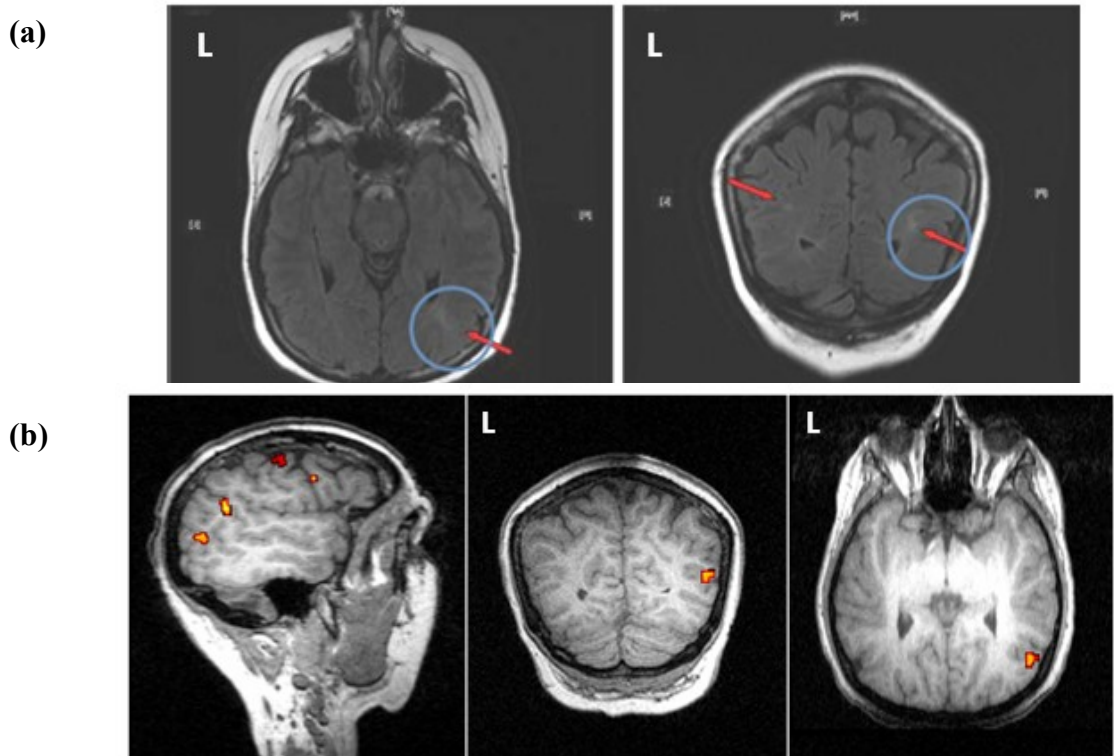


**Figure 7.3: Ictal BOLD changes for patient #1**

(a) Multiple tubers were seen in right parietal lobe and left temporal lobe. Epileptogenic tuber in right parietal lobe is encircled. (b and c) BOLD changes (threshold at  $p < 0.001$  uncorrected for FWE) overlaid on co-registered T1-volume. (b) BOLD map for *Ictal onset* phase was classified to have *Some concordance* with GM BOLD cluster in right middle frontal gyrus (cluster size = 18 voxels,  $F = 6.39$ ) and other BOLD-clusters in right inferior parietal lobule (concordant with the SOZ) and right temporo-parietal junction.

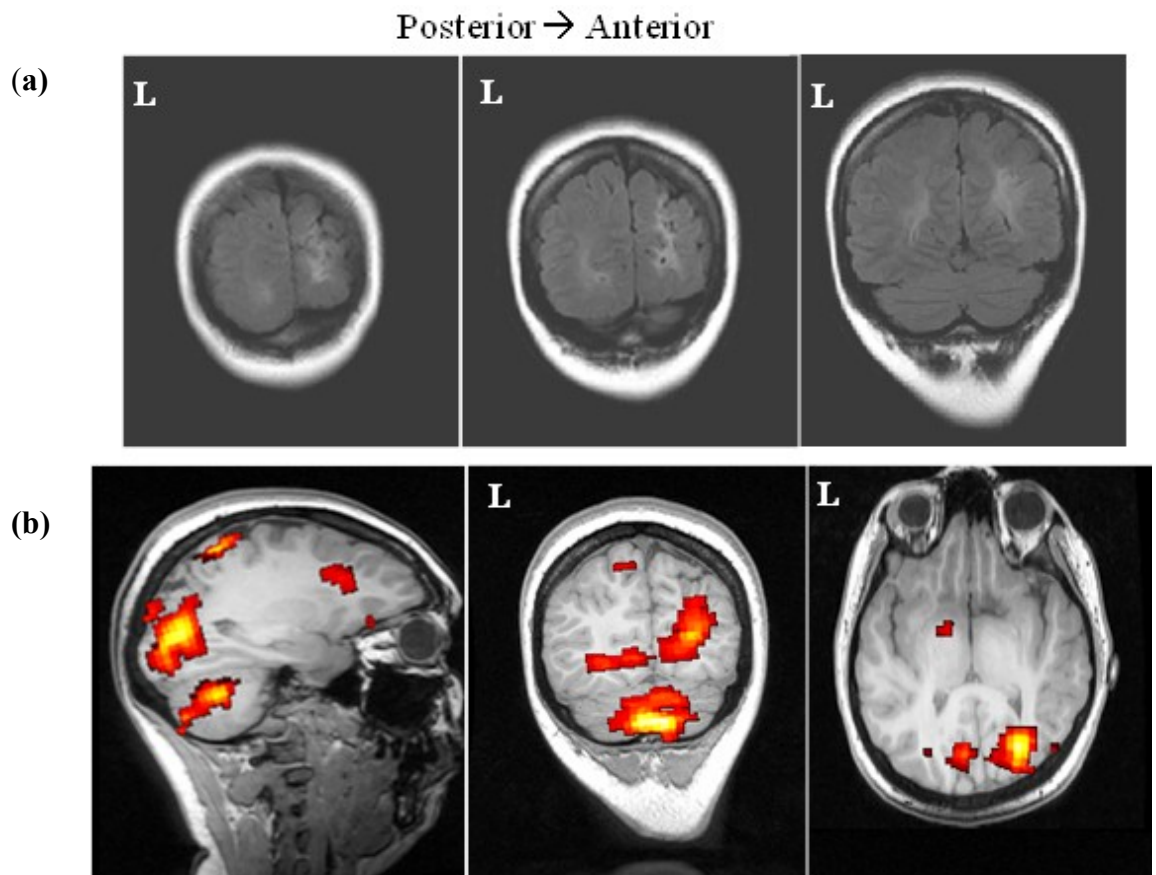


**Figure 7.4: Ictal BOLD changes for patient #10**

One seizure was recorded during vEEG-fMRI acquisition and the ictal pattern was obscured by myogenic-artefact, thus seizure was modelled as single *Ictal* phase. (a) Long standing ischemic damage with malformation of gyri in right occipito-parietal region extending into right posterior temporal lobe on (FLAIR) MRI-scan. (b and c) BOLD changes (threshold at  $p < 0.05$  corrected for FWE) overlaid on co-registered T1-volume. (b) *Concordant plus* BOLD maps for *Ictal* phase showed BOLD changes in right occipito-temporal (GM, cluster size = 4907 voxels,  $F=33.65$ , crosshair), bilateral superior parietal, bilateral medial parieto-occipital and right posterior temporal lobe.

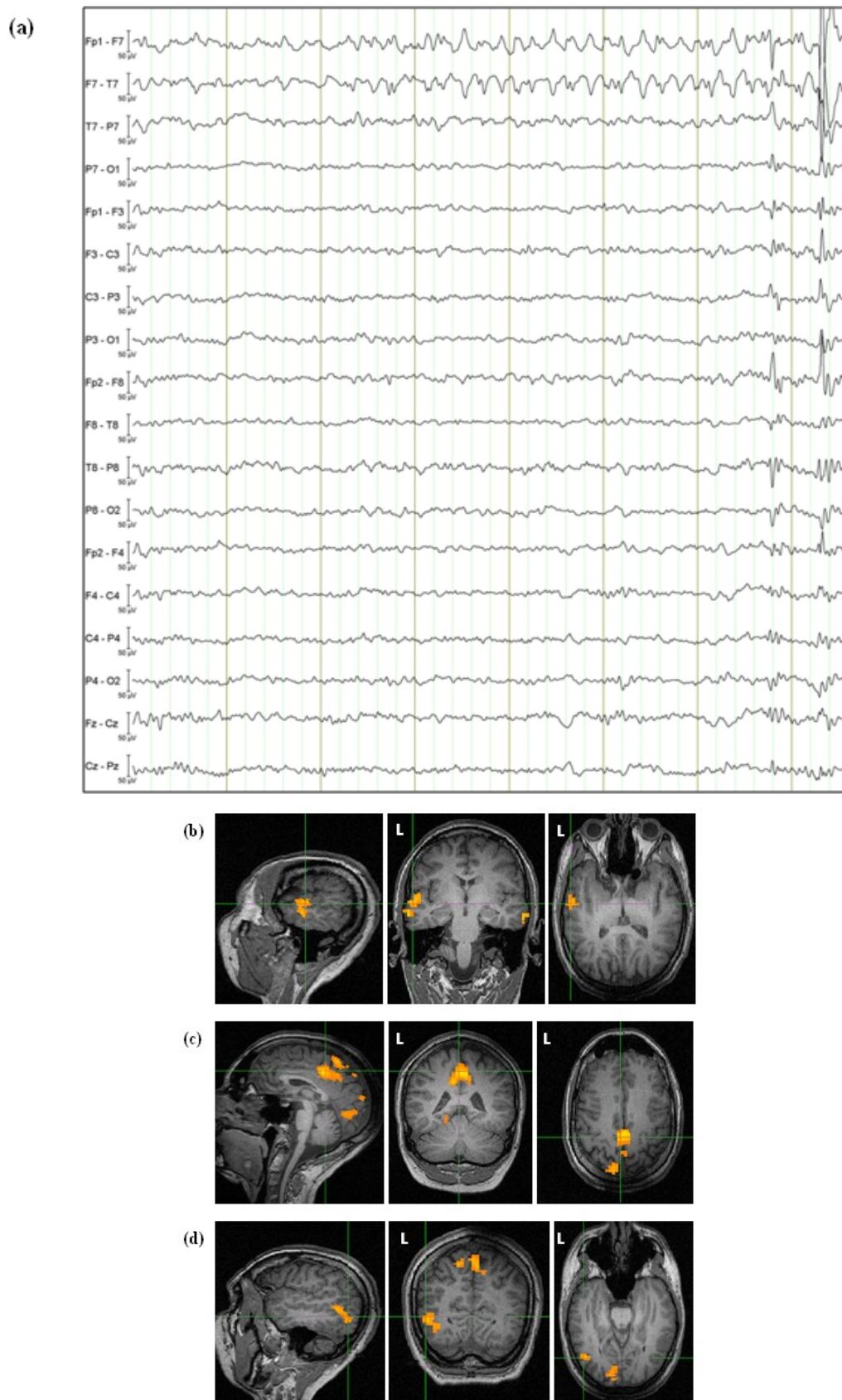
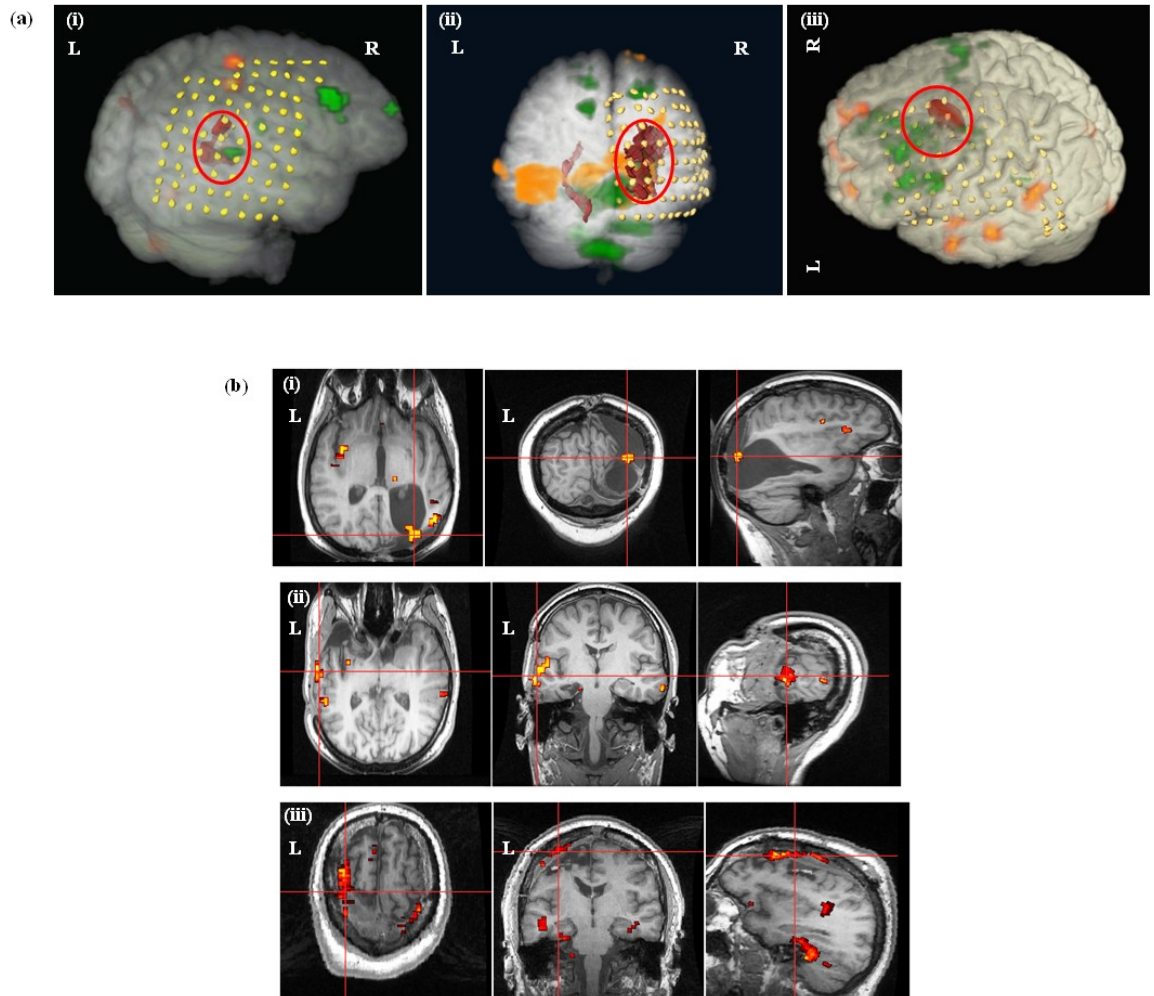


Figure 7.5: Ictal BOLD changes patients #4

(a) Representative EEG sample recorded inside scanner showing a regional left temporal ictal-pattern at seizure-onset (F7, T7). (b, c and d) BOLD changes (threshold at  $p < 0.001$  uncorrected for FWE) overlaid on to T1-volume. (b) *Concordant plus* BOLD-map for *Ictal onset* phase showed BOLD changes in left superior temporal gyrus (GM, cluster size = 37 voxels,  $F = 6.57$ , crosshair), left temporo-occipital region, right superior and middle frontal gyrus, left paracentral lobule and right inferior temporal gyrus. (c) *Discordant* BOLD-map for *Ictal established* phase showed BOLD changes in right superior and middle frontal gyrus (GM, cluster size = 54 voxels,  $F = 7.84$ ), basal ganglia, left cuneus, paracentral lobule (crosshair). (d) *Concordant plus* BOLD map for *Late ictal* phase showed BOLD changes in left temporo-occipital region (GM, cluster size = 31 voxels,  $F = 6.69$ , crosshair), paracentral lobule, right MFG, left precuneus and cuneus and basal ganglia.



**Figure 7.6: Comparison of BOLD changes with implantation and resection**  
**(a)** SPMs of F-statistics for preictal and ictal-onset phase overlaid on 3D-rendered brain in individual space, showing the relationship between preictal and ictal onset-related BOLD changes, implanted electrodes and structural lesion. Colour coding: structural lesion = red; preictal BOLD change = orange; ictal onset-related BOLD change = green; grid, strip and depth electrodes = yellow. Red circle shows invasively defined SOZ. **(i)** Patient #1: For the *Ictal onset* phase, the GM BOLD cluster in right middle frontal gyrus (cluster size = 18 voxels,  $F = 6.39$ ) was 7cm, and the 2<sup>nd</sup> most statistically significant BOLD cluster in right inferior parietal lobe, highlighted non-invasively to be with the presumed SOZ, was 1.9cm from the depth electrode recording first EEG change during seizures. The GM preictal BOLD cluster, highlighted non-invasively to be nearest to the presumed SOZ, in the right superior parietal (GM, cluster size = 11 voxels,  $F=4.87$ ) was 3cm from the depth electrode recording first EEG change during seizures. **(ii)**

Patient #10: For the *Ictal* phase, the GM BOLD cluster, highlighted non-invasively to be with the presumed SOZ, in the right occipito-temporal (cluster size = 4907 voxels,  $F=33.65$ ) was 1.8cm from grid electrode recording first EEG change during seizures. The preictal BOLD cluster, highlighted non-invasively to be nearest to the presumed SOZ, in the right lateral parieto-occipital was 2.5cm from grid electrode recording first EEG change during seizures. **(iii)** Patient #16: For the *Ictal* phase, the GM BOLD cluster in left superior/middle frontal gyrus (GM, cluster size = 182 voxels,  $F=21.63$ ), highlighted non-invasively to be within the presumed SOZ, was 1.5 cm from the intracranial electrode recording first EEG change during seizures. The preictal BOLD cluster, highlighted non-invasively to be nearest to the presumed SOZ, in medial superior frontal gyrus was 2.5cm from the intracranial electrode recording first EEG change during seizures.

**(b)** Ictal onset related BOLD maps (SPMs of F-statistics) overlaid on co-registered postsurgical T1-volume. Cross-hair shows the BOLD-cluster highlighted non-invasively and nearest to the SOZ defined on icEEG. **(i)** Patient #1 had a cortical resection including the right parietal tuber and overlapping ictal onset-related nearest BOLD-cluster (cross-hair) and has ILAE Class I postsurgical outcome at 1.5 year. **(ii)** Patient #4 underwent left anterior temporal lobe resection which did not involve the ictal onset-related nearest BOLD-cluster in superior temporal gyrus (cross-hair) and had ILAE Class III postsurgical outcome at 1 year. **(iii)** Patient #16 had a resection including right posterior superior frontal gyrus, middle frontal gyrus and part of supplementary motor area and ictal onset-related nearest BOLD-cluster (cross-hair) with an ILAE Class I postsurgical outcome at 1 year.

### 7.3.1b Comparison of ictal BOLD changes with presumed SOZ

In the 14 patients who did not undergo icEEG recordings, eight had epileptogenic structural abnormalities: FCD (patients #12, 17, 19), hypothalamic hamartoma (patients #14, 20) and other abnormalities (patients #5, 8, 11; see Table 7.1). For these eight patients BOLD changes were seen within the presumed SOZ overlapping the structural abnormalities. The *Ictal onset / Ictal* phase related maps were classified as (Table 7.4; Figure 7.7): *Concordant plus* = 5/8; *Some concordance* = 1/8; and *Discordant* = 2/8. The *Ictal established* phase was seen in five of these eight patients with structural abnormalities, and the maps were classified as: *Concordant plus* = 2/5; *Some concordance* = 2/5; *Discordant* = 1/8. The *Late ictal* phase was seen in four of these of these eight patients with structural abnormalities, and the maps were classified as: *Some concordance* = 2/4; and *Discordant* = 2/4.

Six patients (#2, 6, 7, 9, 13, 18) who did not undergo icEEG recordings and who did not have structural abnormalities showed BOLD changes within the presumed SOZ (defined on the basis of interictal and ictal discharges on EEG and ictal semiology) at lobar level. The *Ictal onset / Ictal* phase related maps were classified as: *Entirely concordant / Concordant plus* = 3/6; *Some concordance* = 2/6; and *Discordant* = 1/6. The *Ictal established* phase was seen in four patients, and the maps were classified as: *Concordant plus* = 2/4; *Discordant* = 2/4. The *Late ictal* phase was also seen in two patients, and the maps were classified as: *Some concordance* = 1/2; and *Discordant* = 1/2.

For the 8/14 patients with *Entirely concordant / Concordant plus* BOLD maps for the *Ictal onset / Ictal* phase, the GM BOLD cluster was localizable, within the presumed SOZ, to one or two gyri in six patients (patients #2, 6, 7, 8, 11, 12) and was spanning more than two gyri within the same lobe in the remaining two (patients #5, 17). In comparison, using the criteria set out in [Luders *et al.* 2000], the seizure onset scalp EEG pattern was localised to one (patients #2, 12, 17) or multiple lobes (patients #5, 6, 7, 8, 11; Table 7.1). Moreover, in six patients with frontal lobe seizures and difficult to localise ictal EEG, the GM ictal onset related BOLD cluster was localised within the presumed SOZ at sub-lobar level in four patients.

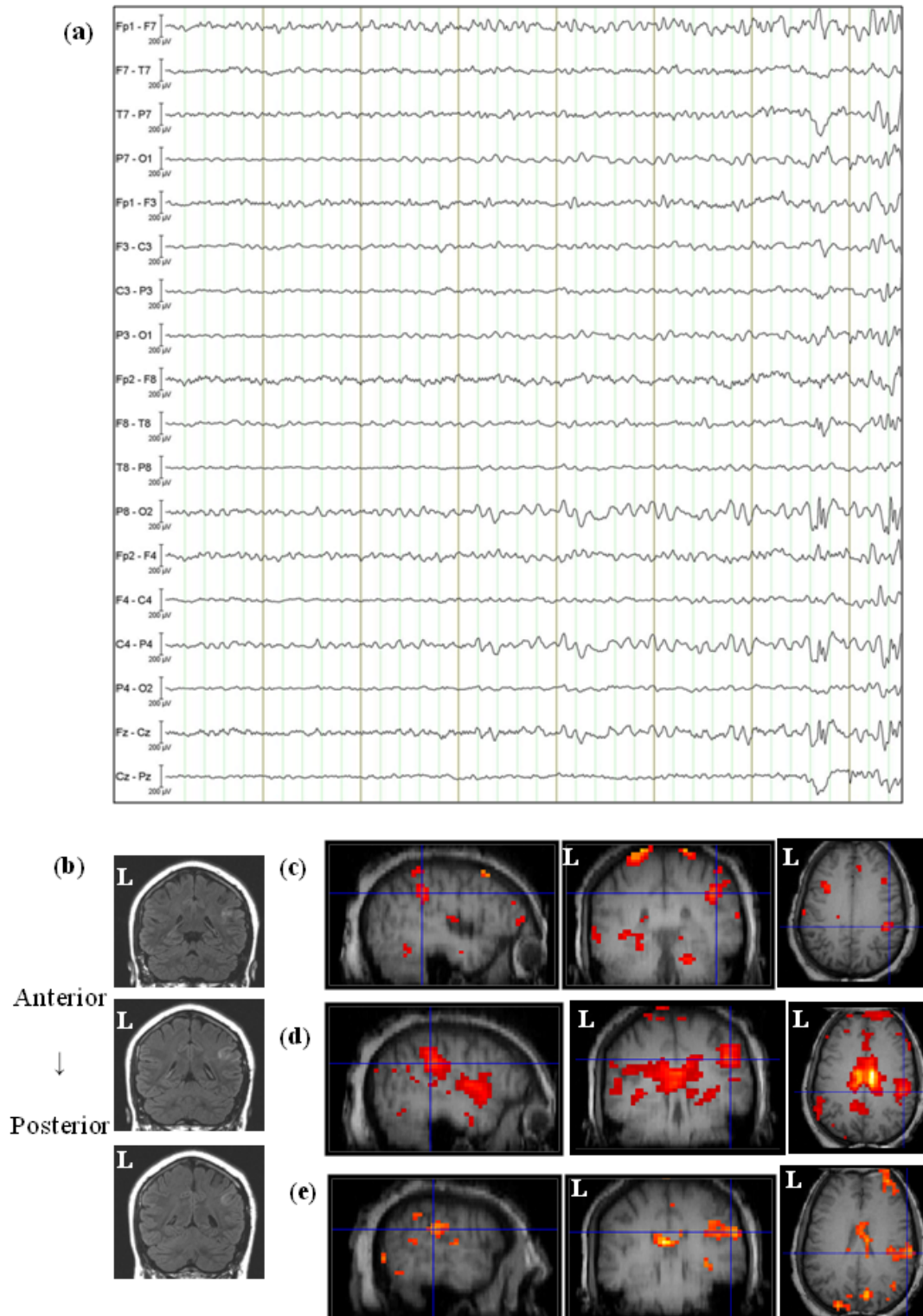


**Figure 7.7: Ictal BOLD changes for patient #19**

(a) Representative EEG sample recorded inside scanner showing a regional right centro-parietal ictal-pattern (b) Focal cortical dysplasia in the right supramarginal gyrus on (FLAIR) MRI-scan. (c, d and e) BOLD changes (threshold at  $p < 0.05$  corrected for FWE) overlaid on to T1-volume. (c) BOLD map with *Some concordance* for *Ictal onset* phase showed BOLD changes in right middle frontal



gyrus (MFG) (GM, cluster size = 713 voxels,  $F = 40.64$ ), superior frontal gyrus (SFG) and right supramarginal gyrus (crosshair). (d) *Concordant plus* BOLD maps for *Ictal established* phase showed BOLD changes in right supramarginal gyrus (GM, cluster size = 583 voxels,  $F = 39.51$ , crosshair) and precuneus. (e) BOLD map with *Some concordance* for *Late ictal* phase showed BOLD changes in right parietal lobe (GM, cluster size = 51 voxels,  $F = 31.47$ ), MFG, SFG, supramarginal gyrus (crosshair).

### 7.3.2 Ictal propagation related BOLD networks

BOLD changes for *Ictal established/Ictal* phases were revealed in symptomatogenic areas and/or eloquent cortex in 9/20 patients (45%; Table 7.4). Three patients had BOLD changes only in symptomatogenic areas, and the rest also had changes in non-symptomatogenic areas. The two groups with changes in symptomatogenic and non-symptomatogenic areas were not statistically significantly different. These areas included: motor cortex for hand, foot or face movements (Patients #2, 6, 17), supplementary motor area/prefrontal cortex for asymmetric tonic limb posturing (figure of 4 sign: striking asymmetry of posturing of oarms, one arm is extended at elbow with fists clenched and the other arm is flexed at elbow; Patient #9), medial or lateral temporal lobes in TLE for automatisms (Patient #15), precentral gyrus and posterior middle frontal gyrus for eye deviation and head turning (Patients #8, 9, 16) hypothalamus for gelastic seizures (Patient #20) and thalamus, limbic temporal structures, cingulum and medial frontal for dialeptic seizures (Patient #7).

In relation to the RSNs [Mantini *et al.* 2007], BOLD changes were seen in the in the precuneus/cuneus, bilateral parietal lobes, posterior cingulate and/or medial frontal lobes reflecting the default mode network (DMN) [Raichle *et al.* 2001] in 13/20 patients (65%; Figure 7.8, Table 7.5) for *all ictal* phase. These were BOLD decreases in eleven patients and increases in two patients. I did not measure the impairment of awareness during vEEG-fMRI; however I compared the association of BOLD changes in the DMN with the loss of awareness assessed during long-term video-EEG monitoring for typical seizures (Figure 7.8). I found a moderate correlation ( $\Phi = 0.3$ ) between the presence of BOLD changes in the DMN and the loss of consciousness which was not statistically significant. However, in the subgroup of patients with BOLD decreases in the DMN, these changes were significantly associated with the loss of consciousness ( $p < 0.05$ ). I also found BOLD changes in relation to other RSNs at  $p < 0.001$ , uncorrected for FWE: dorsal attention network (bilateral dorsolateral frontal and bilateral superior parietal) in 12/20 patients (60%); sensory motor network (pre/post central gyri, medial frontal and supplementary motor area) in 11/20 patients (55%); visual processing network (medial occipital cortex and temporo-occipital regions) in 12/20 patients (60%); auditory phonological network (superior temporal cortices) in 7/20 patients (35%).

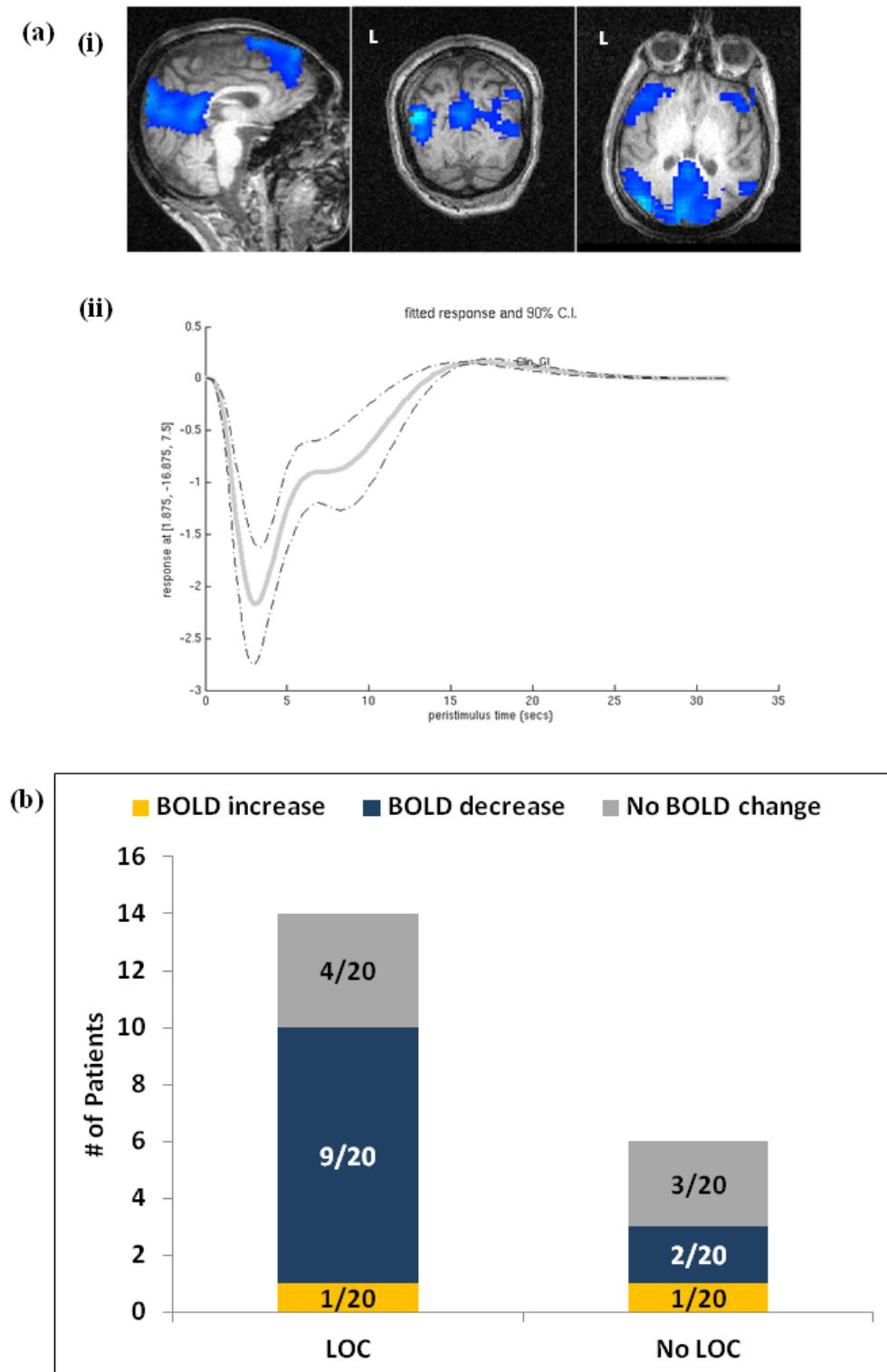


**Figure 7.8: BOLD changes in DMN**

(a) Patient #7. (i) SPM[F] map for *all ictal* (across whole seizure) overlaid on co-registered T1-volume showing BOLD decreases in precuneus, cuneus, bilateral superior parietal, bilateral dorsolateral frontal and medial frontal cortex. (ii) Predicted BOLD response for the GM BOLD change in precuneus showing BOLD decrease. (b) Bar chart showing the proportion of patients with BOLD increases and decreases and loss of consciousness during seizures.

**Table 7.5: BOLD changes in resting state networks during seizure**

<b>ID #</b>	<b>Default mode network</b> Increases = ↑, Decreases = ↓	<b>Dorsal attention network</b> Increases = ↑, Decreases = ↓	<b>Visual processing network</b> Increases = ↑, Decreases = ↓	<b>Sensori-motor network</b> Increases = ↑, Decreases = ↓	<b>Auditory phonological network</b> Increases = ↑, Decreases = ↓
2	-	-	-	↑	-
3	↓↑	↑↓	-	-	-
4	↓	↑↓	↑	↑	↑
6	-	-	-	↓	-
7	↓	↓	↑	-	-
8	-	-	↓	↑	-
9	↓	↑	-	↑	↑
10	-	-	↑	-	-
11	↓	↑	↓↑	↑	-
12	↓	↓	↑↓	-	-
13	↓	-	↓	-	-
14	-	-	↑	↓	↓
15	-	↑	-	↑	↓
16	↓	↑↓	-	-	-
17	↓	↓	↑	↑	↑
18	↓	↓	↑	-	-
19	↓	↓	↑	↓	↓
20	↑	↑	↑	↑	↑

### 7.3.3 Direction of BOLD change

The BOLD maps for the individual ictal phases contained clusters corresponding to a mixture of BOLD increases and decreases in 16/20 patients; increases only for three patients and decreases only for one patient at  $p < 0.001$ , uncorrected for FWE. For the patients with *Entirely concordant / Concordant plus* BOLD maps, the GM BOLD cluster corresponded to an increase in: 8/13 patients for *Ictal onset / Ictal* phase; 2/5 patients for *Ictal established* phase; one patient for *Late ictal* phase. The BOLD clusters for *Ictal established* and *Late ictal* phases were remote from the presumed SOZ and predominantly decreases (Table 7.4).

### 7.3.4 Head motion and ictal BOLD patterns

The mean number of head jerks across all patients with seizures was 37 (95% CI: 16.2 - 57.8). The overall mean inter-scan displacement across all patients with seizures was 0.13 mm (95% CI: 0.06 - 0.2; see Figure 7.9). The level of concordance for the *Ictal onset / Ictal* phase were not significantly associated with number of head jerks ( $p\text{-value} = 0.3$ ), mean inter-scan displacement ( $p\text{-value} = 0.9$ ) or maximum inter-scan displacement ( $p\text{-value} = 0.7$ ).

Six patients (#: 9, 10, 16, 17, 18, 19) showed large BOLD clusters across multiple lobes and the maximum inter-scan head motion was greater than 1mm. However, the spatial distribution of ictal related BOLD clusters was focal in comparison to homogenous BOLD signal changes across whole brain for the motion and pulse-related effects (Figure 7.10).

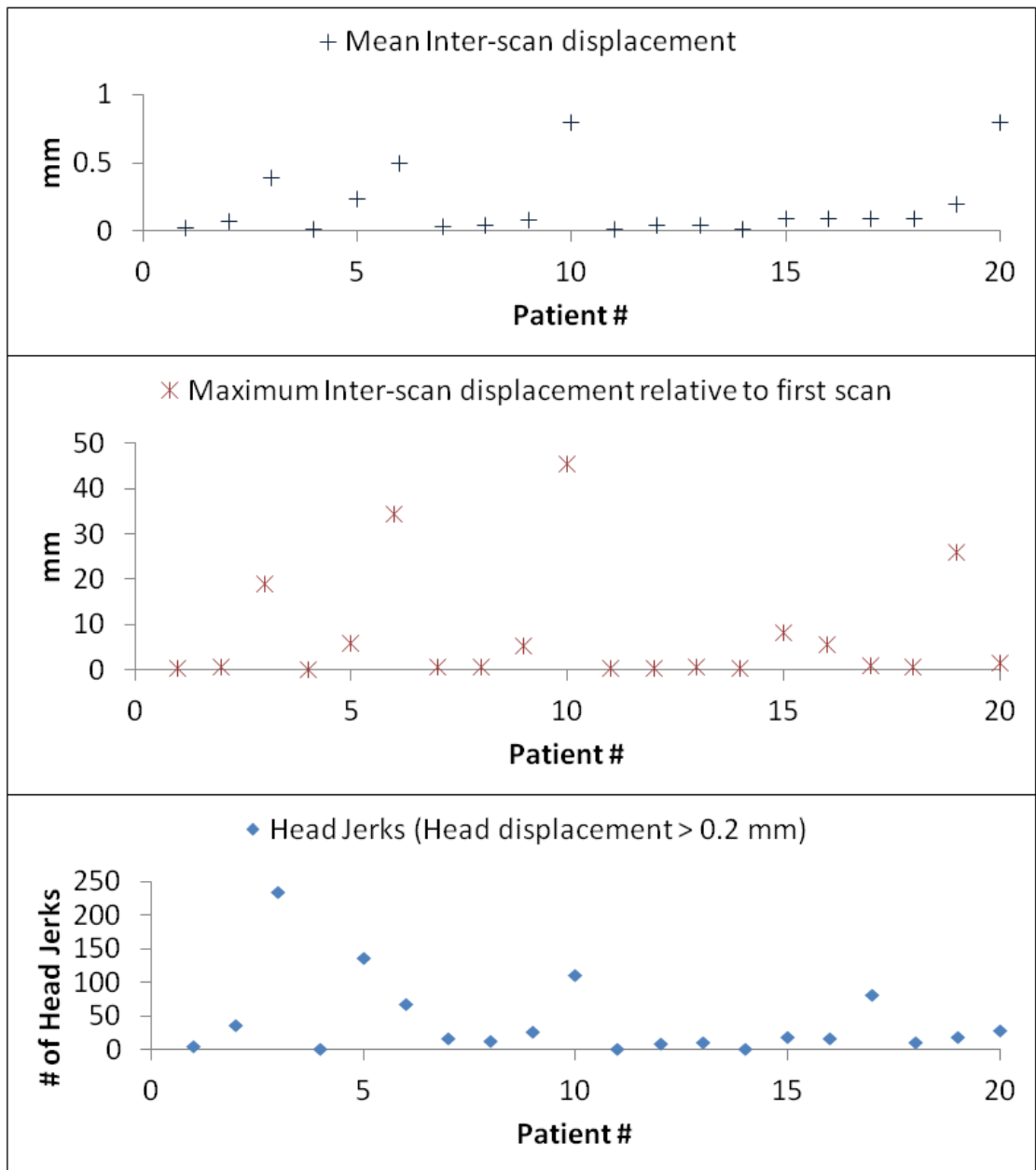


**Figure 7.9: Scatter plots showing inter scan head motion**

Mean inter-scan displacement, maximum inter-scan displacement relative to the first scan and the number of head-jerks (> 0.2 mm) during vEEG-fMRI.

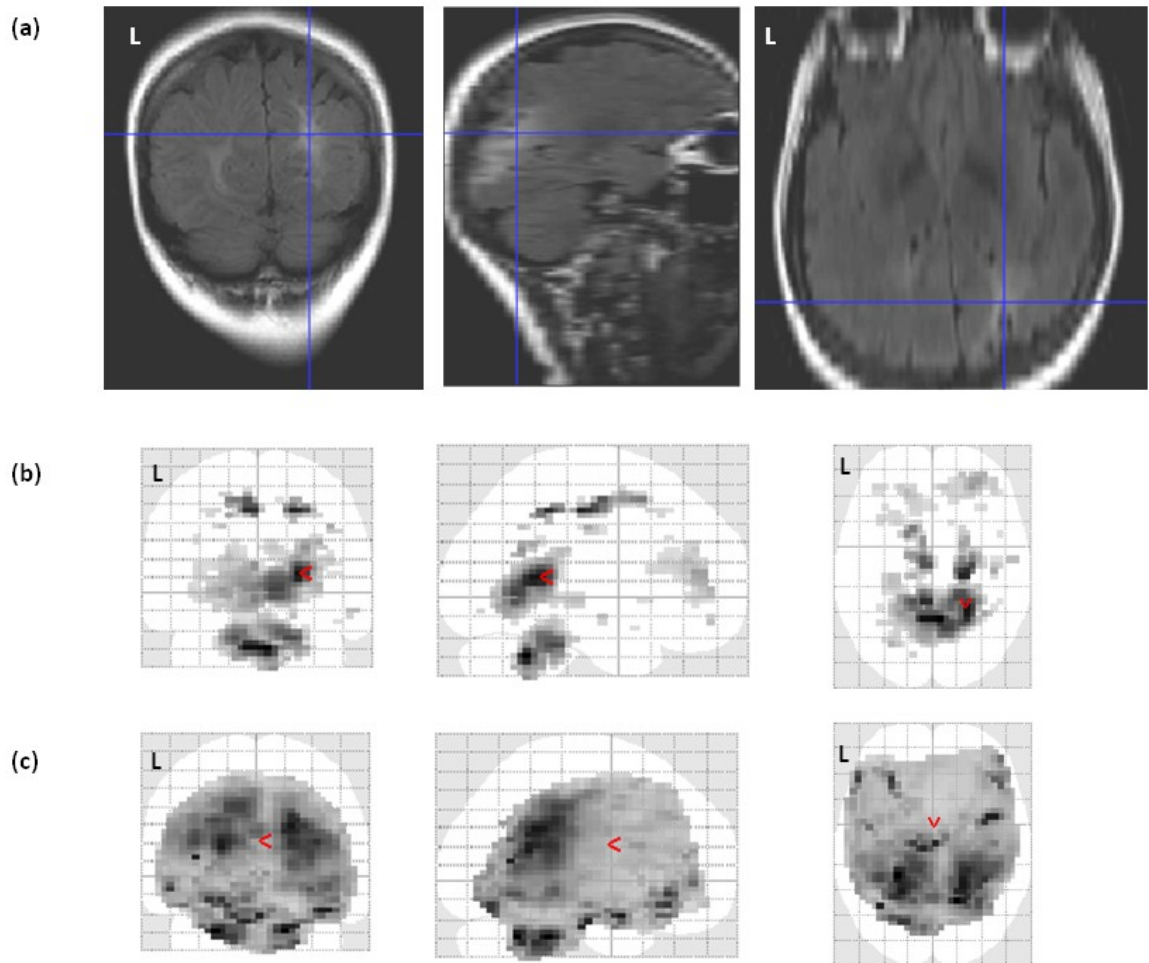


**Figure 7.10: Comparison of BOLD change for seizure, motion and pulse**

Patient #10. (a) Long standing ischemic damage with malformation of gyri in right occipito-parietal region extending into right posterior temporal lobe on (FLAIR) MRI scan. (b) Ictal related BOLD changes (threshold at  $p < 0.05$  corrected for FWE) overlaid on glass brain. Crosshair at GM BOLD cluster concordant with structural damage. (c) Motion and pulse-related BOLD changes (threshold at  $p < 0.05$  corrected for FWE) overlaid on glass brain.

#### 7.4 Discussion

I demonstrated the application of vEEG-fMRI in patients with frequent seizures and identified haemodynamic changes specific to various ictal phases. The main findings are:

- Noninvasive localisation of ictal onset related GM cluster and confirmation by its comparison with the invasively defined SOZ.
- Localisation of ictal onset related GM cluster with good concordance with the presumed SOZ at sub-lobar level as compared to scalp EEG.
- Propagated BOLD changes in symptomatogenic and RSN related areas during seizures.
- Predominant BOLD increases at seizure onset in the SOZ and remote BOLD decreases during later parts of seizure.
- Added advantage of simultaneous video recordings for the identification of seizures during vEEG-fMRI.

These results suggest that vEEG-fMRI may have a useful role in planning the placement of intracranial electrodes.

Previous EEG-fMRI studies have largely recorded seizures fortuitously in the course of studies aimed at mapping IED, and mostly are case reports or case series with low yield [Salek-Haddadi *et al.* 2002;Archer *et al.* 2006;Auer *et al.* 2008;Tyvaert *et al.* 2009;Donaire *et al.* 2009a;LeVan *et al.* 2010b;Thornton *et al.* 2010b]. Here, I focussed on patients with frequent daily seizures.

The level of concordance of the BOLD maps with the SOZ was higher for the *Ictal onset* phase than *Ictal established* phase, *Late ictal* phase or IED related BOLD maps (see Appendix 2), lending support to my approach towards fMRI data modelling based on ictal phases. These findings in the largest sample of seizures investigated with vEEG-fMRI improve on the previous findings from my group [Thornton *et al.* 2010b], and reinforce that localisation for clinical purposes largely depends on the localisation of seizure onset [ILAE 1989]. The distance between the BOLD clusters and invasively defined SOZ has only been measured in one study [Thornton *et al.* 2010b]. Compared to previous findings, I found that the proportion of cases showing ictal related BOLD changes



concordant with the invasively defined SOZ has increased from 4/7 [Thornton *et al.* 2010b] to 6/6 patients undergoing icEEG recording (Table 7.4).

The BOLD changes for the *Ictal established* and *Ictal* phases in symptomatogenic areas, remote from the presumed SOZ, and for *all ictal* phase in areas of the brain which are part of the DMN were predominantly decreases. In comparison, the maps concordant with the SOZ for *Ictal onset* or *Ictal* phases predominantly showed BOLD increases in line with previous studies of ictal and interictal activity [Federico *et al.* 2005b; Tyvaert *et al.* 2008; Jacobs *et al.* 2009; Vulliemoz *et al.* 2009; Donaire *et al.* 2009a]. The BOLD changes for ictal phases, overlapping or adjacent to the structural abnormalities, were usually a mixture of increases and decreases consistent with previous findings [Laufs *et al.* 2007b; Vaudano *et al.* 2009; Thornton *et al.* 2010b; Moeller *et al.* 2010c].

#### 7.4.1 Methodological considerations

The identification of seizures inside the scanner has mostly been dependent on EEG which has limited sensitivity [Tyvaert *et al.* 2008; Thornton *et al.* 2010b], and despite vigorous artefact removal interpretation of the intra-scanner EEG can be difficult [Benar *et al.* 2003] as discussed in Chapter 3, Section 3.2. In these circumstances synchronised video-EEG recording can be very useful to identify seizures based on spatiotemporal evolution of EEG ictal rhythms and ictal semiology [Foldvary *et al.* 2001; Luders *et al.* 2006; Najm *et al.* 2006]. In previous fMRI studies, seizures were represented by single blocks [Tyvaert *et al.* 2008; Salek-Haddadi *et al.* 2009] or by contiguous EEG independent sliding windows [Donaire *et al.* 2009a]. Thornton *et al.* (2010) has previously modelled seizures by dividing them into EEG informed blocks reflecting seizure evolution. Here, I attempted to further improve upon this approach by using video to divide seizures into more physiologically informed phases on the basis of their spatiotemporal evolution [Niedermeyer and Lopes da Silva 2005] on video-EEG, separating ictal onset related changes from the more widespread ictal semiology related and late changes. The value of the ictal phase modelling approach rests on its potential capacity to identify haemodynamic change specifically related to an electrophysiological and/or semiological meaningful part of the seizures. Another novel methodological aspect of this work is the attempt to account for physiological activities of patients to explain a greater amount of nuisance

variance in the fMRI data which can result in improved sensitivity to the effects of interest, as shown in Chapter 6.

When a patient had two or more seizures which were similar electroclinically [Wendling *et al.* 1996], I represented them as a single effect reflecting the assumption that they would be associated with a consistent BOLD pattern and thereby potentially increasing the statistical power of the analysis to map the changes averaged across occurrences [Hamandi *et al.* 2006]. The alternative approach is to treat each seizure as a single event [Tyvaert *et al.* 2009;Donaire *et al.* 2009a] requiring a secondary analysis to identify the features that are common across occurrences which has not been done yet. In this study, I focussed on features that characterise a specific type of seizure in a given patient. The successful identification of significant and meaningful BOLD changes in cases with repeated seizures (N = 11; Table 7.3) confirms the interest in this modelling approach, providing some indication of the core aspects of the epileptogenic and propagation networks. The nature and biological significance of underlying seizure network is debated [Bartolomei *et al.* 2001;Spencer 2002], however, I believe that the identification of seizure related areas averaged across events, as made possible by this approach, should form the basis for the characterisation of BOLD changes in these regions across events and possibly their relationship with ictal onset and semiology.

I convolved the ictal related blocks with the canonical HRF and its derivatives [Friston *et al.* 1995b;Friston 1996], the latter as an attempt to account for a degree of variability in BOLD timing and shape [Salek-Haddadi *et al.* 2006;Thornton *et al.* 2010b].

The distance between GM or other BOLD cluster within the presumed SOZ and the invasively defined SOZ was 1.1 to 3.5cm. Accounting for the co-registration inaccuracies, due to implantation related brain shift [Nimsky *et al.* 2000] and displacement of BOLD clusters due to neurovascular coupling effects [Disbrow *et al.* 2000], I considered these BOLD clusters concordant with the invasively defined SOZ. Other limitations of this comparison include: vEEG-fMRI and icEEG recordings were performed at different times; the conditions under which seizures were recorded on icEEG were different e.g., effects of drug reduction, anaesthesia and sleep deprivation; and icEEG has limited spatial sampling. I also note that due to the fundamentally different nature of the two modalities the lack

of significant ictal related BOLD signal changes in a given region sampled by icEEG does not preclude the occurrence of ictal electrophysiological correlates [Nunez and Silberstein 2000;Tyvaert *et al.* 2009].

One of the weaknesses of fMRI is that it is a correlative technique producing complex BOLD maps containing multiple clusters. I used a concordance classification which has been used previously [Thornton *et al.* 2010b;Grouiller *et al.* 2011] and conservative statistical threshold to summarise and interpret complex maps for clinical purposes. The degree of concordance of the maps was evaluated by comparing the location of GM and other clusters with the SOZ defined independently. *Entirely-concordant* maps can be taken as ‘true-positive’ findings; *Concordant-plus* and *Some-concordance* maps as a mixture of ‘true and false-positive’ results; and *Discordant* maps as ‘false positive’. The GM cluster is usually unique for a given map [Friston *et al.* 1995b;Friston 1996;Worsley *et al.* 2002] and might have special biological or clinical significance as shown by my findings and those of others previously. Therefore, it is possible in future that the GM cluster may be a key marker of epileptogenic network (as defined by icEEG and postsurgical outcome), particularly with advances in fMRI acquisition and modelling for seizures.

In these data, the amount of head motion was comparable to that observed in previous study of seizures [Thornton *et al.* 2010b] but greater than for the study in the interictal state [Salek-Haddadi *et al.* 2006]. It can be argued that one of the limitations of this study is that I included all seizures irrespective of motion which may corrupt fMRI signal. However, this was motivated by the desire to extract as much information from each and every dataset as possible, given its relative rarity and eventual possible importance of the technique to individual patients. Furthermore, the motion related effects were modelled in the design matrix as confounds and the level of concordance was not significantly associated with the amount of head motion. For the patients with large clusters, ictal BOLD changes were focal and did not overlap significantly with spatially uniform motion and pulse related effects [Salek-Haddadi *et al.* 2006;Thornton *et al.* 2010b].

#### 7.4.2 Neurobiological significance

In this study, sustained BOLD increases were seen predominantly for *Ictal onset* and *Ictal* phases and decreases for *Ictal established* and *Late ictal* phases. BOLD increases represent increased oxy-haemoglobin content [Ogawa *et al.* 1990a].

Essentially a differential technique, the sign of fMRI signal change depends as much on the baseline as on the effect of interest [Pasley *et al.* 2007; Shulman *et al.* 2007]. Although the details of the relationship between BOLD and neuronal activity remains to be elucidated [Pasley *et al.* 2007], increases can be linked to increased neuronal activity as measured at the microscopic level [Logothetis *et al.* 2001] and are thought to reflect the local balance between excitation and inhibition [Logothetis *et al.* 2001; Logothetis 2008].

Sustained BOLD decreases may also represent decreased neuronal activity possibly originating from inhibitory inputs from adjacent regions [Shmuel *et al.* 2006] or dysregulated neurovascular coupling [Schridde *et al.* 2008] reflecting a mismatch between demand and perfusion, though there is hyper-oxygenation of the tissue [Raichle *et al.* 2001; Zhao *et al.* 2009]. The temporal dynamics of BOLD changes can result from interactions between neuronal, haemodynamic and metabolic domains [Raichle and Mintun 2006], and both increases and decreases have been seen in relation to seizures [Tyvaert *et al.* 2009; Donaire *et al.* 2009a; Thornton *et al.* 2010b] consistent with my findings. In addition, the sustained BOLD decreases may be different from tissue hypoxia associated with initial transient BOLD decreases [Geneslaw *et al.* 2011]. At the macroscopic scale, the EEG correlates of BOLD changes studied in the resting state and during tasks have shown negative correlations in the alpha frequencies and positive correlations in the gamma range [Mukamel *et al.* 2005; Niessing *et al.* 2005; Goense and Logothetis 2008; Goense *et al.* 2008]. In comparison, paroxysmal fast activity ranging from 13 to 30Hz is a common feature of seizure onset in human and animal studies [Wendling *et al.* 1996; Foldvary *et al.* 2001; Gnatkovsky *et al.* 2008], suggesting predominant BOLD increases at the seizure onset as seen in this work.

Interestingly, cerebral blood flow can be compromised in areas of structural abnormality resulting in BOLD decreases associated with increases in neuronal activity [Sakatani *et al.* 2007]. BOLD decreases have been revealed in relation to interictal and ictal discharges in idiopathic generalized [Hamandi *et al.* 2006], idiopathic (rolandic) / symptomatic focal [Jacobs *et al.* 2009] and cryptogenic focal epilepsy [Vulliemoz *et al.* 2009] irrespective of structural abnormality, consistent with this work. I also found that when seizures became widespread (during *Ictal established* phase) BOLD decreases tended to dominate, which can

reflect neuronal inhibition [Shmuel *et al.* 2006;Logothetis 2008] or may be the result of demand and perfusion mismatch [Raichle *et al.* 2001;Zhao *et al.* 2009]. The relationship between neuronal activity and BOLD and perfusion changes in patients with epilepsy has been investigated on a limited scale showing that neurovascular coupling to BOLD signal is generally maintained [Stefanovic *et al.* 2005;Carmichael *et al.* 2008a]. I suggest that future studies investigating the relationship between different types of epileptic neuronal activity and BOLD and perfusion changes using improved techniques to measure perfusion changes [Petersen *et al.* 2006] may help to understand the presence of BOLD decreases for increased neuronal activity and blood flow.

The ictal related BOLD changes in the RSN may represent neuronal baseline activity [Damoiseaux *et al.* 2006] from which task related networks are modulated [Mantini *et al.* 2007] or underlying brain physiology independent of neuronal activity [Obrig *et al.* 2000;Birn *et al.* 2006]. Given the purely correlative nature of the present analysis, the observed BOLD changes in the RSN may indicate transitions in brain dynamics either as a result of ictal discharges i.e. recruitment during seizure propagation (downstream), or upstream from ictal activity reflecting changes in brain state that are favourable to seizures [Vaudano *et al.* 2009].

### 7.4.3 Clinical significance

In this study, I demonstrated an increased localisation sensitivity of concordant ictal BOLD changes with the SOZ from 44% [Thornton *et al.* 2010b] to 65%. I suggest that this improvement results from the ability of video-EGG to identify and classify seizures better than EEG alone leading to enhanced physiologically informed fMRI modelling of seizures; inclusion of regressors for physiological activities; and refined concordance scheme [Chaudhary *et al.* 2012a].

Ictal pattern may not be visible at all on scalp EEG in simple partial seizures [Binnie and Stefan 1999;Smith 2005]. In this study, seizures were identified on the basis of ictal semiology on video in 15% patients as EEG was not helpful, which might have been disregarded in the absence of video. When seizures were identified on the basis of ictal electrophysiology and semiology on video-EEG (75% patients), video recordings were used to confirm seizure semiology as compared to the long-term video-EEG monitoring.

In this work, I showed that in 65% of patients ictal onset related GM cluster (*Entirely concordant* or *Concordant plus* maps) was co-localised within the presumed SOZ at the sub-lobar level which is superior to scalp EEG. In the implanted cases in this study, the ictal onset related GM or other BOLD cluster within the presumed SOZ was 1.1 to 3.5cm from the invasively defined SOZ at sub-lobar level. This suggests that vEEG-fMRI can capture relevant ictal onset-related localisation information. For example in patient #10, the seizure onset on icEEG was thought to represent a propagated pattern which can be explained if SOZ is located between the implanted electrodes as suggested by the non-invasively highlighted BOLD cluster. Similarly, the investigation of patient #15 where the lack of posterior temporal lobe coverage with intracranial electrodes might have been improved given the presence of ictal onset related BOLD clusters.

I also suggest that the ictal onset related BOLD changes may also provide information on not to implant in cases in whom surgery can risk eloquent cortex as for patient #3, avoiding unnecessary exposure to risks and expenses associated with intracranial electrode implantation. The postsurgical outcome was ILAE class-I when the ictal onset related BOLD cluster, highlighted non-invasively, was resected (patient #1 and 16; Figure 7.7), and class-III when it was not resected (patient #4). Intracranial EEG is an expensive test and not suitable in many cases. Furthermore, the number of intracranial electrode placement is limited by the risk of complications from surgery [Knowlton *et al.* 2008a; Knowlton *et al.* 2008b]. The decision about whether to implant and where to put intracranial electrodes is a consensus decision by undertaking all the information available from non-invasive investigation, formulating one or more hypotheses about the sites of seizure generation and spread. It has been shown that other non-invasive techniques: magnetic source imaging, MEG or FDG-PET, mostly map the irritative zone which is not equivalent to the SOZ, or may miss the ictal onset (Ictal SPECT) [Knowlton 2006; Knowlton *et al.* 2009]. While the limitations of BOLD quantification are also noted, my findings suggest that this sub-lobar localisation of the GM BOLD cluster at the ictal onset using vEEG-fMRI may have a particular significance and may be a useful marker in some case providing further precision in comparison to scalp EEG. However, establishing clinical usefulness will require larger prospective studies to identify predictive power in

terms of icEEG localisation and surgical outcome. It is possible that ictal vEEG-fMRI has a negative predictive power similar to interictal EEG-fMRI [Thornton *et al.* 2011].

In patients who did not have icEEG recordings, the presumed SOZ was localised on the basis of structural abnormality on MRI and scalp EEG or scalp EEG alone. Additionally, it has been shown that 6 to 10cm<sup>2</sup> area of the cortex needs to be recruited for electrophysiological changes to be detected on scalp EEG [Ray *et al.* 2007; Tao *et al.* 2007a]. Therefore, ictal patterns from deep brain structures such as: medial temporal [Pacia and Ebersole 1997] and medial frontal structures [Lee *et al.* 2000; Jobst *et al.* 2000] may not be sufficient to reach scalp EEG before semiological changes set in. In this study, sub-lobar localisation of GM BOLD cluster within the presumed SOZ was superior to the lobar localisation of scalp EEG alone in cases with and without structural abnormalities, further refining the localisation process.

BOLD changes in symptomatogenic areas [Swartz 1994; Luders *et al.* 1998; Lee *et al.* 2002; Loddenkemper and Kotagal 2005; Kameyama *et al.* 2010; Foldvary-Schaefer and Unnwongse 2011], for *Ictal established/Ictal* phase, were seen in 45% of patients, in line with our previous work [Thornton *et al.* 2010b]. In addition to their timing relative to the seizure onset, the location of these BOLD changes broadly reflected ictal semiology suggesting that they correspond to downstream propagation network [Tyvaert *et al.* 2008; Thornton *et al.* 2010b]. BOLD changes were also seen in non symptomatogenic areas in these patients. However, it is difficult to ascertain whether these changes in non-symptomatogenic areas merely reflect motion related signal changes or a propagation network involving fluctuations in the RSN as the seizure evolves.

It has been suggested that BOLD decreases in the DMN may be associated with loss of awareness [Laufs *et al.* 2003; Gotman *et al.* 2005; Laufs *et al.* 2006; Bai *et al.* 2010; Berman *et al.* 2010; Carney *et al.* 2010; Moeller *et al.* 2010b; Thornton *et al.* 2010b]. I found an association between BOLD decreases in the DMN in this study and loss of awareness as assessed during long-term video-EEG monitoring for typical seizures. This is in agreement with over-synchronization of electrical activity in associative cortices during later part of seizures in patients losing consciousness during seizures [Arthuis *et al.* 2009].

The sensitivity of vEEG-fMRI to ictal BOLD changes is high when seizures are captured (36%) as compared to 4% [Tyvaert *et al.* 2008], and 11% [Thornton *et al.* 2010b]. This may be due to the combination of strict selection criteria. The need to scan in real-time combined with limited access to scan time are likely to limit the technique's clinical utility based on current scanner technology and places it on a par with MEG. The technique is at a disadvantage compared to ictal-SPECT in this regard, however vEEG-FMRI's superior temporal resolution compared to ictal-SPECT makes it possible to focus on the interictal-ictal transition. In Chapter 8, I will present my work on investigating haemodynamic networks recruited during interictal to ictal transition and compare their localisation with the SOZ.

### **7.5 Conclusion**

In conclusion, simultaneous vEEG-fMRI can reveal haemodynamic changes specifically related to the seizure onset and evolution and resting state BOLD networks recruited during seizures, in a significant proportion of patients with frequent seizures. Ictal onset related BOLD changes have shown a good level of concordance with the presumed/invasively defined SOZ providing additional information at sub-lobar level which may guide the implantation of intracranial electrodes and avoid unnecessary implantations.



## Chapter 8: Mapping preictal haemodynamic networks using vEEG-fMRI<sup>7</sup>

### 8.1 Background

The transition from interictal to ictal state has been investigated on a limited scale as compared to ictal state considering that the time of actual transition is not known. Simultaneous recordings of scalp and icEEG have demonstrated that larger areas of brain need to be recruited before electrical activity could be seen on scalp EEG and may also be delayed as compared to icEEG reflecting propagated electrical activity [Tao *et al.* 2005; Ray *et al.* 2007]. Similarly, a limited number of fMRI and optical imaging studies focussing on preictal haemodynamic changes have shown that preictal BOLD increases and decrease can start minutes [Federico *et al.* 2005b] to seconds [Zhao *et al.* 2007; Tyvaert *et al.* 2009; Donaire *et al.* 2009a] before the seizure onset on scalp EEG. These preictal changes have been revealed in areas concordant with the SOZ as well as in widespread areas in the DMN as discussed in Chapter 3, Section 3.3d.

In vitro and in vivo studies have shown that qualitatively different preictal discharges from IEDs may precede the seizure onset by seconds to minutes [Bragin *et al.* 2007; Gnatkovsky *et al.* 2008; Huberfeld *et al.* 2011]. It has been shown that networks consisting of brain areas responsible for seizure generation as well as distant regions are recruited before the seizure sets in [Wendling *et al.* 2003; Bartolomei *et al.* 2004; Valton *et al.* 2008; Truccolo *et al.* 2011].

In this chapter, I present my work on investigating haemodynamic changes during interictal to ictal transition. I hypothesized that haemodynamic changes may precede the electrical discharges on scalp EEG. The aim was to assess the localisation of preictal BOLD changes and their time of onset. I therefore, compared the localisation of preictal BOLD changes with the presumed and invasively defined SOZ and also evaluated their time courses prior to the seizure onset on scalp EEG.

---

<sup>7</sup> This chapter forms the basis of the article [Chaudhary *et al.* 2012b]

## 8.2 Methods

The common methods are described in Chapter 4, and the specific methods for this study are described here.

### 8.2.1 Subjects

We studied sixteen patients (Tables 7.1 and 7.2; Patients #1, 3, 4, 5, 6, 7, 8, 10, 11, 13, 14, 15, 16, 17, 19, 20) out of a series of 55 patients with refractory focal epilepsy (as in Chapter 7), who had typical spontaneous seizures during vEEG-fMRI acquisition as recorded during long-term video-EEG monitoring. These patients were invited to undergo vEEG-fMRI scanning as per selection criteria described in Chapter 7, Section 7.2. Drug reduction or sleep deprivation was not used before vEEG-fMRI studies. A summary of the clinical details on these patients can be found in Tables 7.1 and 7.2.

### 8.2.2 MRI acquisition

Two 20-minute EPI sessions were acquired, except in patient #7 in whom three 20-minute EPI sessions were acquired. Scanning was stopped prematurely in patient #6 to limit the risk of adverse incident. The details of MRI acquisition are described in Chapter 4 Section 4.2.

### 8.2.3 Video-EEG recording and artefact correction

Synchronous scalp video-EEG was recorded during the MRI scanning. The details of video-EEG recording and removal of pulse and scanner artefact are described in Chapter 4, Section 4.3.

### 8.2.4 Data processing and analysis

#### 8.2.4a EEG and fMRI Processing

I reviewed video-EEGs jointly with experienced neurophysiologists (Dr. Beate Diehl, Dr. Serge Vulliemoz, Prof. Matthew C Walker) to identify IEDs and ictal rhythms [Luders *et al.* 2000; Foldvary *et al.* 2001] and ictal semiology [Luders *et al.* 1998]. The seizures recorded during vEEG-fMRI were compared with the seizures recorded during long-term video-EEG monitoring, and partitioned into phases as described in Chapter 7, Section 7.2.4a. Physiological activities: spontaneous eye blinks and eye movements, swallowing, jaw clenching, small

head jerk, facial twitches, brief hand/foot movements, as described in Chapter 6, were also identified on video-EEG and distinguished from ictal semiology by comparison with ictal events captured on long-term video-EEG monitoring.

Preictal time window was defined as 30sec preceding the *Ictal onset* phase (see Chapter 7, Section 7.2.4a) on scalp EEG without any visible EEG changes. In case without clear electrographic signature on EEG, or EEG obscured by myogenic artefact the *preictal* phase was defined as 30sec before the first semiological change observed on video. The details of fMRI data pre-processing are described in Chapter 4, Section 4.4.

### **8.2.4b fMRI Modelling**

The fMRI data was analysed within the GLM framework. EPI sessions during which seizures were recorded on video-EEG were analyzed. Eight patients had more than one seizure in more than one recording session and both sessions were included in the same GLM as separate sessions.

A GLM was created specifically to investigate the preictal BOLD changes. I used a more flexible approach based on the Fourier basis set to model BOLD changes during the preictal time window defined as 30sec prior to the *Ictal onset* phase. The Fourier basis set is capable of capturing arbitrarily shaped fluctuations over time scales down to  $2*TR$ , and was not set to zero at the window start and end to capture the actual onset of BOLD changes if they extend beyond the modelled window. The basis set order was set to 5 (combination of 5 sine and 5 cosine functions), and was calculated by dividing the preictal time-window by  $2*TR=6sec$ . All the regressors in Model for Ictal changes (see Chapter 7, Section 7.2.4b) were treated as confounds in the current model.

### **8.2.5 Assessment of BOLD change significance, visualization and level of concordance**

SPM[F] maps were obtained for the preictal phase. The presence of significant BOLD changes was assessed at a threshold of  $p < 0.05$ , corrected for FWE and additionally using a less conservative statistical threshold  $p < 0.001$ , uncorrected for FWE, when there were no BOLD changes seen at  $p < 0.05$ . The resulting

maps were co-registered with the patient's anatomical MRI scans with and without icEEG electrodes and postsurgical T1-weighted MRI scans.

First, the localisation of all BOLD-clusters was visually compared, by an experienced neuro-radiologist (Dr. Caroline Micallef), with the presumed SOZ. The presumed SOZ was defined non-invasively on the basis of IEDs, ictal rhythm, ictal semiology and structural abnormality where available. Preictal BOLD maps were classified as either:

- *Entirely concordant*: All BOLD clusters were within the presumed SOZ (within the same lobe/gyrus).
- *Concordant plus*: The most statistically significant BOLD cluster (global maximum: GM) was within the presumed SOZ (within the same lobe/gyrus) and other clusters were remote from the presumed SOZ.
- *Some concordance*: The GM cluster was remote from the presumed SOZ and one of the other clusters was within the presumed SOZ (within the same lobe/gyrus).
- *Discordant*: all clusters were remote (another lobe or opposite hemisphere) from the presumed SOZ.

The BOLD clusters located in the ventricular system, vascular tree, edges and base of brain and cerebellum were not considered [Chaudhary *et al.* 2012a]. I compared the level of concordance of *Ictal onset / Ictal* phase related and *preictal* BOLD maps with the presumed SOZ using Spearman's rank Correlation ( $r_s$ ) (IBM SPSS Statistics); and also compared the sub-lobar localisation of the GM BOLD cluster within the presumed SOZ with the localisation of ictal rhythm on scalp EEG.

Second, the preictal haemodynamic onset was defined as the time at which the fitted response was more than two standard deviations above or below baseline. A secondary assessment of the preictal changes was performed having found that the fitted values at the start of modelling window were generally not zero. I inspected the fitted time courses, for each preictal BOLD cluster ( $> 5$ voxels), over the period preceding the modelled preictal time window (i.e., backwards from minus 30sec from the *Ictal onset* phase) visually. The purpose was to determine the time

at which the preictal changes were significantly different from zero and later continued into the modelled preictal time-window.

Thirdly, for the patients who underwent icEEG recording during presurgical assessment, I measured the Euclidean distance between the statistical maximum voxel of GM/other BOLD cluster, within the presumed SOZ for the preictal phase, and the invasively defined SOZ using the following formula:

$$|d_1| = \sqrt{((X_1 - X_2)^2 + (Y_1 - Y_2)^2 + (Z_1 - Z_2)^2)}$$

Here,  $X_1$ ,  $Y_1$  and  $Z_1$  represent the position of the icEEG electrode contact in x,y and z plane and  $X_2$ ,  $Y_2$  and  $Z_2$  represent the position of the BOLD change in x,y and z plane. Invasively defined SOZ was assessed by two experienced neurophysiologists (Dr. Beate Diehl, Prof. Matthew C Walker) as the location of depth/grid contacts on icEEG where the first and maximal ictal change was seen.

### 8.3 Results

There were 8 males; median age was 28years and the median age at seizure onset was 8 years. Six patients had frontal lobe seizures, four had multifocal, 2 had temporal lobe, 2 had parietal lobe and 2 had hypothalamic seizures.

Statistically significant preictal changes were revealed at  $p < 0.05$ , corrected for FWE in 2/16 patients only and at  $p < 0.001$ , uncorrected for FWE for 15/16 (93.7%). One patient (#17) did not show any preictal changes.

Preictal BOLD changes had a degree of concordance with the presumed SOZ in 10/16 (62.5%) patients (Table 8.1; Figure 8.1). Preictal BOLD changes were seen in presumed SOZ and IZ and also remote from the presumed SOZ in the areas which were part of the DMN, which are described in Table 8.1 for each patient.

Preictal maps were classified as (see Table 8.1; Figures 8.2-8.3): *Concordant plus* = 4/16 (25%); *Some concordance* = 6/16 (37.5%); and *Discordant* = 5/16 (31.2%). The level of concordance of the BOLD maps (Figure 8.1) for the *Ictal onset / Ictal phase* (85%) was better than preictal phase (62.5%); and was significantly correlated with the *Ictal onset / Ictal phase* ( $r_s = 0.4$ ,  $p < 0.05$ ). Preictal BOLD changes overlapping or adjacent to the epileptogenic structural abnormalities were also seen.

In 3/4 patients with *Concordant plus* preictal maps, the GM BOLD cluster within presumed SOZ was localised to one to two gyri at sub-lobar level as compared to lobar (patient #1) and multi-lobar (patients #3, 8, 11) localisation of ictal pattern on scalp EEG.

Inspection of the preictal time courses across 74 seizures in 15 patients revealed a consistent pattern of BOLD decrease followed by a BOLD increase before the electrical seizure onset during vEEG-fMRI. The onset of BOLD changes varied from 98sec to 0sec before the electrical seizure onset (Figure 8.4; Table 8.1). There was a consistent BOLD decrease starting at -98sec to -14sec, and was followed by an increase starting at -50sec to 0sec. The median onset for preictal BOLD decreases was -31sec (95% confidence interval (CI): -35.7 to -26.3); and the median onset for preictal BOLD increase was -16sec (95% CI: -18.1 to -13.9). Six patients (#1, 3, 4, 10, 15, 16) underwent icEEG recordings for localisation of the SOZ. The distance between the GM or other BOLD cluster, within the presumed SOZ, and the invasively defined SOZ was 2 to 5cm (Table 8.1). Three patients (# 1, 4, 16) underwent surgery, out of which two (#1 and 16) had ILAE Class I postsurgical outcome, and one (#4) had ILAE Class III postsurgical outcome. Preictal BOLD cluster nearest to the invasively defined SOZ was not resected in any of these patients.

**Table 8.1: Preictal BOLD changes and level of concordance with the SOZ**

ID #	Preictal BOLD changes Positive = ↑ Negative = ↓ Biphasic = ↑↓	Concordance with the presumed SOZ	Onset of preictal BOLD changes (sec)		*Delay (sec)	- d
			↓	↑		
1	↓↑ <i>R Superior Parietal, L Parieto-temporal, Medial Frontal, L Temporal</i>	C+	-79	-32	3	3
3	↓↑ <i>L Occipito-temporal, L Temporal-ITG, L motor-cortex, R ITG, B/L Medial Occipital</i>	C+	-30 to -28	-18 to -17	25	SOZ1 = 4.7 SOZ2 = 4.2 SOZ3 = 7.6
4	↓↑ <i>R Orbito-frontal, R Temporal-STG, Post. Cingulate, R Cuneus, L Temporal-MTG</i>	SC	-80 to -20	-26 to 0	8	7.6 / 3
5	↓↑ <i>B/L Fronto-central-SFG/ MFG/ Med.SFG</i>	D	-90 to -14	-50 to -1	NA	NA
6	↓↑ <i>R Frontal lobe-MFG/IFG, R Precuneus, R Superior Parietal</i>	D	-37	-20	NA	NA
7	↓↑ <i>L Temporal (GM), L Frontal</i>	SC	-84 to -19	-25 to -3	NA	NA
8	↓↑ <i>R Frontal-SFG, R Temporal-STG</i>	C+	-74 to -52	-25 to -23	NA	NA
10	↓↑ <i>L Medial Parieto-occipital, R Medial Parieto-occipital, B/L Parieto-occipital</i>	SC	-53	-28	38	SOZ1= 5.9 / 5.3 SOZ2 = 3.7 / 2.5
11	↓↑ <i>R Frontal-SFG, R Cingulate, R Orbito-frontal</i>	C+	-40 to -17	-18 to -5	NA	NA
13	↓↑ <i>R Temporal, L Temporo-occipital</i>	D	-68 to -28	-30 to -28	NA	NA
14	↓↑ <i>L Temporal-MTG</i>	D	-98	-25	NA	NA
15	↓↑ <i>L Fronto-polar, L Frontal-MFG, L Temporal-STG</i>	SC	-25	-4	13	SOZ1 = 5.3 / 3 SOZ2 = 7.9 / 2

**Table 8.1: Contd.**

ID #	Preictal BOLD changes Positive = ↑ Negative = ↓ Biphasic = ↑↓	Concordance with the presumed SOZ	Onset of preictal BOLD changes (sec)		*Delay (sec)	↔  d
			↓	↑		
16	↓↑ <i>R Temporal-MTG, L Temporal-MTG, Medial Frontal-SFG, L posterior Temporo-occipital, L Parietal, Medial occipital, <b>L Frontal-SFG</b></i>	SC	-67	-25	6	9.1 / 2.5
19	↓↑ <i>R Frontal-IFG/MFG/SFG, R Temporal-MTG, R Frontal-motor-cortex, Paracentral lobule, <b>R Parietal-SMG, Medial Frontal</b></i>	SC	-37	-30	NA	NA
20	↓↑ <i>R Frontal-SFG/SMA, L Temporal- ITG, L Frontal-IFG, B/L motor cortex</i>	D	-62	-22	NA	NA

Preictal BOLD changes were revealed at  $p < 0.05$  (FWE-corrected) in two patients. In the remaining patients preictal BOLD changes were seen at less conservative statistical threshold  $p < 0.001$  uncorrected for FWE only (Italicized). The first BOLD cluster for each patient is the most statistically significant cluster (GM); and the cluster within the presumed SOZ is boldened.

\* Delay (sec) between seizure onset on icEEG and clinical seizure onset

↔ |d| = Distance (cm) between the intracranial electrode with first EEG change at seizure onset and GM/nearest BOLD cluster for the preictal phase highlighted non-invasively to be within the presumed SOZ

Abbreviations: Med.SFG = medial superior frontal gyrus, SFG = superior frontal gyrus, MTG = middle temporal gyrus, MFG = middle frontal gyrus, SMA = supplementary motor area, IFG = inferior frontal gyrus, STG = superior temporal gyrus, B/L = bilateral, SMG = supra-marginal gyrus, ITG = inferior temporal gyrus, R = right, L = left, NA = not applicable, sec = seconds, GM = global maximum, SOZ = seizure onset zone, EC = Entirely concordant, C+ = Concordant plus, SC = Some Concordance, D = Discordant



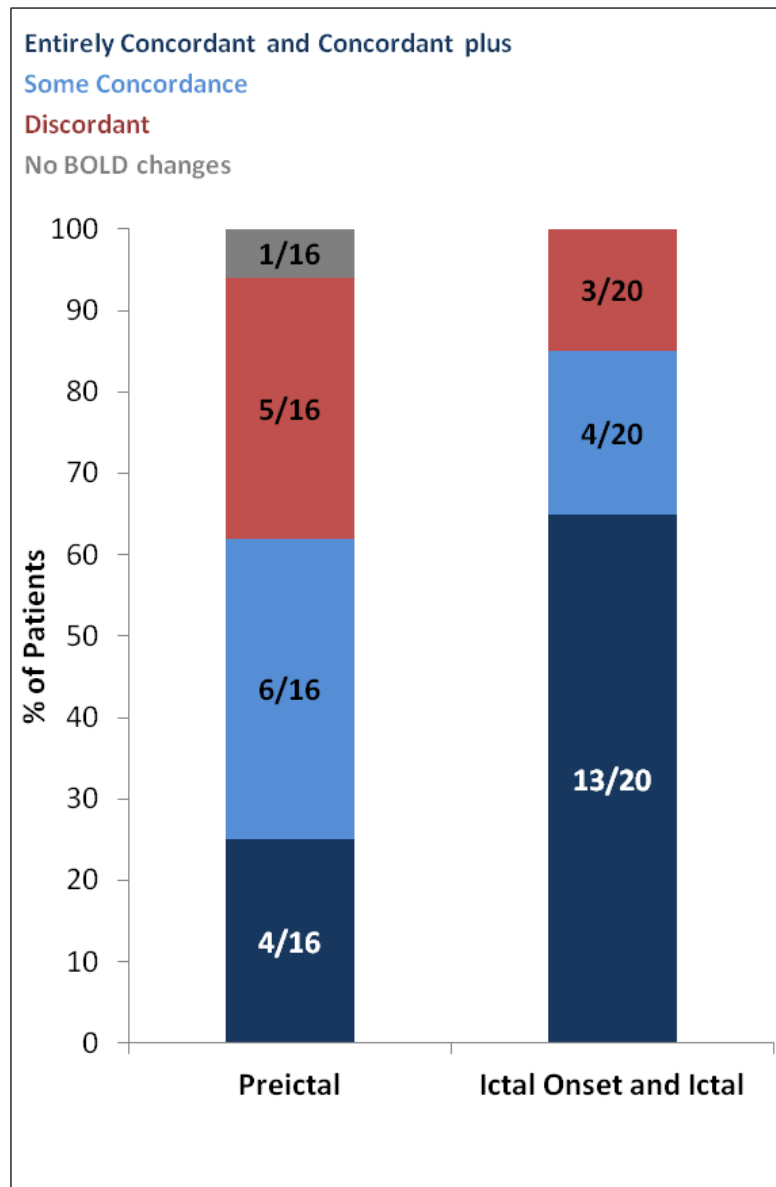


**Figure 8.1: Bar chart showing level of concordance for preictal BOLD changes vs. Ictal onset/Ictal phases**

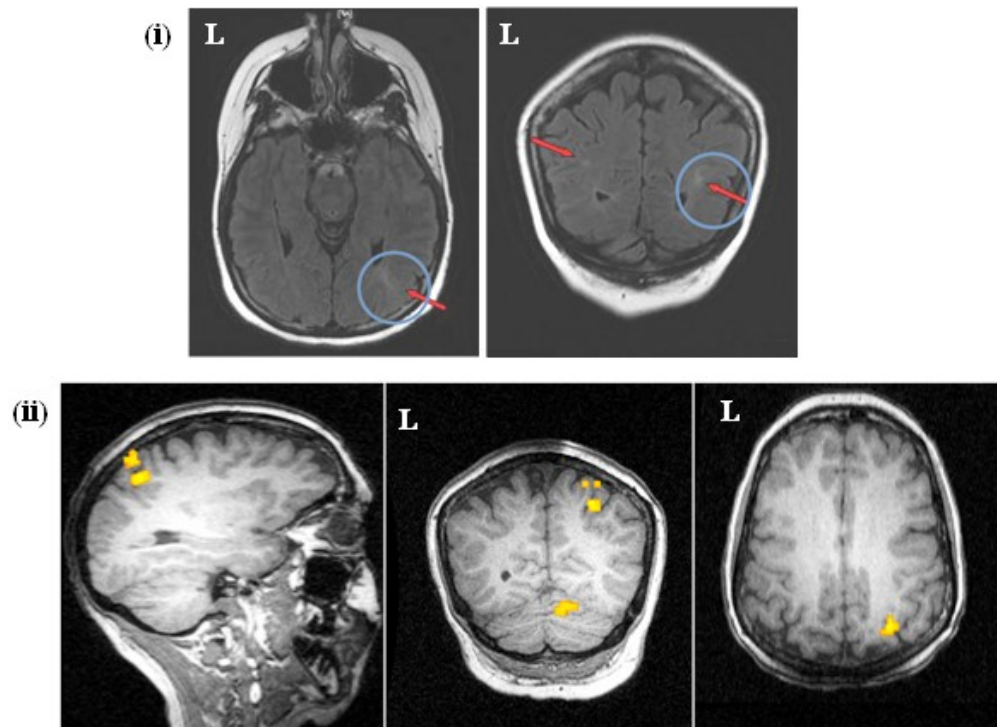


**Figure 8.2: Preictal BOLD changes for patient #1**

(i) Multiple tubers were seen in right parietal lobe and left temporal lobe. Epileptogenic tuber in right parietal lobe is encircled. (ii) BOLD changes (threshold at  $p < 0.001$  uncorrected for FWE) overlaid on co-registered T1-volume. (ii) The preictal BOLD map was classified as *Concordant plus* with GM BOLD cluster in right superior parietal lobule (cluster size = 11 voxels,  $F=4.87$ ) and other BOLD cluster in left parieto-temporal.

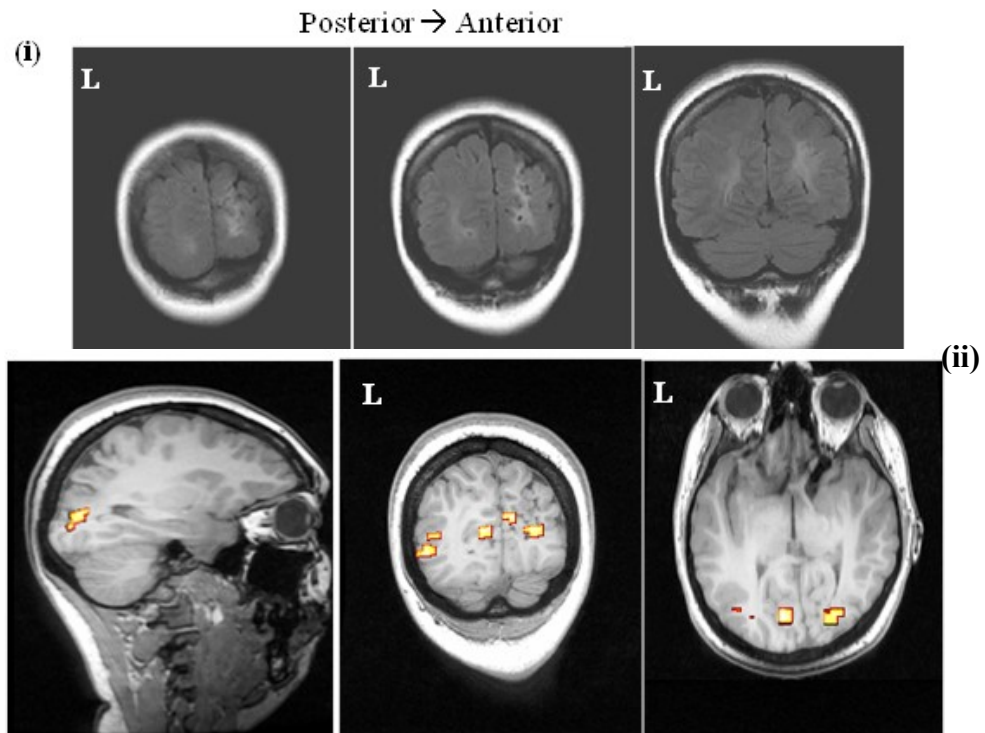


**Figure 8.3: Preictal BOLD changes for patient #10**

(i) Long standing ischemic damage with malformation of gyri in right occipito-parietal region extending into right posterior temporal lobe on (FLAIR) MRI-scan. (ii and iii) BOLD changes (threshold at  $p < 0.05$  corrected for FWE) overlaid on co-registered T1-volume. (iii) Preictal BOLD map had *Some concordance* showing BOLD changes in: left medial parieto-occipital (GM, cluster size = 8 voxels,  $F=3.75$ ), right medial parieto-occipital and right lateral parieto-occipital region (crosshair).

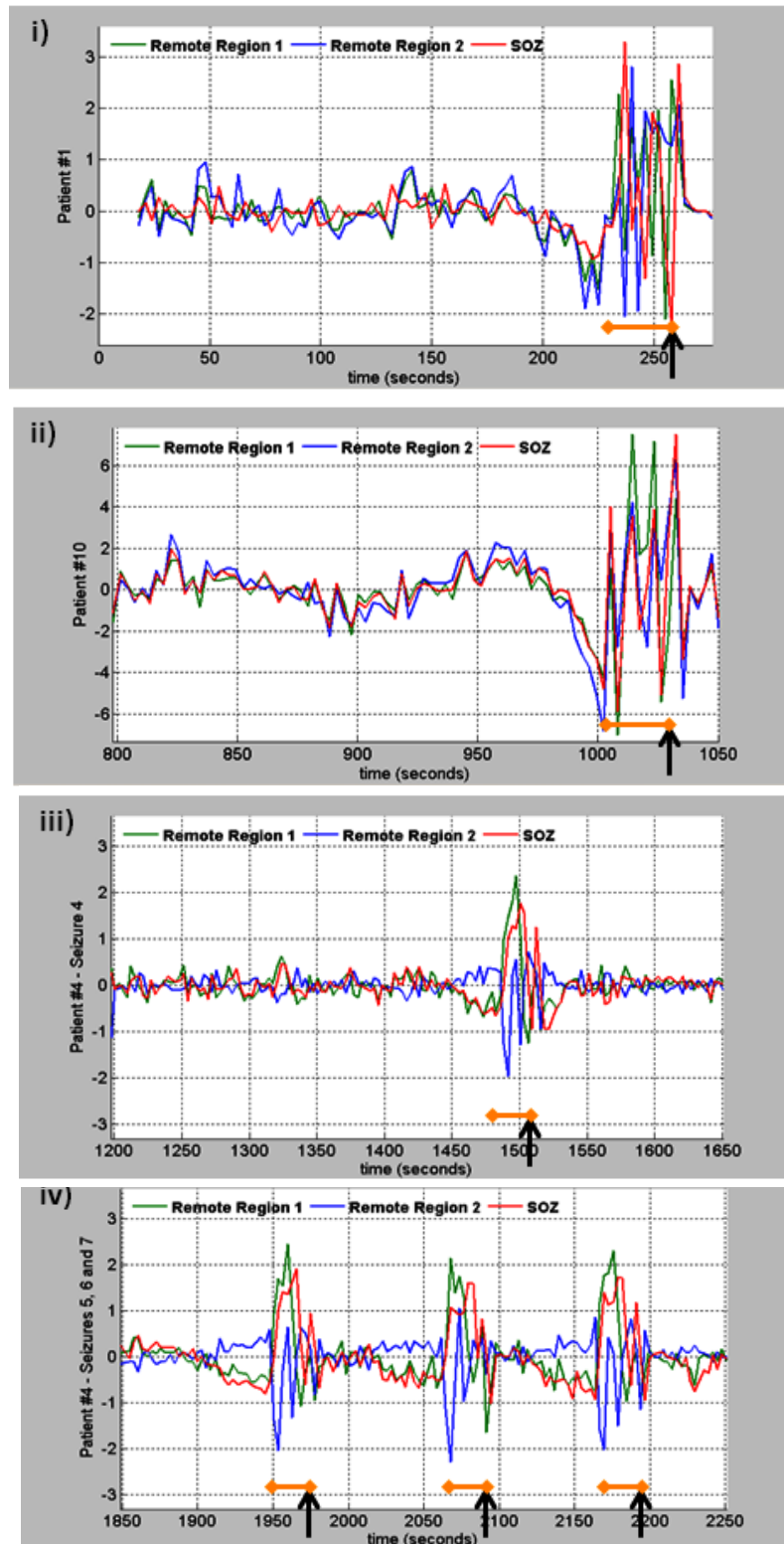


**Figure 8.4: Time courses of preictal BOLD changes**

X-axis: time; Y-axis: % BOLD response. Black arrow indicates seizure onset recorded on vEEG inside scanner and orange bar indicates the 30sec preictal window (Fourier modelling window). There was a consistent BOLD decrease (Median onset: -31sec; 95% CI: -35.7 to -26.3) followed by an increase (Median

onset: -16sec (95% CI: -18.1 to -13.9). (i) Patient #1 had one seizure. Red line represents the time course from the BOLD cluster concordant with the presumed SOZ; green line represents the time course from the BOLD cluster from remote region1 (left temporal lobe also showing IEDs on MEG); blue line represents the time course from the BOLD cluster from remote region2 (left parieto-temporal lobe) (ii) Patient #10 had one seizure. Red line represents the time course from the BOLD cluster concordant with the presumed SOZ (right temporo-occipital region); green line represents the time course from the BOLD cluster from remote region1 (left temporo-occipital); blue line represents the time course from the BOLD cluster from remote region2 (medial occipital); (iii & iv) patient #4 had seven seizures. Red line represents the time course from the BOLD cluster concordant with the presumed SOZ (left temporal lobe); green line represents the time course from the BOLD cluster from remote region1 (right temporal lobe also showing IEDs on scalp EEG and MEG); blue line represents the time course from the BOLD cluster from remote region2 (precuneus).

## 8.4 Discussion

In this work, I compared the localisation of preictal BOLD changes using vEEG-fMRI with the presumed SOZ; and also measured the distance between the GM / other BOLD cluster and the invasively defined SOZ in patients with refractory seizures. The main findings of the study are:

- Noninvasive localisation of preictal BOLD changes which had a degree of concordance with the presumed SOZ in 62.5% patients.
- Identification of a consistent pattern of preictal BOLD decrease -31sec (95% CI: -35.7 to -26.3), followed by an increase -16sec (95% CI: -18.1 to -13.9)

This suggests that vEEG-fMRI can reveal preictal haemodynamic changes before the electrical seizure onset on scalp EEG. Preictal BOLD changes in cortical and subcortical structures have been shown previously in a limited number of cases [Tyvaert *et al.* 2009;Donaire *et al.* 2009a]. The preictal BOLD maps reflected BOLD changes in the SOZ, IZ and DMN related areas in line with other studies [Tyvaert *et al.* 2009;Donaire *et al.* 2009a].

For modelling preictal haemodynamic changes in the GLM framework, I used a more flexible approach based on the Fourier basis set which is capable of capturing arbitrarily shaped fluctuations up to the temporal resolution afforded by a set order. This approach can be justified by the fact that there is no consensus regarding the timeline of preictal haemodynamic changes, and the exact onset and time course of BOLD changes prior to the seizure onset is less well defined. Fourier basis set gives more freedom to capture this less well studied aspects of seizures. This also raises the question: at what time might haemodynamic changes start prior to any behavioural or EEG features? I selected a 30sec window to include the timeline of preictal changes as reported in some fMRI [Donaire *et al.* 2009a] and optical imaging studies [Zhao *et al.* 2007]. This choice is also partly justified by consideration of the inter-seizure interval in these data, which is of the order of 1-minute or greater in all cases (except Patients # 4, 7 and 11: when the inter-seizure interval was less than 30sec, and the following seizure was not included in the design matrix as a separate event, given the need to avoid the effects of overlap between the preictal time window and preceding seizures). I attempted to capture the relative arbitrariness of the haemodynamic changes at the

start of preictal window, i.e. the Fourier basis set was not forced to zero at that point, which permitted me to determine whether the changes are likely to have started  $\geq 30$ sec prior to the electrical seizure onset on scalp EEG. For detecting the onset of preictal BOLD changes, I plotted the fitted time courses of preictal clusters and looked for the time of onset of preictal changes backwards from minus 30sec from the *Ictal onset* phase on scalp EEG.

The basis set approach has been used previously to map interictal [Lemieux *et al.* 2008; Masterton *et al.* 2010] and ictal [Thornton *et al.* 2010b] BOLD changes; I used Fourier basis set to map preictal BOLD changes because: 1) it can capture small deviations from the canonical haemodynamic-response better than finite-impulse-response [Penny *et al.* 2007]; 2) it modelled signal fluctuations taking place over a time-scale of  $\geq 2$ TR, and limited the effects of noise by constraining the estimated time course with proper assessment of statistical significance within the SPM framework, in contrast to averaging time courses; and 3) it can reveal preictal changes throughout the brain independently of the results for the later ictal phases, in contrast with methods based on the analysis of the BOLD signal in regions identified ictally [Bai *et al.* 2010].

The degree of concordance of preictal BOLD maps was evaluated by comparing the location of GM and other clusters with the presumed SOZ using a concordance classification which has been used previously [Thornton *et al.* 2010b; Grouiller *et al.* 2011] as discussed in Chapter 7, Section 7.4.1.

In this work, preictal changes started with a consistent sustained BOLD decrease from -31sec (95% CI: -35.7 to -26.3) followed by an increases from -16sec (95% CI: -18.1 to -13.9) in agreement with previous studies showing preictal changes starting minutes [Federico *et al.* 2005b] to seconds [Tyvaert *et al.* 2009; Donaire *et al.* 2009a] before the seizure onset. It can be argued that the ictal pattern on scalp EEG may be delayed by up to 8sec as compared to icEEG and may represent propagation [Tao *et al.* 2005; Ray *et al.* 2007]; whereas the first electrical change on icEEG preceded the first clinical change by 3 to 38sec (Table 8.1) in the six patients who underwent invasive recordings in this study. This suggests preictal changes hint towards an increase in oxygen demand secondary to the changes in neuronal activity which is yet not powerful or synchronised enough to be seen on scalp EEG [Gavaret *et al.* 2004; Ray *et al.* 2007], as at least 6-10cm<sup>2</sup> area of brain needs to be recruited before electrical activity could be seen

on scalp EEG; and preictal changes may reflect metabolic changes preceding the electrical changes at the seizure onset on scalp EEG.

I found BOLD decreases in the presumed SOZ, irritative zones and other remote areas (Figure 8.4) whereas Donaire et al. (2009) found decreases in putative SOZ in addition to medial frontal, bilateral parietal and posterior cingulum i.e., forming part of the so-called DMN [Raichle et al. 2001]. However, Tyvaert et al. (2009) found preictal increases preceding decreases at lower statistical threshold. I suggest that the initial BOLD decreases in this work may correspond to the active inhibitory circuits [Wendling et al. 2003; Wendling et al. 2005; Gnatkovsky et al. 2008; Trombin et al. 2011] which are over-ridden by the increasing neuronal activity as shown by the later increases: driven by glutamatergic neurons [Huberfeld et al. 2011]. Moreover, the BOLD changes in areas remote from the SOZ may represent fluctuations in the resting state networks before the manifestation of seizures [Schwartz et al. 2011] or involvement of an epileptogenic network before seizure ensues [Bartolomei et al. 2001; Truccolo et al. 2011].

Recently, it has been shown, using transcranial magnetic stimulation, that motor responses during preictal state differ from that during interictal state; this also signifies that the brain state changes immediately prior to the seizure [Richardson and Lopes da Silva 2011]. It can be suggested that preictal haemodynamic changes may reflect: preictal discharges (spatially and morphologically different from interictal discharges) [Huberfeld et al. 2011]; fast oscillatory activity [Wendling et al. 2005; Gnatkovsky et al. 2008; Jacobs et al. 2008a; Engel, Jr. et al. 2009; Khosravani et al. 2009]; or activity from glial cells [Moore and Cao 2008; Figley and Stroman 2011]. Further studies with simultaneous scalp and icEEG-fMRI can help to understand the relationship between early electrical changes on icEEG and their haemodynamic correlates at the seizure onset.

In this study, I demonstrated that preictal BOLD maps had a degree of concordance with the presumed SOZ in larger proportion (62.5%) cases; specifically for *Concordant plus* BOLD maps the GM BOLD cluster was localizable to one to two gyri providing further precision of localisation as compared to scalp EEG which can localise up to lobar level. However, the level of concordance for preictal BOLD maps was lower than ictal onset related BOLD maps, again reflecting that the preictal haemodynamic changes possibly represent



a transition state during which various inhibitory and excitatory circuits are at work before the actual seizure sets in [Wendling *et al.* 2005].

In Chapters 7 and 8, I compared the localisation of seizure related BOLD networks during different ictal phases and interictal-ictal transition with that of independently defined SOZ. I also compared the localisation of BOLD networks with the gold standard i.e., icEEG where available. However, icEEG also has limitations of spatial sampling. In Chapter 9, I will present my work on the localisation of BOLD networks for IEDs on icEEG and their comparison with the surgical resection and postsurgical outcome using icEEG-fMRI.

### **8.5 Conclusion**

vEEG-fMRI can map preictal BOLD changes having a degree of concordance with the SOZ. Moreover, the pattern of preictal haemodynamic changes i.e., BOLD decrease followed by increase suggests an underlying mechanism of the transition from interictal to ictal state which may help to better understand the seizure generation.

## **Chapter 9: Mapping the interictal haemodynamic networks using simultaneous intracranial EEG-fMRI and comparison with postsurgical outcome**

### **9.1 Background**

Scalp EEG suffers from limitations for presurgical evaluation of epilepsy including low sensitivity [Binnie and Stefan 1999;Smith 2005], paradoxical lateralization [Catarino *et al.* 2011] or incongruous localisation [Remi *et al.* 2011]. Invasive evaluation with icEEG is performed to localise the SOZ and IZ because it has higher spatial resolution and greater sensitivity than scalp EEG [Luders *et al.* 2006]; although it has limited spatial sampling and carries surgical risks [Knowlton *et al.* 2008b].

As discussed in Chapter 3, scalp EEG-fMRI has been shown to map BOLD changes related to IEDs [Salek-Haddadi *et al.* 2006;Zijlmans *et al.* 2007;Thornton *et al.* 2011] and seizures [Tyvaert *et al.* 2009;Donaire *et al.* 2009a;Thornton *et al.* 2010b]. Scalp EEG-fMRI is limited by the IED discharge rates, an incomplete understanding of the relationship between IEDs and BOLD changes and low sensitivity of scalp EEG [Al-Asmi *et al.* 2003;Salek-Haddadi *et al.* 2006;Zijlmans *et al.* 2007]. However, IED related BOLD changes in distributed epileptic networks across lobes, in patients with FCDs, have been shown to be associated with poor surgical outcome [Thornton *et al.* 2011]. Recently, simultaneous icEEG-fMRI has been performed following extensive safety testing [Carmichael *et al.* 2008b;Carmichael *et al.* 2010] revealing IED related BOLD changes [Vulliemoz *et al.* 2011] local and remote from the relevant icEEG electrodes.

This raises the question if BOLD changes associated with IEDs localised at subgyral level on icEEG may also predict the surgical outcome. In this work, I investigated the BOLD patterns associated with specific IED types in a larger group of patients undergoing invasive evaluation. In particular, the BOLD changes were mapped for each IED type over the entire brain (network) and compared their relationship to the IZ and the surgical resection and also evaluated

the BOLD distribution for combined all IED types in relation to postsurgical outcome.

## 9.2 Methods

### 9.2.1 Subjects

Ten patients with refractory focal epilepsy having icEEG recording as part of presurgical evaluation at the National Hospital for Neurology and Neurosurgery, Queen Square, London underwent icEEG-fMRI consecutively if they did not have any contraindications as described by [Carmichael *et al.* 2008b; Carmichael *et al.* 2010; Carmichael *et al.* 2012] and gave informed written consent for an additional study with icEEG-fMRI after the clinical recordings for capturing seizures on icEEG had completed. Prior to implantation, all patients had had detailed clinical history and examination, epilepsy protocol MRI [Duncan 2010], neuropsychology assessment. The clinical details for each patient are summarized in Table 9.1.

Seven patients subsequently underwent resective surgery. Postsurgical outcome was assessed as per ILAE classification [Wieser *et al.* 2001] at a median duration of 16 months postoperatively (range: 12-32months); class I to III were defined as good outcome and class IV and V were defined as poor outcome. Four patients (#2, 3, 5, and 7) had good outcome and three patients (#1, 6, 9) had poor outcome. The study was approved by the joint research ethics committee of the National Hospital for Neurology and Neurosurgery (UCLH NHS Foundation Trust) and UCL Institute of Neurology, Queen Square, London, UK. Some of the IED related BOLD results for two patients (#1 and 6), using icEEG-fMRI, have previously been published [Vulliemoz *et al.* 2011; Carmichael *et al.* 2012].

### 9.2.2 Intracranial EEG-fMRI acquisition

The implantation of intracranial electrodes (Figure 9.1) was guided by a hypothesis based consensus decision generated from the results of long-term EEG monitoring, structural MRI and other non-invasive investigations: PET, MEG or ictal-SPECT where available in a given patient.

**Table 9.1: Clinical characteristics**

ID	Age	Sex	Seizure onset age	Epilepsy	Scalp EEG	MRI	Presumed SOZ
1	46	F	18	FLE	Spikes: regional central Seizure: non-localizable	NL	L motor cortex
2	39	M	8	FLE	Sharp: R temporal/centro-parietal Seizure: central fast activity	L HS	R SMA
3	28	M	12	FLE	Spike: L fronto-central Seizure: regional central	FCD: L posterior SFG+MFG	L Frontal Lobe
4	50	F	5	FLE	Spikes: L fronto-central/fronto-temporal Seizure: regional L frontocentral	FCD: L posterior IFG	L Frontal Lobe
5	36	F	7	FLE	Spikes: L inferior frontal/orbito-frontal Seizure: regional L frontal	FCD: L IFG	L Frontal Lobe
6	31	F	6	TLE	Spikes: regional L temporal Seizure: L posterior temporal	NL	L Temporal Lobe
7	26	M	7	TLE	Spikes: Bi temporal Seizure: Regional L temporal	L HS	L Temporal Lobe
8	28	M	10	TLE	Spikes: Bi temporal Seizure: Regional L temporal	NL	L Temporal Lobe
9	24	M	18	TOLE	Spikes: R temporal/posterior temporal, L temporal Seizure: R posterior temporal/ Temporo-occipital	NL	R Temporal Lobe
10	32	F	2	TOLE	Spikes: R mid temporal and fronto-temporal Seizure: R lateralized maximum temporal	R occipital ischemic damage extending into parietal lobe	R Temporo-occipital

Abbreviations: M=male, F=female, FLE=frontal lobe epilepsy, TLE=temporal lobe epilepsy, TOLE=Temporo-occipital lobe epilepsy, R=right, L=left, NL=non-lesional, HS=hippocampal sclerosis, FCD=focal cortical dysplasia, SFG=superior frontal gyrus, MFG=middle frontal gyrus, IFG=inferior frontal gyrus

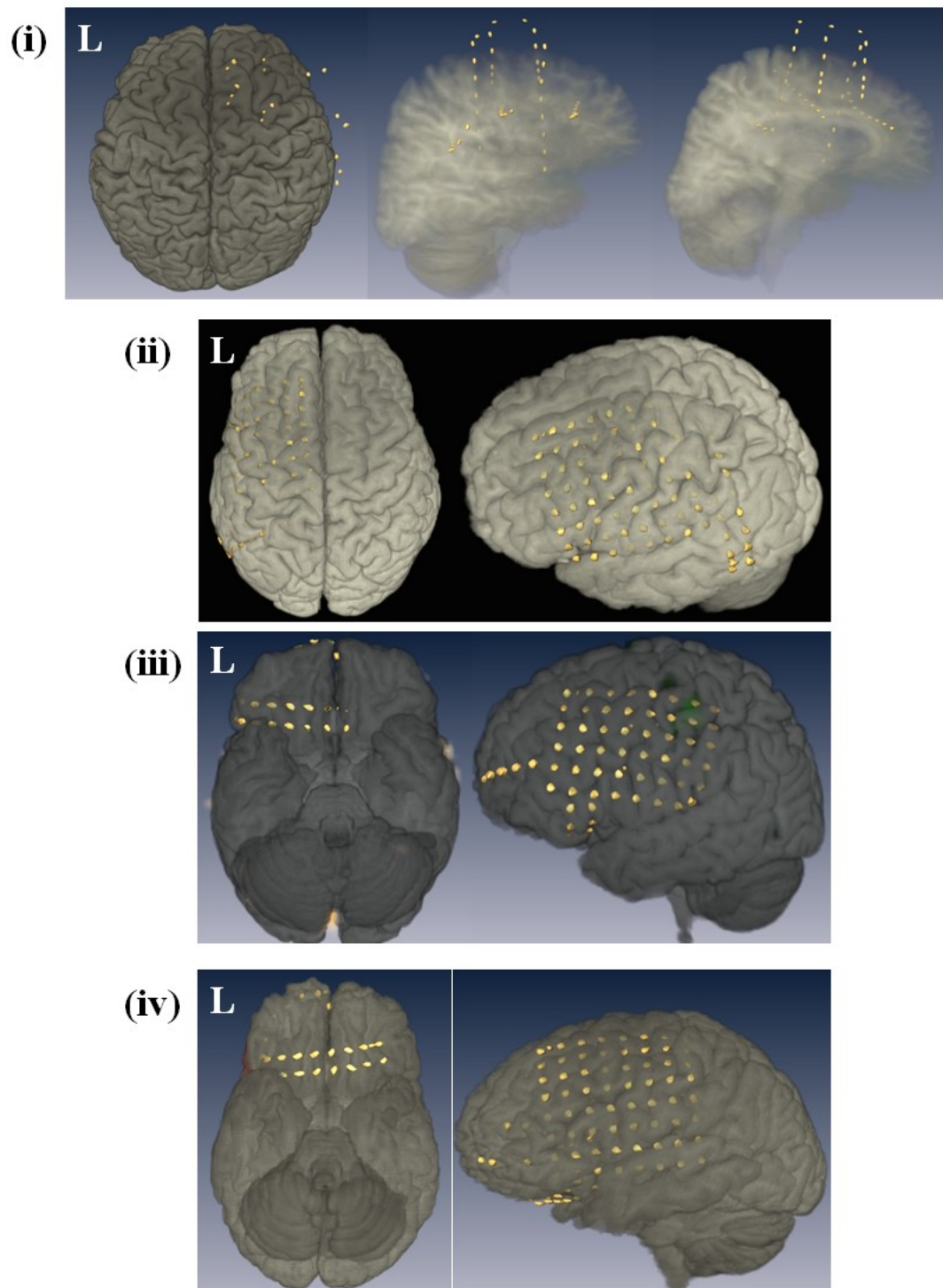


**Figure 9.1: Implantation Scheme**

(i) Patient #2, (ii) Patient #3, (iii) Patient #4, (iv) Patient #5

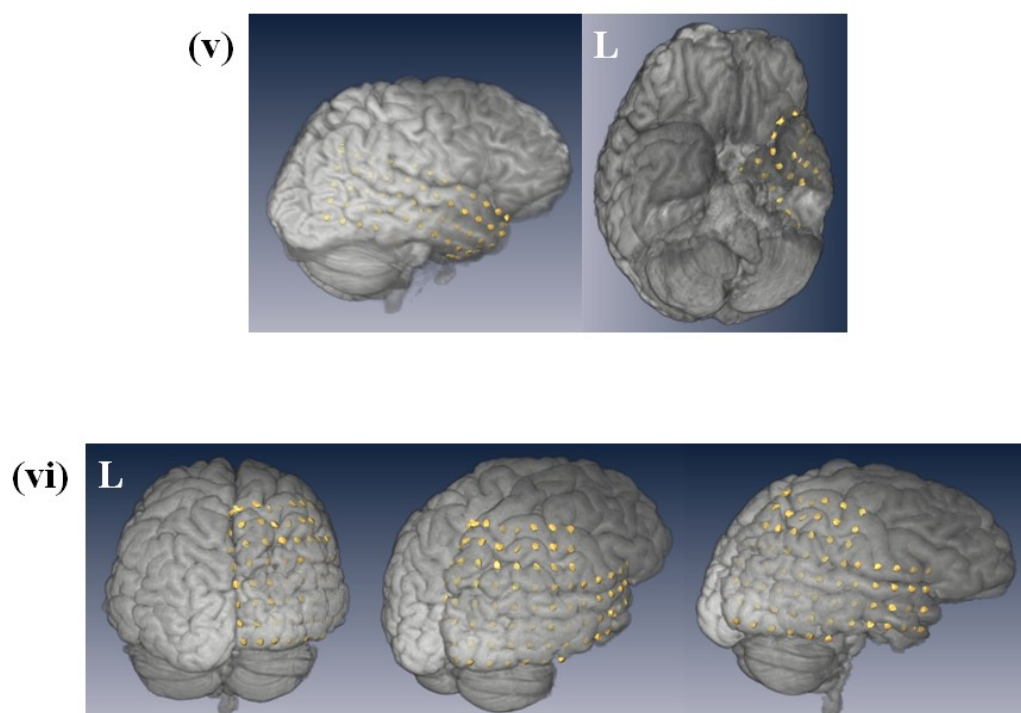


**Figure 9.1 (continued)**

(v) Patient #9, (vi) Patient #10

The IZ and SOZ were defined invasively by two experienced neurophysiologists (Dr. Beate Diehl, Prof. Matthew C Walker) as the location of depth/grid contact on icEEG where the earliest/maximal interictal or ictal change was seen, respectively.

After clinical icEEG recordings were completed for localisation purposes, the case specific 56-90 implanted electrodes were connected to MR-compatible cables and amplifier system [Carmichael *et al.* 2010;Vulliemoz *et al.* 2011] for icEEG-fMRI acquisition. Intracranial EEG was recorded using Brain Vision Recorder version 1 software (Brain Products, Munich, Germany) and displayed without scanner artefacts using RecView software (Brain Products, Munich, Germany) during fMRI acquisitions.

In accordance with our icEEG-fMRI protocol [Carmichael *et al.* 2008b;Carmichael *et al.* 2010;Carmichael *et al.* 2012] MR images were acquired using 1.5T scanner (Siemens, Erlangen, Germany) with a standard transmit/receive head-coil and low specific absorption rate (SAR) sequences ( $\leq 0.1\text{W/kg}$ , head average) to ensure patient safety. One (for patients #4, 5) or two (patients #1, 2, 3, 6, 7, 8, 9, 10) 10-minute resting state EPI sessions (Imaging parameters: TR / TE / flip angle = 3000ms / 40ms / 90°, 64 × 64 acquisition matrix, 38 × 2.5 mm slices with 0.5 mm gap) and T1-weighted structural scans (Imaging parameters: TR / TE / flip angle = 15ms / 4.49ms / 25°, resolution 1.0 × 1.2 × 1.2 mm, FoV 260 × 211 × 170 mm, 256 × 176 × 142) were acquired [Carmichael *et al.* 2012].

### 9.2.3 Data Processing and analysis

#### 9.2.3a Intracranial EEG and fMRI processing

icEEG acquired inside MRI scanner was corrected offline for scanner related artefact [Allen *et al.* 2000] using Brain Vision Analyzer version 2 software (Brain Products, Germany) and reviewed to identify and classify IEDs according to their spatiotemporal and amplitude distribution. I also compared icEEG acquired inside MRI scanner with long-term icEEG monitoring. For one patient (#8) the entire icEEG recorded during icEEG-fMRI could not be corrected satisfactorily due to technical problems at acquisition and one patient (#7) had a

subclinical seizure during one of the two EPI-sessions and therefore these datasets were not considered for further analysis.

Functional time series data for nine patients was analyzed using SPM8 ([www.fil.ion.ucl.ac.uk](http://www.fil.ion.ucl.ac.uk)) after discarding the first two image-volumes to account for the T1-saturation effect. EPI time series data were corrected for slice acquisition time, realigned to the mean and spatially smoothed using an isotropic Gaussian kernel of 8mm FWHM [Friston *et al.* 1995b].

### 9.2.3b fMRI modelling

A GLM was built to map IED related hemodynamic changes. Six patients had two EPI sessions and these were included in a single GLM as separate sessions. IEDs were represented as zero duration stick functions (individual IED) or blocks (runs of IEDs). Each IED type was modelled as a separate effect and convolved with the canonical HRF and its temporal and dispersion derivatives. Twenty four inter-scan realignment parameters (6 realignment parameters from image pre-processing and a Volterra-expansion of these [Friston *et al.* 1996]) were included in the GLMs as confounds to account for motion related effects.

### 9.2.4 Assessment of BOLD changes

Two questions were addressed: what is the anatomical relationship between the BOLD changes related to specific IEDs and the IZ? Given the variety of IEDs on icEEG in any given patient, what is the clinical relevance of a summary representation of BOLD changes for combined all IEDs?

#### 9.2.4a BOLD changes for individual IED types

For each IED type, the presence of significant BOLD changes was assessed across the whole brain in the SPM[F]-maps i.e., network level, at a statistical threshold of  $p < 0.05$  (corrected for FWE), and a less conservative threshold  $p < 0.001$  (uncorrected). The resulting SPMs were co-registered with pre and postsurgical T1-weighted MRI scans. No brain shift correction was applied when co-registering pre and postsurgical images. BOLD time courses based upon the maximum likelihood parameter estimates of the GLM were plotted for each BOLD cluster to classify the BOLD change as increases, decreases or biphasic



(both increases and decreases) according to the value at event onset. The localisation of BOLD clusters was visually compared, along with an experienced neuro-radiologist (Dr. Caroline Micallef), with the IZ. The Euclidean distance was measured between the statistical maximum voxel of the most statistically significant (global maximum: GM) / other BOLD cluster nearest to the IZ and the icEEG electrode contact i.e., the IZ. The degree of concordance of BOLD maps with the IZ for each IED type were then classified [Chaudhary *et al.* 2012a] as:

- *Entirely concordant*: All BOLD clusters in the same lobe/gyrus as and within 2cm of the IZ.
- *Concordant plus*: The GM cluster was in the same lobe/gyrus as and within 2cm of the IZ and other clusters were remote (i.e., different lobe or opposite hemisphere) from the IZ.
- *Some concordance*: The GM cluster was remote from the IZ and one of the other clusters was in the same lobe/gyrus as and within 2cm of the IZ.
- *Discordant*: all clusters were remote (different lobe or opposite hemisphere) from the IZ.

The BOLD clusters located in the ventricular system, vascular tree, edges and base of brain and cerebellum were not considered [Chaudhary *et al.* 2012a].

There is a signal drop within 1cm of the electrode contact [Carmichael *et al.* 2012] and macro electrodes can record within a distance of 1-1.4cm [Lachaux *et al.* 2003]. Therefore, to measure BOLD changes proximal to the sites recording IEDs, I assessed IED related BOLD changes within a volume of interest (VOI) of 2cm radius [Vulliemoz *et al.* 2011] around the icEEG contact recording the earliest / maximum electrical change for each IED type. The VOI approach was implemented in SPM8 using *small volume correction* tool [Ashburner *et al.* 2012] and statistical significance of local BOLD change was assessed at threshold  $p \leq 0.05$  within the VOI [Vulliemoz *et al.* 2011]. The *small volume correction* tool [Ashburner *et al.* 2012] evaluates the presence of any significant finding within the predefined VOI rather correlating the predicted BOLD response with the modelled IED at each voxel over the entire brain, and performs the statistical threshold correction taking into account its shape and volume with strong control for Family wise type-I error. The Euclidean distance between the statistical

maximum voxel of local BOLD change for each IED type and the icEEG electrode contact recording IED was also calculated.

#### **9.2.4b BOLD changes for combined all IEDs in an individual patient**

To provide a summary of BOLD changes linked to all interictal activity in a given patient an SPM[F]-map for combined all IED types (i.e., ‘*combined interictal BOLD map*’) was generated. The Euclidean distance was measured between the statistical maximum voxel of GM / other BOLD cluster nearest to the IZ and the resection margins. The spatial distribution of interictal BOLD changes was further summarized by calculating a laterality index (LI) using ‘*one threshold for all method*’ of SPM8-toolbox [Wilke and Lidzba 2007]. The LI were prefixed with ‘+’ when they lateralized to the hemisphere ipsilateral ( $+0.3 \leq LI \leq +1$ ) to the IZ and with ‘-’ when they lateralized to the hemisphere contralateral ( $-1.0 \leq LI \leq -0.3$ ) to the IZ. BOLD maps with an LI in the range ( $-0.3 < LI < 0.3$ ) were classified as non-lateralizing.

### **9.3 Results**

There were five males, the median age at the time of icEEG-fMRI was 31.5years and the median age at seizure onset was 7.5years. Five patients had FLE, three had TLE and two had TOLE. The implantation scheme, IED classification and statistics and the IZ/SOZ for each patient is summarized in Table 9.2. Significant IED related BOLD changes were revealed for all types of analysis in all cases.

**Table 9.2: IED statistics and local and network level BOLD changes**

ID	Implantation scheme (Labelling of electrodes used during icEEG-fMRI)	Location of IED on Grid/depth electrode (Number)	BOLD changes for individual spike types		1. IZ (most frequent spikes) 2. SOZ
			Network	Concordance	
			Localisation ↑ increase, ↓ decrease, ↑↓ biphasic (cm)	↑↓ (cm)	
1	Grid 8X6: L fronto-parietal (G)	1. G13, 14 (466)	↑L med. SFG, ↑L SMA, ↓L Parietal, ↑↓L MFG, ↑Cingulate, ↓Precuneus	8/2.4	D
	Grid 8X2: L fronto-parieto-temporal				
	Strip 1X6: L anterior frontal (S1)	2. G22, 23 (866)	↑↓R Cuneus, R IFG, L Cuneus	6.2/5.9	D
	Strip 1X6: L frontopolar (S2)	3. G39 (361)	↑L med. SFG/SMA, L IFG, ↓R Parietal, ↑↓R Cuneus, ↓Precuneus	3.4/-	D
		4. G30 (197)	↑↓R Temporo-occipital, ↑R STG, ↑L SMA	5.8/2	D
		5. G42, 43 (42)	↓Med. SFG, ↑↓Cuneus/Precuneus, R IFG	8.4/4.7	D
2		6. G17 (57)	↑L SMC, R Thalamus, L SMA, L SFG	3.6/1.7	D
	Depth: 1X6-R ant. SMA	1. R ant. and post. SMA (476)	↓L SFG, R SFG, B/L MFG, R Cuneus, R post. Cingulate, R Paracentral lobule / SMA	5.7/2	SC
	Depth: 1X6-R post. SMA				
	Depth: 1X8-R ant. Insula	2. R post. SMA (211)	↓SMA, R sup. Parietal, L med. SFG, B/L IFG		
	Depth: 1X8-R post. Insula	3. R ant. SMA (46)	↓Paracentral lobule, Precuneus/ Cuneus, B/L sup. Parietal	1.7/-	C+
	Depth: 1X8-R ant. cingulum				
	Depth: 1X10-R middle cingulum	4. R ant. Insula + R post. Cingulum + R ant. SMA (152)	↓R SFG/MFG, Precuneus / Cuneus, R MFG/SFG, Cingulate, L MFG, ↑B/L post. Temporal, B/L MTG, R SMA	3.1	D
	Depth: 1X10-R post. cingulum			6/1.1	SC
		5. R post. Cingulum + R SMA (150)	↓R MFG, R SFG/SMA, Precuneus/ Cuneus	5.7/2	SC
	3	Grid 8X8: L fronto-parietal (G)	1. G 4,5 (72)	↓L IFG, ↑L post. Temporal, Cuneus/Precuneus	2/-
Grid 2X8: L parieto-temporal (GA)		2. G5 + G13, 22, 23, DP3,4 (244)	↑L MFG, R MTG, ↓post. SMA, post. Cingulate/Precuneus, ↑L post. MFG	1/-	C+
Depth 1X4: L ant. SFG (DA)		3. G5 + G13, 23,29,30 (80)	↑↓L IFG, ↑med. SFG, L Temporo-occipital, ↓L MFG	3.8/0.8	SC
Depth 1X4: L post. SFG (DP)		4. G13,14 (29)	↓L med. Occipital, L IFG/MFG, L parieto- temporal, R Cingulate	11/3.9	D
		5. G13,14 + G21,22 (350)	↓L MFG/IFG, ↑L paracentral lobule/SMA, ↑↓L ant. MFG	0.9/-	C+

Table 9.2: Contd.

ID	Implantation scheme (Labelling of electrodes used during icEEG- fMRI)	Location of IED on Grid/depth electrode (Number)	BOLD changes for individual spike types		Concordance	1. IZ (most frequent spikes) 2. SOZ				
			Network	Localisation ↑increase, ↓decrease, ↑biphasic -  d <sub>i</sub> (cm)						
4	Grid 8X6: L frontoparietal (GA)	1. DL2,3 (909) 2. DL2,3+GA28, 36 (152) 3. GA13, 28, 36, 45 (130)	↑R MFG, Thalamus, R Temporo-parietal, orbito-frontal, L med. SFG	5.8/-	D	1. L posterior IFG (DL3)				
	Depth 1X6: L ant. SMA (DA)						↑R MFG, ↓R post. Temporal, L cingulate, ↑L Insula,	6.6/2.9	D	2. L posterior IFG
	Depth 1X6: L post. SMA (DM)									
5	Depth 1X6: L middle SMA (DP)	1. DA3,4 (770) 2. DA3,4 + G1 18, 27, 35, 43 (227) 3. G2 6,14 (195)	↑L Thalamus, ↓B/L cingulate ↑L IFG	4.9/- 1.9/-	D EC	1. L ant. IFG (DA3,4) 2. L ant. IFG				
	Depth 1X4: L lesion (DL)						↓R sup. Parietal, ↓L Precuneus, L Thalamus, R orbito-frontal, L frontopolar, ↑L MFG/IFG	11.2/1.7	SC	
	Strip 1X6: L frontopolar Grid 8X2: L orbitofrontal									
6	Grid 8X4: L lat. temporal (G)	1. DA1,2+DH1,2 + SB1,2 (284) 2. DH2,3+SB2+DA2 (156) 3. G28,18,10+DH5+DA6+SB1-6 (3) 4. DH2,3+SB2+DA2+G2,11,18 (22)	↑↓L post. SFG, B/L Precuneus, ↑B/L orbitofrontal, R IFG, R parahippocampus, R sup. Parietal, ↑med. Frontal, ↑L MFG, L STG, L SFG, L sup. Parietal, ↑↓R Precuneus, ↓L sup. Parietal, ↑B/L orbitofrontal ↑Med. SFG, ↓L sup. Parietal, ↑R basal Temporo-occipital, R basal ganglia/thalamus ↓B/L Precuneus/post. Cingulate, L post. Basal temporal, ↑med. SFG	8.3/3.7 8.9/-	D D D	1. L hippocampus/ lat. temporal / orbito-frontal (DH2,3 and G28) 2. L hippocampus				
	Strip 8X2: L inf. frontal parietal									
	Strip 1X6: L orbitofrontal (SA)									
	Strip 1X6: L temporal pole (SB)									
	Strip 1X6: L basal temporal (S)									
	Depth 1X6: L hippocampus (DH)									
	Depth 1X6: L amygdala (DA)									

Table 9.2: Contd.

ID	Implantation scheme (Labelling of electrodes used during icEEG- fMRI)	Location of IED on Grid/depth electrode (Number)	BOLD changes for individual spike types		Concordance	1. IZ (most frequent spikes) 2. SOZ
			Network	Localisation ↑increase, ↓decrease, ↑↓biphasic - d  (cm)		
			Localisation			
7	Depth1X6:L. ant. hippocampus (LAH) Depth 1X6: L. post. hippocampus (LPH) Depth1X6:L. amygdale(LA) Depth1X6: R ant. hippocampus (RAH) Depth 1X6: R amygdale (RA)	1. RA1,2 + RAH1,2 (634) 2. LAH1,2 + LPH1,2 + LA3,4(60) 3. RA1,2+RAH1,2 +LAH2,3+LPH2,3(10)	↓R Temporoparietal, B/L sup. Parietal, R med. Temporo-occipital ↑L post. Temporal, B/L Precuneus, R post. Basal Temporal, post. Cingulate, B/L sup. Parietal, L IFG/STG, orbito-frontal, med. SFG, B/L MFG ↑L post. Basal Temporal, R MFG, R post. Basal Temporal, B/L Precuneus, B/L sup. Parietal, orbito-frontal, B/L MFG, med. SFG, LSTG	8.3/5.4 D 6.8/3.1 D 6.9/3.3 D	D D D	1. L hippocampus (LAH 1,2) and / R amygdale (RA1,2) 2. L hippocampus
9	Grid8X4:R lat. temporal(GA) Grid4X5:R post. temporal Strip 1X6:R ant. Inf./basal temporal (SPBT) Strip 1X6: R middle inferior/basal temporal (SMBT) Strip 1X6: R post. inferior /basal temporal (SAT) Depth 1X6: R hippocampus (DH) Depth1X6: R amygdala (DA)	1. GA2, 10, 18 (313) 2. GA2, 10, 18 + SPBT5 (485) 3. GA10,11 (302) 4. SPBT4 + SAT3 + DH2,3 + GA10, (111) 5. SPBT4,5 (116) 6. DH2 + DA3+ SAT3 + SPBT3 (80)	↑R Temporoparietal ↑R sup. Parietal, R IFG, Cingulate, L SMC, IFG ↑L sup. Parietal, orbito-frontal, L STG, ↑↓R IFG ↓Post. Cingulate/Precuneus, B/L sup. Parietal, B/L occipital, B/L Temporo-occipital, SMA, B/L SMC, B/L STG ↓L Occipital, SMA, B/L sup. Parietal, R Temporo-occipital, ↑Precuneus ↑L MFG, B/L SMC, B/L sup. Parietal, L STG, B/L Cuneus, Paracentral Lobule, SMA, R Temporo-occipital	3/- 6.4/- 10/- 4.6/0.6 7.3/2.8 11.3/2.2	D D D SC D D	1. (a) R ant. & med. Temporal (GA2,10, DH2, DA3) (b) R temporo- occipital 2. (a) R med. & ant. temporal (b) R temporo- occipital

Table 9.2: Contd.

ID	Implantation scheme (Labelling of electrodes used during icEEG-fMRI)	Location of IED on Grid/depth electrode (Number)	BOLD changes for individual spike types		Concordance	1. IZ (most frequent spikes) 2. SOZ
			Network	Localisation		
			↑increase, ↓decrease, ↑↓biphasic			
Depth 1X6: R hippocampus (DH) Grid 8X8: R temporo-parieto-occipital (G) Grid 5X4: R lateral temporal (GT)	1. DH 2,3,4 (928) 2. G42 (56) 3. GT7 + GT11 + GT2 + DH3 (1658)	↑R ant. hippocampus ↑Precuneus, L Parieto-occipital, R SFG, ↑↓SMA, R Parietal, ↑R Temporo-parietal, R Temporo-occipital, Paracentral lobule, L post. Hippocampus, L Temporo-parietal, R MTG	1.2 6.8/2.6 2.6/1.5	C D SC	1.(a) R hippocampus DH1-4) (b) R Temporo-occipital (G42), and lateral temporal (GT2, 7) 2. R med. Temporo-occipital	

— distance between GM / other BOLD cluster nearest to the IZ and the IZ  
Abbreviations: C=Entirely concordant, C+=Concordant plus, SC=Some concordance, D=Discordant, NA=Not applicable, ant.=anterior, post.=posterior, med.=medial, lat.=lateral, sup.=superior, inf.=inferior, R=right, L=left, SFG=superior frontal gyrus, MFG=middle frontal gyrus, IFG=inferior frontal gyrus, SMA=supplementary motor area, SMC=sensori-motor cortex, STG=superior temporal gyrus, MTG=middle temporal gyrus, ITG=inferior temporal gyrus

### 9.3.1 Individual IED related BOLD changes

At the network level, IED related BOLD changes were seen (Table 9.2) within 2cm of the IZ for at least one IED type for six patients (#1, 2, 3, 5, 9, 10; BOLD increases: 5 patients and BOLD decreases: 3 patients, Figures 9.2 and 9.3); and in remote areas including DMN related areas i.e., bilateral superior parietal lobes, precuneus/cuneus and cingulate [Raichle *et al.* 2001] for all patients (BOLD increases: 5 patients, BOLD decreases: 3 patients, biphasic BOLD change: 2 patients). Across the group, the distance ( $|d|$ ) between the IZ and the GM / other BOLD cluster nearest to the IZ varied between 0.6 and 10 cm (Median: 2.9cm; 95% CI: 2.2-3.6; Table 9.2). BOLD maps for 38 different IED types in nine patients had a degree of concordance with the IZ for 13/38 (*Entirely concordant*: 2; *Concordant plus*: 4; *Some concordance*: 7; Table 9.2, Figures 9.2 and 9.3) and were discordant for 25/38.

All nine patients revealed IED related BOLD changes within the VOI for different IED types around the icEEG contact within a distance of 0.3 to 2cm (Median: 1.6cm; 95%CI: 1.4-1.7).

In the operated cases with good postsurgical outcome (patients #: 2, 3, 5, 7), BOLD maps for different IED types in a given patient predominantly had a degree of concordance with the IZ in 3/4 patients, and the GM / other BOLD cluster nearest to the IZ for individual IED type was at a median distance of 2cm (95%CI:1.4-2.6) from the IZ and were also within the area resected (Figures 9.2 and 9.3; Table 9.2).

In the operated cases with poor postsurgical outcome (patients #: 1,6,9), BOLD maps for different IED types in a given patient were predominantly discordant with the IZ for all patients and the GM / other BOLD cluster nearest to the IZ for individual IED type was at a median distance of 3.5cm (95%CI: 2.2-4.8; Table 9.2) from the IZ.

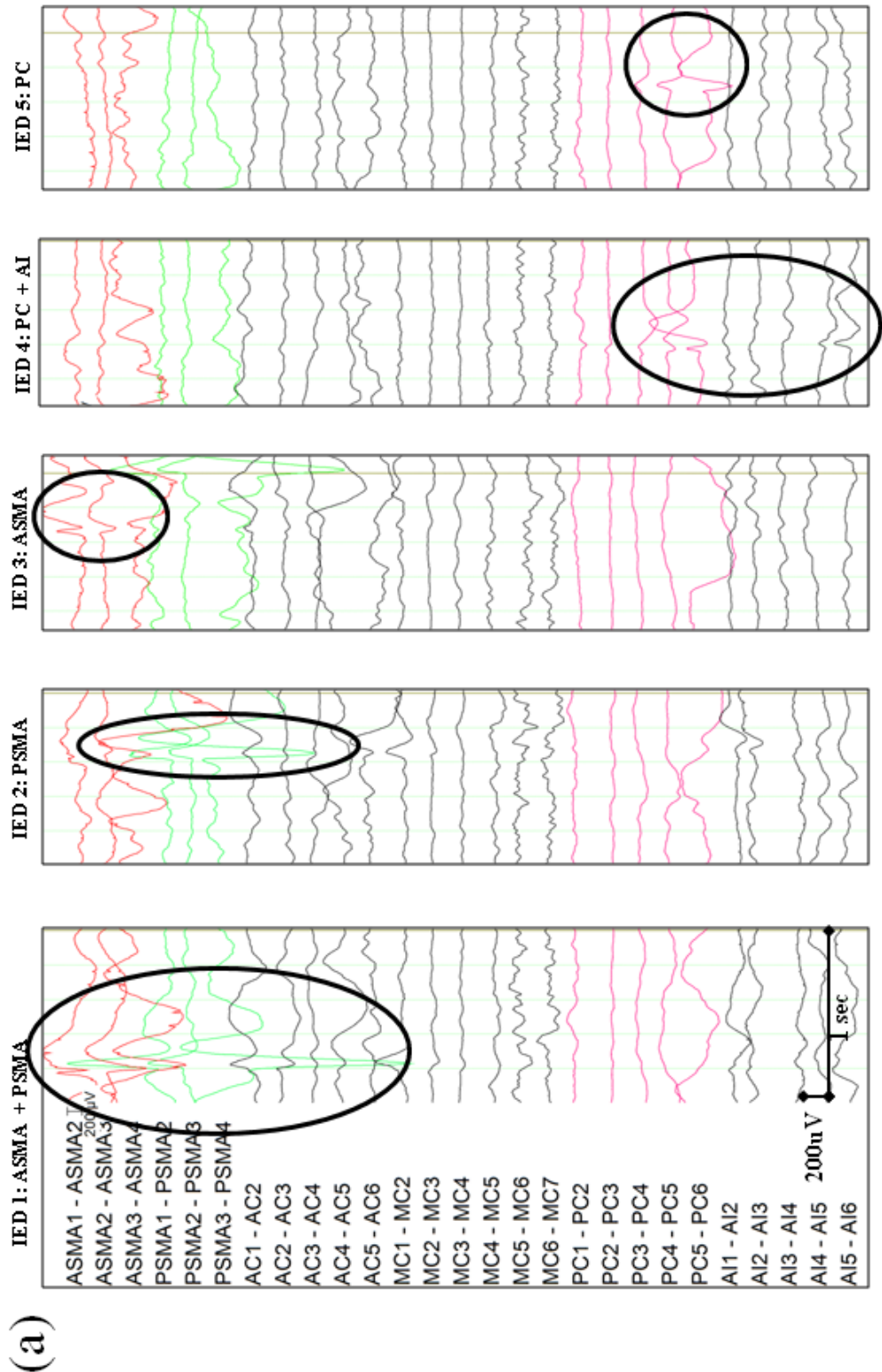


**Figure 9.2: IEDs and BOLD changes for Patient #2**

(a) Representative sample of EEG showing different IEDs modelled as separate regressors in the GLM framework.



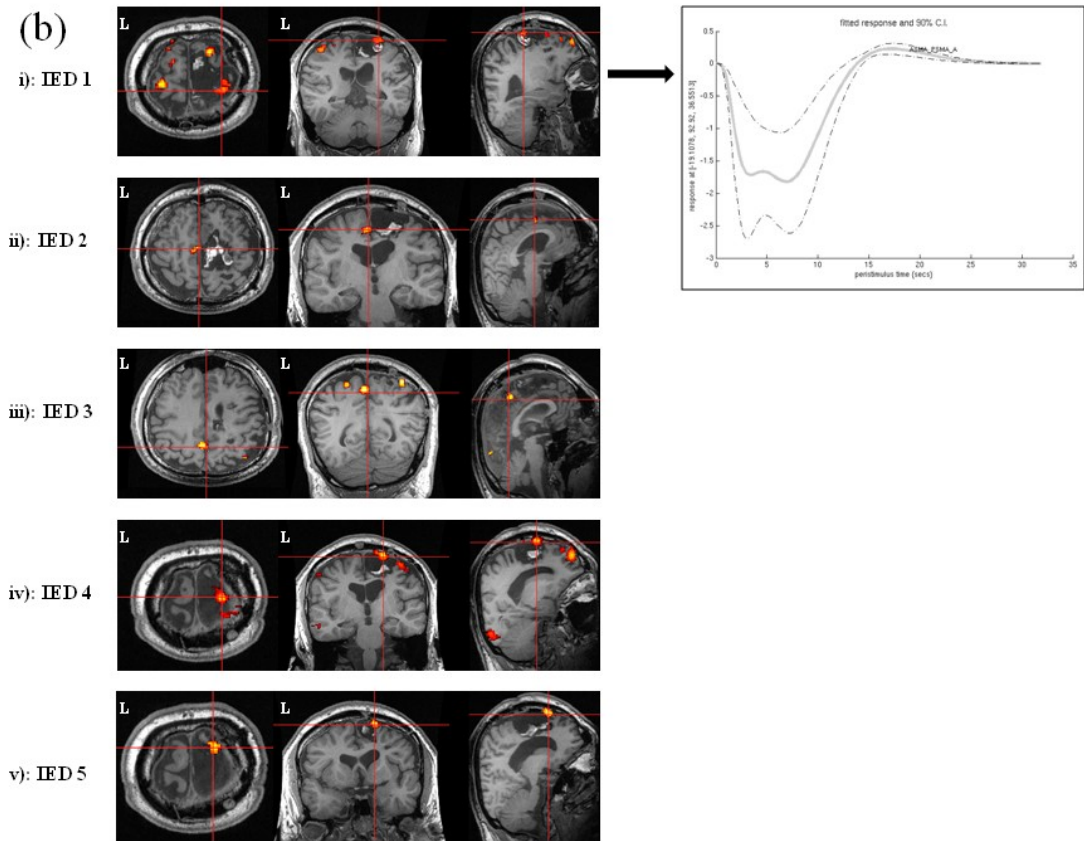


**Figure 9.2: contd.**

(b) SPM[F] map ( $p < 0.001$ ) for individual IEDs at network level overlaid on co-registered postsurgical T1-volume; i) BOLD map for IED 1 was classified to have some concordance and changes were revealed in L SFG (GM; 5.7cm from the IZ), R SFG (2cm from the IZ and within resection cavity, crosshair), bilateral MFG, R Cuneus, R post. Cingulate, R Paracentral lobule, which were BOLD decreases as shown in the plotted HRF; ii) BOLD map for IED 2 was classified as concordant plus and changes were revealed in SMA (GM: 1.7cm from the IZ and within the resection cavity), R sup. Parietal, L med. SFG, B/L IFG; iii) BOLD map for IED 3 was classified as discordant and changes were seen in Paracentral lobule (GM: 3.1 cm from the IZ), Precuneus/ Cuneus, B/L sup. Parietal; iv) BOLD map for IED 4 was classified to have some concordance and changes were revealed in R SFG/MFG (GM: 6cm from the IZ), Precuneus / Cuneus, R MFG/SFG (1.1 cm from the IZ and within the resection cavity, crosshair), Cingulate, L MFG, B/L post. Temporal, B/L MTG, R SMA; v) BOLD map for IED 5 was classified to have some concordance and changes were seen in R MFG (GM: 5.7cm), R SFG (2cm from the IZ and within the resection cavity(crosshair), Precuneus/ Cuneus.

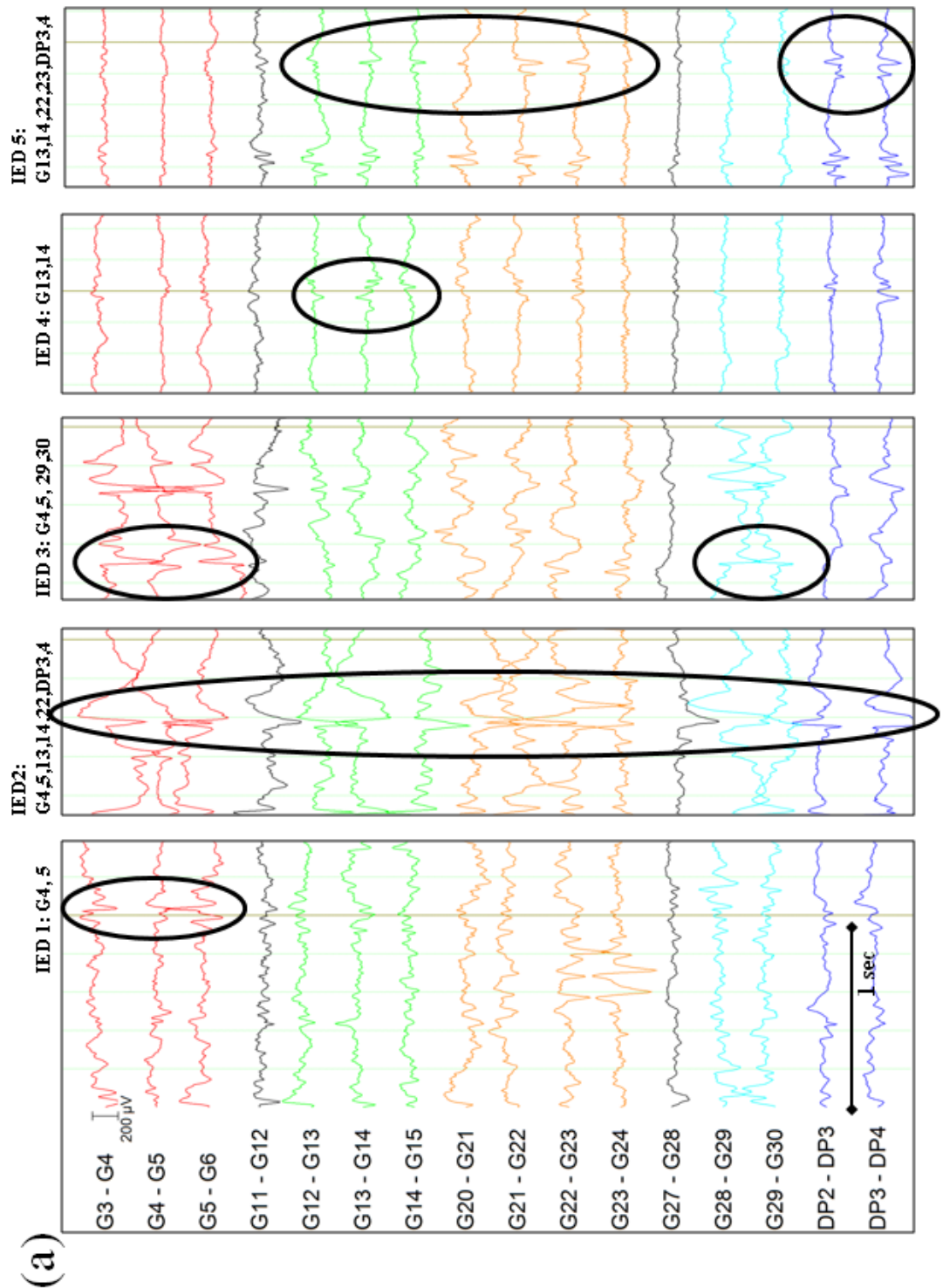


**Figure 9.3: IEDs and BOLD changes for Patient #3**

(a) Representative sample of EEG showing different IEDs modelled as separate regressors in the GLM framework.

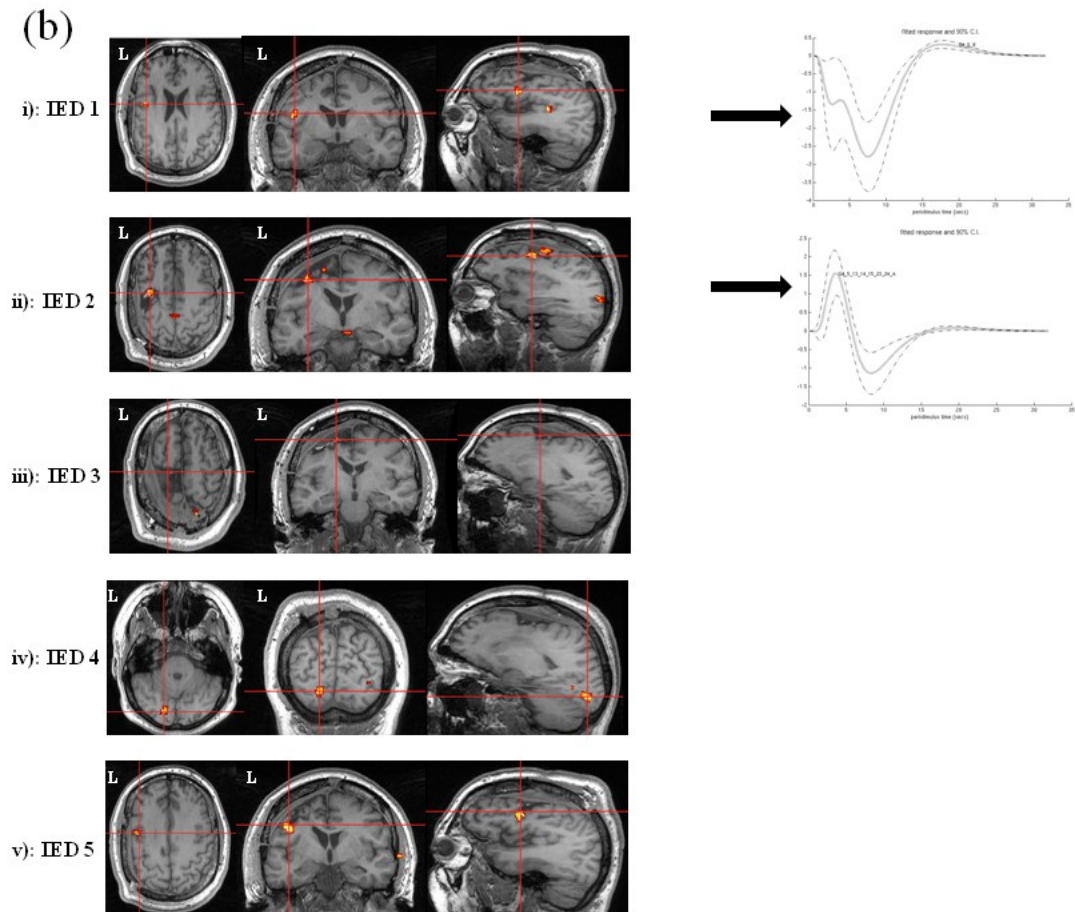


**Figure 9.3: contd.**

(b) SPM[F] map ( $p < 0.001$ ) for individual IEDs at network level overlaid on co-registered postsurgical T1-volume; i) BOLD map for IED 1 was classified as concordant plus and changes were revealed in L IFG (GM: 2cm from the IZ , BOLD decrease as shown in the plotted HRF), L post. Temporal, Cuneus/Precuenus; ii) BOLD map for IED 2 was classified as concordant plus and changes were revealed in L MFG (GM: 1cm from the IZ and within the resection cavity, BOLD increase as shown in the plotted HRF), R MTG, post. SMA, post. Cingulate/Precuenus, L post. MFG; iii) BOLD map for IED 3 was classified to have some concordance and changes were revealed in L IFG (GM: 3.8cm from the IZ) , med. SFG (0.8cm from the IZ and within the resection cavity), L Temporo-occipital, ↓L MFG; iv) BOLD map for IED 4 was classified as discordant and changes were revealed in L med. Occipital (GM: 11cm from the IZ), L IFG/MFG (3.9cm from the IZ), L parieto-temporal, R Cingulate; v) BOLD map for IED 5 was classified as concordant plus and changes were seen in L MFG/IFG (GM: 0.9cm from the IZ), L paracentral lobule/SMA, L ant. MFG.

### 9.3.2 Combined IED related BOLD changes

The summary ‘*combined interictal BOLD maps*’ revealed clusters within the area resected or at resection margins (Figure 9.4; Table 9.3) in addition to remote changes for four patients with good postsurgical outcome. In 2/3 patients with poor postsurgical outcome, the BOLD cluster nearest to the IZ was located more than 2cm from the resection margin (Table 9.3). One patient (#1) did not have postsurgical MRI. The ‘*combined interictal BOLD maps*’ lateralized to the hemisphere ipsilateral to the IZ in 3/4 patients (LI in the range [0.3-0.7]) with good postsurgical outcome and were non-lateralizing in all three patients (LI in the range [0.05-0.2]) with poor postsurgical outcome (Table 9.3; Figure 9.5). One patient (#7) with a non-lateralizing ‘*combined interictal BOLD map*’ for bilateral hippocampal IEDs had good postsurgical outcome.

**Table 9.3: BOLD changes for combined all IED types, laterality index and postsurgical outcome**

ID	BOLD changes for all IEDs	~ d <sub>i</sub> (cm) GM/other	*Laterality Index	Resection	Postsurgical outcome (IL/AE)
1	B/L med. SFG/SMA, R Precuneus, R SMC, L IFG, R sup. Parietal, R occipito-temporal	NA	-0.2	L pre/post central around hand area	Class IV @ 16months
2	R frontopolar SFG, R Precuneus, <b>R SFG/MFG</b> , Cuneus, L SFG/MFG, R Parieto-temporal, R MTG, R Cingulate, L STG, L MFG, R post. SMA, B/L sup. Parietal	1.8 / Within resection cavity	0.7	R SMA + SFG	Class I @ 12months
3	<b>L MFG/IFG</b> , L SMG, R sup. Parietal, med. Occipital, Paracentral lobule/ <b>SMA</b> / post. Cingulate, ant. Cingulate, L basal ganglia	0.5 / Within resection cavity	0.6	L post. SFG + MFG	Class I @ 12months
5	R inferior parietal, <b>L IFG</b> , L inferior parietal, R IFG, L basal ganglia, Precuneus	12 / 0.2	0.3	L ant. IFG / MFG	Class I @ 12months
6	B/L Precuneus, R orbitofrontal, med. SFG, L SMC, R MFG, L post. Basal temporal, L sup. Parietal, L MFG, R paracentral lobule	6.6/2.9	0.2	L anterior temporal lobe	Class IV @ 32months
7	L post. Basal Temporal, B/L Precuneus, B/L MFG, R post. Temporal, orbito-frontal, <b>L STG</b> , L IFG, med. SFG, B/L sup. Parietal	7 / Within resection cavity	-0.1	L anterior temporal lobe	Class I @ 24months
9	L Temporo-occipital, B/L sup. Parietal, R Temporo-occipital, L MTG, post. Cingulate/Precuneus, SMA, B/L MFG, R STG	8.3 / 3	-0.05	R anterior and posterior temporal lobe	Class IV @ 19months

Bolded and italicized BOLD change is the cluster resected during surgery or <1cm to the resection margins. \* -0.2 to 0.2= Non Lateralizing; -0.3 to -1= lateralized to hemisphere contralateral to the IZ; 0.3 to 1= lateralized to hemisphere ipsilateral to the IZ. ~ |d<sub>i</sub>|=distance between GM/other BOLD cluster within 2cm of the IZ and the margin of resection cavity  
Abbreviations: R=right, L=left, SFG=superior frontal gyrus, MFG=middle frontal gyrus, IFG=inferior frontal gyrus, ant.=anterior, post.=posterior, med.=medial, lat.=lateral, sup.=superior, inf.=inferior, SMA=supplementary motor area, SMC=sensori-motor cortex, STG=superior temporal gyrus, MTG=middle temporal gyrus, ITG=inferior temporal gyrus, B/L=bilateral, SMG=supramarginal gyrus, NA=postsurgical MRI not available

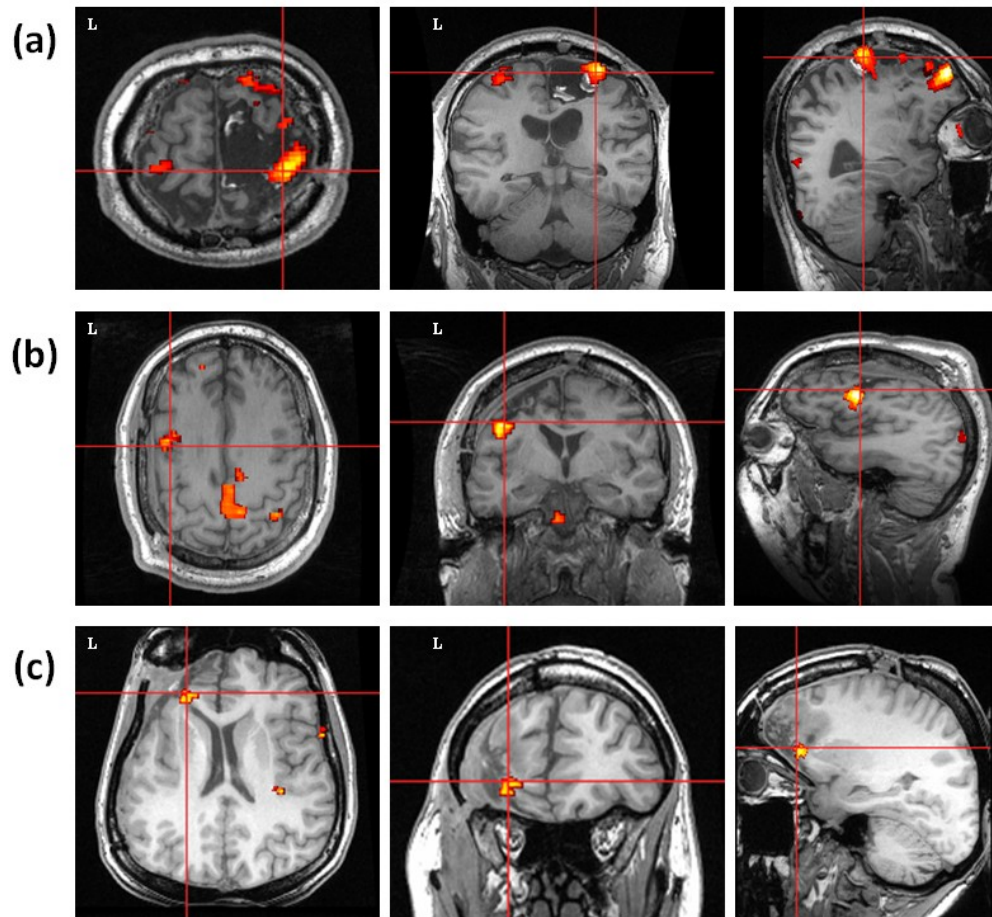


**Figure 9.4: BOLD changes for combined all IED types and surgical resection** SPM[F] map ( $p < 0.001$ ) for *all interictal* at global level overlaid on co-registered postsurgical T1-volume. (a) Patient #2: BOLD changes were seen in R frontopolar SFG, R Precuneus, R SFG/MFG, Cuneus, L SFG/MFG, R Parieto-temporal, R MTG, R Cingulate, L STG, L MFG, R post. SMA, and bilateral sup. Parietal. GM BOLD cluster in R frontopolar SFG was 1.8cm from the resection margin and another cluster in R SFG/MFG (cross hair: +) was within the resection cavity. (b) Patient # 3: BOLD changes were seen in L MFG/IFG, L SMG, R sup. Parietal, med. Occipital, Paracentral lobule/ SMA/ post. Cingulate, ant. Cingulate, and L basal ganglia. GM BOLD cluster in L MFG/IFG was 0.5cm (cross hair: +) from the resection margin and another cluster in L SMA was within the resection cavity. (c) Patient # 5: BOLD changes were seen in R inferior parietal, L IFG, L inferior parietal, R IFG, L basal ganglia, and precuneus. GM BOLD cluster in R inferior parietal was 12cm from the resection margin and another cluster in L IFG was 0.2cm (cross hair: +) from the resection margin.

(a)

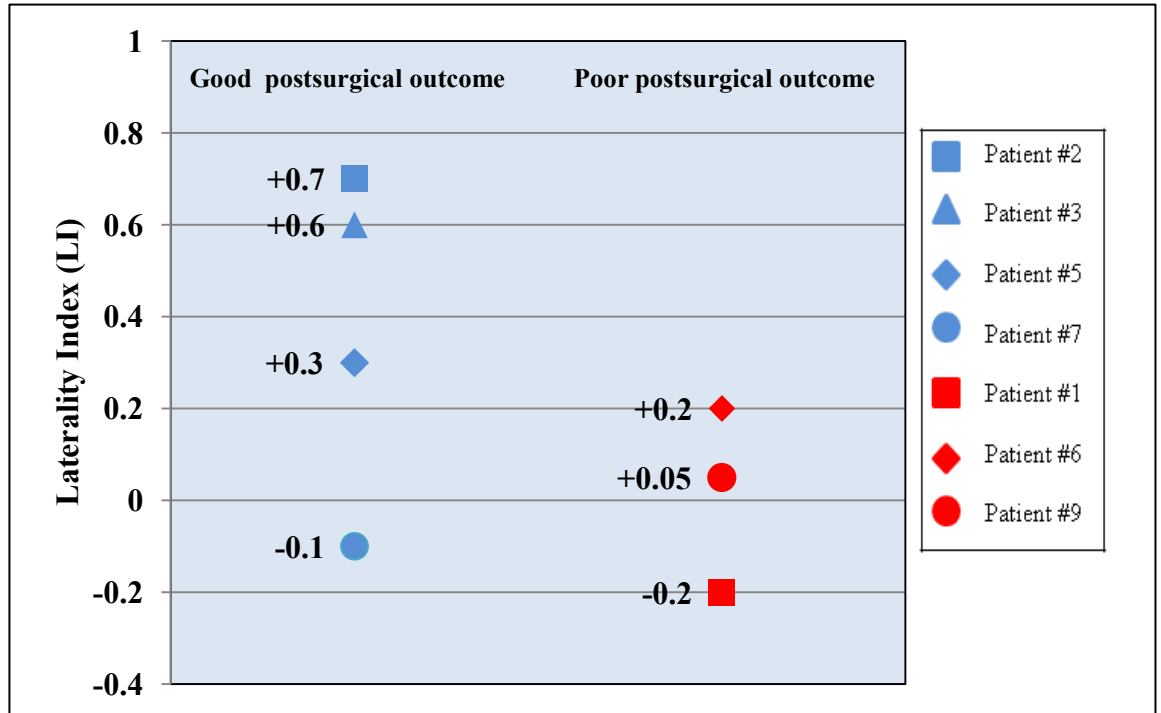


**Figure 9.5: BOLD changes, laterality index and postsurgical outcome**

(a) Scatter plot comparing the laterality indices in two groups of patients with good (ILAE Class I-III: blue) and poor (ILAE Class IV-VI: red) postsurgical outcome.

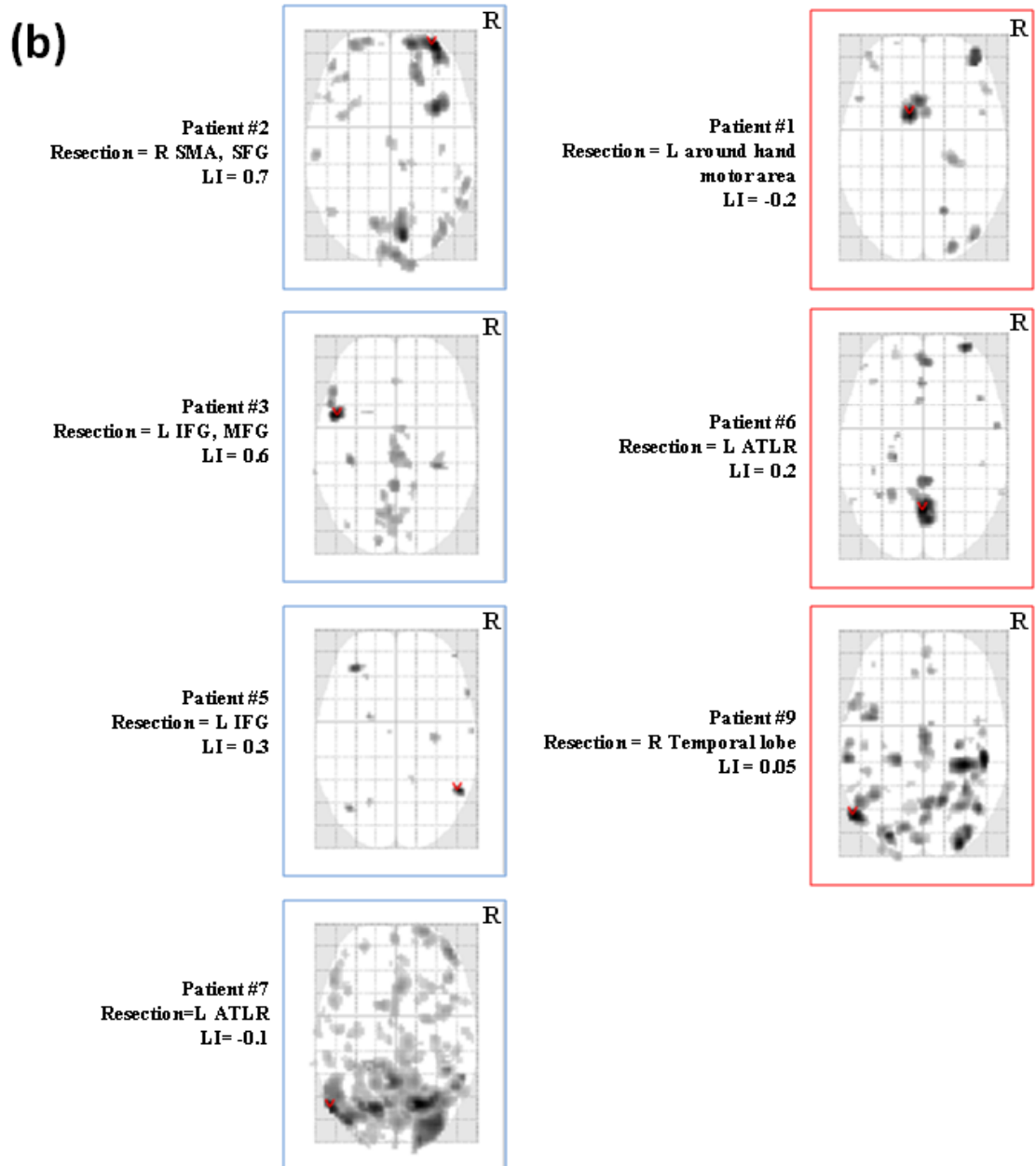


**Figure 9.5: contd.**

(b) SPM[F] maps ( $p < 0.001$ ) for *all interictal* at global level overlaid on glass brain for each patient undergoing surgery to demonstrate the lateralization of BOLD changes. Cross hair (<) is fixed on GM BOLD cluster.



#### 9.4 Discussion

In this work, I demonstrated that icEEG-fMRI can map haemodynamic changes locally within a VOI and across whole brain for very focal IEDs on icEEG. The main findings are:

- At the network level, individual IED related BOLD maps had a degree of concordance with the IZ for 13/38 IED types.
- In patients with good postsurgical outcome, BOLD maps predominantly had a degree of concordance with the IZ for different IED types in a given patient, and the GM / other BOLD cluster for individual IED type was within 2cm of the IZ (Figures 9.2 and 9.3).
- In patients with good postsurgical outcome, ‘*combined interictal BOLD maps*’ revealed changes lateralized to the hemisphere ipsilateral to the IZ, and the GM / other BOLD clusters were within the resection cavity or at resection margin (Figures 9.4 and 9.5).

These results suggest that icEEG-fMRI can be a useful tool for mapping epileptic networks and may have a role in predicting postsurgical outcome in patients undergoing icEEG recordings.

IED related BOLD changes concordant with the IZ in patients undergoing presurgical evaluation have been revealed using scalp EEG-fMRI previously [Al-Asmi *et al.* 2003; Zijlmans *et al.* 2007; Tyvaert *et al.* 2008]. There are only a few studies comparing the localisation of BOLD changes with postsurgical outcome [Thornton *et al.* 2010a; Thornton *et al.* 2011]. In addition, there is only one study [Vulliemoz *et al.* 2011] using icEEG-fMRI for localising IED related BOLD changes. In this study, I compared the localisation of BOLD changes for different types of focal IEDs on icEEG with the IZ at two levels across whole brain i.e., for individual IED type and combined all interictal activity. The localisation of BOLD changes was also compared with the resection margins and postsurgical outcome, and LI was calculated to assess the predictive value of the technique.

### 9.4.1 Methodological considerations

Simultaneous icEEG-fMRI is a new method and its feasibility and safety has been established [Carmichael *et al.* 2010;Vulliemoz *et al.* 2011;Carmichael *et al.* 2012] provided a well tested protocol is strictly observed. Signal degradation is observed within 1cm of the electrode contacts and is orientation dependent [Deichmann *et al.* 2002;Carmichael *et al.* 2012]. However, BOLD effects are generally more widespread [Carmichael *et al.* 2012]. IED related BOLD changes within a VOI of 2cm radius around the electrode contact recording IED were seen in all patients within a median distance of 1.6cm (95%CI: 1.4-1.7) in accordance with [Carmichael *et al.* 2012]. This is in line with the findings that macro intracranial electrodes can record electric signal within a distance of about 1-1.4cm [Lachaux *et al.* 2003].

IEDs were represented as single or series of events in separate regressors for each IED type to evaluate specific BOLD pattern in a GLM framework [Hamandi *et al.* 2006;Salek-Haddadi *et al.* 2006;Tyvaert *et al.* 2008;Thornton *et al.* 2011;Vulliemoz *et al.* 2011] using canonical HRF and its derivatives as a haemodynamic kernel [Friston *et al.* 1995b] to account for a degree of variability in BOLD timing and shape [Salek-Haddadi *et al.* 2006;Thornton *et al.* 2010a]. One limitation of this study is that BOLD changes around the electrode contacts were not revealed, at whole brain level, for very frequent continuous IEDs (~600 to 900 spike and wave discharges/10minutes; Patient #1(IED #2), 4(IED #1), 5(IED #1), 7(IED #1); Table 9.2). This might be because of the absence of a rest period in between IEDs, making it an inefficient experimental design for very frequent events.

The level of concordance of BOLD changes with the IZ was assessed using a scheme implemented previously [Thornton *et al.* 2010a;Thornton *et al.* 2011;Grouiller *et al.* 2011;Chaudhary *et al.* 2012a] as discussed in Chapter 7, section 7.4.1. Thus, I interpreted complex BOLD maps for clinical purposes to find out if there is one area or a network [Bartolomei *et al.* 2001;Spencer 2002] responsible for epileptogenicity as reflected by IED related BOLD changes. The distance was measured between the GM / other BOLD cluster nearest to the IZ and the IZ / resection margin. BOLD changes were considered concordant when

they were within 2cm of the IZ / resection margin in the same lobe and gyrus taking into account implantation and co-registration related brain shift [Nimsky *et al.* 2000] and neurovascular coupling effects [Disbrow *et al.* 2000].

The distribution of BOLD changes for combined all IEDs was quantified by calculating LI [Wilke and Lidzba 2007] and compared with postsurgical outcome. LI is an established tool to assess language and memory lateralization pre and post-operatively [Bonelli *et al.* 2011; Bonelli *et al.* 2012]. The statistical significance of BOLD changes was assessed at thresholds corrected and also uncorrected for FWE. Confounding factors such as motion were modelled in the design matrix to regress out their influence on the BOLD results [Friston *et al.* 1995b; Friston *et al.* 1996]. Pulse related artefact did not affect IED identification on icEEG [Vulliemoz *et al.* 2011; Carmichael *et al.* 2012] and was not included in the design matrix as were included in the models in Chapters 6, 7 and 8 to maintain sufficient number of degrees of freedom [Friston *et al.* 1995b].

#### 9.4.2 Neurobiological significance

These findings provide further evidence to the findings demonstrated by recent scalp EEG-fMRI [Thornton *et al.* 2011] and icEEG [Bartolomei *et al.* 2001; Spencer 2002] studies that an underlying network may be responsible for epileptogenicity. In consensus with this hypothesis, IED related BOLD networks were observed involving the areas which were within the area resected as well as in the adjacent and remote healthy cortex. I suggest that BOLD changes in the areas remote from the resection margin but concordant with secondary IZs may represent the propagated activity in agreement with scalp EEG-fMRI [Thornton *et al.* 2011] and electric source imaging studies [Vulliemoz *et al.* 2010]. It is difficult to ascertain whether the whole epileptic network or a principal node of the network (single focus) define epileptogenicity in a given scenario especially with the level of evidence and understanding currently available. Further studies comparing BOLD networks with postsurgical outcome, using icEEG-fMRI, may provide further evidence.

IED related BOLD changes were also seen in the resting state network such as DMN [Raichle *et al.* 2001; Laufs *et al.* 2007b] reflecting that it may be associated with awareness at some level. I will present my work on the effect of the presence

of generalized spike wave discharges on the functional networks during performance of a working memory task in the next chapter.

I found predominant BOLD increases in the IZ and decreases in the DMN in accordance with previous scalp EEG-fMRI studies [Tyvaert *et al.* 2008;Vulliemoz *et al.* 2009;Thornton *et al.* 2011;Chaudhary *et al.* 2012a]. It can be suggested that the sustained BOLD decreases as seen in this work in some patients may reflect neuronal inhibition [Shmuel *et al.* 2006;Logothetis 2008] or demand and perfusion mismatch [Raichle *et al.* 2001;Zhao *et al.* 2009]

### 9.4.3 Clinical significance

These results demonstrate a very high yield of icEEG-fMRI (~100%) as compared to scalp EEG-fMRI (30-70%) [Salek-Haddadi *et al.* 2006;Thornton *et al.* 2011;Grouiller *et al.* 2011]. All nine patients had IEDs and associated statistically significant BOLD changes with a degree of concordance with the IZ in 6/9 patients during icEEG-fMRI. In comparison, scalp EEG-fMRI results (see Appendix 3) for these patients showed that 4/8 patients had IEDs and BOLD maps had a degree of concordance with the IZ in 3/8 patients. This high yield of icEEG-fMRI is because of high sensitivity, specificity and spatial resolution of icEEG as compared to scalp EEG to detect and localise IEDs [Luders *et al.* 2006]. IEDs were classified according to their spatiotemporal and amplitude distribution [Luders *et al.* 2000] which might not be the optimal model for detecting BOLD changes but aids interpretation.

In patients with one focal SOZ there may be more than one type of IED reflecting different IZs and not all of these require removal for good surgical outcome [Luders *et al.* 2006]. Therefore, I compared the localisation of IED related BOLD changes with the IZ and resection margins rather the SOZ.

These findings suggest that icEEG-fMRI may have a clinical role in predicting the postsurgical outcome in patients undergoing invasive evaluation because IED related BOLD maps for different IED types in a given patient with good outcome had a degree of concordance with the IZ (except patient #7) and GM / other BOLD cluster was localised within 2cm of the IZ (Figures 9.2 and 9.3). Similarly, 'combined interictal BOLD maps' for patients with good postsurgical outcome showed GM / other BOLD cluster within the resected area or at resection margin (Figure 9.4; Table 9.3), and the maps lateralized (Figure 9.5) to the hemisphere

ipsilateral to the IZ. In comparison, patients with poor outcome had BOLD maps discordant with the IZ for different IED types, and '*combined interictal BOLD maps*' were non-lateralizing. Moreover, the GM / other cluster nearest to the IZ in BOLD map for individual IED type as well as in '*combined interictal BOLD maps*' was located at a distance of more than 2cm from the IZ and resection margin. My findings in this group using icEEG-fMRI further corroborate the previous findings with scalp EEG-fMRI in patients with focal cortical dysplasia [Thornton *et al.* 2011] and with electrocorticography in patients with intractable FLE [Wennberg *et al.* 1999] that IED related BOLD changes distributed across both hemisphere and epileptic activity distant from the resection margin respectively are associated with poor outcome.

In this work, IED related BOLD changes were seen in a network distribution consistent with the epileptic network hypothesis [Bartolomei *et al.* 2001; Spencer 2002]. It may be suggested that the resection of the GM / other cluster within 1-2cm of the IZ for individual IED type and combined all interictal activity may disconnect the underlying epileptic network [Bartolomei *et al.* 2001; Spencer 2002] resulting in good postsurgical outcome specially when '*combined interictal BOLD maps*' also lateralize to the hemisphere ipsilateral to the IZ.

Patients #7 who had good outcome but discordant and non-lateralizing BOLD maps had clinical seizures from left temporal lobe and subclinical seizures from right temporal lobe. IEDs and associated BOLD changes were seen in both temporal lobes. The patient remains seizure free postsurgically after left temporal lobectomy. BOLD maps for IEDs from left temporal lobe revealed BOLD changes in distributed network across both hemisphere but lateralized to left side and IEDs from right temporal lobe revealed BOLD changes only in right temporal lobe.

Other non-invasive techniques including, scalp EEG-fMRI [Tyvaert *et al.* 2008; Thornton *et al.* 2011] PET and MEG [Knowlton 2006] may have a role in the presurgical evaluation. It is suggested that icEEG-fMRI is superior specifically in patients undergoing invasive evaluation. It provides a direct comparison of the epileptic activity from very limited sources up to sub-gyral level on icEEG, 'gold standard' with the localisation of IED related BOLD network in individual patients at whole brain level suggesting that it may circumvent the limited spatial sampling of icEEG [Rosenow and Luders 2001].

Alternatively, indirect comparison e.g., BOLD networks from scalp EEG-fMRI with the gold standard may be influenced by drug reductions, recent anaesthesia etc. during invasive evaluation.

The number of patients being suitable for this type of investigation will be limited to those undergoing invasive evaluation and its true value may be to better predict patients who are likely to have a poor surgical outcome. If IEDs are associated with non-lateralizing and discordant BOLD maps these results suggest that a poor outcome is likely.

### **9.5 Conclusion**

Simultaneous icEEG-fMRI is a new investigation technique which can address the limited spatial sampling of icEEG during invasive evaluation of patients undergoing epilepsy surgery. It can lateralize and localise BOLD changes for very focal interictal discharges on icEEG in a limited number of patients undergoing invasive evaluation and may predict surgical outcome, suggesting that the test may have clinical utility in future.

## Chapter 10: Imaging the interaction: epileptic discharges, working memory and behaviour<sup>8</sup>

### 10.1 Background

The effect of interictal epileptic discharges on cognitive function remains controversial [Aldenkamp *et al.* 1996; Aldenkamp *et al.* 2005]. An impairment of cognitive function during epileptic discharges was described in 1939 [Schwab RS 1939]. Whilst both, generalized and focal discharges were found to impair cognition in up to 50% of patients [Aarts *et al.* 1984; Binnie *et al.* 1987; Shewmon and Erwin 1988; Rugland 1990], the mechanism by which short lasting interictal epileptic discharges affect cognition remains unknown [Binnie 2003]. The nature of the cognitive task is key, as complex tasks with increasing difficulty such as working memory tasks are more sensitive for detecting cognitive impairment than less demanding tasks [Hutt and Gilbert 1980; Aarts *et al.* 1984; Binnie *et al.* 1987].

Neuropsychological studies indicate that interictal epileptic discharges and cognition have a complex bidirectional relationship: cognitive tasks may suppress interictal epileptic discharges, but also may increase their rate with increasing task difficulty [TIZARD and MARGERISON 1963; Binnie *et al.* 1987; Binnie 2003]; thus facilitate the detection of cognitive impairment associated with interictal epileptic discharges.

Recent functional imaging studies investigating the brain structures involved in the interaction between generalized spike wave discharges (GSWDs) and task performance used simple reaction time tasks under continuous attention [Bai *et al.* 2010; Berman *et al.* 2010; Moeller *et al.* 2010b]. I hypothesized that GSWDs during the task may affect well established working memory related activations in prefrontal cortex. I tested this hypothesis by using a spatial working memory task and assessing for regionally specific interactions between GSWDs and working memory task related haemodynamic responses using vEEG-fMRI.

---

<sup>8</sup> This chapter forms the basis of the article [Chaudhary *et al.* 2012c].

## 10.2 Methods

The common methods are described in Chapter 4, and the specific methods for this study are described here.

### 10.2.1 Subjects

I studied eight patients with IGE performing a spatial working memory task using vEEG-fMRI. One patient, a 39 year old, right handed woman (IGE subtype: childhood absence epilepsy) had GSWDs during the performance of spatial working memory task and is presented here.

Birth and early development were normal and there were no learning disabilities. The seizure onset was at age 7 years with typical absences and generalized tonic clonic seizures. Neurological examination and high resolution structural imaging were normal. Repeat long-term video-EEG monitoring had shown frequent bilaterally synchronous 2.5-3Hz GSWDs with anterior predominance lasting 1 to 3sec. The discharges were more marked with stressful conditions and lack of sleep and were not increased with hyperventilation. The discharges associated with unresponsiveness were accurately recalled by the patient. Several anti-epileptic medications including Valproate, Carbamazepine, Ethosuximide, Lamotrigine, Clobazam, Phenytoin, Topiramate and Clonazepam had been tried without any significant improvement to control absences. Written informed consent was obtained and the study was approved by the local hospital research ethics committee.

### 10.2.2 MRI acquisition and working memory task

An EPI sequence was used to acquire 240 BOLD sensitive scans. During scanning, the patient performed a continuously updating parametric spatial working memory task of the n-back type with three levels of working memory load: 0-back, 1-back and 2-back (Vollmar et al., 2011). During the task dots randomly appeared in one of the four corners of a diamond shaped box and the patient had to move a joystick with her right hand to the position of the dot. Each dot was displayed for 2sec in one position. The patient was instructed to move the joystick to the position of the current dot in the 0-back condition; to the position of the previous dot in 1-back condition; and to the position of the dot two presentations earlier in the 2-back condition. Performance parameters ('correct', 'wrong' and 'no' responses derived from the movement of joystick) during the



task were recorded simultaneously. Each of the three active conditions: 0-back, 1-back and 2-back lasted 30sec and was repeated five times ( $30 \times 5 = 150$  sec) in a pseudo-random order alternating with a 15sec rest condition consisting of a static display of all four dots. The total duration of the task inside the scanner was twelve minutes and the patient underwent task familiarization before scanning.

### **10.2.3 Video-EEG recording and artefact correction**

Video-EEG recording was performed during the MRI scanning. The details of video-EEG recording and removal of pulse and scanner artefact are described in Chapter 4, Section 4.3.

### **10.2.4 Data processing and analysis**

#### **10.2.4a EEG and fMRI processing**

The 2.5-3Hz GSWDs identified on inside scanner EEG were identical with the GSWDs during long-term video-EEG monitoring. All GSWDs identified on EEG recorded inside the scanner were used for further fMRI analysis. All fMRI data was pre-processed (realigned, normalized to Montreal Neurological Institute (MNI) space and smoothed) and analysed using SPM8 ([www.fil.ion.ucl.ac.uk/spm](http://www.fil.ion.ucl.ac.uk/spm)).

#### **10.2.4b fMRI modelling**

A GLM was specified based on factorial design: task x GSWDs (Factor 1 = Task with 4 levels: rest, 0-back, 1-back, 2-back, and Factor 2 = GSWDs with 2 levels: presence, absence). As a result the GLM had eight regressors of interest (Figure 10.1): rest with GSWDs, 0-back with GSWDs, 1-back with GSWDs, 2-back with GSWDs, rest without GSWDs, 0-back without GSWDs, 1-back without GSWDs, 2-back without GSWDs. GSWDs and stimulus presentation (for 0-back, 1-back and 2-back) were represented as “0” duration stick functions and convolved with canonical HRF [Friston *et al.* 1995b; Price *et al.* 1997]. The six realignment parameters from image pre-processing were included in the GLM as covariates of no interest [Friston *et al.* 1995b], explaining head movement related MR signal variance.

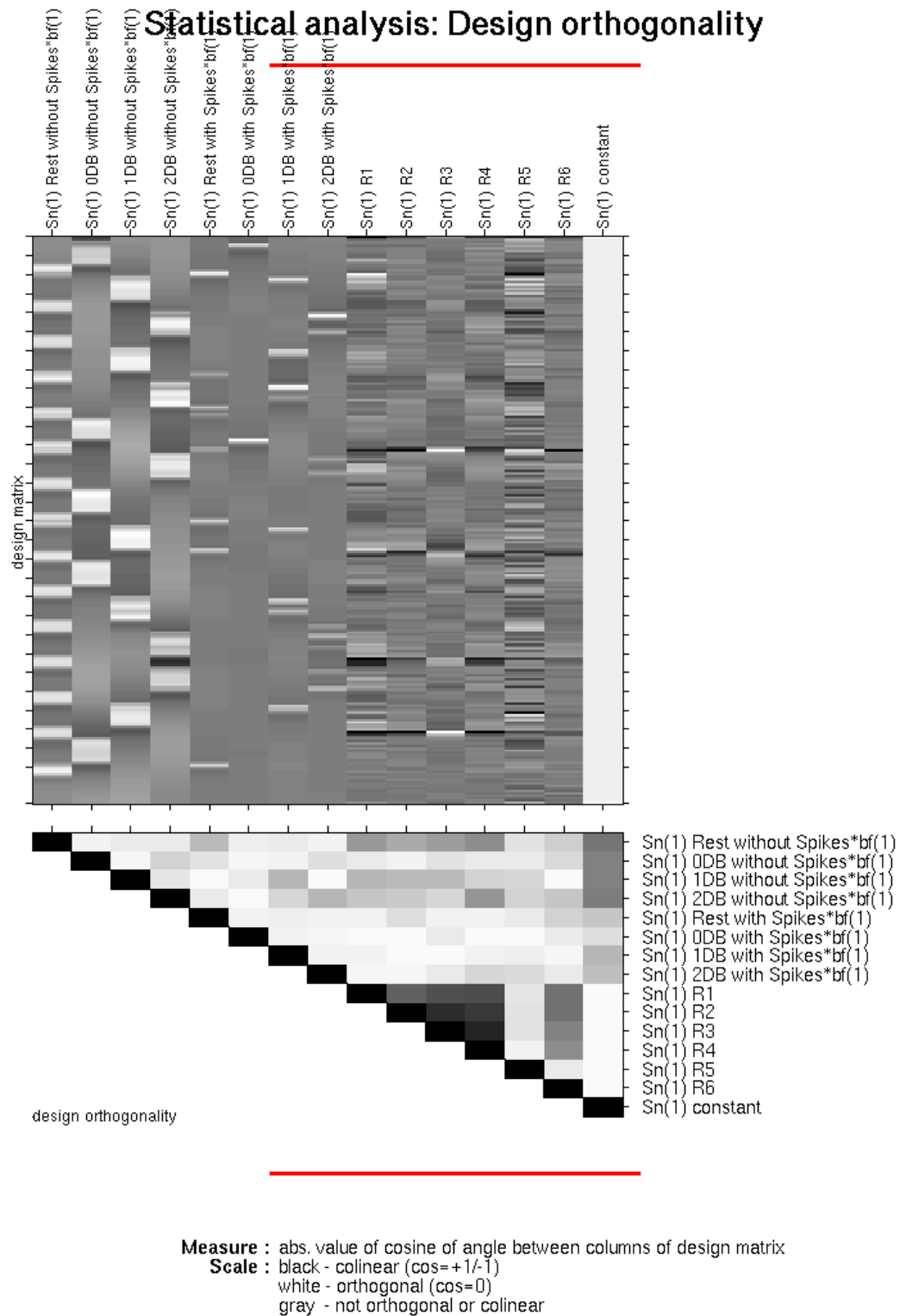


**Figure 10.1: Design matrix**

### 10.2.5 Assessment of BOLD changes, significance and visualization

The SPM contrasts were defined for the ‘task’: by including the memory load (1-back and 2-back) and the control task (0-back, as it does not have a memory load and represents only motor-related changes); and for the working memory (excluding motor related changes): ‘WM’: by comparing task with memory load (1-back and 2-back) against the control task (0-back) [Vollmar *et al.* 2011]. Statistical parametric maps of the  $F$  statistic were computed to test for the (simple) main effects of: GSWDs (during rest and task) showing GSWDs related BOLD changes; and task (with and without GSWDs) showing BOLD responses in task sensitive brain regions. SPMs testing for main effect of the task were used as an inclusive mask in SPM contrast building to restrict the search for regions showing an effect (SPMs of the  $t$ -statistics) of:

- task-with-GSWDs
- task-without-GSWDs
- WM-with-GSWDs
- WM-without-GSWDs

and the following interactions:

- task-level (task-without-GSWDs > task-with-GSWDs)
- WM-level (WM-without-GSWDs > WM-with-GSWDs)

SPMs were threshold at  $p < 0.05$  (FWE corrected) to test for the main effects of GSWDs and task (with and without GSWDs), and also for  $p < 0.001$  (uncorrected for FWE). The effects: task-with-GSWDs, task-without-GSWDs, WM-with-GSWDs, WM-without-GSWDs and the following interactions: task-level (task-without-GSWDs > task-with-GSWDs) and WM-level (WM-without-GSWDs > WM-with-GSWDs) were tested at a significance of  $p < 0.001$  (uncorrected) within the task-sensitive brain regions (as described above). The results were overlaid on a 3D-rendered normalized brain in MNI space. I confirmed the location of visually identified BOLD clusters using automated anatomical labelling (AAL) atlas in SPM tool box: xjView.

### 10.2.6 Statistical analysis

For the purpose of statistical analysis each 2sec (time for the display of dot at one position) was counted as one event. The numbers of GSWDs and performance parameters (correct responses and wrong/no responses) during different task

phases were compared using chi-squared tests in the statistical package Stata/IC 11.1 (StataCorp LP).

### 10.3 Results

The patient had 52 GSWDs lasting 0.2-2sec (mode:0.3, standard error:  $\pm 0.05$ ) during vEEG-fMRI recording session. The number of GSWDs was significantly different (*chi-squared test, p-value*  $< 0.001$ ) during the task (43/225 observations) and rest conditions (9/135 observations) and increased with increasing complexity of the task (*chi-squared test for trend: Z* = 4.25, *p*  $< 0.001$ ) (Figure 10.2). Furthermore, correct responses were significantly different for 2-back (9/75) than 1-back (22/75) than 0-back (58/75) and decreased with increasing complexity of the task (*chi-squared test for trend: Z* = 7.56, *p*  $< 0.001$ ) (Figure 10.2). I did not find a significant association between presence of GSWDs and the performance parameters i.e., correct and wrong responses in either of the active task conditions (0-back, 1-back, 2-back) at the time of stimulus presentation or at the time of actual response corrected for delay in 1-back and 2-back.

The GSWDs recorded during the task and rest conditions were similar (Figure 10.3) to the discharges recorded during standard EEG. The main effect of GSWDs revealed significant BOLD decreases in the precuneus and lateral parietal and frontal lobes (Figure 10.4).

The main effect of task irrespective of the presence of GSWDs showed significant BOLD changes in task sensitive areas: bilateral middle and inferior frontal gyrus, bilateral pre and post-central gyrus, bilateral parietal lobe, precuneus, paracentral lobule, supplementary motor area (SMA), medial superior frontal gyrus, thalamus and occipital lobe (Figure 10.4).

Task related effects in the absence of GSWDs (task-without-GSWDs) showed significant BOLD increases in the pre and post-central gyri bilaterally extending into the middle and inferior frontal gyri, superior parietal lobes, thalamus, SMA and cerebellum, with BOLD decreases in the precuneus, lateral parietal, frontal and medial frontal lobes, and right pre-central gyrus (Figure 10.5.a.i). For the task related effects during GSWDs (task-with-GSWDs), BOLD increases were observed only in the left pre-central gyrus, and bilateral superior parietal lobes, and BOLD decreases in precuneus, left lateral parietal and frontal lobes, and right pre-central gyrus (Figure 10.5.a.ii).

The effect of WM-without-GSWDs revealed significant BOLD increases in a fronto-parieto-striato-thalamo-cerebellar network: bilateral middle and inferior frontal gyri extending into pre and post-central gyri, SMA, superior parietal lobes, superior temporal gyrus, occipital lobes, caudate, globus palladium, thalamus and cerebellum, and BOLD decreases in the default mode network (DMN) related areas: precuneus, lateral parietal and medial frontal lobes (Figure 10.5.b.i). For the WM-related effects during GSWDs, smaller clusters of BOLD increases were observed only in the occipital lobes, SMA, parieto-temporo-occipital junction, bilateral pre/post-central gyrus, thalamus, left inferior frontal gyrus and cerebellum; other smaller clusters of BOLD decreases were seen in the frontal and parietal lobes (Figure 10.5.b.ii).

The interaction between the task and GSWDs (task-without-GSWDs > task-with-GSWDs; Figure 10.5.c) revealed activation differences in areas including: bilateral inferior frontal gyri extending into the pre and post-central gyri. I also plotted the time course of the BOLD signal change for the global statistical maximum cluster in the contrast task-without-GSWDs > task-with-GSWDs (Figure 10.5.c.i, crosshair shows the global statistical maximum cluster). I found greater BOLD changes for task-without-GSWDs than task-with-GSWDs reflecting that these areas were active during different phases of the task (0-back, 1-back, 2-back) without GSWDs and deactivated for task-with-GSWDs as shown in Figure 10.6. There were no greater BOLD decreases for task-without-GSWDs than task-with-GSWDs.

The interaction between WM and GSWDs showed greater BOLD increases in right inferior and middle frontal gyri and bilateral parietal lobes for WM-without-GSWDs than WM-with-GSWDs.

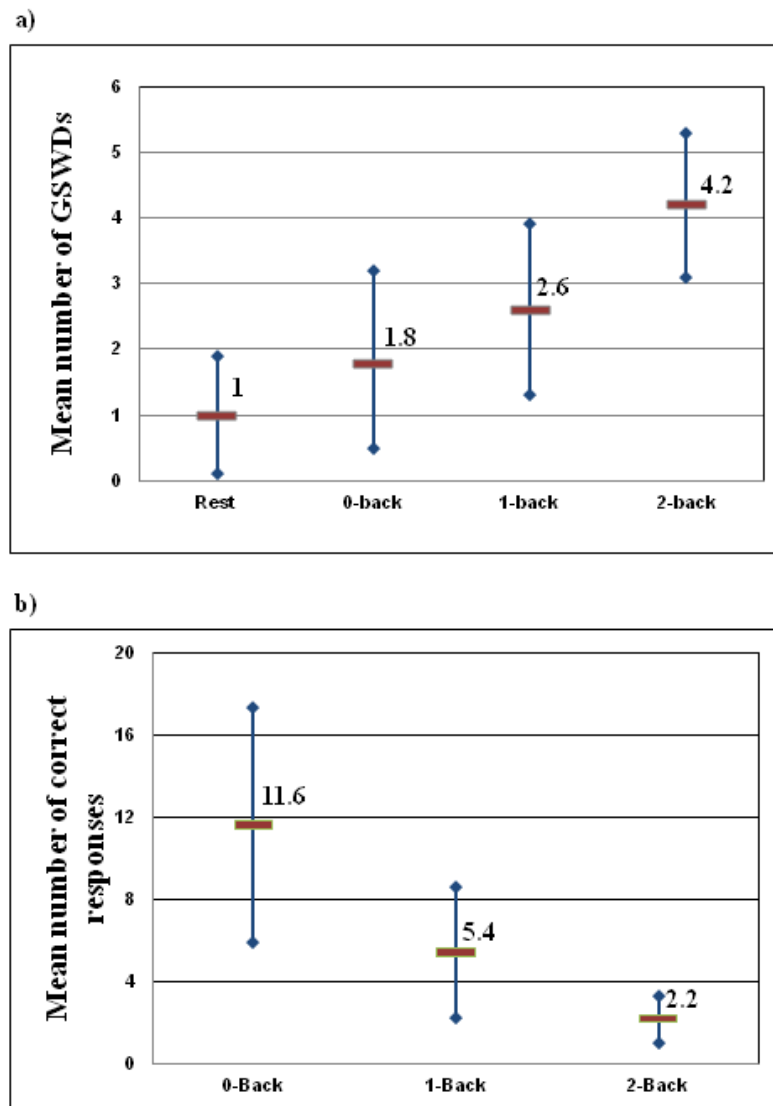


**Figure 10.2: Dot chart showing number of GSWDs and responses**

(a) Mean number of GSWDs with 95% confidence intervals ( $\text{Mean} \pm 1.96 \cdot (\text{Standard Deviation} / \sqrt{n})$ ) during each 30 sec block of active conditions (0-back (total duration = 150 sec), 1-back (total duration = 150 sec), 2-back (total duration = 150 sec)) and 15 sec block of rest (total duration = 270 sec). The GSWDs increased from rest to 0-back to 1-back to 2-back which was statistically significantly (Chi-squared test for trend:  $Z=4.25$ ,  $p < 0.001$ ). (b) Mean number of correct responses with 95% confidence intervals ( $\text{Mean} \pm 1.96 \cdot (\text{Standard Deviation} / \sqrt{n})$ ) during each 30 sec block of active conditions (0-back (total duration = 150 sec), 1-back (total duration = 150 sec), 2-back (total duration = 150 sec)). The correct responses decreased linearly with increasing task complexity from 0-back to 1-back to 2-back (Chi-squared test for trend:  $Z=7.56$ ,  $p < 0.001$ ).

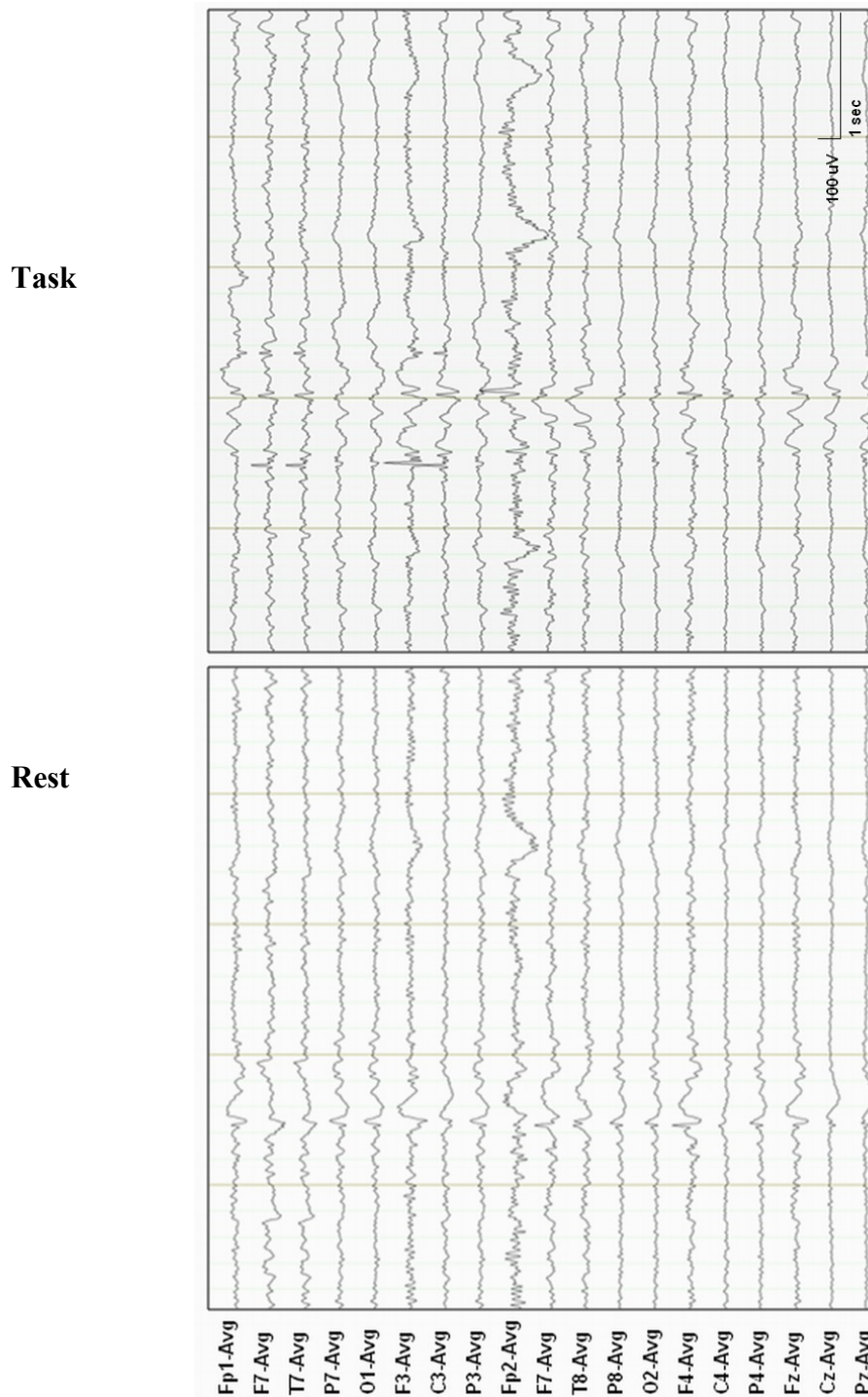


**Figure 10.3: Representative sample of EEG**

EEG during rest and task periods. 2.5-3Hz GSWDs during 270s of rest (N=9) and 450s (N=43) of task lasting 0.2 to 2 seconds were counted, which were significantly higher during the task (Chi-squared test,  $p = 0.001$ ).

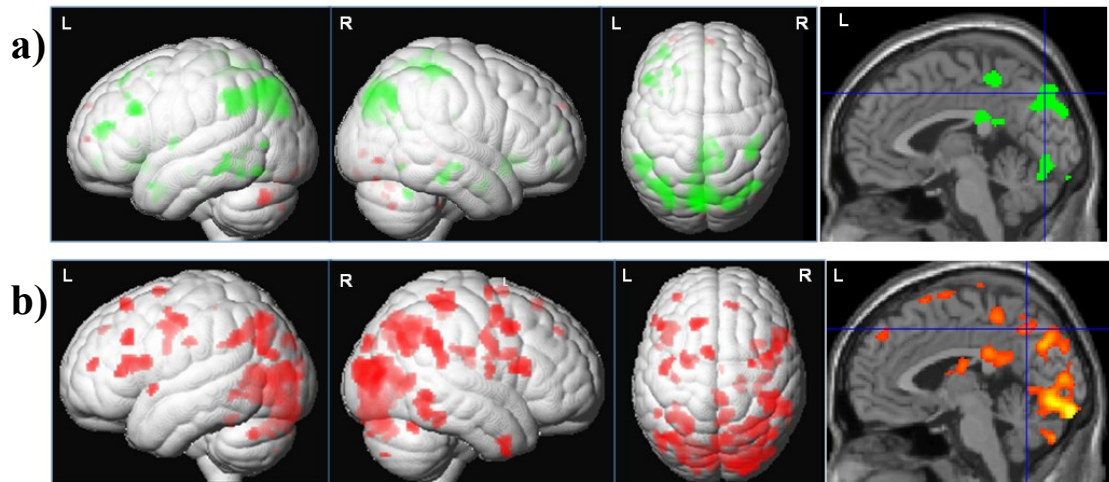


**Figure 10.4: BOLD changes for GSWDs and task**

(a) Main effect of GSWDs: SPM of  $F$ -statistics ( $p < 0.001$ ) overlaid on a 3D-rendered normalized brain in MNI space. GSWDs during rest and task were associated with BOLD decreases (green clusters) in precuneus (left sagittal medial surface view), lateral parietal lobes, lateral and basal frontal lobes and small clusters of BOLD increases (red clusters) in frontal and parietal lobe and cerebellum. The crosshair in the medial surface view showing BOLD changes in precuneus. (b) Main effect of task (memory load (1-back and 2-back) and control condition (0-back)) irrespective of GSWDs: SPM of  $F$ -statistics ( $p < 0.001$ ) overlaid on a 3D-rendered normalized brain in MNI space. Significant BOLD changes were seen in bilateral middle and inferior frontal gyrus, bilateral pre and post-central gyrus, bilateral lateral parietal lobe, precuneus, paracentral lobule, supplementary motor area, medial superior frontal gyrus, thalamus and occipital lobe (left sagittal medial surface view). The crosshair in the medial surface view showing BOLD changes in precuneus.



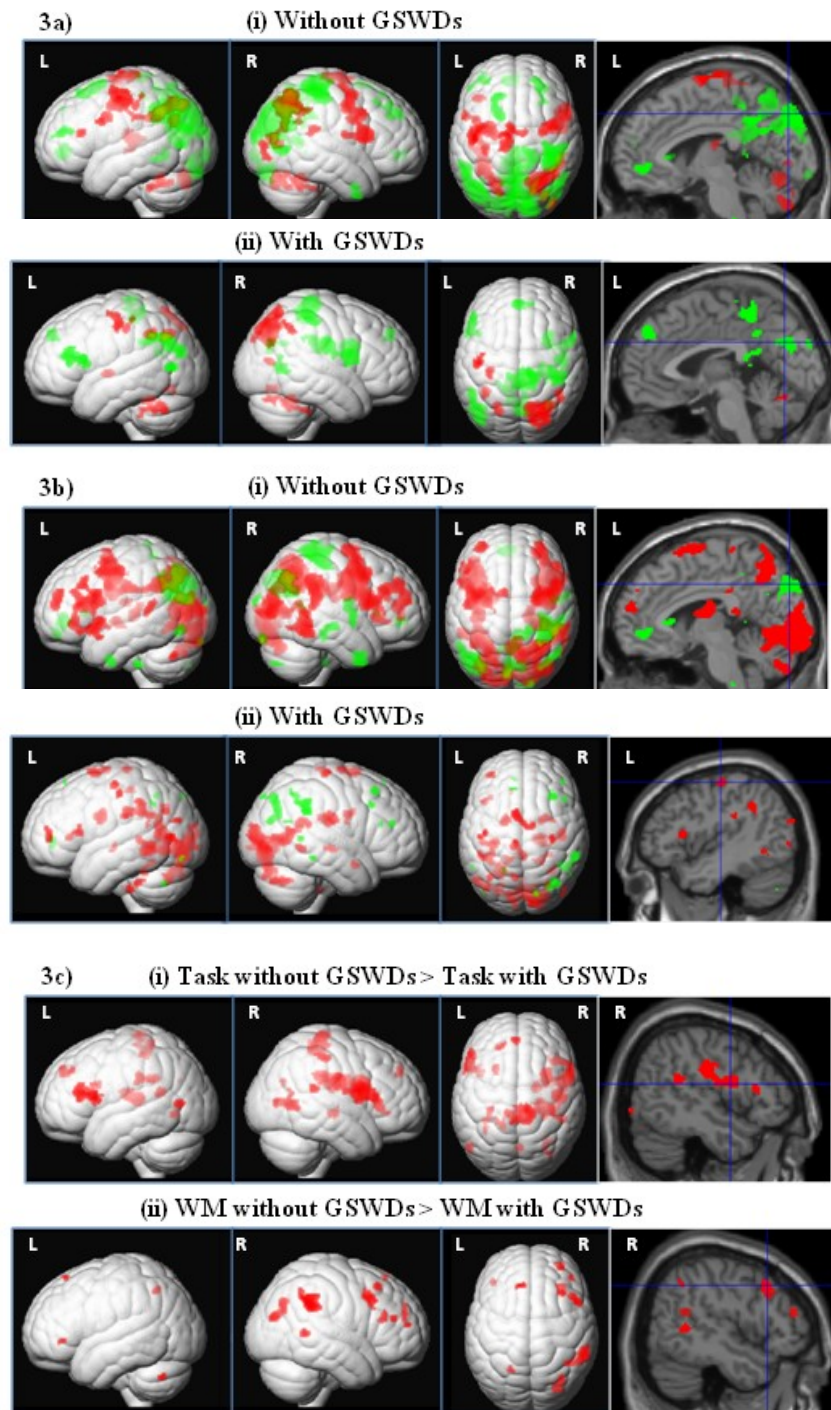


**Figure 10.5: Working memory related BOLD changes with/without GSWDs**  
 SPMs of  $T$ -statistics ( $p < 0.001$ ) masked by main effect of task and overlaid on 3D-rendered normalized brain in MNI space. Red clusters represent BOLD increases and green clusters represent BOLD decreases.

(a.i) Task-without-GSWDs showed BOLD increased in bilateral pre and post-central gyri extending into middle and inferior frontal gyri, superior parietal lobes, thalamus, supplementary motor area and cerebellum. BOLD decreases involved precuneus, lateral parietal and frontal and medial frontal lobes, and right pre-

central gyrus. Left sagittal medial surface view showing BOLD changes in the midline structures (crosshair: precuneus). (a.ii) BOLD increases for the task-with-GSWDs were seen in left pre-central gyrus, and bilateral superior parietal lobes, and BOLD decreases in precuneus, left lateral parietal and frontal lobes, and right pre-central gyrus. Left sagittal medial surface view showing BOLD changes in the midline structures (crosshair: precuneus).

(b.i) BOLD increases for the WM-without-GSWDs were present in bilateral middle and inferior frontal gyri, pre and post-central gyri, superior parietal lobes, superior temporal gyrus, occipital lobes, thalamus and cerebellum, and BOLD decreases in precuneus and lateral parietal and medial frontal lobes. Left sagittal medial surface view showing BOLD changes in the midline structures (crosshair: cuneus/precuneus). (b.ii) BOLD increases for the WM-with-GSWDs were observed in occipital lobes, supplementary motor area, parieto-temporo-occipital junction, left pre-central gyrus, thalamus and cerebellum, and small clusters of BOLD decreases in frontal lobes. Left sagittal view showing BOLD changes in the left hemisphere (crosshair: precentral gyrus).

(c.i) Interaction between task and GSWDs showed greater BOLD increases for the task-without-GSWDs than task-with-GSWDs in bilateral inferior frontal gyrus extending into pre and post-central gyrus. Right sagittal view showing BOLD changes in right hemisphere (crosshair: inferior frontal gyrus). (c.ii) Interaction between working memory and GSWDs, showing BOLD increases for WM-without-GSWDs more than WM-with-GSWDs in right inferior and middle frontal gyrus and bilateral parietal lobes. Right sagittal view showing BOLD changes in right hemisphere (crosshair: inferior/middle frontal gyrus).

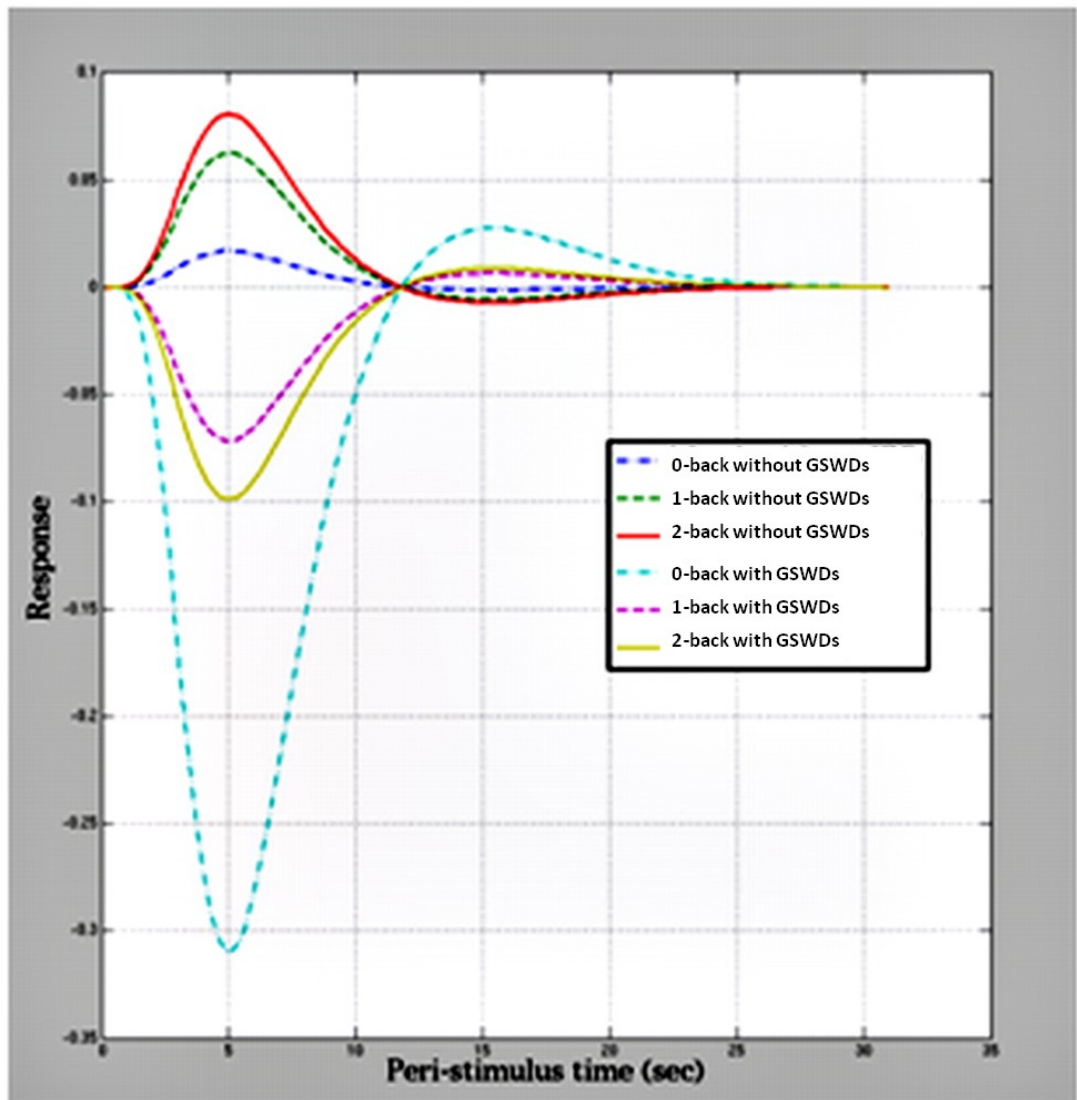


**Figure 10.6: Predicted BOLD responses**

Predicted BOLD responses based upon the maximum likelihood parameter estimates of the GLM for regions showing a significant interaction with task. These quantitative estimates demonstrate that these areas are more active during task-without-GSWDs than task-with-GSWDs.

#### 10.4 Discussion

My observations suggest a bidirectional relationship: cognitive processing of a high demanding task influences GSWDs which in turn may affect the functional networks active during working memory. This is consistent with previous reports that cognitive demand provoked GSWDs [Aarts *et al.* 1984;Binnie *et al.* 1987].

The task and working memory related frontal lobe networks were suppressed when GSWDs were present during the task, despite preserved motor performance and visual spatial processing as evident by button presses related BOLD changes in motor cortex and visual attention related BOLD changes in occipital lobes and superior parietal lobes [Owen *et al.* 2005] (Figure 10.5). During the task performance (without GSWDs), the task and working memory related network of BOLD increases was consistent with the “fronto-parieto-striato-thalamo-cerebellar network” described previously [Kumari *et al.* 2009;Takeuchi *et al.* 2011]. Similarly, during the task performance without GSWDs, the task and working memory related BOLD decreases seen in DMN related areas were also consistent with previous findings [Takeuchi *et al.* 2011].

Nonetheless, the working memory related frontal lobe network was found to be activated more strongly with the task without GSWDs, than with the task in the presence of GSWDs as shown in Figure 10.5. It is possible that the presence of GSWDs introduced increased variability in the fMRI signal causing some of the task related fMRI changes to be more difficult to detect because of their reduced amplitude relative to baseline variability, and thus failed reaching statistical significance. The parametric increase of task related BOLD response (in the absence of GSWDs) in the working memory related frontal lobe network, as shown in Figure 10.6, was similar to that observed previously [Kumari *et al.* 2009]. In addition, the presence of GSWDs during the task was associated with BOLD decreases in the same areas active for the task without GSWDs (Figure 10.6). This is in agreement with the findings that interictal discharges are associated with focal tissue hypoxia [Geneslaw *et al.* 2011], which in turn may result in poor performance for a high demanding task.

The effect of GSWDs was also consistent during rest and the task (Figure 10.7), and with the previously reported BOLD decreases in the DMN in IGE [Bai *et al.* 2010;Berman *et al.* 2010;Moeller *et al.* 2010b]. I did not observe GSWDs related BOLD signal changes in the thalamus which may be due to the relatively short

duration of the discharges in this patient (always less than 3sec). It has been observed previously that thalamic signal changes were seen in patients with discharges of longer durations [Hamandi *et al.* 2006]. The duration of GSWDs is important when investigating cognitive impairment secondary to GSWDs or seizures [Aarts *et al.* 1984]. My findings are also supported by recent studies [Bai *et al.* 2010;Berman *et al.* 2010;Moeller *et al.* 2010b] investigating the interaction between behaviour and epileptiform discharges of longer durations in IGE, using either simple motor or attention tasks. Cortico-thalamic BOLD network changes were noticed in association with behavioural interruptions, i.e. typical absence seizures [Bai *et al.* 2010;Berman *et al.* 2010;Moeller *et al.* 2010b]. In this work, I focussed on short lasting discharges without clinical change and a task with high cognitive demand. The differences in the working memory related BOLD network in the presence and absence of GSWDs are in line with the findings that functional changes underlie the impaired interictal attention [Killory *et al.* 2011].

Increased task complexity was associated with a significant increase in the number of GSWDs (Figure 10.2.a) and a significant decrease in correct responses (Figure 10.2.b) [Aarts *et al.* 1984;Binnie *et al.* 1987]. It can be argued that the level of statistical significance for correct responses would be different if the three performance parameters (wrong, correct and no response) were included separately rather combining wrong and no response as one performance parameter. I verified this by comparing the three performance parameters separately and confirmed that there was a significant decrease in correct responses (*chi-squared test for trend: Z = 2.20, p=0.03*) with increased task complexity. It is difficult to associate the presence of GSWDs with individual behavioural response categories (correct, wrong and no responses) during different task phases for the following reasons:

- 1) The complexity of the design with a continuously updating working memory task with possible interaction between GSWDs and response to a stimulus occurring 2 seconds earlier (retrieval) or later (encoding)
- 2) Limited number of discharges during each active condition of the task. Behaviourally the performance parameters were not significantly different by the occurrence of GSWDs. It is argued that for a GSWD to produce a measureable

behavioural correlate, it needs to be of certain duration (more than 3 seconds) [Aarts *et al.* 1984;Aldenkamp *et al.* 2001].

Confounding factors such as motion were included in the design matrix by modelling realignment parameters from fMRI pre-processing to regress out their influence on the BOLD results [Friston *et al.* 1995b;Friston 1996]. Pulse related artefact and Volterra-expansion of realignment parameters were not included in the design matrix as were included in the fMRI models in Chapters 6, 7 and 8 to maintain sufficient number of degrees of freedom [Friston *et al.* 1995b].

The imaging data suggests an interaction between GSWDs and the working memory related BOLD network in the presence of short lasting GSWDs, as compared to the working memory related BOLD network in the absence of GSWDs, despite there was no statistically significant association between wrong responses and the presence of short lasting GSWDs.

Designing such studies, combining three modalities (hemodynamic, electrophysiological and behavioural), is challenging and can be very demanding on patients who need to have sufficient number of GSWDs during the limited time inside the scanner when performing the task. For example, I scanned eight IGE patients with frequent GSWDs on repeat standard EEG and only the patient reported here had increased GSWDs during task performance inside the scanner. It may be possible that GSWDs were suppressed by the complexity of the task in seven patients, as suggested by other studies that increasing complexity of the task performance may also suppress the focal and generalized interictal and ictal discharges [TIZARD and MARGERISON 1963;Aarts *et al.* 1984;Binnie *et al.* 1987;Matsuoka *et al.* 2000;Binnie 2003;Berman *et al.* 2010]. However, there was no obvious cumulative effect of GSWDs on the task performance as the task related network was similar in patients with and without GSWDs (Figure 10.8).

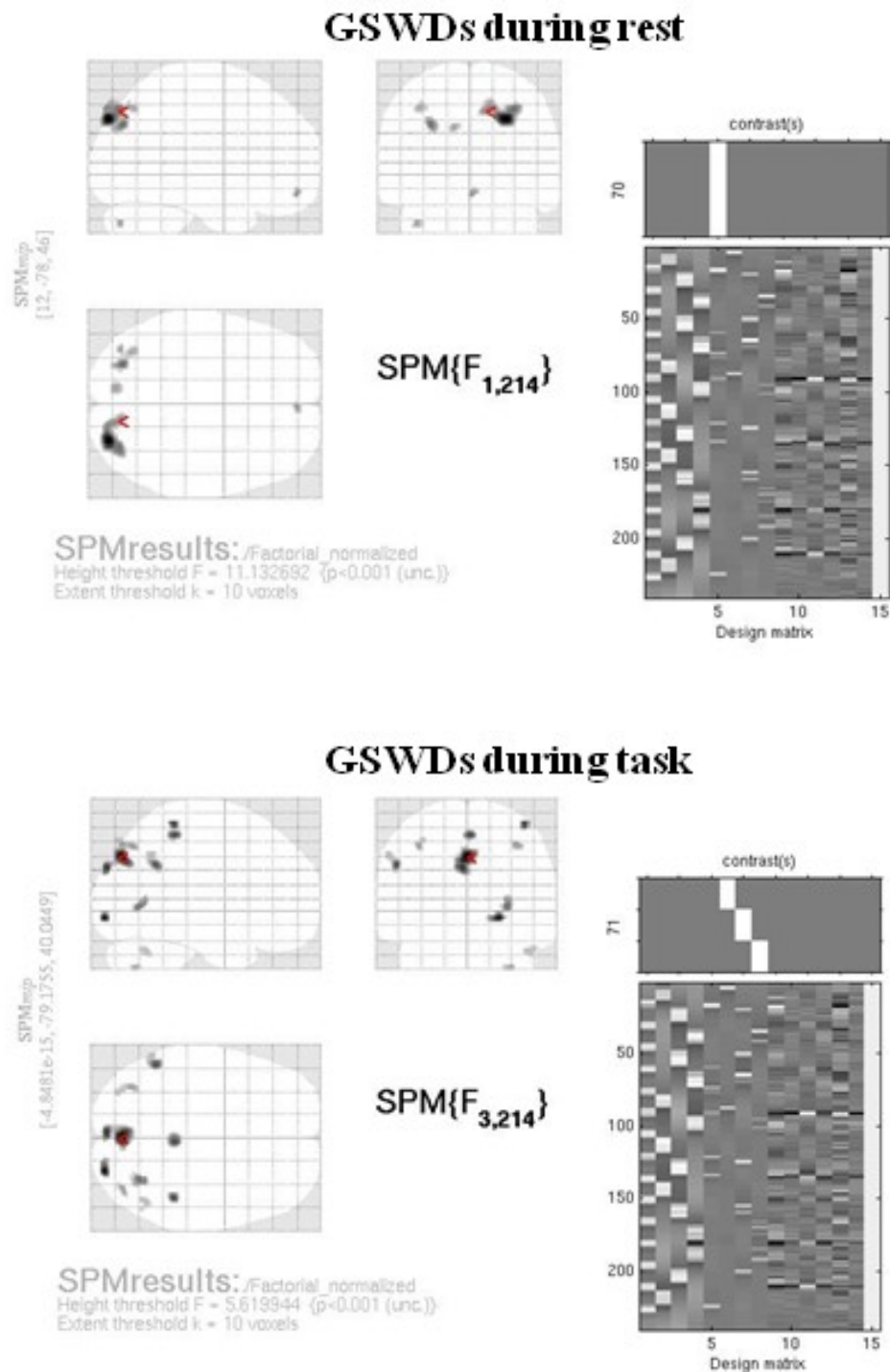


**Figure 10.7: BOLD changes for GSWDs during rest and task**

SPM of  $F$ -statistics ( $p < 0.001$ ) overlaid on glass brain normalized in MNI space. GSWDs during rest and task were associated with BOLD changes in precuneus, lateral parietal lobes and medial frontal lobes.

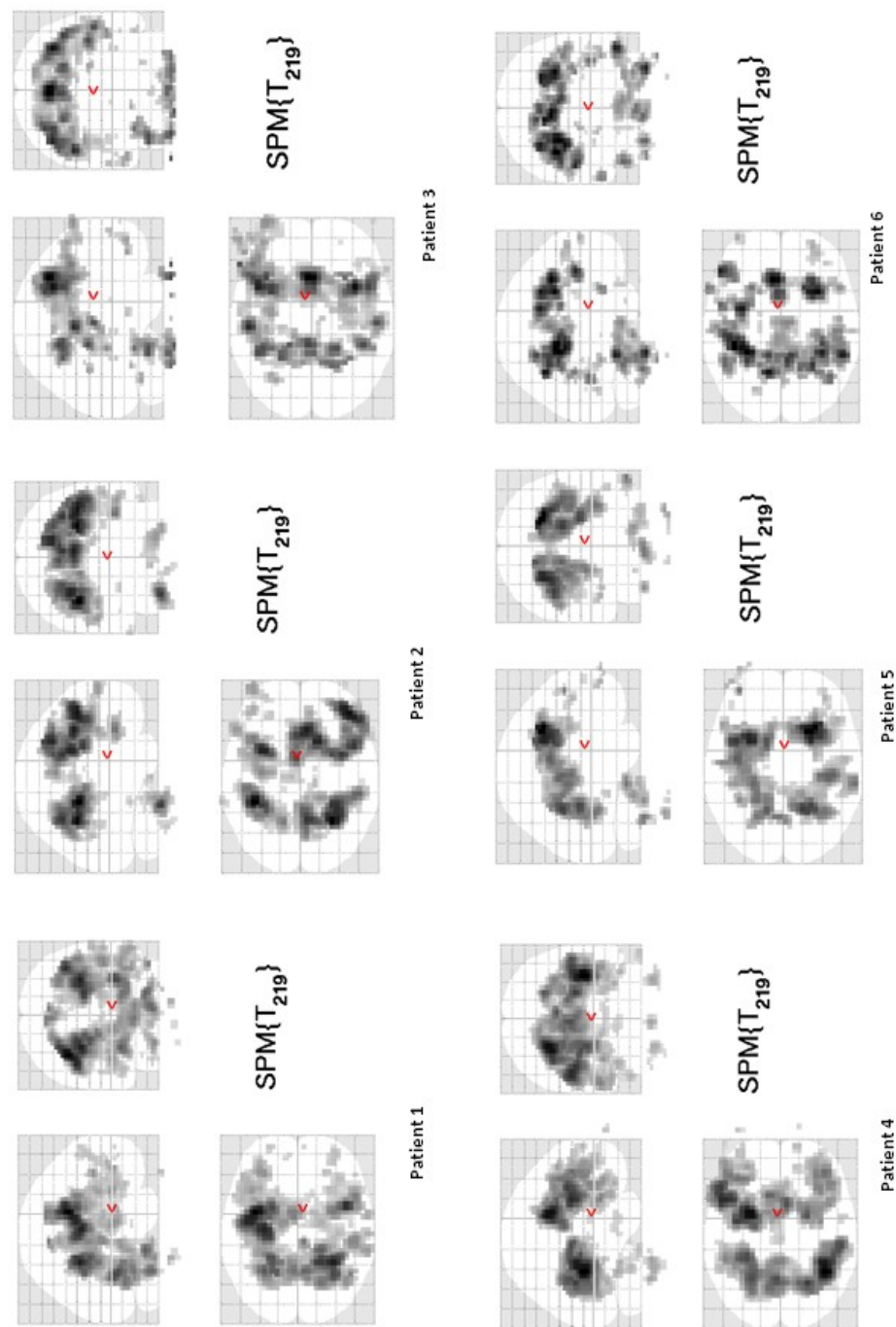


**Figure 10.8: BOLD changes for working memory task**

SPM of  $F$ -statistics ( $p < 0.001$ ) overlaid on glass brain normalized in MNI space. BOLD changes for working memory task in fronto-parieto-striato-thalamo-cerebellar network for patient 1 who had GSWDs during working memory task were similar to other patients who did not have GSWDs during working memory task.



**10.5 Conclusion**

My observations in one patient cannot be generalized, but these findings suggest that the functional networks active during a high demanding cognitive task may change in the presence of shorter lasting GSWDs, generating interesting hypotheses on how interictal discharges may affect cognition.

## SECTION 3: DISCUSSION & CONCLUSION

### Chapter 11: General discussion and future perspectives

In Chapters 5 to 10, I demonstrated the application of simultaneous vEEG-fMRI and simultaneous icEEG-fMRI in patients with focal and generalized epilepsy.

The main findings of the studies in this thesis are:

- Synchronised video recordings can be incorporated in simultaneous EEG-fMRI system without significantly compromising fMRI image and EEG quality.
- Including additional regressors for physiological activities, identified on video-EEG such as eye movements and blinks, head jerks, hand movements and swallowing, in the design matrix for fMRI data analysis can reveal additional IED related BOLD changes, thus improving the sensitivity of vEEG-fMRI studies of epileptic activity.
- Synchronised video recording during simultaneous vEEG-fMRI can be helpful in the identification and partition of seizures into phases according to the spatiotemporal evolution of ictal EEG rhythm and semiology.
- Simultaneous vEEG-fMRI can localise BOLD networks at the seizure onset with good concordance with the SOZ and can separate them from seizure propagation related BOLD networks.
- Preictal BOLD changes have a consistent pattern: BOLD decreases followed by increases, across patients prior to the seizure onset on scalp EEG and have a degree of concordance with the SOZ which is less than that at seizure onset.
- Simultaneous icEEG-fMRI can localise and lateralize IED related BOLD networks circumventing the limited spatial sampling of icEEG, and may have some ability to predict postsurgical outcome.
- The presence of GSWDs during the performance of a highly demanding working memory task may alter the working memory related frontal lobe network.

What do these findings suggest about the future role of EEG-fMRI? Here, I present my perspective on the development of EEG-fMRI in the context of my research work described in earlier chapters.

### 11.1 BOLD mapping for interictal discharges

Simultaneous scalp EEG-fMRI can map IED related BOLD changes having a degree of concordance with the IZ [Zijlmans *et al.* 2007; Tyvaert *et al.* 2008; Thornton *et al.* 2010a] and has been shown to have some predictive power in relation to postsurgical outcome in patients with FCDs [Thornton *et al.* 2011]. Dependence of the technique on EEG for recording and identifying IEDs for conventional GLM based fMRI data analysis is a major limitation towards its sensitivity, specially because sensitivity of scalp EEG to detect IEDs is low (~ 30 to 50%) [Smith 2005]. In Chapter 6, I showed that modelling of fMRI data for vEEG-fMRI studies of IEDs in individual patients can be improved by explaining more nuisance variance, which can also increase the sensitivity to some extent. In my work, the number of channels recorded inside the scanner was limited to 64, corresponding to two 32-channel amplification units. In future, the identification and labelling of physiological activities such as: eye blinks, chewing and respiration can be automated by adding extra electrodes around the eyes for electro-oculography and around the face for EMG and using respiration belt respectively; this would involve either sacrificing a number of EEG channels or increasing the total number of channels with additional amplifier cost. Moreover, EMG recordings can also be very beneficial to investigate BOLD correlates of myoclonus [Richardson *et al.* 2006b]. It has also been shown that despite recording IEDs during EEG-fMRI acquisition, BOLD changes for IEDs may not been seen in ~30% of cases [Salek-Haddadi *et al.* 2006] using conventional GLM based analysis. A possible solution may be to parametrise IEDs for features including amplitude, duration, frequency etc.

However, the problem of low sensitivity persists if there are no IEDs recorded on EEG during MRI scanning. In this regard, it is possible that weaker IEDs associated with smaller cortical generators are not reflected on scalp EEG, particularly when atleast 6-10cm<sup>2</sup> area of cortex needs to be recruited to produce an IED on scalp EEG [Ray *et al.* 2007]. Topographical map correlation based analysis approach [Grouiller *et al.* 2011] may reveal BOLD changes associated with weaker IEDs which are not seen on scalp EEG recorded during EEG-fMRI

acquisition. This approach has been applied on a limited scale and in future can be combined with the analysis approach described in Chapter 6, where by including all regressors: IEDs on the EEG inside the scanner, topographical map correlation, physiological activities, and confounds: motion and pulse-related in the same GLM may improve the sensitivity of EEG-fMRI greatly.

The clinical significance of the various characteristics of IED related BOLD maps remain largely unexplored. The position of the GM voxel itself and the total extent of the cluster containing the GM voxel might have different degrees of clinical significance. The nominal resolution of BOLD fMRI being of the order of 3-5mm (EPI voxel size: 3.75 x 3.75 x 3) at sub-lobar [Grouiller *et al.* 2011] and gyral level [Thornton *et al.* 2010b] is possible when considering the position of the GM voxel. Whether such precision is achieved in practice and clinically meaningful will require detailed comparison with the clinical gold standard i.e., icEEG and also postsurgical outcome. Furthermore, a comparison of the localisation sensitivity of EEG-fMRI with other non-invasive imaging techniques: PET, ictal SPECT and MEG, and its role in planning the placement of intracranial electrodes will demonstrate its true utility during the presurgical evaluation of patients with refractory focal epilepsy. A prospective study investigating the role of scalp EEG-fMRI during presurgical evaluation is currently ongoing at the National Hospital for Neurology and Neurosurgery, London.

In Chapter 9, I demonstrated that simultaneous icEEG-fMRI can map IED related BOLD networks with some predictive value. This technique is potentially useful but only for the relatively small number of patients who undergo invasive evaluation prior to surgery. Future studies comparing BOLD localisation on scalp EEG-fMRI, using combination of conventional GLM based analysis and topographical map correlation based analysis [Grouiller *et al.* 2011], with that of icEEG-fMRI may reveal if the former has the same power and can guide implantation of intracranial electrodes. The application of icEEG-fMRI has opened new horizons to investigate epileptic activity specific to icEEG such as high frequency oscillations. However, it remains an open question as to how to build an appropriate model of BOLD changes for very frequent/continuous IEDs on icEEG without sufficient resting period in this context. For frequent events to measure changes it is likely that inter event differences need to be parameterized for example by their amplitude, frequency and duration. Evaluation of the transfer

function (coupling) linking BOLD changes to IEDs on icEEG will be an important avenue of future research.

An interesting question which needs to be addressed in future study is if there is a single focus or a network responsible for a particular type of epileptic activity and if it has an impact on the surgical outcome? Recent scalp EEG-fMRI studies [Vulliemoz *et al.* 2010;Thornton *et al.* 2010a;Thornton *et al.* 2011] and my work on IEDs using icEEG-fMRI point towards the existence of a network including a statistical maximum BOLD cluster concordant with the epileptic focus which is responsible for focal IEDs in individual patients. Laufs *et al.*, [Laufs *et al.* 2011] has shown that frontal piriform cortex ipsilateral to the presumed focus of epilepsy might be a common area involved in the epileptic activity in different types of epilepsy. Moreover, it has also been shown that the resting state BOLD networks associated with IEDs in patients with TLE are recruited differently in comparison to patients with extra-TLE [Laufs *et al.* 2007b]. Future group studies in sub-types of epilepsy exploring the existence of a common IED related BOLD network in patients with good versus poor postsurgical outcome may answer this question.

Recently, it has been shown in a pilot study that BOLD changes in DMN related areas during performance of a cognitive task are different under the influence of Topiramate as compared to other AEDs [Yasuda *et al.* 2012]. This is an interesting observation. IED related BOLD changes have been shown in DMN related areas previously [Laufs *et al.* 2007b], therefore, it will be valuable to investigate the effect of different AEDs on IED related BOLD networks.

## 11.2 BOLD mapping for seizures

I demonstrated that vEEG-fMRI studies on seizures can map BOLD changes at seizure onset with good concordance with the SOZ and can differentiate them from propagation related BOLD changes in symptomatogenic and DMN related areas. Considering the clinical importance of video-EEG to identify seizures, the use of video-EEG based GLM, using a system of event representation of seizures as dynamic entities can be a first line approach. In the GLM based analysis approach, I attempted to characterise the BOLD patterns using a measure of concordance, based on the presumed SOZ, and measuring the distance between the GM/other BOLD cluster within the presumed SOZ and the SOZ on icEEG.

At the National Hospital for Neurology and Neurosurgery many other epilepsy surgery centres, icEEG is considered the clinical gold standard to localise the SOZ which is meant to represent a circumscribed brain region [Rosenow and Luders 2001; Luders *et al.* 2006]. Above and beyond considerations related to the way in which the BOLD maps are summarised the question of the nature of the seizure onset, conceived as a single region in contrast to a network, arises with implications for the interpretation and suitability of the concordance scheme. If the seizure related BOLD maps represent genuine epileptogenic networks [Bartolomei *et al.* 2001; Spencer 2002; Truccolo *et al.* 2011] then one can question the relevance of the concordance scheme used in this work considering the emphasis given to GM BOLD cluster for the localization purposes. Answering this question would require means to obtain complete characterisation of the SOZ/network beyond currently available means. Given the current presurgical evaluation techniques, I believe that the approach used here remains the most appropriate way of summarising the relationship between the BOLD maps and independently obtained localising information. Nonetheless, it must be acknowledged that deviations from my concordance scheme are to be expected, particularly in view of the epileptogenic network hypothesis. On the other hand, if the BOLD map consists of a single BOLD cluster at onset would tend to support, though not prove, the focus hypothesis. Furthermore when available, postsurgical imaging and seizure outcome data constitute the ultimate criterion in the evaluation of the utility of localisation techniques.

The approach used in my work and that of others [Tyvaert *et al.* 2008; Thornton *et al.* 2010b] can show the BOLD changes in areas recruited during the whole seizure or during different ictal phases represented in the design matrix as variable duration blocks; however it cannot show the evolutionary recruitment of these areas on a temporal scale within a single ictal phase. Further exploration of seizure related fMRI data with dynamic modelling approaches e.g., sequential window based analysis [Donaire *et al.* 2009b], real-time ICA [Esposito *et al.* 2003] or with dynamic causal modelling to understand the connectivity between these regions can improve our knowledge regarding seizure spread and associated mechanisms. In the context of seizure spread, the GLM based group analysis approach for seizures may also highlight a common area or network.

The clinical value in the context of technique's sensitivity and specificity remains to be assessed prospectively which can be very complex considering the way multiple test are done [Knowlton 2006]. The sensitivity of ictal EEG-fMRI can be increased by using video-EEG to detect seizures rather EEG only as shown in Chapter 7. Moreover, selecting patients carefully i.e., who are likely to have seizures during vEEG-fMRI acquisition and could benefit from the test, can also help to define the clinical utility. As for specificity, my study in Chapter 7 cannot provide a statistical measure of specificity in view of the small number of patients studied.

EEG-fMRI studies [Tyvaert *et al.* 2008;Thornton *et al.* 2010b] and my work on seizures related haemodynamic changes in Chapter 7 demonstrated the technique's ability to localise the seizure focus confirmed by icEEG. This suggests that vEEG-fMRI has potential to provide a non-invasive way of better planning the placement of subdural grids and intracranial electrodes to outline the SOZ for patients undergoing presurgical evaluation. However, establishing clinical usefulness will require future prospective studies to evaluate the effect of reviewing ictal related BOLD changes on implantation scheme prior to implantation and to determine technique's true predictive value in terms of icEEG localisation or surgical outcome. It is possible that ictal vEEG-fMRI has a negative predictive power similar to interictal EEG-fMRI as determined in patients with FCDs [Thornton *et al.* 2011].

I demonstrated that vEEG-fMRI can reveal significant preictal BOLD changes in agreement with previous studies [Tyvaert *et al.* 2008;Tyvaert *et al.* 2009;Donaire *et al.* 2009a;LeVan *et al.* 2010b]. The observed pattern of sustained BOLD decreases followed by increases supports the hypothesis that an inhibitory network is active which is overridden at the seizure onset [Wendling *et al.* 2003;Wendling *et al.* 2005;Gnatkovsky *et al.* 2008;Trombin *et al.* 2011;Truccolo *et al.* 2011]. Further studies recording scalp EEG during simultaneous icEEG-fMRI may be helpful to address if these BOLD changes reflect early electrical changes e.g., preictal discharges on icEEG which are not reflected on scalp EEG or true metabolic changes starting before seizure onset even on icEEG. Such studies would also allow to explore the connectivity between different regions of interest e.g., IZ, SOZ and remote healthy cortex showing BOLD changes but not being part of the epileptic network.

Other limitations of current vEEG-fMRI studies on seizures include: motion during seizures as a confounding factor to deteriorate data quality and to increase false positive results, and low temporal resolution of fMRI (~3 seconds) being unable to separate propagation related BOLD changes from onset related BOLD changes if occurring too fast. Future studies using fMRI sequences with online motion correction [Thesen *et al.* 2000] and higher temporal resolution [Liou *et al.* 2011] may map activity patterns over the entire brain at the second time scale and improve our understanding of seizure initiation and propagation and help us answer clinically relevant questions. However, it remains to be explored if simultaneous recording of EEG during scanning will be compatible with fMRI sequences with online motion correction and higher temporal resolution

### 11.3 Assessment of loss of awareness and EEG-fMRI

IEDs [Laufs *et al.* 2007b] and seizure [Donaire *et al.* 2009b; Thornton *et al.* 2010b] related BOLD decreases have been shown in DMN related areas which are thought to be involved in maintaining awareness. Berman and colleagues [Berman *et al.* 2010] has shown that GSWDs associated with poor performance on continuous performance task have BOLD decreases in DMN related areas. I found seizure related BOLD decreases in DMN related areas during later phases of focal seizures especially in patients with documented loss of awareness for seizures recorded during clinical long-term video-EEG monitoring as shown in Chapter 7. Moreover, the presence of shorter lasting GSWDs (0.2-2sec) can alter the working memory related frontal lobe BOLD network as shown in Chapter 10. These findings suggest that EEG-fMRI may be able to show a functional signature for loss of awareness associated with seizures and possibly with IEDs. This would require a thorough assessment of awareness during EEG-fMRI studies of epileptic activity. This will not be an easy undertaking and study design may have many possible confounding factors: type of epilepsy, nature and number of epileptic discharges and sensitivity of the task being performed to assess the awareness. As I discussed in Chapter 10 that performance of a cognitive task may have a bidirectional relationship with IEDs i.e., cognitive task may increase the number of IEDs which in turn can alter the task associated BOLD network. However, performance of a task may also suppress IEDs and seizures [TIZARD and MARGERISON 1963; Aarts *et al.* 1984; Binnie *et al.* 1987; Matsuoka *et al.* 2000; Binnie 2003; Berman *et al.* 2010]. This will require a careful selection of an



appropriately sensitive task to detect loss of awareness in the future studies of EEG-fMRI on seizures. More specifically icEEG-fMRI studies can be more helpful to assess the relationship between awareness and IEDs as they do not suffer from the low sensitivity of scalp EEG.

## Chapter 12: Conclusion

EEG-fMRI is a developing technique which combines information from two different modalities bridging the gap between neurophysiology and imaging of epilepsy. The experimental studies presented in this thesis are a continuation of this developing phase. I presented the means to improve the data acquisition by incorporating video recordings into the EEG-fMRI set up which can help to identify seizures and divide them into phases; and data analysis by including video-EEG based information into the design matrices of vEEG-fMRI data modelling. I demonstrated that vEEG-fMRI can localise BOLD networks at the seizure onset and during seizure propagation in patients with focal seizures. This information can be particularly helpful in patients undergoing invasive evaluation to localise the SOZ and planning the placement of intracranial electrodes. Preictal BOLD changes further corroborate the theory that during interictal to ictal transition an active inhibitory network is overridden by an excitatory network at the seizure onset. IED related BOLD networks revealed by icEEG-fMRI had some power to predict postsurgical outcome in patients undergoing invasive evaluation and provided further evidence to the epileptogenic network hypothesis. In addition, my work on the interaction between GSWDs and cognition suggested that the former can affect the working memory related functional network. These findings suggest that EEG-fMRI holds great promise in the future to help better localise the epileptic focus/network for clinical purposes and may provide a cost-effective red flag to avoid invasive studies or surgery in patients who may possibly have a worse outcome postsurgically. Moreover, it may also help to understand the mechanism of seizure generation and loss of awareness during IEDs and seizures.

## APPENDICES

## Appendix 1: Examples of epileptiform discharges

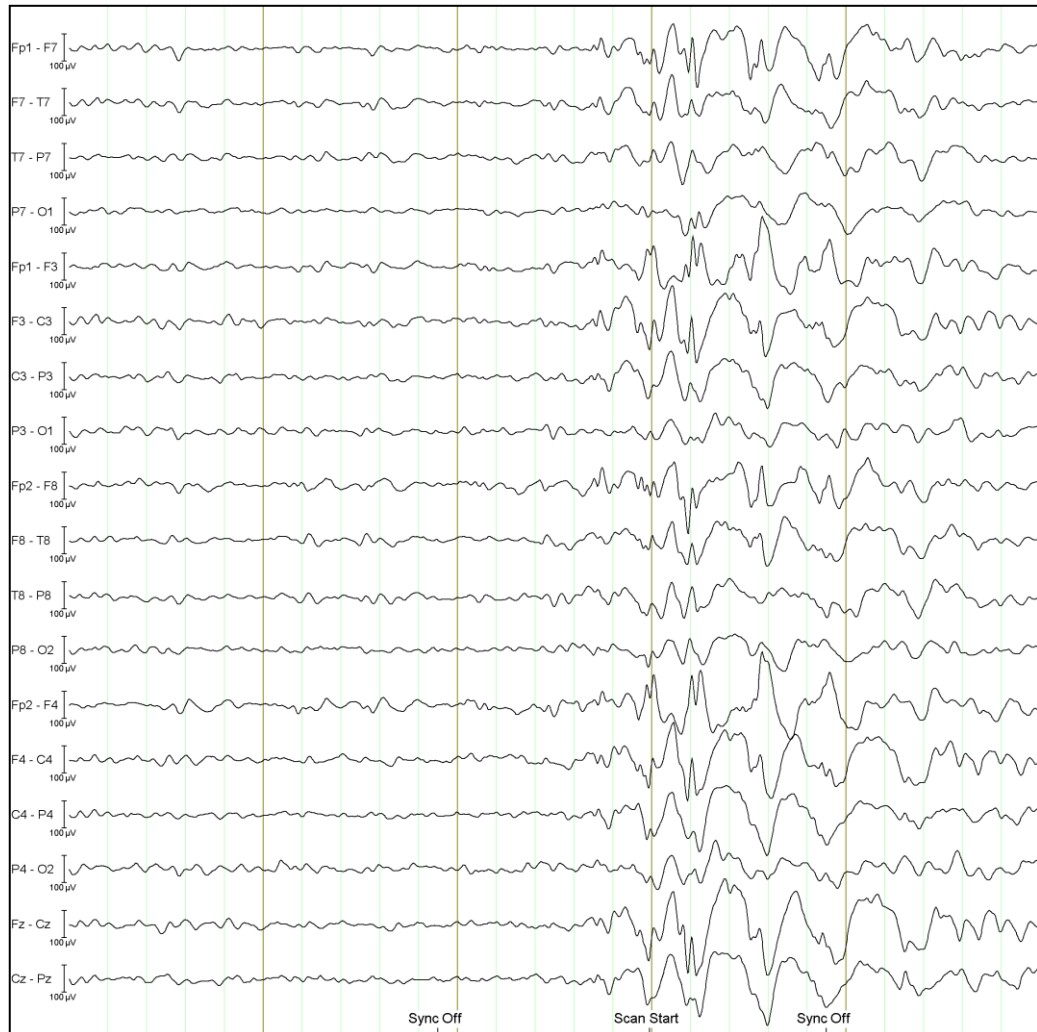


**Figure S1: Example of generalized spike wave discharges**

EEG recorded during simultaneous video-EEG-fMRI showing 2.5-3Hz generalized spike wave discharges (bipolar montage) in a patient with IGE.

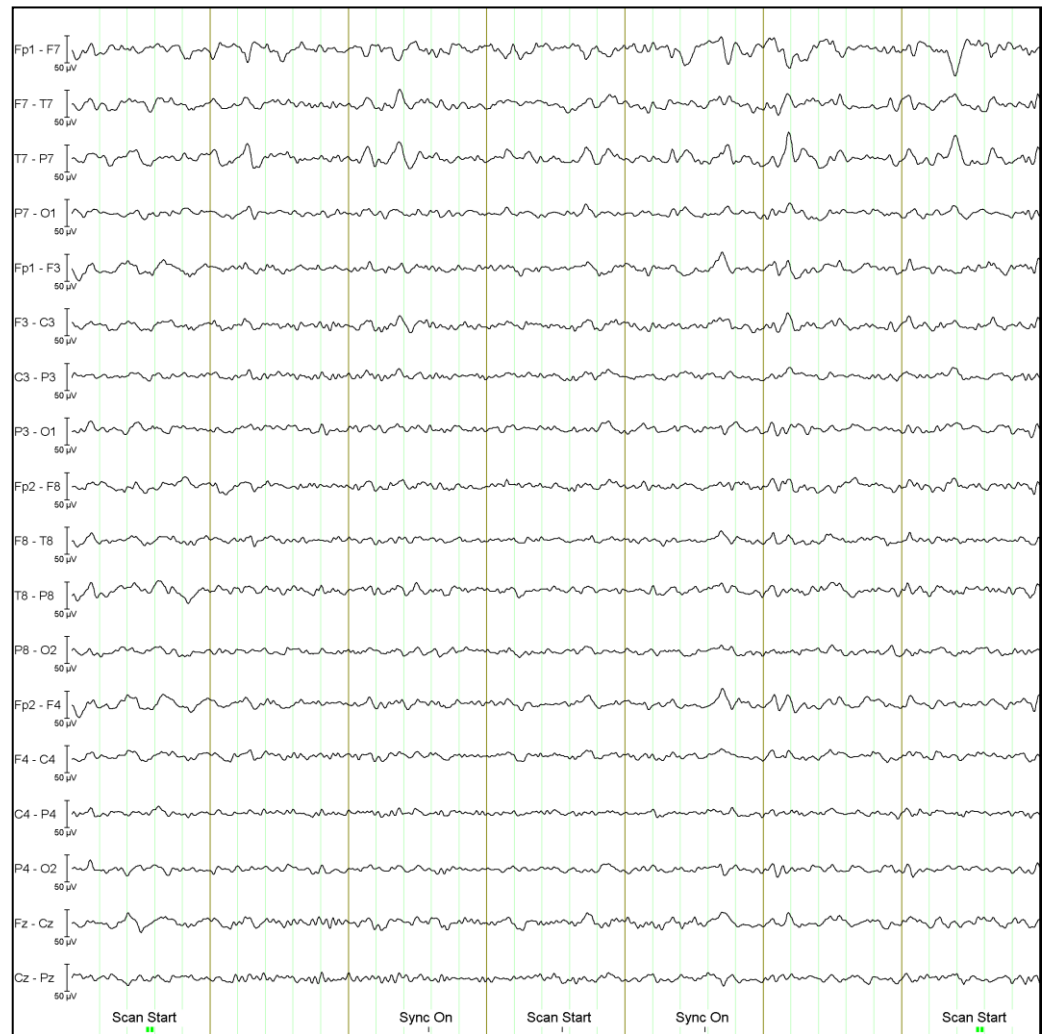


**Figure S2: Example of focal interictal epileptiform discharges**

EEG recorded during simultaneous video-EEG-fMRI showing left focal interictal epileptiform discharges (bipolar montage: T7, F7) in a patient with left TLE.

## **Appendix 2: IED related BOLD changes for data presented in Chapter 7**

For the 20 patients with typical seizures recorded during scalp EEG-fMRI (i.e., data presented in Chapter 7), IEDs were also included in the design matrix for fMRI data analysis as described in Chapter 7, Section 7.2.4. In order to assess, IED related BOLD changes SPM[F] maps were generated for individual type of IEDs.

IEDs were recorded on scalp EEG during scalp EEG-fMRI in 15/20 patients. IED related BOLD changes were seen at conservative statistical threshold  $p < 0.05$  corrected for FWE in four patients, and at less conservative statistical threshold  $p < 0.001$ , uncorrected, in none patients.

BOLD maps had a degree of concordance with the presumed SOZ in 8/15 (53%) patients (Table S1); and were discordant in 5/15 (33%) patients. No BOLD changes were seen for IEDs in two (13%) patients.

**Table S1: IED related BOLD changes for patients who had seizures during scalp EEG-fMRI**

ID	IED recorded during scalp EEG-fMRI	Localization of BOLD changes	*Concordance with the Presumed SOZ
3	L post. temporal sharp	<i>L MFG, R STG, L IFG</i>	D
	R fronto-temporal sharp	None	NA
4	L temporal spike	<i>L IFG, L med. Temporal, L temporal pole, Med. SFG</i>	SC
5	L fronto-temporal spikes	None	NA
	B/L GSW	None	NA
	Slow waves: Left fronto-temporal	None	NA
7	B/L GSW	<b>R sup. Parietal, Precuneus, L sup. Parietal, B/L dorsolateral Frontal, Med. SFG, B/L Temporal</b>	SC
8	L mid temporal spike	<i>Cingulate gyrus, Med. SFG</i>	D
	R temporal spike	<i>R MFG, R MTG, L med. Temporal, R STG</i>	C+
	R frontal SW	<i>L med. Temporal, R MFG, R basal Temporal</i>	SC
	1-1.5 Hz widespread GSW	<i>R ITG, R MFG, Med. SFG</i>	C+
	B/L temporal spikes	<i>R ITG, R basal post. Temporal, R STG</i>	C+
9	Fronto-central spikes	None	NA
10	R mid. temporal sharp	<i>B/L med. occipital</i>	EC
11	B/L GSW R > L	<b>R MFG/IFG, B/L sup. Parietal, L IFG, Precuneus, Med. SFG</b>	C+
12	L fronto-central spikes	<i>Med. SFG, L Inf. Parietal, B/L MFG, Precuneus</i>	C+
13	1.5-2 Hz fronto-central SW	<b>R Parietal, Thalamus, L STG, L MFG, Med. SFG, R STG,</b>	D
14	B/L temporal slow	<b>R Temporal pole, B/L sup. Parietal, Med. SFG</b>	D
15	Polyspikes and wave max. L temporal	<i>L basal and post. Temporal, L sup. Parietal, Post. Cingulate, Precuneus, R sup. Parietal, B/L MFG</i>	C+
16	Bi-frontal and L frontal sharp/spikes	<i>L MFG, R MFG, L sup. Parietal</i>	C+
19	R parietal sharp/slow	<i>R IFG, L STG, L Med. Temporal, B/L MFG</i>	D
20	R fronto-central	<i>R cingulate, L STG, Med. SFG, L SFG</i>	D

\*Concordance with the presumed SOZ was assessed as described in Chapter 7, Section 7.2.4.

First BOLD cluster is the global statistical maximum (GM) cluster.

Italicized BOLD clusters were revealed at less conservative statistical threshold  $p < 0.001$  uncorrected, and boldened BOLD clusters were revealed at conservative statistical threshold  $p < 0.05$  corrected for FWE.

Abbreviations: R = Right, L = Left, MFG = middle frontal gyrus, MTG = middle temporal gyrus, STG = superior temporal gyrus, B/L = Bilateral, sup. = superior, med. / Med. = medial, SFG = superior frontal gyrus, IFG = inferior frontal gyrus, inf. = inferior, GSW = generalized spike wave, EC = *Entirely concordant*, C+ = *Concordant plus*, SC = *Some concordance*, D = *Discordant*.

### **Appendix 3: IED related BOLD changes on scalp EEG-fMRI for data presented in Chapter 9**

All patients who had icEEG-fMRI (i.e., data presented in Chapter 9) also had scalp EEG-fMRI prior to the implantation of icEEG electrodes, except patient #5. For one patient (#8), the entire icEEG recorded during icEEG-fMRI acquisition could not be corrected due to technical reasons; therefore, scalp EEG-fMRI data for patient #8 will not be considered for further analysis. Scalp EEG-fMRI data from these eight patients was analyzed in the GLM framework as described in Chapter 6 [Chaudhary *et al.* 2012a] to assess IED related BOLD changes.

In 4/8 patients (#2, 3, 7, 10), IEDs were recorded on scalp EEG during scalp EEG-fMRI acquisition and revealed IED related BOLD changes. BOLD maps were had a degree of concordance with the IZ (Table S2) in 3/8 patients; and were discordant in one patient.

**Table S2: IED related BOLD changes during scalp EEG-fMRI for patients who also underwent icEEG-fMRI**

<b>ID</b>	<b>IED recorded during scalp EEG-fMRI</b>	<b>Localization of BOLD Changes</b>	<b>*Concordance with the IZ</b>
2	Sharpened slow: R Centro-parietal	R superior Parietal	D
3	Sharp/Spikes: Bi-frontal L frontal	L MFG, R MFG, L superior Parietal	C+
7	Sharp/Spikes: L Temporal Bi-temporal	L posterior MTG	EC
10	Sharp waves: R mid Temporal	Bilateral medial Occipital	EC

Abbreviations: R = Right, L = Left, MFG = middle frontal gyrus, MTG = middle temporal gyrus, STG = superior temporal gyrus, EC = *Entirely concordant*, C+ = *Concordant plus*, D = *Discordant*, \*Concordance with the irritative zone was assessed as described in Chapter 9, Section 9.2.4a.



## REFERENCES

- Aarts JH, Binnie CD, Smit AM, Wilkins AJ. Selective cognitive impairment during focal and generalized epileptiform EEG activity. *Brain* 1984; 107 ( Pt 1): 293-308.
- Ackermann RF, Finch DM, Babb TL, Engel J, Jr. Increased glucose metabolism during long-duration recurrent inhibition of hippocampal pyramidal cells. *J Neurosci* 1984; 4: 251-264.
- Aghakhani Y, Bagshaw AP, Benar CG, Hawco C, Andermann F, Dubeau F, Gotman J. fMRI activation during spike and wave discharges in idiopathic generalized epilepsy. *Brain* 2004; 127: 1127-1144.
- Aghakhani Y, Kobayashi E, Bagshaw AP, Hawco C, Benar CG, Dubeau F, Gotman J. Cortical and thalamic fMRI responses in partial epilepsy with focal and bilateral synchronous spikes. *Clin Neurophysiol* 2006; 117: 177-191.
- Agirre-Arrizubieta Z, Huiskamp GJ, Ferrier CH, van Huffelen AC, Leijten FS. Interictal magnetoencephalography and the irritative zone in the electrocorticogram. *Brain* 2009; 132: 3060-3071.
- Ahnlide JA, Rosen I, Linden-Mickelsson TP, Kallen K. Does SISCOM contribute to favorable seizure outcome after epilepsy surgery? *Epilepsia* 2007; 48: 579-588.
- Al-Asmi A, Benar CG, Gross DW, Khani YA, Andermann F, Pike B, Dubeau F, Gotman J. fMRI activation in continuous and spike-triggered EEG-fMRI studies of epileptic spikes. *Epilepsia* 2003; 44: 1328-1339.
- Alarcon G, Guy CN, Binnie CD, Walker SR, Elwes RD, Polkey CE. Intracerebral propagation of interictal activity in partial epilepsy: implications for source localisation. *J Neurol Neurosurg Psychiatry* 1994; 57: 435-449.
- Alarcon G, Binnie CD, Elwes RD, Polkey CE. Power spectrum and intracranial EEG patterns at seizure onset in partial epilepsy. *Electroencephalogr Clin Neurophysiol* 1995; 94: 326-337.
- Alavi A, Hirsch LJ. Studies of central nervous system disorders with single photon emission computed tomography and positron emission tomography: evolution over the past 2 decades. *Semin Nucl Med* 1991; 21: 58-81.
- Albowitz B, Kuhnt U. Epileptiform activity in the guinea-pig neocortical slice spreads preferentially along supragranular layers--recordings with voltage-sensitive dyes. *Eur J Neurosci* 1995; 7: 1273-1284.
- Aldenkamp AP, Overweg J, Gutter T, Beun AM, Diepman L, Mulder OG. Effect of epilepsy, seizures and epileptiform EEG discharges on cognitive function. *Acta Neurol Scand* 1996; 93: 253-259.
- Aldenkamp AP, Arends J, Overweg-Plandsoen TC, van Bronswijk KC, Schyns-Soeterboek A, Linden I, Diepman L. Acute cognitive effects of nonconvulsive difficult-to-detect epileptic seizures and epileptiform electroencephalographic discharges. *J Child Neurol* 2001; 16: 119-123.
- Aldenkamp AP, Beitler J, Arends J, van dL, I, Diepman L. Acute effects of subclinical epileptiform EEG discharges on cognitive activation. *Funct Neurol* 2005; 20: 23-28.
- Allen PJ, Fish DR, Smith SJ. Very high-frequency rhythmic activity during SEEG suppression in frontal lobe epilepsy. *Electroencephalogr Clin Neurophysiol* 1992; 82: 155-159.
- Allen PJ, Polizzi G, Krakow K, Fish DR, Lemieux L. Identification of EEG events in the MR scanner: the problem of pulse artifact and a method for its subtraction. *Neuroimage* 1998; 8: 229-239.
- Allen PJ, Josephs O, Turner R. A method for removing imaging artifact from continuous EEG recorded during functional MRI. *Neuroimage* 2000; 12: 230-239.

## REFERENCES

- Archer JS, Briellmann RS, Syngeniotis A, Abbott DF, Jackson GD. Spike-triggered fMRI in reading epilepsy: involvement of left frontal cortex working memory area. *Neurology* 2003a; 60: 415-421.
- Archer JS, Briellman RS, Abbott DF, Syngeniotis A, Wellard RM, Jackson GD. Benign epilepsy with centro-temporal spikes: spike triggered fMRI shows somato-sensory cortex activity. *Epilepsia* 2003b; 44: 200-204.
- Archer JS, Waites AB, Abbott DF, Federico P, Jackson GD. Event-related fMRI of myoclonic jerks arising from dysplastic cortex. *Epilepsia* 2006; 47: 1487-1492.
- Archer JS, Abbott DF, Masterton RA, Palmer SM, Jackson GD. Functional MRI interactions between dysplastic nodules and overlying cortex in periventricular nodular heterotopia. *Epilepsy Behav* 2010; 19: 631-634.
- Arthuis M, Valton L, Regis J, Chauvel P, Wendling F, Naccache L, Bernard C, Bartolomei F. Impaired consciousness during temporal lobe seizures is related to increased long-distance cortical-subcortical synchronization. *Brain* 2009; 132: 2091-2101.
- Ashburner J, Friston K. Multimodal image coregistration and partitioning--a unified framework. *Neuroimage* 1997; 6: 209-217.
- Ashburner J, Flandin G, Henson R, Kiebel S, Kilner J, Mattout J, Pennt W, Stephan K, Hutton C. SPM5 Manual; The FIL Methods Group. 2008.
- Ashburner J, Barnes G, Chen C, Daunizeau J, Flandin G, Friston K, Kiebel S, Kilner J, Litvak V, Moran R, Penny W, Rosa M, Stephan K, Gitelman D, Henson R, Hutton C, Glauche V, Mattout J, Phillips C. SPM8 Manual; The FIL Methods Group. 2012.
- Attwell D, Laughlin SB. An energy budget for signaling in the grey matter of the brain. *J Cereb Blood Flow Metab* 2001; 21: 1133-1145.
- Attwell D, Iadecola C. The neural basis of functional brain imaging signals. *Trends Neurosci* 2002; 25: 621-625.
- Auer T, Veto K, Doczi T, Komoly S, Juhos V, Janszky J, Schwarcz A. Identifying seizure-onset zone and visualizing seizure spread by fMRI: a case report. *Epileptic Disord* 2008; 10: 93-100.
- Avanzini G, de CM, Marescaux C, Panzica F, Spreafico R, Vergnes M. Role of the thalamic reticular nucleus in the generation of rhythmic thalamo-cortical activities subserving spike and waves. *J Neural Transm Suppl* 1992; 35: 85-95.
- Avoli M, Gloor P. The effects of transient functional depression of the thalamus on spindles and on bilateral synchronous epileptic discharges of feline generalized penicillin epilepsy. *Epilepsia* 1981; 22: 443-452.
- Avoli M, Gloor P. Interaction of cortex and thalamus in spike and wave discharges of feline generalized penicillin epilepsy. *Exp Neurol* 1982; 76: 196-217.
- Avoli M, Kostopoulos G. Participation of corticothalamic cells in penicillin-induced generalized spike and wave discharges. *Brain Res* 1982; 247: 159-163.
- Avoli M, Rogawski MA, Avanzini G. Generalized epileptic disorders: an update. *Epilepsia* 2001; 42: 445-457.
- Avoli M, Biagini G, de CM. Do interictal spikes sustain seizures and epileptogenesis? *Epilepsy Curr* 2006; 6: 203-207.
- Aziz H, Guvener A, Akhtar SW, Hasan KZ. Comparative epidemiology of epilepsy in Pakistan and Turkey: population-based studies using identical protocols. *Epilepsia* 1997; 38: 716-722.
- Babb TL, Wilson CL, Isokawa-Akesson M. Firing patterns of human limbic neurons during stereoencephalography (SEEG) and clinical temporal lobe seizures. *Electroencephalogr Clin Neurophysiol* 1987; 66: 467-482.
- Bagshaw AP, Aghakhani Y, Benar CG, Kobayashi E, Hawco C, Dubeau F, Pike GB, Gotman J. EEG-fMRI of focal epileptic spikes: analysis with multiple haemodynamic functions and comparison with gadolinium-enhanced MR angiograms. *Hum Brain Mapp* 2004; 22: 179-192.
- Bagshaw AP, Hawco C, Benar CG, Kobayashi E, Aghakhani Y, Dubeau F, Pike GB, Gotman J. Analysis of the EEG-fMRI response to prolonged bursts of interictal epileptiform activity. *Neuroimage* 2005; 24: 1099-1112.

## REFERENCES

- Bagshaw AP, Kobayashi E, Dubeau F, Pike GB, Gotman J. Correspondence between EEG-fMRI and EEG dipole localisation of interictal discharges in focal epilepsy. *Neuroimage* 2006; 30: 417-425.
- Bai X, Vestal M, Berman R, Negishi M, Spann M, Vega C, Desalvo M, Novotny EJ, Constable RT, Blumenfeld H. Dynamic time course of typical childhood absence seizures: EEG, behavior, and functional magnetic resonance imaging. *J Neurosci* 2010; 30: 5884-5893.
- Bakhtiar L, Cameron O, Shah MH. *The canon of medicine*. Chicago: Great Books of the Islamic World, Kazi Publications; 1999.
- Bal T, von KM, McCormick DA. Role of the ferret perigeniculate nucleus in the generation of synchronized oscillations in vitro. *J Physiol* 1995a; 483 ( Pt 3): 665-685.
- Bal T, von KM, McCormick DA. Synaptic and membrane mechanisms underlying synchronized oscillations in the ferret lateral geniculate nucleus in vitro. *J Physiol* 1995b; 483 ( Pt 3): 641-663.
- Bancaud J. The physiopathogenesis of generalized epilepsies of organic nature (stereoencephalographic study). In: Gastaut H, Jasper HH, Bancaud J, Waltregny A, editors. *The physiopathogenesis of the epilepsies*. Springfield, III: Charles C Thomas Publisher; 1969. p. 158-85.
- Bandettini PA, Jesmanowicz A, Wong EC, Hyde JS. Processing strategies for time-course data sets in functional MRI of the human brain. *Magn Reson Med* 1993; 30: 161-173.
- Barba C, Barbati G, Minotti L, Hoffmann D, Kahane P. Ictal clinical and scalp-EEG findings differentiating temporal lobe epilepsies from temporal 'plus' epilepsies. *Brain* 2007; 130: 1957-1967.
- Barbarosie M, Avoli M. CA3-driven hippocampal-entorhinal loop controls rather than sustains in vitro limbic seizures. *J Neurosci* 1997; 17: 9308-9314.
- Bartlett PA, Richardson MP, Duncan JS. Measurement of amygdala T2 relaxation time in temporal lobe epilepsy. *J Neurol Neurosurg Psychiatry* 2002; 73: 753-755.
- Bartolomei F, Wendling F, Bellanger JJ, Regis J, Chauvel P. Neural networks involving the medial temporal structures in temporal lobe epilepsy. *Clin Neurophysiol* 2001; 112: 1746-1760.
- Bartolomei F, Wendling F, Regis J, Gavaret M, Guye M, Chauvel P. Pre-ictal synchronicity in limbic networks of mesial temporal lobe epilepsy. *Epilepsy Res* 2004; 61: 89-104.
- Beckmann CF, Smith SM. Probabilistic independent component analysis for functional magnetic resonance imaging. *IEEE Trans Med Imaging* 2004; 23: 137-152.
- Beghi E, Berg A, Carpio A, Forsgren L, Hesdorffer DC, Hauser WA, Malmgren K, Shinnar S, Temkin N, Thurman D, Tomson T. Comment on epileptic seizures and epilepsy: definitions proposed by the International League Against Epilepsy (ILAE) and the International Bureau for Epilepsy (IBE). *Epilepsia* 2005; 46: 1698-1699.
- Beghi E. The concept of the epilepsy syndrome: how useful is it in clinical practice? *Epilepsia* 2009; 50 Suppl 5: 4-10.
- Beghi E. New classification proposals for epilepsy: a real advancement in the nosography of the disease? *Epilepsia* 2011; 52: 1197-1198.
- Beleza P. Refractory epilepsy: a clinically oriented review. *Eur Neurol* 2009; 62: 65-71.
- Benar C, Aghakhani Y, Wang Y, Izenberg A, Al-Asmi A, Dubeau F, Gotman J. Quality of EEG in simultaneous EEG-fMRI for epilepsy. *Clin Neurophysiol* 2003; 114: 569-580.
- Benar CG, Gross DW, Wang Y, Petre V, Pike B, Dubeau F, Gotman J. The BOLD response to interictal epileptiform discharges. *Neuroimage* 2002; 17: 1182-1192.
- Benar CG, Grova C, Kobayashi E, Bagshaw AP, Aghakhani Y, Dubeau F, Gotman J. EEG-fMRI of epileptic spikes: concordance with EEG source localization and intracranial EEG. *Neuroimage* 2006; 30: 1161-1170.
- Benn EK, Hauser WA, Shih T, Leary L, Bagiella E, Dayan P, Green R, Andrews H, Thurman DJ, Hesdorffer DC. Estimating the incidence of first unprovoked seizure and

## REFERENCES

- newly diagnosed epilepsy in the low-income urban community of Northern Manhattan, New York City. *Epilepsia* 2008; 49: 1431-1439.
- Berg AT, Berkovic SF, Brodie MJ, Buchhalter J, Cross JH, van Emde BW, Engel J, French J, Glauser TA, Mathern GW, Moshe SL, Nordli D, Plouin P, Scheffer IE. Revised terminology and concepts for organization of seizures and epilepsies: report of the ILAE Commission on Classification and Terminology, 2005-2009. *Epilepsia* 2010; 51: 676-685.
- Berg AT, Scheffer IE. Response to Commentaries: What is at stake in a classification? *Epilepsia* 2011; 52: 1205-1208.
- Bergey GK. Evidence-based treatment of idiopathic generalized epilepsies with new antiepileptic drugs. *Epilepsia* 2005; 46 Suppl 9: 161-168.
- Berkovic SF, McIntosh AM, Kalnins RM, Jackson GD, Fabinyi GC, Brazenor GA, Bladin PF, Hopper JL. Preoperative MRI predicts outcome of temporal lobectomy: an actuarial analysis. *Neurology* 1995; 45: 1358-1363.
- Berman R, Negishi M, Vestal M, Spann M, Chung MH, Bai X, Purcaro M, Motelow JE, Danielson N, Dix-Cooper L, Enev M, Novotny EJ, Constable RT, Blumenfeld H. Simultaneous EEG, fMRI, and behavior in typical childhood absence seizures. *Epilepsia* 2010; 51: 2011-2022.
- Billings JS. The Surgical Treatment of Epilepsy. *Cincinnati Lancet & Observer* 1861; 334-341.
- Binnie CD, Rowan AJ, Overweg J, Meinardi H, Wisman T, Kamp A, Lopes da SF. Telemetric EEG and video monitoring in epilepsy. *Neurology* 1981; 31: 298-303.
- Binnie CD, Kasteleijn-Nolst Trenite DG, Smit AM, Wilkins AJ. Interactions of epileptiform EEG discharges and cognition. *Epilepsy Res* 1987; 1: 239-245.
- Binnie CD, Prior PF. Electroencephalography. *J Neurol Neurosurg Psychiatry* 1994; 57: 1308-1319.
- Binnie CD, Stefan H. Modern electroencephalography: its role in epilepsy management. *Clin Neurophysiol* 1999; 110: 1671-1697.
- Binnie CD. Cognitive impairment during epileptiform discharges: is it ever justifiable to treat the EEG? *Lancet Neurol* 2003; 2: 725-730.
- Birn RM, Bandettini PA, Cox RW, Jesmanowicz A, Shaker R. Magnetic field changes in the human brain due to swallowing or speaking. *Magn Reson Med* 1998; 40: 55-60.
- Birn RM, Bandettini PA, Cox RW, Shaker R. Event-related fMRI of tasks involving brief motion. *Hum Brain Mapp* 1999; 7: 106-114.
- Birn RM, Cox RW, Bandettini PA. Experimental designs and processing strategies for fMRI studies involving overt verbal responses. *Neuroimage* 2004; 23: 1046-1058.
- Birn RM, Diamond JB, Smith MA, Bandettini PA. Separating respiratory-variation-related fluctuations from neuronal-activity-related fluctuations in fMRI. *Neuroimage* 2006; 31: 1536-1548.
- Birn RM, Murphy K, Handwerker DA, Bandettini PA. fMRI in the presence of task-correlated breathing variations. *Neuroimage* 2009; 47: 1092-1104.
- Blumcke I. Neuropathology of focal epilepsies: a critical review. *Epilepsy Behav* 2009; 15: 34-39.
- Blumcke I, Vinters HV, Armstrong D, Aronica E, Thom M, Spreafico R. Malformations of cortical development and epilepsies: neuropathological findings with emphasis on focal cortical dysplasia. *Epileptic Disord* 2009; 11: 181-193.
- Blumcke I, Thom M, Aronica E, Armstrong DD, Vinters HV, Palmieri A, Jacques TS, Avanzini G, Barkovich AJ, Battaglia G, Becker A, Cepeda C, Cendes F, Colombo N, Crino P, Cross JH, Delalande O, Dubeau F, Duncan J, Guerrini R, Kahane P, Mathern G, Najm I, Ozkara C, Raybaud C, Represa A, Roper SN, Salamon N, Schulze-Bonhage A, Tassi L, Vezzani A, Spreafico R. The clinicopathologic spectrum of focal cortical dysplasias: a consensus classification proposed by an ad hoc Task Force of the ILAE Diagnostic Methods Commission. *Epilepsia* 2011; 52: 158-174.
- Blume WT, Luders HO, Mizrahi E, Tassinari C, van Emde BW, Engel J, Jr. Glossary of descriptive terminology for ictal semiology: report of the ILAE task force on classification and terminology. *Epilepsia* 2001; 42: 1212-1218.

## REFERENCES

- Bodis-Wollner I, Bucher SF, Seelos KC. Cortical activation patterns during voluntary blinks and voluntary saccades. *Neurology* 1999; 53: 1800-1805.
- Boecker H, Kleinschmidt A, Requardt M, Hanicke W, Merboldt KD, Frahm J. Functional cooperativity of human cortical motor areas during self-paced simple finger movements. A high-resolution MRI study. *Brain* 1994; 117 ( Pt 6): 1231-1239.
- Bonelli SB, Powell RH, Yogarajah M, Samson RS, Symms MR, Thompson PJ, Koepp MJ, Duncan JS. Imaging memory in temporal lobe epilepsy: predicting the effects of temporal lobe resection. *Brain* 2010; 133: 1186-1199.
- Bonelli SB, Powell R, Thompson PJ, Yogarajah M, Focke NK, Stretton J, Vollmar C, Symms MR, Price CJ, Duncan JS, Koepp MJ. Hippocampal activation correlates with visual confrontation naming: fMRI findings in controls and patients with temporal lobe epilepsy. *Epilepsy Res* 2011; 95: 246-254.
- Bonelli SB, Thompson PJ, Yogarajah M, Vollmar C, Powell RH, Symms MR, McEvoy AW, Micallef C, Koepp MJ, Duncan JS. Imaging language networks before and after anterior temporal lobe resection: results of a longitudinal fMRI study. *Epilepsia* 2012; 53: 639-650.
- Bonilha L, Halford JJ, Rorden C, Roberts DR, Rumboldt Z, Eckert MA. Automated MRI analysis for identification of hippocampal atrophy in temporal lobe epilepsy. *Epilepsia* 2009; 50: 228-233.
- Bonmassar G, Purdon PL, Jaaskelainen IP, Chiappa K, Solo V, Brown EN, Belliveau JW. Motion and ballistocardiogram artifact removal for interleaved recording of EEG and EPs during MRI. *Neuroimage* 2002; 16: 1127-1141.
- Bracco P, Anastasi G, Piancino MG, Frongia G, Milardi D, Favaloro A, Bramanti P. Hemispheric prevalence during chewing in normal right-handed and left-handed subjects: a functional magnetic resonance imaging preliminary study. *Cranio* 2010; 28: 114-121.
- Bragin A, Wilson CL, Engel J, Jr. Chronic epileptogenesis requires development of a network of pathologically interconnected neuron clusters: a hypothesis. *Epilepsia* 2000; 41 Suppl 6: S144-S152.
- Bragin A, Claeys P, Vonck K, Van RD, Wilson C, Boon P, Engel J, Jr. Analysis of initial slow waves (ISWs) at the seizure onset in patients with drug resistant temporal lobe epilepsy. *Epilepsia* 2007; 48: 1883-1894.
- Brinker G, Bock C, Busch E, Krep H, Hossmann KA, Hoehn-Berlage M. Simultaneous recording of evoked potentials and T2\*-weighted MR images during somatosensory stimulation of rat. *Magn Reson Med* 1999; 41: 469-473.
- Bristow D, Frith C, Rees G. Two distinct neural effects of blinking on human visual processing. *Neuroimage* 2005a; 27: 136-145.
- Bristow D, Haynes JD, Sylvester R, Frith CD, Rees G. Blinking suppresses the neural response to unchanging retinal stimulation. *Curr Biol* 2005b; 15: 1296-1300.
- Browne EG. Islamic medicine : Fitzpatrick lectures delivered at the Royal College of Physicians in 1919-1920. New Delhi: Goodword; 2001.
- Buchwald JS, Hala ES, Schramm S. A comparison of multi-unit activity and EEG activity recorded from the same brain site in chronic cats during behavioural conditioning. *Nature* 1965; 205: 1012-1014.
- Buzsaki G. The thalamic clock: emergent network properties. *Neuroscience* 1991; 41: 351-364.
- Byrd KE, Romito LM, Dziedzic M, Wong D, Talavage TM. fMRI study of brain activity elicited by oral parafunctional movements. *J Oral Rehabil* 2009; 36: 346-361.
- Calhoun VD, Adali T, Pearlson GD, Pekar JJ. Spatial and temporal independent component analysis of functional MRI data containing a pair of task-related waveforms. *Hum Brain Mapp* 2001; 13: 43-53.
- Capovilla G, Berg AT, Cross JH, Solomon LM, Vigeveno F, Wolf P, Avanzini G. Monreale workshop: conceptual dichotomies in classifying epilepsies: partial versus generalized and idiopathic versus symptomatic (April 18-20, 2008, Monreale, Italy). *Epilepsia* 2009; 50: 1645-1649.

## REFERENCES

- Cappelletti V. Giorgio Baglivi on mechanism and Hippocrates. *Med Secoli* 2000; 12: 9-18.
- Carmichael DW, Hamandi K, Laufs H, Duncan JS, Thomas DL, Lemieux L. An investigation of the relationship between BOLD and perfusion signal changes during epileptic generalised spike wave activity. *Magn Reson Imaging* 2008a; 26: 870-873.
- Carmichael DW, Thornton JS, Rodionov R, Thornton R, McEvoy A, Allen PJ, Lemieux L. Safety of localizing epilepsy monitoring intracranial electroencephalograph electrodes using MRI: radiofrequency-induced heating. *J Magn Reson Imaging* 2008b; 28: 1233-1244.
- Carmichael DW, Thornton JS, Rodionov R, Thornton R, McEvoy AW, Ordidge RJ, Allen PJ, Lemieux L. Feasibility of simultaneous intracranial EEG-fMRI in humans: a safety study. *Neuroimage* 2010; 49: 379-390.
- Carmichael DW, Vulliemoz S, Rodionov R, Thornton JS, McEvoy AW, Lemieux L. Simultaneous intracranial EEG-fMRI in humans: Data quality. *Neuroimage* 2012.
- Carney PW, Masterton RA, Harvey AS, Scheffer IE, Berkovic SF, Jackson GD. The core network in absence epilepsy. Differences in cortical and thalamic BOLD response. *Neurology* 2010; 75: 904-911.
- Cascino GD. Video-EEG monitoring in adults. *Epilepsia* 2002; 43 Suppl 3: 80-93.
- Catarino CB, Vollmar C, Noachtar S. Paradoxical lateralization of non-invasive electroencephalographic ictal patterns in extra-temporal epilepsies. *Epilepsy Res* 2011.
- Celsus. *Celsus: De medicina*, with an English translation by W.G.Spencer. London: William Heinemann Limited; 1938.
- Chainay H, Krainik A, Tanguy ML, Gerardin E, Le BD, Lehericy S. Foot, face and hand representation in the human supplementary motor area. *Neuroreport* 2004; 15: 765-769.
- Chamberlin NL, Traub RD, Dingledine R. Role of EPSPs in initiation of spontaneous synchronized burst firing in rat hippocampal neurons bathed in high potassium. *J Neurophysiol* 1990; 64: 1000-1008.
- Chandler SH, Hsiao CF, Inoue T, Goldberg LJ. Electrophysiological properties of guinea pig trigeminal motoneurons recorded in vitro. *J Neurophysiol* 1994; 71: 129-145.
- Chassagnon S, Hawko CS, Bernasconi A, Gotman J, Dubeau F. Coexistence of symptomatic focal and absence seizures: video-EEG and EEG-fMRI evidence of overlapping but independent epileptogenic networks. *Epilepsia* 2009; 50: 1821-1826.
- Chaudhary UJ, Kokkinos V, Carmichael DW, Rodionov R, Gasston D, Duncan JS, Lemieux L. Implementation and evaluation of simultaneous video-electroencephalography and functional magnetic resonance imaging. *Magn Reson Imaging* 2010; 28: 1192-1199.
- Chaudhary UJ, Duncan JS, Lemieux L. A dialogue with historical concepts of epilepsy from the Babylonians to Hughlings Jackson: persistent beliefs. *Epilepsy Behav* 2011; 21: 109-114.
- Chaudhary UJ, Rodionov R, Carmichael DW, Thornton RC, Duncan JS, Lemieux L. Improving the sensitivity of EEG-fMRI studies of epileptic activity by modelling eye blinks, swallowing and other video-EEG detected physiological confounds. *Neuroimage* 2012a; 61: 1383-1393.
- Chaudhary UJ, Carmichael DW, Rodionov R, Thornton RC, Bartlett P, Vulliemoz S, Micallef C, McEvoy AW, Diehl B, Walker MC, Duncan JS, Lemieux L. Mapping preictal and ictal haemodynamic networks using video-electroencephalography and functional imaging. *Brain* 2012b; 135: 3645-3663.
- Chaudhary UJ, Centeno M, Carmichael DW, Vollmar C, Rodionov R, Bonelli S, Stretton J, Pressler R, Eriksson SH, Sisodiya S, Friston K, Duncan JS, Lemieux L, Koepp M. Imaging the interaction: Epileptic discharges, working memory, and behavior. *Hum Brain Mapp* 2012c.
- Chaudhary UJ, Duncan JS, Lemieux L. Mapping hemodynamic correlates of seizures using fMRI: A review. *Hum Brain Mapp* 2013; 34: 447-466.
- Christensen J, Kjeldsen MJ, Andersen H, Friis ML, Sidenius P. Gender differences in epilepsy. *Epilepsia* 2005; 46: 956-960.

## REFERENCES

- Chugani HT, Rintahaka PJ, Shewmon DA. Ictal patterns of cerebral glucose utilization in children with epilepsy. *Epilepsia* 1994; 35: 813-822.
- Clusmann H, Kral T, Gleissner U, Sassen R, Urbach H, Blumcke I, Bogucki J, Schramm J. Analysis of different types of resection for pediatric patients with temporal lobe epilepsy. *Neurosurgery* 2004; 54: 847-859.
- Cobb SR, Buhl EH, Halasy K, Paulsen O, Somogyi P. Synchronization of neuronal activity in hippocampus by individual GABAergic interneurons. *Nature* 1995; 378: 75-78.
- Colloquium on Status Epilepticus. Proceedings and abstracts of the First London Colloquium on Status Epilepticus, University College London, April 12-15, 2007. *Epilepsia* 2007; 48 Suppl 8: 1-109.
- Colloquium on Status Epilepticus. Proceedings of the Innsbruck Colloquium on Status Epilepticus. Innsbruck, Austria. April 2-5, 2009. *Epilepsia* 2009; 50 Suppl 12: 1-80.
- Connors BW, Gutnick MJ, Prince DA. Electrophysiological properties of neocortical neurons in vitro. *J Neurophysiol* 1982; 48: 1302-1320.
- Contreras D, Destexhe A, Sejnowski TJ, Steriade M. Control of spatiotemporal coherence of a thalamic oscillation by corticothalamic feedback. *Science* 1996; 274: 771-774.
- Contreras D, Steriade M. State-dependent fluctuations of low-frequency rhythms in corticothalamic networks. *Neuroscience* 1997; 76: 25-38.
- Cook MJ, Fish DR, Shorvon SD, Straughan K, Stevens JM. Hippocampal volumetric and morphometric studies in frontal and temporal lobe epilepsy. *Brain* 1992; 115 ( Pt 4): 1001-1015.
- Czisch M, Wehrle R, Kaufmann C, Wetter TC, Holsboer F, Pollmacher T, Auer DP. Functional MRI during sleep: BOLD signal decreases and their electrophysiological correlates. *Eur J Neurosci* 2004; 20: 566-574.
- Dale AM. Optimal experimental design for event-related fMRI. *Hum Brain Mapp* 1999; 8: 109-114.
- Damoiseaux JS, Rombouts SA, Barkhof F, Scheltens P, Stam CJ, Smith SM, Beckmann CF. Consistent resting-state networks across healthy subjects. *Proc Natl Acad Sci U S A* 2006; 103: 13848-13853.
- Danober L, Deransart C, Depaulis A, Vergnes M, Marescaux C. Pathophysiological mechanisms of genetic absence epilepsy in the rat. *Prog Neurobiol* 1998; 55: 27-57.
- Dasheiff RM. The first American epileptologists: William P. Spratling, MD, and Rosewell Park, MD. *Neurology* 1994; 44: 171-174.
- Debener S, Strobel A, Sorger B, Peters J, Kranczioch C, Engel AK, Goebel R. Improved quality of auditory event-related potentials recorded simultaneously with 3-T fMRI: removal of the ballistocardiogram artefact. *Neuroimage* 2007; 34: 587-597.
- Debener S, Herrmann CS. Integration of EEG and fMRI. Editorial. *Int J Psychophysiol* 2008; 67: 159-160.
- Debener S, Mullinger KJ, Niazy RK, Bowtell RW. Properties of the ballistocardiogram artefact as revealed by EEG recordings at 1.5, 3 and 7 T static magnetic field strength. *Int J Psychophysiol* 2008; 67: 189-199.
- Debets RM, van Veelen CW, Maquet P, van Huffelen AC, van Emde BW, Sadzot B, Overweg J, Velis DN, Dive D, Franck G. Quantitative analysis of 18/FDG-PET in the presurgical evaluation of patients suffering from refractory partial epilepsy. Comparison with CT, MRI, and combined subdural and depth. EEG. *Acta Neurochir Suppl (Wien)* 1990; 50: 88-94.
- deCurtis M, Avanzini G. Thalamic regulation of epileptic spike and wave discharges. *Funct Neurol* 1994; 9: 307-326.
- deCurtis M, Radici C, Forti M. Cellular mechanisms underlying spontaneous interictal spikes in an acute model of focal cortical epileptogenesis. *Neuroscience* 1999; 88: 107-117.
- Deichmann R, Josephs O, Hutton C, Corfield DR, Turner R. Compensation of susceptibility-induced BOLD sensitivity losses in echo-planar fMRI imaging. *Neuroimage* 2002; 15: 120-135.

## REFERENCES

- DeMartino F, Gentile F, Esposito F, Balsi M, Di SF, Goebel R, Formisano E. Classification of fMRI independent components using IC-fingerprints and support vector machine classifiers. *Neuroimage* 2007; 34: 177-194.
- Derchansky M, Jahromi SS, Mamani M, Shin DS, Sik A, Carlen PL. Transition to seizures in the isolated immature mouse hippocampus: a switch from dominant phasic inhibition to dominant phasic excitation. *J Physiol* 2008; 586: 477-494.
- deTisi J, Bell GS, Peacock JL, McEvoy AW, Harkness WF, Sander JW, Duncan JS. The long-term outcome of adult epilepsy surgery, patterns of seizure remission, and relapse: a cohort study. *Lancet* 2011; 378: 1388-1395.
- Detre JA, Sirven JI, Alsop DC, O'Connor MJ, French JA. Localization of subclinical ictal activity by functional magnetic resonance imaging: correlation with invasive monitoring. *Ann Neurol* 1995; 38: 618-624.
- Detre JA, Alsop DC, Aguirre GK, Sperling MR. Coupling of cortical and thalamic ictal activity in human partial epilepsy: demonstration by functional magnetic resonance imaging. *Epilepsia* 1996; 37: 657-661.
- Devor A, Tian P, Nishimura N, Teng IC, Hillman EM, Narayanan SN, Ulbert I, Boas DA, Kleinfeld D, Dale AM. Suppressed neuronal activity and concurrent arteriolar vasoconstriction may explain negative blood oxygenation level-dependent signal. *J Neurosci* 2007; 27: 4452-4459.
- Di Bonaventura C, Vaudano AE, Carni M, Pantano P, Nucciarelli V, Garreffa G, Maraviglia B, Prencipe M, Bozzao L, Manfredi M, Giallonardo AT. Long-term reproducibility of fMRI activation in epilepsy patients with Fixation Off Sensitivity. *Epilepsia* 2005; 46: 1149-1151.
- Di Bonaventura C, Carnfi M, Vaudano AE, Pantano P, Garreffa G, Le PE, Maraviglia B, Bozzao L, Manfredi M, Prencipe M, Giallonardo AT. Ictal hemodynamic changes in late-onset rasmussen encephalitis. *Ann Neurol* 2006a; 59: 432-433.
- Di Bonaventura C, Vaudano AE, Carni M, Pantano P, Nucciarelli V, Garreffa G, Maraviglia B, Prencipe M, Bozzao L, Manfredi M, Giallonardo AT. EEG/fMRI study of ictal and interictal epileptic activity: methodological issues and future perspectives in clinical practice. *Epilepsia* 2006b; 47 Suppl 5: 52-58.
- Diamantis A, Sidiropoulou K, Magiorkinis E. Epilepsy during the Middle Ages, the Renaissance and the Enlightenment. *J Neurol* 2010; 257: 691-698.
- Diehl B, Knecht S, Deppe M, Young C, Stodieck SR. Cerebral hemodynamic response to generalized spike-wave discharges. *Epilepsia* 1998; 39: 1284-1289.
- Disbrow EA, Slutsky DA, Roberts TP, Krubitzer LA. Functional MRI at 1.5 tesla: a comparison of the blood oxygenation level-dependent signal and electrophysiology. *Proc Natl Acad Sci U S A* 2000; 97: 9718-9723.
- Donaire A, Bargallo N, Falcon C, Maestro I, Carreno M, Setoain J, Rumia J, Fernandez S, Pintor L, Boget T. Identifying the structures involved in seizure generation using sequential analysis of ictal-fMRI data. *Neuroimage* 2009a; 47: 173-183.
- Donaire A, Falcon C, Carreno M, Bargallo N, Rumia J, Setoain J, Maestro I, Boget T, Pintor L, Agudo R, Falip M, Fernandez S. Sequential analysis of fMRI images: A new approach to study human epileptic networks. *Epilepsia* 2009b; 50: 2526-2537.
- Doss RC, Zhang W, Risse GL, Dickens DL. Lateralizing language with magnetic source imaging: validation based on the Wada test. *Epilepsia* 2009; 50: 2242-2248.
- Dowd CF, Dillon WP, Barbaro NM, Laxer KD. Magnetic resonance imaging of intractable complex partial seizures: pathologic and electroencephalographic correlation. *Epilepsia* 1991; 32: 454-459.
- DRABKIN IE. Soranus and his system of medicine. *Bull Hist Med* 1951; 25: 503-518.
- Duffy FH. Masturbation and clitoridectomy: A nineteenth century view. *JAMA* 1963; 186: 246-248.
- Duffy FH, Burchfiel JL, Lombroso CT. Brain electrical activity mapping (BEAM): a method for extending the clinical utility of EEG and evoked potential data. *Ann Neurol* 1979; 5: 309-321.
- Duncan JD, Moss SD, Bandy DJ, Manwaring K, Kaplan AM, Reiman EM, Chen K, Lawson MA, Wodrich DL. Use of positron emission tomography for presurgical



## REFERENCES

- localization of eloquent brain areas in children with seizures. *Pediatr Neurosurg* 1997a; 26: 144-156.
- Duncan JS. Imaging and epilepsy. *Brain* 1997; 120 ( Pt 2): 339-377.
- Duncan JS, Bartlett P, Barker GJ. Measurement of hippocampal T2 in epilepsy. *AJNR* 1997b; 18: 1791-1792.
- Duncan JS. Epilepsy surgery. *Clin Med* 2007; 7: 137-142.
- Duncan JS. Imaging in the surgical treatment of epilepsy. *Nat Rev Neurol* 2010; 6: 537-550.
- Duncan JS. The evolving classification of seizures and epilepsies. *Epilepsia* 2011a; 52: 1204-1205.
- Duncan JS. Epilepsy in 2010: Refinement of optimal medical and surgical treatments. *Nat Rev Neurol* 2011b; 7: 72-74.
- Duncan JS. Selecting patients for epilepsy surgery: synthesis of data. *Epilepsy Behav* 2011c; 20: 230-232.
- Eadie M. Louis Francois Bravais and Jacksonian epilepsy. *Epilepsia* 2010; 51: 1-6.
- Eadie MJ. A pathology of the animal spirits -- the clinical neurology of Thomas Willis (1621-1675). Part II -- disorders of intrinsically abnormal animal spirits. *J Clin Neurosci* 2003; 10: 146-157.
- Ebersole JS, Ebersole SM. Combining MEG and EEG source modeling in epilepsy evaluations. *J Clin Neurophysiol* 2010; 27: 360-371.
- Edelstein WA, Hutchison JM, Johnson G, Redpath T. Spin warp NMR imaging and applications to human whole-body imaging. *Phys Med Biol* 1980; 25: 751-756.
- Elferink JG. Epilepsy and its treatment in the ancient cultures of America. *Epilepsia* 1999; 40: 1041-1046.
- Ellingson ML, Liebenthal E, Spanaki MV, Prieto TE, Binder JR, Ropella KM. Ballistocardiogram artifact reduction in the simultaneous acquisition of auditory ERPS and fMRI. *Neuroimage* 2004; 22: 1534-1542.
- Engel J. Surgical treatment of the epilepsies. New York: Raven Press; 1993.
- Engel J, Jr. Classifications of the International League Against Epilepsy: time for reappraisal. *Epilepsia* 1998; 39: 1014-1017.
- Engel J, Jr. A proposed diagnostic scheme for people with epileptic seizures and with epilepsy: report of the ILAE Task Force on Classification and Terminology. *Epilepsia* 2001; 42: 796-803.
- Engel J, Jr. Report of the ILAE classification core group. *Epilepsia* 2006; 47: 1558-1568.
- Engel J. Epilepsy: A Comprehensive Textbook. Lippincott Williams & Wilkins; 2007.
- Engel J, Jr., Bragin A, Staba R, Mody I. High-frequency oscillations: what is normal and what is not? *Epilepsia* 2009; 50: 598-604.
- Esposito F, Seifritz E, Formisano E, Morrone R, Scarabino T, Tedeschi G, Cirillo S, Goebel R, Di SF. Real-time independent component analysis of fMRI time-series. *Neuroimage* 2003; 20: 2209-2224.
- Evans P. Henri Ey's concepts of the organization of consciousness and its disorganization: an extension of Jacksonian theory. *Brain* 1972; 95: 413-440.
- Faingold CL. Brainstem Networks: Reticulo-Cortical Synchronization in Generalized Convulsive Seizures. In: Noebels JL, Avoli M, Rogawski MA, Olsen RW, Delgado-Escueta AV, editors. *Jasper's Basic Mechanisms of the Epilepsies*. Oxford University Press; 2012.
- Faraci FM, Breese KR. Nitric oxide mediates vasodilatation in response to activation of N-methyl-D-aspartate receptors in brain. *Circ Res* 1993; 72: 476-480.
- Federico P, Archer JS, Abbott DF, Jackson GD. Cortical/subcortical BOLD changes associated with epileptic discharges: an EEG-fMRI study at 3 T. *Neurology* 2005a; 64: 1125-1130.
- Federico P, Abbott DF, Briellmann RS, Harvey AS, Jackson GD. Functional MRI of the pre-ictal state. *Brain* 2005b; 128: 1811-1817.
- Fergus A, Lee KS. Regulation of cerebral microvessels by glutamatergic mechanisms. *Brain Res* 1997; 754: 35-45.

## REFERENCES

- Ferrie CD. Terminology and organization of seizures and epilepsies: radical changes not justified by new evidence. *Epilepsia* 2010; 51: 713-714.
- Figley CR, Stroman PW. The role(s) of astrocytes and astrocyte activity in neurometabolism, neurovascular coupling, and the production of functional neuroimaging signals. *Eur J Neurosci* 2011; 33: 577-588.
- Fisher RS, van Emde BW, Blume W, Elger C, Genton P, Lee P, Engel J, Jr. Epileptic seizures and epilepsy: definitions proposed by the International League Against Epilepsy (ILAE) and the International Bureau for Epilepsy (IBE). *Epilepsia* 2005; 46: 470-472.
- Focke NK, Symms MR, Burdett JL, Duncan JS. Voxel-based analysis of whole brain FLAIR at 3T detects focal cortical dysplasia. *Epilepsia* 2008; 49: 786-793.
- Focke NK, Bonelli SB, Yogarajah M, Scott C, Symms MR, Duncan JS. Automated normalized FLAIR imaging in MRI-negative patients with refractory focal epilepsy. *Epilepsia* 2009; 50: 1484-1490.
- Foldvary N, Klem G, Hammel J, Bingaman W, Najm I, Luders H. The localizing value of ictal EEG in focal epilepsy. *Neurology* 2001; 57: 2022-2028.
- Foldvary-Schaefer N, Unnwongse K. Localizing and lateralizing features of auras and seizures. *Epilepsy Behav* 2011; 20: 160-166.
- Forsgren L, Bucht G, Eriksson S, Bergmark L. Incidence and clinical characterization of unprovoked seizures in adults: a prospective population-based study. *Epilepsia* 1996; 37: 224-229.
- Forti M, Biella G, Caccia S, de CM. Persistent excitability changes in the piriform cortex of the isolated guinea-pig brain after transient exposure to bicuculline. *Eur J Neurosci* 1997; 9: 435-451.
- Fountain NB, Bear J, Bertram EH, III, Lothman EW. Responses of deep entorhinal cortex are epileptiform in an electrogenic rat model of chronic temporal lobe epilepsy. *J Neurophysiol* 1998; 80: 230-240.
- Fox MD, Zhang D, Snyder AZ, Raichle ME. The global signal and observed anticorrelated resting state brain networks. *J Neurophysiol* 2009; 101: 3270-3283.
- Fox PT, Raichle ME, Mintun MA, Dence C. Nonoxidative glucose consumption during focal physiologic neural activity. *Science* 1988; 241: 462-464.
- Frahm J, Kruger G, Merboldt KD, Kleinschmidt A. Dynamic uncoupling and recoupling of perfusion and oxidative metabolism during focal brain activation in man. *Magn Reson Med* 1996; 35: 143-148.
- Friedman L, Glover GH. Reducing interscanner variability of activation in a multicenter fMRI study: controlling for signal-to-fluctuation-noise-ratio (SFNR) differences. *Neuroimage* 2006; 33: 471-481.
- Friston KJ, Jezzard P, Turner R. Analysis of functional MRI time series. *Human Brain Mapping* 1994; 1: 153-171.
- Friston KJ, Ashburner J, Frith C, Poline JB, Heather JD, Frackowiak RSJ. Spatial Registration and Normalization of Images. *Human Brain Mapping* 1995a; 3: 165-189.
- Friston KJ, Holmes AP, Worsley KJ, Poline JB, Firth CD, Frackowiak RSJ. Statistical parametric maps in functional imaging: a general linear approach. *Hum Brain Mapp* 1995b; 2: 189-210.
- Friston KJ. Statistical parametric mapping and other analyses of functional imaging data. In: Toga AW, Mazziotta JC, editors. *Brain Mapping: The Methods*. San Diego: Academic Press; 1996. p. 363-96.
- Friston KJ, Williams S, Howard R, Frackowiak RS, Turner R. Movement-related effects in fMRI time-series. *Magn Reson Med* 1996; 35: 346-355.
- Friston KJ, Fletcher P, Josephs O, Holmes A, Rugg MD, Turner R. Event-related fMRI: characterizing differential responses. *Neuroimage* 1998; 7: 30-40.
- Friston KJ, Holmes AP, Worsley KJ. How many subjects constitute a study? *Neuroimage* 1999a; 10: 1-5.
- Friston KJ, Zarahn E, Josephs O, Henson RN, Dale AM. Stochastic designs in event-related fMRI. *Neuroimage* 1999b; 10: 607-619.

## REFERENCES

- Fromm GH, Bond HW. SLOW CHANGES IN THE ELECTROCORTICOGRAM AND THE ACTIVITY OF CORTICAL NEURONS. *Electroencephalogr Clin Neurophysiol* 1964; 17: 520-523.
- Fromm GH, Bond HW. The relationship between neuron activity and cortical steady potentials. *Electroencephalogr Clin Neurophysiol* 1967; 22: 159-166.
- Frye RE, Rezaie R, Papanicolaou AC. Functional Neuroimaging of Language Using Magnetoencephalography. *Phys Life Rev* 2009; 6: 1-10.
- Fukuda M, Masuda H, Honma J, Kameyama S, Tanaka R. Ictal SPECT analyzed by three-dimensional stereotactic surface projection in frontal lobe epilepsy patients. *Epilepsy Res* 2006; 68: 95-102.
- Garcia-Albea RE. [Aretaeus of Cappadocia (2nd century AD) and the earliest neurological descriptions]. *Rev Neurol* 2009; 48: 322-327.
- Gastaut H. Clinical and electroencephalographical classification of epileptic seizures. *Epilepsia* 1970; 11: 102-113.
- Gavaret M, McGonigal A, Badier JM, Chauvel P. Physiology of frontal lobe seizures: pre-ictal, ictal and inter-ictal relationships. *Suppl Clin Neurophysiol* 2004; 57: 400-407.
- Geneslaw AS, Zhao M, Ma H, Schwartz TH. Tissue hypoxia correlates with intensity of interictal spikes. *J Cereb Blood Flow Metab* 2011; 31: 1394-1402.
- Gloor P. Generalized cortico-reticular epilepsies. Some considerations on the pathophysiology of generalized bilaterally synchronous spike and wave discharge. *Epilepsia* 1968; 9: 249-263.
- Gloor P. Neurophysiological basis of generalized seizures termed centrencephalic. In: Gastaut H, Jasper HH, Bancaud J, Walgreny A, editors. *The physiopathogenesis of the epilepsies*. Springfield, III: Charles C Thomas Publisher; 1969. p. 209-36.
- Gloor P, Avoli M, Kostopoulos G. Thalamocortical relationships in generalized epilepsy with bilateral synchronous spike and wave discharges. In: Avoli M, Gloor P, Kostopoulos G, Naquet R, editors. *Generalized Epilepsy. Neurobiological Approaches*. Boston: Birkhauser; 1990. p. 190-212.
- Glover GH, Lai S. Self-navigated spiral fMRI: interleaved versus single-shot. *Magn Reson Med* 1998; 39: 361-368.
- Glover GH, Li TQ, Ress D. Image-based method for retrospective correction of physiological motion effects in fMRI: RETROICOR. *Magn Reson Med* 2000; 44: 162-167.
- Glover GH, Law CS. Spiral-in/out BOLD fMRI for increased SNR and reduced susceptibility artifacts. *Magn Reson Med* 2001; 46: 515-522.
- Gnatkovsky V, Librizzi L, Trombin F, de CM. Fast activity at seizure onset is mediated by inhibitory circuits in the entorhinal cortex in vitro. *Ann Neurol* 2008; 64: 674-686.
- Goense JB, Logothetis NK. Neurophysiology of the BOLD fMRI signal in awake monkeys. *Curr Biol* 2008; 18: 631-640.
- Goense JB, Ku SP, Merkle H, Tolias AS, Logothetis NK. fMRI of the temporal lobe of the awake monkey at 7 T. *Neuroimage* 2008; 39: 1081-1093.
- Goldman RI, Stern JM, Engel J, Jr., Cohen MS. Acquiring simultaneous EEG and functional MRI. *Clin Neurophysiol* 2000; 111: 1974-1980.
- Gotman J. Quantitative measurements of epileptic spike morphology in the human EEG. *Electroencephalogr Clin Neurophysiol* 1980; 48: 551-557.
- Gotman J. Automatic recognition of interictal spikes. *Electroencephalogr Clin Neurophysiol Suppl* 1985; 37: 93-114.
- Gotman J, Grova C, Bagshaw A, Kobayashi E, Aghakhani Y, Dubeau F. Generalized epileptic discharges show thalamocortical activation and suspension of the default state of the brain. *Proc Natl Acad Sci U S A* 2005; 102: 15236-15240.
- Gowers WR. *Epilepsy and Other Chronic Convulsive Diseases*. Churchill, London; 1881.
- GRANIT R, KERNELL D, SMITH RS. Delayed depolarization and the repetitive response to intracellular stimulation of mammalian motoneurons. *J Physiol* 1963; 168: 890-910.

## REFERENCES

- Gray CM, Maldonado PE, Wilson M, McNaughton B. Tetrodes markedly improve the reliability and yield of multiple single-unit isolation from multi-unit recordings in cat striate cortex. *J Neurosci Methods* 1995; 63: 43-54.
- Green RM. *A Translation of Galen's Hygiene*. Illinois: Springfield; 1951.
- Grouiller F, Thornton RC, Groening K, Spinelli L, Duncan JS, Schaller K, Siniatchkin M, Lemieux L, Seeck M, Michel CM, Vulliemoz S. With or without spikes: localization of focal epileptic activity by simultaneous electroencephalography and functional magnetic resonance imaging. *Brain* 2011; 134: 2867-2886.
- Grover FS, Buchwald JS. Correlation of cell size with amplitude of background fast activity in specific brain nuclei. *J Neurophysiol* 1970; 33: 160-171.
- Gusnard DA, Akbudak E, Shulman GL, Raichle ME. Medial prefrontal cortex and self-referential mental activity: relation to a default mode of brain function. *Proc Natl Acad Sci U S A* 2001; 98: 4259-4264.
- Guye M, Ranjeva JP, Bartolomei F, Confort-Gouny S, McGonigal A, Regis J, Chauvel P, Cozzone PJ. What is the significance of interictal water diffusion changes in frontal lobe epilepsies? *Neuroimage* 2007; 35: 28-37.
- Haas HL, Jefferys JG. Low-calcium field burst discharges of CA1 pyramidal neurones in rat hippocampal slices. *J Physiol* 1984; 354: 185-201.
- Haas HL, Jefferys JG, Slater NT, Carpenter DO. Modulation of low calcium induced field bursts in the hippocampus by monoamines and cholinomimetics. *Pflugers Arch* 1984; 400: 28-33.
- Hajnal JV, Myers R, Oatridge A, Schwieso JE, Young IR, Bydder GM. Artifacts due to stimulus correlated motion in functional imaging of the brain. *Magn Reson Med* 1994; 31: 283-291.
- Halgren E, Marinkovic K, Chauvel P. Generators of the late cognitive potentials in auditory and visual oddball tasks. *Electroencephalogr Clin Neurophysiol* 1998; 106: 156-164.
- Hamandi K, Salek-Haddadi A, Laufs H, Liston A, Friston K, Fish DR, Duncan JS, Lemieux L. EEG-fMRI of idiopathic and secondarily generalized epilepsies. *Neuroimage* 2006; 31: 1700-1710.
- Hamandi K, Laufs H, Noth U, Carmichael DW, Duncan JS, Lemieux L. BOLD and perfusion changes during epileptic generalised spike wave activity. *Neuroimage* 2008; 39: 608-618.
- Harada Y, Takahashi T. The calcium component of the action potential in spinal motoneurons of the rat. *J Physiol* 1983; 335: 89-100.
- Harris KD, Henze DA, Csicsvari J, Hirase H, Buzsaki G. Accuracy of tetrode spike separation as determined by simultaneous intracellular and extracellular measurements. *J Neurophysiol* 2000; 84: 401-414.
- Hart YM, Sander JW, Johnson AL, Shorvon SD. National General Practice Study of Epilepsy: recurrence after a first seizure. *Lancet* 1990; 336: 1271-1274.
- Hauser WA, Annegers JF, Kurland LT. Incidence of epilepsy and unprovoked seizures in Rochester, Minnesota: 1935-1985. *Epilepsia* 1993; 34: 453-468.
- Hauser WA, Beghi E. First seizure definitions and worldwide incidence and mortality. *Epilepsia* 2008; 49 Suppl 1: 8-12.
- Hawco CS, Bagshaw AP, Lu Y, Dubeau F, Gotman J. BOLD changes occur prior to epileptic spikes seen on scalp EEG. *Neuroimage* 2007; 35: 1450-1458.
- Head H. Aphasia: An Historical Review: The Hughlings Jackson Lecture for 1920. *Proc R Soc Med* 1921; 14: 1-22.
- Higashi H, Tanaka E, Inokuchi H, Nishi S. Ionic mechanisms underlying the depolarizing and hyperpolarizing afterpotentials of single spike in guinea-pig cingulate cortical neurons. *Neuroscience* 1993; 55: 129-138.
- Hippocrates. *Hippocrates, with an English Translation by W H S Jones*. London: William Heinemann Ltd.; 1923.
- Hitiris N, Brodie MJ. Evidence-based treatment of idiopathic generalized epilepsies with older antiepileptic drugs. *Epilepsia* 2005; 46 Suppl 9: 149-153.

## REFERENCES

- Hoffmann A, Jager L, Werhahn KJ, Jaschke M, Noachtar S, Reiser M. Electroencephalography during functional echo-planar imaging: detection of epileptic spikes using post-processing method. *Magn Reson Med* 2000; 44: 791-798.
- Hu X, Le TH, Ugurbil K. Evaluation of the early response in fMRI in individual subjects using short stimulus duration. *Magn Reson Med* 1997; 37: 877-884.
- Huberfeld G, Habert MO, Clemenceau S, Maksud P, Baulac M, Adam C. Ictal brain hyperperfusion contralateral to seizure onset: the SPECT mirror image. *Epilepsia* 2006; 47: 123-133.
- Huberfeld G, Menendez dIP, Pallud J, Cohen I, Le Van QM, Adam C, Clemenceau S, Baulac M, Miles R. Glutamatergic pre-ictal discharges emerge at the transition to seizure in human epilepsy. *Nat Neurosci* 2011; 14: 627-634.
- Huguenard JR, Prince DA. Clonazepam suppresses GABAB-mediated inhibition in thalamic relay neurons through effects in nucleus reticularis. *J Neurophysiol* 1994; 71: 2576-2581.
- Hutt SJ, Gilbert S. Effects of evoked spike-wave discharges upon short term memory in patients with epilepsy. *Cortex* 1980; 16: 445-457.
- Hyder F, Renken R, Kennan RP, Rothman DL. Quantitative multi-modal functional MRI with blood oxygenation level dependent exponential decays adjusted for flow attenuated inversion recovery (BOLD-ED AFFAIR). *Magn Reson Imaging* 2000; 18: 227-235.
- Hyvarinen A, Oja E. Independent component analysis: algorithms and applications. *Neural Netw* 2000; 13: 411-430.
- Iannetti GD, Di BC, Pantano P, Giallonardo AT, Romanelli PL, Bozzao L, Manfredi M, Ricci GB. fMRI/EEG in paroxysmal activity elicited by elimination of central vision and fixation. *Neurology* 2002; 58: 976-979.
- ILAE. Proposal for revised clinical and electroencephalographic classification of epileptic seizures. From the Commission on Classification and Terminology of the International League Against Epilepsy. *Epilepsia* 1981; 22: 489-501.
- ILAE. Proposal for classification of epilepsies and epileptic syndromes. Commission on Classification and Terminology of the International League Against Epilepsy. *Epilepsia* 1985; 26: 268-278.
- ILAE. Proposal for revised classification of epilepsies and epileptic syndromes. Commission on Classification and Terminology of the International League Against Epilepsy. *Epilepsia* 1989; 30: 389-399.
- ILAE. ILAE classification of epilepsies: its applicability and practical value of different diagnostic categories. *Osservatorio Regionale per L'Epilessia (OREp), Lombardy. Epilepsia* 1996; 37: 1051-1059.
- ILAE. Guidelines for neuroimaging evaluation of patients with uncontrolled epilepsy considered for surgery. *Epilepsia* 1998; 39: 1375-1376.
- Ives JR, Warach S, Schmitt F, Edelman RR, Schomer DL. Monitoring the patient's EEG during echo planar MRI. *Electroencephalogr Clin Neurophysiol* 1993; 87: 417-420.
- Jackson JH. Selected writings of John Hughlings Jackson. New York: Basic Books; 1958.
- Jackson G. Classification of the epilepsies 2011. *Epilepsia* 2011; 52: 1203-1204.
- Jackson GD, Connelly A, Cross JH, Gordon I, Gadian DG. Functional magnetic resonance imaging of focal seizures. *Neurology* 1994; 44: 850-856.
- Jacobs J, Kobayashi E, Boor R, Muhle H, Stephan W, Hawco C, Dubeau F, Jansen O, Stephani U, Gotman J, Siniatchkin M. Hemodynamic responses to interictal epileptiform discharges in children with symptomatic epilepsy. *Epilepsia* 2007; 48: 2068-2078.
- Jacobs J, LeVan P, Chander R, Hall J, Dubeau F, Gotman J. Interictal high-frequency oscillations (80-500 Hz) are an indicator of seizure onset areas independent of spikes in the human epileptic brain. *Epilepsia* 2008a; 49: 1893-1907.
- Jacobs J, Rohr A, Moeller F, Boor R, Kobayashi E, LeVan MP, Stephani U, Gotman J, Siniatchkin M. Evaluation of epileptogenic networks in children with tuberous sclerosis complex using EEG-fMRI. *Epilepsia* 2008b; 49: 816-825.

## REFERENCES

- Jacobs J, LeVan P, Moeller F, Boor R, Stephani U, Gotman J, Siniatchkin M. Hemodynamic changes preceding the interictal EEG spike in patients with focal epilepsy investigated using simultaneous EEG-fMRI. *Neuroimage* 2009; 45: 1220-1231.
- Jansen M, White TP, Mullinger KJ, Liddle EB, Gowland PA, Francis ST, Bowtell R, Liddle PF. Motion-related artefacts in EEG predict neuronally plausible patterns of activation in fMRI data. *Neuroimage* 2012; 59: 261-270.
- Jefferys JG. Gap junctions and diseases of the nervous system. *Trends Neurosci* 1995a; 18: 520-521.
- Jefferys JG. Nonsynaptic modulation of neuronal activity in the brain: electric currents and extracellular ions. *Physiol Rev* 1995b; 75: 689-723.
- Jobst BC, Siegel AM, Thadani VM, Roberts DW, Rhodes HC, Williamson PD. Intractable seizures of frontal lobe origin: clinical characteristics, localizing signs, and results of surgery. *Epilepsia* 2000; 41: 1139-1152.
- Johnston D, Hablitz JJ, Wilson WA. Voltage clamp discloses slow inward current in hippocampal burst-firing neurones. *Nature* 1980; 286: 391-393.
- Jueptner M, Weiller C. Review: does measurement of regional cerebral blood flow reflect synaptic activity? Implications for PET and fMRI. *Neuroimage* 1995; 2: 148-156.
- Juergens E, Guettler A, Eckhorn R. Visual stimulation elicits locked and induced gamma oscillations in monkey intracortical- and EEG-potentials, but not in human EEG. *Exp Brain Res* 1999; 129: 247-259.
- Kameyama S, Masuda H, Murakami H. Ictogenesis and symptomatogenesis of gelastic seizures in hypothalamic hamartomas: an ictal SPECT study. *Epilepsia* 2010; 51: 2270-2279.
- Kaplan PW, Lesser RP. *Noninvasive EEG*. Baltimore: Williams & Wilkins; 1996.
- Karbowski K. Samuel Auguste Tissot (1728-1797). *J Neurol* 2001; 248: 1109-1110.
- Khalsa SS, Moore SA, Van Hoesen GW. Hughlings Jackson and the role of the entorhinal cortex in temporal lobe epilepsy: from patient A to Doctor Z. *Epilepsy Behav* 2006; 9: 524-531.
- Khosravani H, Mehrotra N, Rigby M, Hader WJ, Pinnegar CR, Pillay N, Wiebe S, Federico P. Spatial localization and time-dependant changes of electrographic high frequency oscillations in human temporal lobe epilepsy. *Epilepsia* 2009; 50: 605-616.
- Kida I, Kennan RP, Rothman DL, Behar KL, Hyder F. High-resolution CMR(O2) mapping in rat cortex: a multiparametric approach to calibration of BOLD image contrast at 7 Tesla. *J Cereb Blood Flow Metab* 2000; 20: 847-860.
- Killory BD, Bai X, Negishi M, Vega C, Spann MN, Vestal M, Guo J, Berman R, Danielson N, Trejo J, Shisler D, Novotny EJ, Jr., Constable RT, Blumenfeld H. Impaired attention and network connectivity in childhood absence epilepsy. *Neuroimage* 2011.
- Kim LG, Johnson TL, Marson AG, Chadwick DW. Prediction of risk of seizure recurrence after a single seizure and early epilepsy: further results from the MESS trial. *Lancet Neurol* 2006; 5: 317-322.
- Kim U, Sanchez-Vives MV, McCormick DA. Functional dynamics of GABAergic inhibition in the thalamus. *Science* 1997; 278: 130-134.
- Knake S, Halgren E, Shiraishi H, Hara K, Hamer HM, Grant PE, Carr VA, Foxe D, Camposano S, Busa E, Witzel T, Hamalainen MS, Ahlfors SP, Bromfield EB, Black PM, Bourgeois BF, Cole AJ, Cosgrove GR, Dworetzky BA, Madsen JR, Larsson PG, Schomer DL, Thiele EA, Dale AM, Rosen BR, Stufflebeam SM. The value of multichannel MEG and EEG in the presurgical evaluation of 70 epilepsy patients. *Epilepsy Res* 2006; 69: 80-86.
- Knowlton RC, Laxer KD, Ende G, Hawkins RA, Wong ST, Matson GB, Rowley HA, Fein G, Weiner MW. Presurgical multimodality neuroimaging in electroencephalographic lateralized temporal lobe epilepsy. *Ann Neurol* 1997; 42: 829-837.
- Knowlton RC. The role of FDG-PET, ictal SPECT, and MEG in the epilepsy surgery evaluation. *Epilepsy Behav* 2006; 8: 91-101.

## REFERENCES

- Knowlton RC, Elgavish RA, Bartolucci A, Ojha B, Limdi N, Blount J, Burneo JG, Ver HL, Paige L, Faught E, Kankirawatana P, Riley K, Kuzniecky R. Functional imaging: II. Prediction of epilepsy surgery outcome. *Ann Neurol* 2008a; 64: 35-41.
- Knowlton RC, Elgavish RA, Limdi N, Bartolucci A, Ojha B, Blount J, Burneo JG, Ver HL, Paige L, Faught E, Kankirawatana P, Riley K, Kuzniecky R. Functional imaging: I. Relative predictive value of intracranial electroencephalography. *Ann Neurol* 2008b; 64: 25-34.
- Knowlton RC, Razdan SN, Limdi N, Elgavish RA, Killen J, Blount J, Burneo JG, Ver HL, Paige L, Faught E, Kankirawatana P, Bartolucci A, Riley K, Kuzniecky R. Effect of epilepsy magnetic source imaging on intracranial electrode placement. *Ann Neurol* 2009; 65: 716-723.
- Kobayashi E, Hawco CS, Grova C, Dubeau F, Gotman J. Widespread and intense BOLD changes during brief focal electrographic seizures. *Neurology* 2006a; 66: 1049-1055.
- Kobayashi E, Bagshaw AP, Grova C, Dubeau F, Gotman J. Negative BOLD responses to epileptic spikes. *Hum Brain Mapp* 2006b; 27: 488-497.
- Kobayashi E, Bagshaw AP, Grova C, Gotman J, Dubeau F. Grey matter heterotopia: what EEG-fMRI can tell us about epileptogenicity of neuronal migration disorders. *Brain* 2006c; 129: 366-374.
- Kobayashi E, Bagshaw AP, Benar CG, Aghakhani Y, Andermann F, Dubeau F, Gotman J. Temporal and extratemporal BOLD responses to temporal lobe interictal spikes. *Epilepsia* 2006d; 47: 343-354.
- Kobayashi E, Bagshaw AP, Gotman J, Dubeau F. Metabolic correlates of epileptic spikes in cerebral cavernous angiomas. *Epilepsy Res* 2007; 73: 98-103.
- Kobayashi E, Grova C, Tyvaert L, Dubeau F, Gotman J. Structures involved at the time of temporal lobe spikes revealed by interindividual group analysis of EEG/fMRI data. *Epilepsia* 2009; 50: 2549-2556.
- Kobayashi M, Inoue T, Matsuo R, Masuda Y, Hidaka O, Kang Y, Morimoto T. Role of calcium conductances on spike afterpotentials in rat trigeminal motoneurons. *J Neurophysiol* 1997; 77: 3273-3283.
- Koehler PJ. Brown-Sequard's spinal epilepsy. *Med Hist* 1994; 38: 189-203.
- Konings MK, Bartels LW, Smits HF, Bakker CJ. Heating around intravascular guidewires by resonating RF waves. *J Magn Reson Imaging* 2000; 12: 79-85.
- Kotsopoulos IA, van MT, Kessels FG, de Krom MC, Knottnerus JA. Systematic review and meta-analysis of incidence studies of epilepsy and unprovoked seizures. *Epilepsia* 2002; 43: 1402-1409.
- Krakov K, Woermann FG, Symms MR, Allen PJ, Lemieux L, Barker GJ, Duncan JS, Fish DR. EEG-triggered functional MRI of interictal epileptiform activity in patients with partial seizures. *Brain* 1999; 122 ( Pt 9): 1679-1688.
- Krakov K, Allen PJ, Lemieux L, Symms MR, Fish DR. Methodology: EEG-correlated fMRI. *Adv Neurol* 2000a; 83: 187-201.
- Krakov K, Allen PJ, Symms MR, Lemieux L, Josephs O, Fish DR. EEG recording during fMRI experiments: image quality. *Hum Brain Mapp* 2000b; 10: 10-15.
- Krakov K, Baxendale SA, Maguire EA, Krishnamoorthy ES, Lemieux L, Scott CA, Smith SJ. Fixation-off sensitivity as a model of continuous epileptiform discharges: electroencephalographic, neuropsychological and functional MRI findings. *Epilepsy Res* 2000c; 42: 1-6.
- Krings T, Topper R, Reinges MH, Foltys H, Spetzger U, Chiappa KH, Gilsbach JM, Thron A. Hemodynamic changes in simple partial epilepsy: a functional MRI study. *Neurology* 2000; 54: 524-527.
- Kubota F, Kikuchi S, Ito M, Shibata N, Akata T, Takahashi A, Sasaki T, Oya N, Aoki J. Ictal brain hemodynamics in the epileptic focus caused by a brain tumor using functional magnetic resonance imaging (fMRI). *Seizure* 2000; 9: 585-589.
- Kumari V, Peters ER, Fannon D, Antonova E, Premkumar P, Anilkumar AP, Williams SC, Kuipers E. Dorsolateral prefrontal cortex activity predicts responsiveness to cognitive-behavioral therapy in schizophrenia. *Biol Psychiatry* 2009; 66: 594-602.

## REFERENCES

- Kuzniecky R, Murro A, King D, Morawetz R, Smith J, Powers R, Yaghmai F, Faught E, Gallagher B, Snead OC. Magnetic resonance imaging in childhood intractable partial epilepsies: pathologic correlations. *Neurology* 1993; 43: 681-687.
- Kwan P, Brodie MJ. Early identification of refractory epilepsy. *N Engl J Med* 2000; 342: 314-319.
- Kwan P, Sander JW. The natural history of epilepsy: an epidemiological view. *J Neurol Neurosurg Psychiatry* 2004; 75: 1376-1381.
- Kwong KK, Belliveau JW, Chesler DA, Goldberg IE, Weisskoff RM, Poncelet BP, Kennedy DN, Hoppel BE, Cohen MS, Turner R, . Dynamic magnetic resonance imaging of human brain activity during primary sensory stimulation. *Proc Natl Acad Sci U S A* 1992; 89: 5675-5679.
- la Fougere C, Rominger A, Forster S, Geisler J, Bartenstein P. PET and SPECT in epilepsy: a critical review. *Epilepsy Behav* 2009; 15: 50-55.
- Labate A, Briellmann RS, Abbott DF, Waites AB, Jackson GD. Typical childhood absence seizures are associated with thalamic activation. *Epileptic Disord* 2005; 7: 373-377.
- Lachaux JP, Rudrauf D, Kahane P. Intracranial EEG and human brain mapping. *J Physiol Paris* 2003; 97: 613-628.
- Lai CW, Lai YH. History of epilepsy in Chinese traditional medicine. *Epilepsia* 1991; 32: 299-302.
- Lama A, vanWijngaarden D. Boerhaave: a brilliant mind and a virtuous character. *Rev Med Chil* 2002; 130: 1067-1072.
- Langslow DR. *Medical Latin in the Roman Empire*. Oxford: Oxford University Press; 2000.
- Laufs H, Krakow K, Sterzer P, Eger E, Beyerle A, Salek-Haddadi A, Kleinschmidt A. Electroencephalographic signatures of attentional and cognitive default modes in spontaneous brain activity fluctuations at rest. *Proc Natl Acad Sci U S A* 2003; 100: 11053-11058.
- Laufs H, Lengler U, Hamandi K, Kleinschmidt A, Krakow K. Linking generalized spike-and-wave discharges and resting state brain activity by using EEG/fMRI in a patient with absence seizures. *Epilepsia* 2006; 47: 444-448.
- Laufs H, Duncan JS. Electroencephalography/functional MRI in human epilepsy: what it currently can and cannot do. *Curr Opin Neurol* 2007; 20: 417-423.
- Laufs H, Walker MC, Lund TE. Brain activation and hypothalamic functional connectivity during human non-rapid eye movement sleep: an EEG/fMRI study'--its limitations and an alternative approach. *Brain* 2007a; 130: e75.
- Laufs H, Hamandi K, Salek-Haddadi A, Kleinschmidt AK, Duncan JS, Lemieux L. Temporal lobe interictal epileptic discharges affect cerebral activity in "default mode" brain regions. *Hum Brain Mapp* 2007b; 28: 1023-1032.
- Laufs H, Daunizeau J, Carmichael DW, Kleinschmidt A. Recent advances in recording electrophysiological data simultaneously with magnetic resonance imaging. *Neuroimage* 2008; 40: 515-528.
- Laufs H, Richardson MP, Salek-Haddadi A, Vollmar C, Duncan JS, Gale K, Lemieux L, Loscher W, Koepp MJ. Converging PET and fMRI evidence for a common area involved in human focal epilepsies. *Neurology* 2011; 77: 904-910.
- Lauterbur PC. Image formation by induced local interactions. Examples employing nuclear magnetic resonance. 1973. *Clin Orthop Relat Res* 1989; 3-6.
- Lazeyras F, Blanke O, Zimine I, Delavelle J, Perrig SH, Seeck M. MRI, (1)H-MRS, and functional MRI during and after prolonged nonconvulsive seizure activity. *Neurology* 2000a; 55: 1677-1682.
- Lazeyras F, Blanke O, Perrig S, Zimine I, Golay X, Delavelle J, Michel CM, de TN, Villemure JG, Seeck M. EEG-triggered functional MRI in patients with pharmacoresistant epilepsy. *J Magn Reson Imaging* 2000b; 12: 177-185.
- Lee BI, Heo K, Kim JS, Kim OJ, Park SA, Lim SR, Kim DI, Yoon PH, Kim DK. Syndromic diagnosis at the epilepsy clinic: role of MRI in lobar epilepsies. *Epilepsia* 2002; 43: 496-504.



## REFERENCES

- Lee SK, Kim JY, Hong KS, Nam HW, Park SH, Chung CK. The clinical usefulness of ictal surface EEG in neocortical epilepsy. *Epilepsia* 2000; 41: 1450-1455.
- Lee SK, Lee SY, Yun CH, Lee HY, Lee JS, Lee DS. Ictal SPECT in neocortical epilepsies: clinical usefulness and factors affecting the pattern of hyperperfusion. *Neuroradiology* 2006; 48: 678-684.
- Legatt AD, Arezzo J, Vaughan HG, Jr. Averaged multiple unit activity as an estimate of phasic changes in local neuronal activity: effects of volume-conducted potentials. *J Neurosci Methods* 1980; 2: 203-217.
- Lemieux L, Allen PJ, Franconi F, Symms MR, Fish DR. Recording of EEG during fMRI experiments: patient safety. *Magn Reson Med* 1997; 38: 943-952.
- Lemieux L, Salek-Haddadi A, Josephs O, Allen P, Toms N, Scott C, Krakow K, Turner R, Fish DR. Event-related fMRI with simultaneous and continuous EEG: description of the method and initial case report. *Neuroimage* 2001; 14: 780-787.
- Lemieux L, Salek-Haddadi A, Lund TE, Laufs H, Carmichael D. Modelling large motion events in fMRI studies of patients with epilepsy. *Magn Reson Imaging* 2007; 25: 894-901.
- Lemieux L, Laufs H, Carmichael D, Paul JS, Walker MC, Duncan JS. Noncanonical spike-related BOLD responses in focal epilepsy. *Hum Brain Mapp* 2008; 29: 329-345.
- Lennie P. The cost of cortical computation. *Curr Biol* 2003; 13: 493-497.
- Lerner JT, Salamon N, Hauptman JS, Velasco TR, Hemb M, Wu JY, Sankar R, Donald SW, Engel J, Jr., Fried I, Cepeda C, Andre VM, Levine MS, Miyata H, Yong WH, Vinters HV, Mathern GW. Assessment and surgical outcomes for mild type I and severe type II cortical dysplasia: a critical review and the UCLA experience. *Epilepsia* 2009; 50: 1310-1335.
- LeVan Quyen M, Martinerie J, Navarro V, Baulac AM, Varela FJ. Characterizing neurodynamic changes before seizures. *J Clin Neurophysiol* 2001a; 18: 191-208.
- LeVan Quyen M, Martinerie J, Navarro V, Boon P, D'Have M, Adam C, Renault B, Varela F, Baulac M. Anticipation of epileptic seizures from standard EEG recordings. *Lancet* 2001b; 357: 183-188.
- LeVan P, Gotman J. Independent component analysis as a model-free approach for the detection of BOLD changes related to epileptic spikes: a simulation study. *Hum Brain Mapp* 2009; 30: 2021-2031.
- LeVan P, Tyvaert L, Gotman J. Modulation by EEG features of BOLD responses to interictal epileptiform discharges. *Neuroimage* 2010a; 50: 15-26.
- LeVan P, Tyvaert L, Moeller F, Gotman J. Independent component analysis reveals dynamic ictal BOLD responses in EEG-fMRI data from focal epilepsy patients. *Neuroimage* 2010b; 49: 366-378.
- Lhatoo SD, Solomon JK, McEvoy AW, Kitchen ND, Shorvon SD, Sander JW. A prospective study of the requirement for and the provision of epilepsy surgery in the United Kingdom. *Epilepsia* 2003; 44: 673-676.
- Li J, Iadecola C. Nitric oxide and adenosine mediate vasodilation during functional activation in cerebellar cortex. *Neuropharmacology* 1994; 33: 1453-1461.
- Li Q, Luo C, Yang T, Yao Z, He L, Liu L, Xu H, Gong Q, Yao D, Zhou D. EEG-fMRI study on the interictal and ictal generalized spike-wave discharges in patients with childhood absence epilepsy. *Epilepsy Res* 2009; 87: 160-168.
- Liou ST, Witzel T, Numenmaa A, Chang WT, Tsai KW, Kuo WJ, Chung HW, Lin FH. Functional magnetic resonance inverse imaging of human visuomotor systems using eigenspace linearly constrained minimum amplitude (eLCMA) beamformer. *Neuroimage* 2011; 55: 87-100.
- Lishman WA, McConnell H, Snyder PJ. Psychiatric comorbidity in epilepsy : basic mechanisms, diagnosis, and treatment. Washington, London: American Psychiatric Press; 1998.
- Liston AD, Lund TE, Salek-Haddadi A, Hamandi K, Friston KJ, Lemieux L. Modelling cardiac signal as a confound in EEG-fMRI and its application in focal epilepsy studies. *Neuroimage* 2006; 30: 827-834.

## REFERENCES

- Liu Y, Yang T, Liao W, Yang X, Liu I, Yan B, Chen H, Gong Q, Stefan H, Zhou D. EEG-fMRI study of the ictal and interictal epileptic activity in patients with eyelid myoclonia with absences. *Epilepsia* 2008; 49: 2078-2086.
- Loddenkemper T, Kotagal P. Lateralizing signs during seizures in focal epilepsy. *Epilepsy Behav* 2005; 7: 1-17.
- Logothetis NK, Guggenberger H, Peled S, Pauls J. Functional imaging of the monkey brain. *Nat Neurosci* 1999; 2: 555-562.
- Logothetis NK, Pauls J, Augath M, Trinath T, Oeltermann A. Neurophysiological investigation of the basis of the fMRI signal. *Nature* 2001; 412: 150-157.
- Logothetis NK, Pfeuffer J. On the nature of the BOLD fMRI contrast mechanism. *Magn Reson Imaging* 2004; 22: 1517-1531.
- Logothetis NK, Wandell BA. Interpreting the BOLD signal. *Annu Rev Physiol* 2004; 66: 735-769.
- Logothetis NK. What we can do and what we cannot do with fMRI. *Nature* 2008; 453: 869-878.
- Lotze M, Erb M, Flor H, Huelsmann E, Godde B, Grodd W. fMRI evaluation of somatotopic representation in human primary motor cortex. *Neuroimage* 2000; 11: 473-481.
- Luders H, Acharya J, Baumgartner C, Benbadis S, Bleasel A, Burgess R, Dinner DS, Ebner A, Foldvary N, Geller E, Hamer H, Holthausen H, Kotagal P, Morris H, Meencke HJ, Noachtar S, Rosenow F, Sakamoto A, Steinhoff BJ, Tuxhorn I, Wyllie E. Semiological seizure classification. *Epilepsia* 1998; 39: 1006-1013.
- Luders H, Comair YG. *Epilepsy surgery*. Philadelphia: Lippincott Williams & Wilkins; 2000.
- Luders H, Noachtar S, Benson JK. *Atlas and classification of electroencephalography*. Philadelphia: Saunders; 2000.
- Luders HO, Najm I, Nair D, Widdess-Walsh P, Bingman W. The epileptogenic zone: general principles. *Epileptic Disord* 2006; 8 Suppl 2: S1-S9.
- Luders HO, Turnbull J, Kaffashi F. Are the dichotomies generalized versus focal epilepsies and idiopathic versus symptomatic epilepsies still valid in modern epileptology? *Epilepsia* 2009; 50: 1336-1343.
- Lund TE, Norgaard MD, Rostrup E, Rowe JB, Paulson OB. Motion or activity: their role in intra- and inter-subject variation in fMRI. *Neuroimage* 2005; 26: 960-964.
- Lund TE, Madsen KH, Sidaros K, Luo WL, Nichols TE. Non-white noise in fMRI: does modelling have an impact? *Neuroimage* 2006; 29: 54-66.
- MacDonald BK, Cockerell OC, Sander JW, Shorvon SD. The incidence and lifetime prevalence of neurological disorders in a prospective community-based study in the UK. *Brain* 2000; 123 ( Pt 4): 665-676.
- Magiorkinis E, Sidiropoulou K, Diamantis A. Hallmarks in the history of epilepsy: epilepsy in antiquity. *Epilepsy Behav* 2010; 17: 103-108.
- Magistretti PJ, Sorg O, Naichen Y, Pellerin L, de RS, Martin JL. Regulation of astrocyte energy metabolism by neurotransmitters. *Ren Physiol Biochem* 1994; 17: 168-171.
- Magistretti PJ, Pellerin L, Rothman DL, Shulman RG. Energy on demand. *Science* 1999; 283: 496-497.
- Malonek D, Grinvald A. Interactions between electrical activity and cortical microcirculation revealed by imaging spectroscopy: implications for functional brain mapping. *Science* 1996; 272: 551-554.
- Mandelkow H, Halder P, Boesiger P, Brandeis D. Synchronization facilitates removal of MRI artefacts from concurrent EEG recordings and increases usable bandwidth. *Neuroimage* 2006; 32: 1120-1126.
- Mantini D, Perrucci MG, Del GC, Romani GL, Corbetta M. Electrophysiological signatures of resting state networks in the human brain. *Proc Natl Acad Sci U S A* 2007; 104: 13170-13175.
- Manuel DE. *Marshall Hall (1790-1857): Science & Medicine in Early Victorian Society*. Amsterdam/Atlanta, GA.: Rodopi BV Editions; 1996.

## REFERENCES

- Marciani MG, Gotman J, Andermann F, Olivier A. Patterns of seizure activation after withdrawal of antiepileptic medication. *Neurology* 1985; 35: 1537-1543.
- Markand ON, Salanova V, Worth R, Park HM, Wellman HN. Comparative study of interictal PET and ictal SPECT in complex partial seizures. *Acta Neurol Scand* 1997; 95: 129-136.
- Marrosu F, Barberini L, Puligheddu M, Bortolato M, Mascia M, Tuveri A, Muroi A, Mallarini G, Avanzini G. Combined EEG/fMRI recording in musicogenic epilepsy. *Epilepsy Res* 2009; 84: 77-81.
- Marson A, Jacoby A, Johnson A, Kim L, Gamble C, Chadwick D. Immediate versus deferred antiepileptic drug treatment for early epilepsy and single seizures: a randomised controlled trial. *Lancet* 2005; 365: 2007-2013.
- Marson AG, Al-Kharusi AM, Alwaidh M, Appleton R, Baker GA, Chadwick DW, Cramp C, Cockerell OC, Cooper PN, Doughty J, Eaton B, Gamble C, Goulding PJ, Howell SJ, Hughes A, Jackson M, Jacoby A, Kellett M, Lawson GR, Leach JP, Nicolaidis P, Roberts R, Shackley P, Shen J, Smith DF, Smith PE, Smith CT, Vanoli A, Williamson PR. The SANAD study of effectiveness of valproate, lamotrigine, or topiramate for generalised and unclassifiable epilepsy: an unblinded randomised controlled trial. *Lancet* 2007; 369: 1016-1026.
- Masterton RA, Harvey AS, Archer JS, Lillywhite LM, Abbott DF, Scheffer IE, Jackson GD. Focal epileptiform spikes do not show a canonical BOLD response in patients with benign rolandic epilepsy (BECTS). *Neuroimage* 2010; 51: 252-260.
- Mathiesen C, Caesar K, Akgoren N, Lauritzen M. Modification of activity-dependent increases of cerebral blood flow by excitatory synaptic activity and spikes in rat cerebellar cortex. *J Physiol* 1998; 512 ( Pt 2): 555-566.
- Matsuoka H, Takahashi T, Sasaki M, Matsumoto K, Yoshida S, Numachi Y, Saito H, Ueno T, Sato M. Neuropsychological EEG activation in patients with epilepsy. *Brain* 2000; 123 ( Pt 2): 318-330.
- Mauguiere F, Ryvlin P. The role of PET in presurgical assessment of partial epilepsies. *Epileptic Disord* 2004; 6: 193-215.
- McCormick DA, Contreras D. On the cellular and network bases of epileptic seizures. *Annu Rev Physiol* 2001; 63: 815-846.
- McDonald CR, Thesen T, Hagler DJ, Jr., Carlson C, Devinsky O, Kuzniecky R, Barr W, Gharapetian L, Trongnetrpunya A, Dale AM, Halgren E. Distributed source modeling of language with magnetoencephalography: application to patients with intractable epilepsy. *Epilepsia* 2009; 50: 2256-2266.
- McGirr EM. William Cullen MD (1710-1790). *Scott Med J* 1991; 36: 6.
- McIntyre DC, Wong RK. Cellular and synaptic properties of amygdala-kindled pyriform cortex in vitro. *J Neurophysiol* 1986; 55: 1295-1307.
- McIntyre N. Robert Bentley Todd (1809-60). *J Med Biogr* 2008; 16: 2.
- McKeown MJ, Sejnowski TJ. Independent component analysis of fMRI data: examining the assumptions. *Hum Brain Mapp* 1998; 6: 368-372.
- McKeown MJ, Makeig S, Brown GG, Jung TP, Kindermann SS, Bell AJ, Sejnowski TJ. Analysis of fMRI data by blind separation into independent spatial components. *Hum Brain Mapp* 1998; 6: 160-188.
- McKeown MJ, Humphries C, Iragui V, Sejnowski TJ. Spatially fixed patterns account for the spike and wave features in absence seizures. *Brain Topogr* 1999; 12: 107-116.
- McKeown MJ, Hansen LK, Sejnowski TJ. Independent component analysis of functional MRI: what is signal and what is noise? *Curr Opin Neurobiol* 2003; 13: 620-629.
- McLachlan RS, Nicholson RL, Black S, Carr T, Blume WT. Nuclear magnetic resonance imaging, a new approach to the investigation of refractory temporal lobe epilepsy. *Epilepsia* 1985; 26: 555-562.
- Meeren H, van LG, Lopes da SF, Coenen A. Evolving concepts on the pathophysiology of absence seizures: the cortical focus theory. *Arch Neurol* 2005; 62: 371-376.
- Meeren HK, Pijn JP, van Luijckelaar EL, Coenen AM, Lopes da Silva FH. Cortical focus drives widespread corticothalamic networks during spontaneous absence seizures in rats. *J Neurosci* 2002; 22: 1480-1495.

## REFERENCES

- Meinardi H. International League against Epilepsy and its Journal Epilepsia. 2009.
- Menon V, Ford JM, Lim KO, Glover GH, Pfefferbaum A. Combined event-related fMRI and EEG evidence for temporal-parietal cortex activation during target detection. *Neuroreport* 1997; 8: 3029-3037.
- Menzler K, Thiel P, Hermsen A, Chen X, Benes L, Miller D, Sure U, Knake S, Rosenow F. The role of underlying structural cause for epilepsy classification: clinical features and prognosis in mesial temporal lobe epilepsy caused by hippocampal sclerosis versus cavernoma. *Epilepsia* 2011; 52: 707-711.
- Miller JW, Cole AJ. Is it necessary to define the ictal onset zone with EEG prior to performing resective epilepsy surgery? *Epilepsy Behav* 2011; 20: 178-181.
- Mirsattari SM, Lee DH, Jones D, Bihari F, Ives JR. MRI compatible EEG electrode system for routine use in the epilepsy monitoring unit and intensive care unit. *Clin Neurophysiol* 2004; 115: 2175-2180.
- Mitzdorf U. Properties of the evoked potential generators: current source-density analysis of visually evoked potentials in the cat cortex. *Int J Neurosci* 1987; 33: 33-59.
- Mody I, Heinemann U. NMDA receptors of dentate gyrus granule cells participate in synaptic transmission following kindling. *Nature* 1987; 326: 701-704.
- Mody I, Lambert JD, Heinemann U. Low extracellular magnesium induces epileptiform activity and spreading depression in rat hippocampal slices. *J Neurophysiol* 1987; 57: 869-888.
- Moeller F, Siebner HR, Wolff S, Muhle H, Granert O, Jansen O, Stephani U, Siniatchkin M. Simultaneous EEG-fMRI in drug-naive children with newly diagnosed absence epilepsy. *Epilepsia* 2008a; 49: 1510-1519.
- Moeller F, Siebner HR, Wolff S, Muhle H, Boor R, Granert O, Jansen O, Stephani U, Siniatchkin M. Changes in activity of striato-thalamo-cortical network precede generalized spike wave discharges. *Neuroimage* 2008b; 39: 1839-1849.
- Moeller F, Siebner HR, Wolff S, Muhle H, Granert O, Jansen O, Stephani U, Siniatchkin M. Mapping brain activity on the verge of a photically induced generalized tonic-clonic seizure. *Epilepsia* 2009a; 50: 1632-1637.
- Moeller F, Siebner HR, Ahlgrimm N, Wolff S, Muhle H, Granert O, Boor R, Jansen O, Gotman J, Stephani U, Siniatchkin M. fMRI activation during spike and wave discharges evoked by photic stimulation. *Neuroimage* 2009b; 48: 682-695.
- Moeller F, LeVan P, Gotman J. Independent component analysis (ICA) of generalized spike wave discharges in fMRI: Comparison with general linear model-based EEG-fMRI. *Hum Brain Mapp* 2010a.
- Moeller F, Muhle H, Wiegand G, Wolff S, Stephani U, Siniatchkin M. EEG-fMRI study of generalized spike and wave discharges without transitory cognitive impairment. *Epilepsy Behav* 2010b; 18: 313-316.
- Moeller F, LeVan P, Muhle H, Stephani U, Dubeau F, Siniatchkin M, Gotman J. Absence seizures: individual patterns revealed by EEG-fMRI. *Epilepsia* 2010c; 51: 2000-2010.
- Monto S, Vanhatalo S, Holmes MD, Palva JM. Epileptogenic neocortical networks are revealed by abnormal temporal dynamics in seizure-free subdural EEG. *Cereb Cortex* 2007; 17: 1386-1393.
- Moore CI, Cao R. The hemo-neural hypothesis: on the role of blood flow in information processing. *J Neurophysiol* 2008; 99: 2035-2047.
- Moritz CH, Meyerand ME, Cordes D, Haughton VM. Functional MR imaging activation after finger tapping has a shorter duration in the basal ganglia than in the sensorimotor cortex. *AJNR Am J Neuroradiol* 2000a; 21: 1228-1234.
- Moritz CH, Haughton VM, Cordes D, Quigley M, Meyerand ME. Whole-brain functional MR imaging activation from a finger-tapping task examined with independent component analysis. *AJNR Am J Neuroradiol* 2000b; 21: 1629-1635.
- Morocz IA, Karni A, Haut S, Lantos G, Liu G. fMRI of triggerable auras in musicogenic epilepsy. *Neurology* 2003; 60: 705-709.
- Moshe SL. In support of the ILAE Commission classification proposal. *Epilepsia* 2011; 52: 1200-1201.

## REFERENCES

- Mosier K, Bereznaya I. Parallel cortical networks for volitional control of swallowing in humans. *Exp Brain Res* 2001; 140: 280-289.
- Mukamel R, Gelbard H, Arieli A, Hasson U, Fried I, Malach R. Coupling between neuronal firing, field potentials, and fMRI in human auditory cortex. *Science* 2005; 309: 951-954.
- Mulert C, Lemieux L. EEG-fMRI: physiological basis, technique, and applications. Heidelberg: Springer; 2010.
- Murakami S, Okada Y. Contributions of principal neocortical neurons to magnetoencephalography and electroencephalography signals. *J Physiol* 2006; 575: 925-936.
- Nagarajan L, Schaul N, Eidelberg D, Dhawan V, Fraser R, Labar DR. Contralateral temporal hypometabolism on positron emission tomography in temporal lobe epilepsy. *Acta Neurol Scand* 1996; 93: 81-84.
- Najm IM, Naugle R, Busch RM, Bingaman W, Luders H. Definition of the epileptogenic zone in a patient with non-lesional temporal lobe epilepsy arising from the dominant hemisphere. *Epileptic Disord* 2006; 8 Suppl 2: S27-S35.
- Negishi M, Abildgaard M, Nixon T, Constable RT. Removal of time-varying gradient artifacts from EEG data acquired during continuous fMRI. *Clin Neurophysiol* 2004; 115: 2181-2192.
- Neuner I, Wegener P, Stoecker T, Kircher T, Schneider F, Shah NJ. Development and implementation of an MR-compatible whole body video system. *Neurosci Lett* 2007; 420: 122-127.
- Ngugi AK, Bottomley C, Kleinschmidt I, Sander JW, Newton CR. Estimation of the burden of active and life-time epilepsy: a meta-analytic approach. *Epilepsia* 2010; 51: 883-890.
- Niazy RK, Beckmann CF, Iannetti GD, Brady JM, Smith SM. Removal of fMRI environment artifacts from EEG data using optimal basis sets. *Neuroimage* 2005; 28: 720-737.
- Nicoletti A, Reggio A, Bartoloni A, Failla G, Sofia V, Bartalesi F, Roselli M, Gamboa H, Salazar E, Osinaga R, Paradisi F, Tempera G, Dumas M, Hall AJ. Prevalence of epilepsy in rural Bolivia: a door-to-door survey. *Neurology* 1999; 53: 2064-2069.
- Niedermeyer E, Lopes da Silva FH. *Electroencephalography: basic principles, clinical applications, and related fields*. Philadelphia: Lippincott Williams & Wilkins; 2005.
- Niessing J, Ebisch B, Schmidt KE, Niessing M, Singer W, Galuske RA. Hemodynamic signals correlate tightly with synchronized gamma oscillations. *Science* 2005; 309: 948-951.
- Nimsky C, Ganslandt O, Cerny S, Hastreiter P, Greiner G, Fahlbusch R. Quantification of, visualization of, and compensation for brain shift using intraoperative magnetic resonance imaging. *Neurosurgery* 2000; 47: 1070-1079.
- Nishizawa S, Tanada S, Yonekura Y, Fujita T, Mukai T, Saji H, Fukuyama H, Miyoshi T, Harada K, Ishikawa M, . Regional dynamics of N-isopropyl-(123I)p-iodoamphetamine in human brain. *J Nucl Med* 1989; 30: 150-156.
- Nudo RJ, Masterton RB. Stimulation-induced [<sup>14</sup>C]2-deoxyglucose labeling of synaptic activity in the central auditory system. *J Comp Neurol* 1986; 245: 553-565.
- Nuland SB. Astley Cooper of Guy's Hospital. *Conn Med* 1976; 40: 190-193.
- Nunez PL, Silberstein RB. On the relationship of synaptic activity to macroscopic measurements: does co-registration of EEG with fMRI make sense? *Brain Topogr* 2000; 13: 79-96.
- O'Brien TJ, O'Connor MK, Mullan BP, Brinkmann BH, Hanson D, Jack CR, So EL. Subtraction ictal SPET co-registered to MRI in partial epilepsy: description and technical validation of the method with phantom and patient studies. *Nucl Med Commun* 1998; 19: 31-45.
- Obrig H, Neufang M, Wenzel R, Kohl M, Steinbrink J, Einhaupl K, Villringer A. Spontaneous low frequency oscillations of cerebral hemodynamics and metabolism in human adults. *Neuroimage* 2000; 12: 623-639.

## REFERENCES

- Ogawa S, Lee TM, Kay AR, Tank DW. Brain magnetic resonance imaging with contrast dependent on blood oxygenation. *Proc Natl Acad Sci U S A* 1990a; 87: 9868-9872.
- Ogawa S, Lee TM, Nayak AS, Glynn P. Oxygenation-sensitive contrast in magnetic resonance image of rodent brain at high magnetic fields. *Magn Reson Med* 1990b; 14: 68-78.
- Ogawa S, Tank DW, Menon R, Ellermann JM, Kim SG, Merkle H, Ugurbil K. Intrinsic signal changes accompanying sensory stimulation: functional brain mapping with magnetic resonance imaging. *Proc Natl Acad Sci U S A* 1992; 89: 5951-5955.
- Ogawa S, Lee TM, Stepanoski R, Chen W, Zhu XH, Ugurbil K. An approach to probe some neural systems interaction by functional MRI at neural time scale down to milliseconds. *Proc Natl Acad Sci U S A* 2000; 97: 11026-11031.
- Oishi M, Otsubo H, Kameyama S, Morota N, Masuda H, Kitayama M, Tanaka R. Epileptic spikes: magnetoencephalography versus simultaneous electrocorticography. *Epilepsia* 2002; 43: 1390-1395.
- Olafsson E, Ludvigsson P, Gudmundsson G, Hesdorffer D, Kjartansson O, Hauser WA. Incidence of unprovoked seizures and epilepsy in Iceland and assessment of the epilepsy syndrome classification: a prospective study. *Lancet Neurol* 2005; 4: 627-634.
- Oun A, Haldre S, Magi M. Incidence of adult epilepsy in Estonia. *Acta Neurol Scand* 2003; 108: 245-251.
- Owen AM, McMillan KM, Laird AR, Bullmore E. N-back working memory paradigm: a meta-analysis of normative functional neuroimaging studies. *Hum Brain Mapp* 2005; 25: 46-59.
- Pacia SV, Ebersole JS. Intracranial EEG substrates of scalp ictal patterns from temporal lobe foci. *Epilepsia* 1997; 38: 642-654.
- Pan JW, Stein DT, Telang F, Lee JH, Shen J, Brown P, Cline G, Mason GF, Shulman GI, Rothman DL, Hetherington HP. Spectroscopic imaging of glutamate C4 turnover in human brain. *Magn Reson Med* 2000; 44: 673-679.
- Panayiotopoulos CP. The new ILAE report on terminology and concepts for organization of epileptic seizures: a clinician's critical view and contribution. *Epilepsia* 2011; 52: 2155-2160.
- Parkes LM, Bastiaansen MC, Norris DG. Combining EEG and fMRI to investigate the post-movement beta rebound. *Neuroimage* 2006; 29: 685-696.
- Pasley BN, Inglis BA, Freeman RD. Analysis of oxygen metabolism implies a neural origin for the negative BOLD response in human visual cortex. *Neuroimage* 2007; 36: 269-276.
- Pearce JM. Bromide, the first effective antiepileptic agent. *J Neurol Neurosurg Psychiatry* 2002; 72: 412.
- Peck KK, Branski RC, Lazarus C, Cody V, Kraus D, Haupage S, Ganz C, Holodny AI, Kraus DH. Cortical activation during swallowing rehabilitation maneuvers: a functional MRI study of healthy controls. *Laryngoscope* 2010; 120: 2153-2159.
- Pellerin L, Magistretti PJ. Glutamate uptake into astrocytes stimulates aerobic glycolysis: a mechanism coupling neuronal activity to glucose utilization. *Proc Natl Acad Sci U S A* 1994; 91: 10625-10629.
- Penfield W, Jasper HH. *Epilepsy and the functional anatomy of the human brain*. Boston: Mass: Little Brown & Co; 1954.
- Penny W, Holmes A. Random-Effects Analysis. In: Frackowiak RSJ, Friston KJ, Frith CD *et al*, editors. *Human Brain Function*. London: Academic Press; 2004. p. 843-50.
- Penny W, Flandin G, Trujillo-Barreto N. Bayesian comparison of spatially regularised general linear models. *Hum Brain Mapp* 2007; 28: 275-293.
- Perlberg V, Bellec P, Anton JL, Pelegrini-Issac M, Doyon J, Benali H. CORSICA: correction of structured noise in fMRI by automatic identification of ICA components. *Magn Reson Imaging* 2007; 25: 35-46.
- Petersen ET, Lim T, Golay X. Model-free arterial spin labeling quantification approach for perfusion MRI. *Magn Reson Med* 2006; 55: 219-232.

## REFERENCES

- Polack PO, Guillemain I, Hu E, Deransart C, Depaulis A, Charpier S. Deep layer somatosensory cortical neurons initiate spike-and-wave discharges in a genetic model of absence seizures. *J Neurosci* 2007; 27: 6590-6599.
- Prevett MC, Duncan JS, Jones T, Fish DR, Brooks DJ. Demonstration of thalamic activation during typical absence seizures using H2(15)O and PET. *Neurology* 1995; 45: 1396-1402.
- Price CJ, Moore CJ, Friston KJ. Subtractions, conjunctions, and interactions in experimental design of activation studies. *Hum Brain Mapp* 1997; 5: 264-272.
- Raichle ME, MacLeod AM, Snyder AZ, Powers WJ, Gusnard DA, Shulman GL. A default mode of brain function. *Proc Natl Acad Sci U S A* 2001; 98: 676-682.
- Raichle ME, Mintun MA. Brain work and brain imaging. *Annu Rev Neurosci* 2006; 29: 449-476.
- Ray A, Tao JX, Hawes-Ebersole SM, Ebersole JS. Localizing value of scalp EEG spikes: a simultaneous scalp and intracranial study. *Clin Neurophysiol* 2007; 118: 69-79.
- Rees G, Friston K, Koch C. A direct quantitative relationship between the functional properties of human and macaque V5. *Nat Neurosci* 2000; 3: 716-723.
- Regis J, Bartolomei F, Hayashi M, Roberts D, Chauvel P, Peragut JC. The role of gamma knife surgery in the treatment of severe epilepsies. *Epileptic Disord* 2000; 2: 113-122.
- Remi J, Vollmar C, de MA, Heinlin J, Peraud A, Noachtar S. Congruence and discrepancy of interictal and ictal EEG with MRI lesions in focal epilepsies. *Neurology* 2011; 77: 1383-1390.
- Reynolds EH. Jackson, Todd, and the concept of "discharge" in epilepsy. *Epilepsia* 2007; 48: 2016-2022.
- Reynolds EH, Andrew M. Hughlings Jackson's early education. *J Neurol Neurosurg Psychiatry* 2007; 78: 92.
- Reynolds EH, Wilson JVK. Psychoses of epilepsy in Babylon: the oldest account of the disorder. *Epilepsia* 2008; 49: 1488-1490.
- Riccio CA, Reynolds CR, Lowe P, Moore JJ. The continuous performance test: a window on the neural substrates for attention? *Arch Clin Neuropsychol* 2002; 17: 235-272.
- Richardson MP, Strange BA, Thompson PJ, Baxendale SA, Duncan JS, Dolan RJ. Pre-operative verbal memory fMRI predicts post-operative memory decline after left temporal lobe resection. *Brain* 2004; 127: 2419-2426.
- Richardson MP, Strange BA, Duncan JS, Dolan RJ. Memory fMRI in left hippocampal sclerosis: optimizing the approach to predicting postsurgical memory. *Neurology* 2006a; 66: 699-705.
- Richardson MP, Grosse P, Allen PJ, Turner R, Brown P. BOLD correlates of EMG spectral density in cortical myoclonus: description of method and case report. *Neuroimage* 2006b; 32: 558-565.
- Richardson MP, Lopes da Silva FH. TMS studies of preictal cortical excitability change. *Epilepsy Res* 2011; 97: 273-277.
- Richmond C. Sir Godfrey Hounsfield. *British Medical Journal* 2004; 329: 687.
- Roche-Labarbe N, Zaaïmi B, Mahmoudzadeh M, Osharina V, Wallois A, Nehlig A, Grebe R, Wallois F. NIRS-measured oxy- and deoxyhemoglobin changes associated with EEG spike-and-wave discharges in a genetic model of absence epilepsy: the GAERS. *Epilepsia* 2010; 51: 1374-1384.
- Rodionov R, De MF, Laufs H, Carmichael DW, Formisano E, Walker M, Duncan JS, Lemieux L. Independent component analysis of interictal fMRI in focal epilepsy: comparison with general linear model-based EEG-correlated fMRI. *Neuroimage* 2007; 38: 488-500.
- Rosenow F, Luders H. Presurgical evaluation of epilepsy. *Brain* 2001; 124: 1683-1700.
- Rothman DL, Sibson NR, Hyder F, Shen J, Behar KL, Shulman RG. In vivo nuclear magnetic resonance spectroscopy studies of the relationship between the glutamate-glutamine neurotransmitter cycle and functional neuroenergetics. *Philos Trans R Soc Lond B Biol Sci* 1999; 354: 1165-1177.
- Roy CS, Sherrington CS. On the Regulation of the Blood-supply of the Brain. *J Physiol* 1890; 11: 85-158.

## REFERENCES

- Rugland AL. Neuropsychological assessment of cognitive functioning in children with epilepsy. *Epilepsia* 1990; 31 Suppl 4: S41-S44.
- Rutecki PA, Lebeda FJ, Johnston D. Epileptiform activity induced by changes in extracellular potassium in hippocampus. *J Neurophysiol* 1985; 54: 1363-1374.
- Sakatani K, Murata Y, Fujiwara N, Hoshino T, Nakamura S, Kano T, Katayama Y. Comparison of blood-oxygen-level-dependent functional magnetic resonance imaging and near-infrared spectroscopy recording during functional brain activation in patients with stroke and brain tumors. *J Biomed Opt* 2007; 12: 062110.
- Salek-Haddadi A, Merschhemke M, Lemieux L, Fish DR. Simultaneous EEG-Correlated Ictal fMRI. *Neuroimage* 2002; 16: 32-40.
- Salek-Haddadi A, Friston KJ, Lemieux L, Fish DR. Studying spontaneous EEG activity with fMRI. *Brain Res Brain Res Rev* 2003a; 43: 110-133.
- Salek-Haddadi A, Lemieux L, Merschhemke M, Friston KJ, Duncan JS, Fish DR. Functional magnetic resonance imaging of human absence seizures. *Ann Neurol* 2003b; 53: 663-667.
- Salek-Haddadi A, Diehl B, Hamandi K, Merschhemke M, Liston A, Friston K, Duncan JS, Fish DR, Lemieux L. Hemodynamic correlates of epileptiform discharges: an EEG-fMRI study of 63 patients with focal epilepsy. *Brain Res* 2006; 1088: 148-166.
- Salek-Haddadi A, Mayer T, Hamandi K, Symms M, Josephs O, Fluegel D, Woermann F, Richardson MP, Noppeney U, Wolf P, Koepp MJ. Imaging seizure activity: a combined EEG/EMG-fMRI study in reading epilepsy. *Epilepsia* 2009; 50: 256-264.
- Salmenpera TM, Symms MR, Rugg-Gunn FJ, Boulby PA, Free SL, Barker GJ, Yousry TA, Duncan JS. Evaluation of quantitative magnetic resonance imaging contrasts in MRI-negative refractory focal epilepsy. *Epilepsia* 2007; 48: 229-237.
- Sanchez-Vives MV, McCormick DA. Functional properties of perigeniculate inhibition of dorsal lateral geniculate nucleus thalamocortical neurons in vitro. *J Neurosci* 1997; 17: 8880-8893.
- Sanchez-Vives MV, Bal T, McCormick DA. Inhibitory interactions between perigeniculate GABAergic neurons. *J Neurosci* 1997; 17: 8894-8908.
- Sander JW, Hart YM, Johnson AL, Shorvon SD. National General Practice Study of Epilepsy: newly diagnosed epileptic seizures in a general population. *Lancet* 1990; 336: 1267-1271.
- Sander JW, Shorvon SD. Epidemiology of the epilepsies. *J Neurol Neurosurg Psychiatry* 1996; 61: 433-443.
- Schierhout G, Roberts I. Anti-epileptic drugs for preventing seizures following acute traumatic brain injury. *Cochrane Database Syst Rev* 2000; CD000173.
- Schmitt F, Stehling MK, Turner R. *Echo-Planar Imaging: theory, technique, and application*. Berlin: Springer-Verlag; 1998.
- Schott. Bravais-Jackson epilepsy. *Lyon Med* 1968; 219: 1240.
- Schouten J. Gerard van Swieten, a pioneer in the field of geriatrics. *Gerontol Clin (Basel)* 1974; 16: 231-235.
- Schridde U, Khubchandani M, Motelow JE, Sanganahalli BG, Hyder F, Blumenfeld H. Negative BOLD with large increases in neuronal activity. *Cereb Cortex* 2008; 18: 1814-1827.
- Schwab RS. A method of measuring consciousness in petit-mal epilepsy. *J Nerv Ment Dis* 1939; 89: 690-691.
- Schwartz TH, Hong SB, Bagshaw AP, Chauvel P, Benar CG. Preictal changes in cerebral haemodynamics: review of findings and insights from intracerebral EEG. *Epilepsy Res* 2011; 97: 252-266.
- Schwartzkroin PA, Wyler AR. Mechanisms underlying epileptiform burst discharge. *Ann Neurol* 1980; 7: 95-107.
- Seeck M, Lazeyras F, Michel CM, Blanke O, Gericke CA, Ives J, Delavelle J, Golay X, Haenggeli CA, de TN, Landis T. Non-invasive epileptic focus localization using EEG-triggered functional MRI and electromagnetic tomography. *Electroencephalogr Clin Neurophysiol* 1998; 106: 508-512.



## REFERENCES

- Shewmon DA, Erwin RJ. The effect of focal interictal spikes on perception and reaction time. I. General considerations. *Electroencephalogr Clin Neurophysiol* 1988; 69: 319-337.
- Shinagawa H, Ono T, Honda E, Sasaki T, Taira M, Iriki A, Kuroda T, Ohyama K. Chewing-side preference is involved in differential cortical activation patterns during tongue movements after bilateral gum-chewing: a functional magnetic resonance imaging study. *J Dent Res* 2004; 83: 762-766.
- Shinnar S. The new ILAE classification. *Epilepsia* 2010; 51: 715-717.
- Shmuel A, Yacoub E, Pfeuffer J, van de Moortele PF, Adriany G, Hu X, Ugurbil K. Sustained negative BOLD, blood flow and oxygen consumption response and its coupling to the positive response in the human brain. *Neuron* 2002; 36: 1195-1210.
- Shmuel A, Augath M, Oeltermann A, Logothetis NK. Negative functional MRI response correlates with decreases in neuronal activity in monkey visual area V1. *Nat Neurosci* 2006; 9: 569-577.
- Shorvon SD. Using etiology as one axis of classification. *Epilepsia* 2011a; 52: 1208-1209.
- Shorvon SD. The etiologic classification of epilepsy. *Epilepsia* 2011b; 52: 1052-1057.
- Shulman RG, Rothman DL. Interpreting functional imaging studies in terms of neurotransmitter cycling. *Proc Natl Acad Sci U S A* 1998; 95: 11993-11998.
- Shulman RG, Rothman DL, Hyder F. A BOLD search for baseline. *Neuroimage* 2007; 36: 277-281.
- Sigerist HE. *Bulletin of the history of medicine*. Baltimore: Johns Hopkins, 1941.
- Silvester A. Jean Martin Charcot (1825-93) and John Hughlings Jackson (1835-1911): neurology in France and England in the 19th century. *J Med Biogr* 2009; 17: 210-213.
- Siniatchkin M, Groening K, Moehring J, Moeller F, Boor R, Brodbeck V, Michel CM, Rodionov R, Lemieux L, Stephani U. Neuronal networks in children with continuous spikes and waves during slow sleep. *Brain* 2010; 133: 2798-2813.
- Smith AJ, Blumenfeld H, Behar KL, Rothman DL, Shulman RG, Hyder F. Cerebral energetics and spiking frequency: the neurophysiological basis of fMRI. *Proc Natl Acad Sci U S A* 2002; 99: 10765-10770.
- Smith S. *The Surgical Treatment of Epilepsy, with statistical tables, comprising all the recorded cases of ligature of the carotid artery: and also of trphining the cranium by American Surgeons*. New York Journal of Medicine 1852; 220-242.
- Smith SJ. EEG in the diagnosis, classification, and management of patients with epilepsy. *J Neurol Neurosurg Psychiatry* 2005; 76 Suppl 2: ii2-ii7.
- Sokoloff L. Relation between physiological function and energy metabolism in the central nervous system. *J Neurochem* 1977; 29: 13-26.
- Sokoloff L, Reivich M, Kennedy C, Des Rosiers MH, Patlak CS, Pettigrew KD, Sakurada O, Shinohara M. The [<sup>14</sup>C]deoxyglucose method for the measurement of local cerebral glucose utilization: theory, procedure, and normal values in the conscious and anesthetized albino rat. *J Neurochem* 1977; 28: 897-916.
- Spanaki MV, Spencer SS, Corsi M, MacMullan J, Seibyl J, Zubal IG. Sensitivity and specificity of quantitative difference SPECT analysis in seizure localization. *J Nucl Med* 1999; 40: 730-736.
- Spencer SS. Neural networks in human epilepsy: evidence of and implications for treatment. *Epilepsia* 2002; 43: 219-227.
- Srivastava G, Crottaz-Herbette S, Lau KM, Glover GH, Menon V. ICA-based procedures for removing ballistocardiogram artifacts from EEG data acquired in the MRI scanner. *Neuroimage* 2005; 24: 50-60.
- Stefanovic B, Warnking JM, Pike GB. Hemodynamic and metabolic responses to neuronal inhibition. *Neuroimage* 2004; 22: 771-778.
- Stefanovic B, Warnking JM, Kobayashi E, Bagshaw AP, Hawco C, Dubeau F, Gotman J, Pike GB. Hemodynamic and metabolic responses to activation, deactivation and epileptic discharges. *Neuroimage* 2005; 28: 205-215.

## REFERENCES

- Steriade M, Amzica F, Neckelmann D, Timofeev I. Spike-wave complexes and fast components of cortically generated seizures. II. Extra- and intracellular patterns. *J Neurophysiol* 1998; 80: 1456-1479.
- Strandberg M, Larsson EM, Backman S, Kallen K. Pre-surgical epilepsy evaluation using 3T MRI. Do surface coils provide additional information? *Epileptic Disord* 2008; 10: 83-92.
- Stretton J, Winston G, Sidhu M, Centeno M, Vollmar C, Bonelli S, Symms M, Koepp M, Duncan JS, Thompson PJ. Neural correlates of working memory in Temporal Lobe Epilepsy - An fMRI study. *Neuroimage* 2012; 60: 1696-1703.
- Suzuki M, Asada Y, Ito J, Hayashi K, Inoue H, Kitano H. Activation of cerebellum and basal ganglia on volitional swallowing detected by functional magnetic resonance imaging. *Dysphagia* 2003; 18: 71-77.
- Swartz BE. Electrophysiology of bimanual-bipedal automatisms. *Epilepsia* 1994; 35: 264-274.
- Swartz BE. The advantages of digital over analog recording techniques. *Electroencephalogr Clin Neurophysiol* 1998; 106: 113-117.
- Swartz BE, Goldensohn ES. Timeline of the history of EEG and associated fields. *Electroencephalogr Clin Neurophysiol* 1998; 106: 173-176.
- Swash M. John Hughlings Jackson (1835-1911). *J Neurol* 2005; 252: 745-746.
- Symms MR, Allen PJ, Woermann FG, Polizzi G, Krakow K, Barker GJ, Fish DR, Duncan JS. Reproducible localization of interictal epileptiform discharges using EEG-triggered fMRI. *Phys Med Biol* 1999; 44: N161-N168.
- Takahashi S, Driscoll BF, Law MJ, Sokoloff L. Role of sodium and potassium ions in regulation of glucose metabolism in cultured astroglia. *Proc Natl Acad Sci U S A* 1995; 92: 4616-4620.
- Takeuchi H, Taki Y, Hashizume H, Sassa Y, Nagase T, Nouchi R, Kawashima R. Failing to deactivate: the association between brain activity during a working memory task and creativity. *Neuroimage* 2011; 55: 681-687.
- Tao JX, Ray A, Hawes-Ebersole S, Ebersole JS. Intracranial EEG substrates of scalp EEG interictal spikes. *Epilepsia* 2005; 46: 669-676.
- Tao JX, Baldwin M, Hawes-Ebersole S, Ebersole JS. Cortical substrates of scalp EEG epileptiform discharges. *J Clin Neurophysiol* 2007a; 24: 96-100.
- Tao JX, Baldwin M, Ray A, Hawes-Ebersole S, Ebersole JS. The impact of cerebral source area and synchrony on recording scalp electroencephalography ictal patterns. *Epilepsia* 2007b; 48: 2167-2176.
- Tellez-Zenteno JF, Dhar R, Wiebe S. Long-term seizure outcomes following epilepsy surgery: a systematic review and meta-analysis. *Brain* 2005; 128: 1188-1198.
- Temkin O. Galens Advice for an Epileptic Boy. *Bull Hist Med* 1934; 2: 179-189.
- Temkin O. The falling sickness: a history of epilepsy from the Greeks to the beginning of modern neurology. --. Baltimore: John Hopkins Press; 1971.
- Temkin O. Hippocrates as the physician of Democritus. *Gesnerus* 1985; 42: 455-464.
- Tettamanti M, Alkadhi H, Moro A, Perani D, Kollias S, Weniger D. Neural correlates for the acquisition of natural language syntax. *Neuroimage* 2002; 17: 700-709.
- Theodore WH, Holmes MD, Dorwart RH, Porter RJ, Di CG, Sato S, Rose D. Complex partial seizures: cerebral structure and cerebral function. *Epilepsia* 1986; 27: 576-582.
- Theodore WH, Sato S, Kufta CV, Gaillard WD, Kelley K. FDG-positron emission tomography and invasive EEG: seizure focus detection and surgical outcome. *Epilepsia* 1997; 38: 81-86.
- Theodore WH, Fisher RS. Brain stimulation for epilepsy. *Lancet Neurol* 2004; 3: 111-118.
- Thesen S, Heid O, Mueller E, Schad LR. Prospective acquisition correction for head motion with image-based tracking for real-time fMRI. *Magn Reson Med* 2000; 44: 457-465.
- Thivard L, Adam C, Hasboun D, Clemenceau S, Dezamis E, Lehericy S, Dormont D, Chiras J, Baulac M, Dupont S. Interictal diffusion MRI in partial epilepsies explored with intracerebral electrodes. *Brain* 2006; 129: 375-385.

## REFERENCES

- Thornton R, Laufs H, Rodionov R, Cannadathu S, Carmichael DW, Vulliemoz S, Salek-Haddadi A, McEvoy AW, Smith SM, Lhatoo S, Elwes RD, Guye M, Walker MC, Lemieux L, Duncan JS. EEG correlated functional MRI and postoperative outcome in focal epilepsy. *J Neurol Neurosurg Psychiatry* 2010a; 81: 922-927.
- Thornton R, Vulliemoz S, Rodionov R, Carmichael DW, Chaudhary UJ, Diehl B, Laufs H, Vollmar C, McEvoy AW, Walker MC, Bartolomei F, Guye M, Chauvel P, Duncan JS, Lemieux L. Epileptic networks in focal cortical dysplasia revealed using electroencephalography-functional magnetic resonance imaging. *Ann Neurol* 2011; 70: 822-837.
- Thornton RC, Rodionov R, Laufs H, Vulliemoz S, Vaudano A, Carmichael D, Cannadathu S, Guye M, McEvoy A, Lhatoo S, Bartolomei F, Chauvel P, Diehl B, De MF, Elwes RD, Walker MC, Duncan JS, Lemieux L. Imaging haemodynamic changes related to seizures: comparison of EEG-based general linear model, independent component analysis of fMRI and intracranial EEG. *Neuroimage* 2010b; 53: 196-205.
- TIZARD B, MARGERISON JH. The relationship between generalized paroxysmal EEG discharges and various test situations in two epileptic patients. *J Neurol Neurosurg Psychiatr* 1963; 26: 308-313.
- Todd RB. *Clinical Lectures on Paralysis, Certain Diseases of the Brain, and other Affections of the Nervous System*. Philadelphia: Lindsay & Blakiston; 1855.
- Todman D. Epilepsy in the Graeco-Roman world: Hippocratic medicine and Asklepien temple medicine compared. *J Hist Neurosci* 2008a; 17: 435-441.
- Todman D. Soranus of Ephesus (AD 98-138) and the Methodist sect. *J Med Biogr* 2008b; 16: 51.
- Trombin F, Gnatkovsky V, de CM. Changes in action potential features during focal seizure discharges in the entorhinal cortex of the in vitro isolated guinea pig brain. *J Neurophysiol* 2011; 106: 1411-1423.
- Truccolo W, Donoghue JA, Hochberg LR, Eskandar EN, Madsen JR, Anderson WS, Brown EN, Halgren E, Cash SS. Single-neuron dynamics in human focal epilepsy. *Nat Neurosci* 2011; 14: 635-641.
- Tsakiridou E, Bertollini L, de CM, Avanzini G, Pape HC. Selective increase in T-type calcium conductance of reticular thalamic neurons in a rat model of absence epilepsy. *J Neurosci* 1995; 15: 3110-3117.
- Tucker DM, Brown M, Luu P, Holmes MD. Discharges in ventromedial frontal cortex during absence spells. *Epilepsy Behav* 2007; 11: 546-557.
- Tucker DM, Waters AC, Holmes MD. Transition from cortical slow oscillations of sleep to spike-wave seizures. *Clin Neurophysiol* 2009; 120: 2055-2062.
- Tyler KL. Hughlings Jackson: the early development of his ideas on epilepsy. *J Hist Med Allied Sci* 1984; 39: 55-64.
- Tyvaert L, Hawco C, Kobayashi E, LeVan P, Dubeau F, Gotman J. Different structures involved during ictal and interictal epileptic activity in malformations of cortical development: an EEG-fMRI study. *Brain* 2008; 131: 2042-2060.
- Tyvaert L, LeVan P, Dubeau F, Gotman J. Noninvasive dynamic imaging of seizures in epileptic patients. *Hum Brain Mapp* 2009; 30: 3993-4011.
- Uijl SG, Leijten FS, Arends JB, Parra J, van Huffelen AC, Moons KG. The added value of [18F]-fluoro-D-deoxyglucose positron emission tomography in screening for temporal lobe epilepsy surgery. *Epilepsia* 2007; 48: 2121-2129.
- Valton L, Guye M, McGonigal A, Marquis P, Wendling F, Regis J, Chauvel P, Bartolomei F. Functional interactions in brain networks underlying epileptic seizures in bilateral diffuse periventricular heterotopia. *Clin Neurophysiol* 2008; 119: 212-223.
- Van Bogaert P, Massager N, Tugendhaft P, Wikler D, Damhaut P, Levivier M, Brotschi J, Goldman S. Statistical parametric mapping of regional glucose metabolism in mesial temporal lobe epilepsy. *Neuroimage* 2000; 12: 129-138.
- van den Heuvel MP, Mandl RC, Kahn RS, Hulshoff Pol HE. Functionally linked resting-state networks reflect the underlying structural connectivity architecture of the human brain. *Hum Brain Mapp* 2009; 30: 3127-3141.

## REFERENCES

- van Houdt PJ, Ossenblok PP, Boon PA, Leijten FS, Velis DN, Stam CJ, de Munck JC. Correction for pulse height variability reduces physiological noise in functional MRI when studying spontaneous brain activity. *Hum Brain Mapp* 2010; 31: 311-325.
- Van Paesschen W, Dupont P, Van DG, Van BH, Maes A. SPECT perfusion changes during complex partial seizures in patients with hippocampal sclerosis. *Brain* 2003; 126: 1103-1111.
- Van Paesschen W, Dupont P, Sunaert S, Goffin K, Van LK. The use of SPECT and PET in routine clinical practice in epilepsy. *Curr Opin Neurol* 2007; 20: 194-202.
- Vanzan A, Paladin F. Epilepsy and Persian culture: an overview. *Epilepsia* 1992; 33: 1057-1064.
- Vaudano AE, Laufs H, Kiebel SJ, Carmichael DW, Hamandi K, Guye M, Thornton R, Rodionov R, Friston KJ, Duncan JS, Lemieux L. Causal hierarchy within the thalamo-cortical network in spike and wave discharges. *PLoS One* 2009; 4: e6475.
- Volkman FC. Human visual suppression. *Vision Res* 1986; 26: 1401-1416.
- Vollmar C, O'Muircheartaigh J, Barker GJ, Symms MR, Thompson P, Kumari V, Duncan JS, Janz D, Richardson MP, Koeppe MJ. Motor system hyperconnectivity in juvenile myoclonic epilepsy: a cognitive functional magnetic resonance imaging study. *Brain* 2011; 134: 1710-1719.
- Vulliemoz S, Thornton R, Rodionov R, Carmichael DW, Guye M, Lhatoo S, McEvoy AW, Spinelli L, Michel CM, Duncan JS, Lemieux L. The spatio-temporal mapping of epileptic networks: combination of EEG-fMRI and EEG source imaging. *Neuroimage* 2009; 46: 834-843.
- Vulliemoz S, Lemieux L, Daunizeau J, Michel CM, Duncan JS. The combination of EEG source imaging and EEG-correlated functional MRI to map epileptic networks. *Epilepsia* 2010; 51: 491-505.
- Vulliemoz S, Carmichael DW, Rosenkranz K, Diehl B, Rodionov R, Walker MC, McEvoy AW, Lemieux L. Simultaneous intracranial EEG and fMRI of interictal epileptic discharges in humans. *Neuroimage* 2011; 54: 182-190.
- Wagner K, Hader C, Metternich B, Buschmann F, Schwarzwald R, Schulze-Bonhage A. Who needs a Wada test? Present clinical indications for amobarbital procedures. *J Neurol Neurosurg Psychiatry* 2012.
- Walton K, Fulton BP. Ionic mechanisms underlying the firing properties of rat neonatal motoneurons studied in vitro. *Neuroscience* 1986; 19: 669-683.
- Wandell BA. Computational neuroimaging of human visual cortex. *Annu Rev Neurosci* 1999; 22: 145-173.
- Warach S, Ives JR, Schlaug G, Patel MR, Darby DG, Thangaraj V, Edelman RR, Schomer DL. EEG-triggered echo-planar functional MRI in epilepsy. *Neurology* 1996; 47: 89-93.
- Weil S, Noachtar S, Arnold S, Yousry TA, Winkler PA, Tatsch K. Ictal ECD-SPECT differentiates between temporal and extratemporal epilepsy: confirmation by excellent postoperative seizure control. *Nucl Med Commun* 2001; 22: 233-237.
- Wendling F, Bellanger JJ, Badier JM, Coatrieux JL. Extraction of spatio-temporal signatures from depth EEG seizure signals based on objective matching in warped vectorial observations. *IEEE Trans Biomed Eng* 1996; 43: 990-1000.
- Wendling F, Bartolomei F, Bellanger JJ, Chauvel P. Epileptic fast activity can be explained by a model of impaired GABAergic dendritic inhibition. *Eur J Neurosci* 2002; 15: 1499-1508.
- Wendling F, Bartolomei F, Bellanger JJ, Bourien J, Chauvel P. Epileptic fast intracerebral EEG activity: evidence for spatial decorrelation at seizure onset. *Brain* 2003; 126: 1449-1459.
- Wendling F, Hernandez A, Bellanger JJ, Chauvel P, Bartolomei F. Interictal to ictal transition in human temporal lobe epilepsy: insights from a computational model of intracerebral EEG. *J Clin Neurophysiol* 2005; 22: 343-356.
- Wennberg R, Quesney LF, Lozano A, Olivier A, Rasmussen T. Role of electrocorticography at surgery for lesion-related frontal lobe epilepsy. *Can J Neurol Sci* 1999; 26: 33-39.

## REFERENCES

- Westmijse I, Ossenblok P, Gunning B, van LG. Onset and propagation of spike and slow wave discharges in human absence epilepsy: A MEG study. *Epilepsia* 2009; 50: 2538-2548.
- WHO Media centre. Epilepsy: historical overview. 2001.
- Wichert-Ana L, de Azevedo-Marques PM, Oliveira LF, Fernandes RM, Velasco TR, Santos AC, Araujo D, Kato M, Bianchin MM, Sakamoto AC. Ictal technetium-99 m ethyl cysteinate dimer single-photon emission tomographic findings in epileptic patients with polymicrogyria syndromes: a subtraction of ictal-interictal SPECT coregistered to MRI study. *Eur J Nucl Med Mol Imaging* 2008a; 35: 1159-1170.
- Wichert-Ana L, de Azevedo-Marques PM, Oliveira LF, Terra-Bustamante VC, Fernandes RM, Santos AC, Araujo WM, Bianchin MM, Simoes MV, Sakamoto AC. Interictal hyperemia correlates with epileptogenicity in polymicrogyric cortex. *Epilepsy Res* 2008b; 79: 39-48.
- Wieser HG, Blume WT, Fish D, Goldensohn E, Hufnagel A, King D, Sperling MR, Luders H, Pedley TA. ILAE Commission Report. Proposal for a new classification of outcome with respect to epileptic seizures following epilepsy surgery. *Epilepsia* 2001; 42: 282-286.
- Wild B, Erb M, Lemke N, Scholz P, Bartels M, Grodd W. Video camera and light system for application in magnetic resonance scanners. *Magn Reson Imaging* 2000; 18: 893-896.
- Wilke M, Lidzba K. LI-tool: a new toolbox to assess lateralization in functional MR-data. *J Neurosci Methods* 2007; 163: 128-136.
- Willmann O, Wennberg R, May T, Woermann FG, Pohlmann-Eden B. The contribution of 18F-FDG PET in preoperative epilepsy surgery evaluation for patients with temporal lobe epilepsy A meta-analysis. *Seizure* 2007; 16: 509-520.
- Wilson JVK, Reynolds EH. Texts and Documents. Translation and analysis of a cuneiform text forming part of a Babylonian treatise on epilepsy. *Medical History* 1990; 34: 185-198.
- Wolf P. Of cabbages and kings: some considerations on classifications, diagnostic schemes, semiology, and concepts. *Epilepsia* 2003; 44: 1-4.
- Wolf P. Networks and systems, conceptualizations, and research. *Epilepsia* 2011; 52: 1198-1200.
- Wong M. Epilepsy is both a symptom and a disease: a proposal for a two-tiered classification system. *Epilepsia* 2011; 52: 1201-1203.
- Worsley KJ, Liao CH, Aston J, Petre V, Duncan GH, Morales F, Evans AC. A general statistical analysis for fMRI data. *Neuroimage* 2002; 15: 1-15.
- Yan WX, Mullinger KJ, Geirsdottir GB, Bowtell R. Physical modeling of pulse artefact sources in simultaneous EEG/fMRI. *Hum Brain Mapp* 2010; 31: 604-620.
- Yang G, Iadecola C. Glutamate microinjections in cerebellar cortex reproduce cerebrovascular effects of parallel fiber stimulation. *Am J Physiol* 1996; 271: R1568-R1575.
- Yasuda C, Vollmar C, Centeno M, Stretton J, Symms M, Cendes F, Mehta M, Thompson P, Duncan J, Koepp M. The effect of topiramate on verbal fluency fMRI: a longitudinal pilot study. *Epilepsy Currents* 2012; 12: 371.
- Yogarajah M, Focke NK, Bonelli SB, Thompson P, Vollmar C, McEvoy AW, Alexander DC, Symms MR, Koepp MJ, Duncan JS. The structural plasticity of white matter networks following anterior temporal lobe resection. *Brain* 2010; 133: 2348-2364.
- York GK, Steinberg DA. Hughlings Jackson's suggestion for the treatment of epilepsy. *Neurology* 2009; 73: 1155-1158.
- Zaknun JJ, Bal C, Maes A, Tepmongkol S, Vazquez S, Dupont P, Dondi M. Comparative analysis of MR imaging, ictal SPECT and EEG in temporal lobe epilepsy: a prospective IAEA multi-center study. *Eur J Nucl Med Mol Imaging* 2008; 35: 107-115.
- Zhao M, Suh M, Ma H, Perry C, Geneslaw A, Schwartz TH. Focal increases in perfusion and decreases in hemoglobin oxygenation precede seizure onset in spontaneous human epilepsy. *Epilepsia* 2007; 48: 2059-2067.

## REFERENCES

- Zhao M, Ma H, Suh M, Schwartz TH. Spatiotemporal dynamics of perfusion and oximetry during ictal discharges in the rat neocortex. *J Neurosci* 2009; 29: 2814-2823.
- Ziburkus J, Cressman JR, Barreto E, Schiff SJ. Interneuron and pyramidal cell interplay during in vitro seizure-like events. *J Neurophysiol* 2006; 95: 3948-3954.
- Zijlmans M, Huiskamp G, Hersevoort M, Seppenwoolde JH, van Huffelen AC, Leijten FS. EEG-fMRI in the preoperative work-up for epilepsy surgery. *Brain* 2007; 130: 2343-2353.